



SCUOLA INTERNAZIONALE SUPERIORE DI STUDI AVANZATI - INTERNATIONAL SCHOOL FOR ADVANCED STUDIES

ASPECTS OF KAON PHYSICS IN CHIRAL PERTURBATION  
THEORY AND CHIRAL QUARK MODEL

Thesis submitted for the degree of  
*“Doctor Philosophiæ”*

CANDIDATE

Vito Antonelli

SUPERVISORS

Dr. S. Bertolini and Dr. M. Fabbrichesi

October 1996



# Contents

<b>1</b>	<b>Introduction</b>	<b>9</b>
<b>2</b>	<b><math>\Delta S = 1</math> Weak non Leptonic Interactions</b>	<b>17</b>
2.1	Weak non Leptonic Decays of Kaons . . . . .	17
2.1.1	Classification of Weak Kaon Decays . . . . .	17
2.1.2	Non Leptonic Decays . . . . .	19
2.1.3	Low Energies Effective Hamiltonian . . . . .	19
2.1.4	The Wilson Coefficients . . . . .	26
2.1.5	Hadronic Matrix Elements . . . . .	29
<b>3</b>	<b>Chiral Perturbation Theory and Chiral Quark Model</b>	<b>31</b>
3.1	Basics of Chiral Perturbation Theory . . . . .	31
3.1.1	The Strong Chiral Lagrangian at $O(p^2)$ . . . . .	33
3.1.2	$O(p^4)$ Corrections to the Chiral Lagrangian . . . . .	37
3.2	The Chiral Quark Model . . . . .	39
<b>4</b>	<b>Chiral Lagrangian for <math>\Delta S = 1</math> non Leptonic Decays</b>	<b>47</b>
4.1	The Model . . . . .	47
4.2	Bosonization . . . . .	48
4.3	The Weak Chiral Lagrangian . . . . .	52
4.3.1	Determination of the $\Delta S = 1$ Chiral Lagrangian Coefficients . .	53
4.3.2	General outlines of the calculation . . . . .	53
4.3.3	Non Perturbative Gluonic Corrections . . . . .	55
4.3.4	Divergencies Regularization . . . . .	56
4.3.5	Scheme Dependence and t'Hooft-Veltman Fake Anomalies . . .	57
4.3.6	Fierz Transformation Properties of the Operators . . . . .	60
4.3.7	HV Coefficients . . . . .	64

4.3.8	NDR Coefficients . . . . .	66
4.4	The Choice of the Input Parameters . . . . .	68
4.4.1	Gluon Condensate . . . . .	69
4.4.2	Quark Condensate . . . . .	69
4.4.3	The parameter $M$ . . . . .	71
4.5	Comments about the Results . . . . .	71
4.6	Meson Loop Corrections . . . . .	73
<b>5</b>	<b>The <math>\Delta I = 1/2</math> Selection Rule</b>	<b>79</b>
5.1	Status of the $\Delta I = 1/2$ Rule . . . . .	79
5.2	Hadronic Matrix Elements for $K \rightarrow \pi\pi$ in the Chiral Quark Model . . .	81
5.2.1	HV Results . . . . .	82
5.2.2	NDR Results . . . . .	83
5.3	Wilson Coefficients . . . . .	86
5.4	Choice of the Input Parameters . . . . .	91
5.5	Results of Other Approaches . . . . .	92
5.6	Numerical Results in the Chiral Quark Model . . . . .	94
5.6.1	Dependence on the Input Parameters . . . . .	97
5.6.2	$\gamma_5$ -scheme Independence . . . . .	100
5.7	Comments about our Results . . . . .	104
<b>6</b>	<b>CP Violation in Kaon Systems</b>	<b>109</b>
6.1	The Ratio $\varepsilon'/\varepsilon$ . . . . .	109
6.1.1	The Present Status of Experimental and Theoretical Knowledge . . . . .	113
6.1.2	$\varepsilon'/\varepsilon$ in the Chiral Quark Model . . . . .	114
<b>7</b>	<b><math>\Delta S = 2</math> Processes</b>	<b>117</b>
7.1	Analysis of $K^0 - \bar{K}^0$ Mixing . . . . .	117
7.1.1	Effective Lagrangian for $\Delta S = 2$ Transitions . . . . .	118
7.1.2	The $\Delta S = 2$ Weak Chiral Lagrangian . . . . .	122
7.1.3	Meson Loop Corrections . . . . .	123
7.2	The $\hat{B}_K$ Parameter . . . . .	126
7.2.1	Input Parameters . . . . .	126
7.2.2	Numerical Results for $\hat{B}_K$ . . . . .	127
7.2.3	Next to Leading Order $\eta$ Factors . . . . .	130

7.2.4	The Mixing Parameter $\text{Im } \lambda_t$ . . . . .	131
7.3	The $K_L - K_S$ Mass Difference . . . . .	133
7.3.1	Calculation of Long Distance Contribution . . . . .	134
7.3.2	The Wilson Coefficients . . . . .	135
7.3.3	Numerical Analysis . . . . .	135
<b>8</b>	<b>Conclusions and Overview of Future Perspectives</b>	<b>139</b>
<b>A</b>	<b>Chiral Quark Model</b>	<b>143</b>
A.1	Feynman Rules . . . . .	143
A.2	Fierz Transformations and Clebsh-Gordan Coefficients . . . . .	144
A.3	Dimensional Regularization . . . . .	145
<b>B</b>	<b>Table of Input Parameters</b>	<b>147</b>
<b>C</b>	<b>Feynman Rules for the Chiral Loops</b>	<b>149</b>
C.1	Feynman Rules for the Strong Chiral Lagrangian . . . . .	149
C.2	Feynman Rules for the $\Delta S = 1$ Chiral Lagrangian . . . . .	151
C.3	Feynman Rules for the $\Delta S = 2$ Chiral Lagrangian . . . . .	162

## List of Tables

5.1	NLO Wilson coefficients at $\mu = 0.8$ GeV in the NDR scheme for $\bar{m}_t(m_W) = 183$ GeV, which corresponds to $m_t^{pole} = 180$ GeV. The corresponding values at $\mu = m_W$ are given in parenthesis ( $\alpha = 1/128$ ). In addition one has $y_{1,2}(\mu) = 0$ . The coefficients $z_i(\mu)$ do not depend on $m_t$ . . . . .	87
5.2	Same as in table 1 in the HV scheme. . . . .	88
5.3	Same as in table 1 for $\mu = 1$ GeV. . . . .	89
5.4	Same as in table 2 for $\mu = 1$ GeV . . . . .	90
5.5	Matching scale and $\gamma_5$ scheme dependence of $A_0$ (in units of $10^{-7}$ GeV) and $A_2$ (in units of $10^{-8}$ GeV) in the VSA approach with NLO Wilson coefficients. The amplitudes are computed for $\Lambda_{\text{QCD}}^{(4)} = 350$ MeV and $\langle \bar{q}q \rangle$ given in eq. (5.47). The two values quoted for the $\mu$ -dependence of the amplitudes correspond to the NDR and HV scheme results in the range between 0.8 and 1.0 GeV. . . . .	93

5.6	Same as in table 5 in the $\chi$ QM approach, for different values of $\Lambda_{\text{QCD}}^{(4)}$ . We take for the gluon condensate the central value $\langle\alpha_s GG/\pi\rangle = (376 \text{ MeV})^4$ and for the quark condensate $\langle\bar{q}q\rangle$ eq. (5.47). For the chiral quark model parameter we choose $M = 220 \text{ MeV}$ . . . . .	96
5.7	The $B_i$ factors in the $\chi$ QM (including meson-loop renormalizations) for all the ten operators $Q_i$ , at two different scales: $\mu = 0.8$ and $1.0 \text{ GeV}$ . We have taken the gluon condensate at the central value of eq. (5.56), while the range given for $B_{5,6}$ corresponds to varying the quark condensate according to eq. (5.45). The results shown are given in both schemes for $M = 220 \text{ MeV}$ . . . . .	105
7.1	Values of $\hat{B}_K$ obtained in different approaches. . . . .	120
7.2	Matching scale and $\gamma_5$ scheme dependence of $\hat{B}_K$ in the $\chi$ QM with NLO Wilson coefficient, for three different values of $\Lambda_{\text{QCD}}^{(4)}$ . We take for the gluon condensate the value $\langle\alpha_s GG/\pi\rangle = (360 \text{ MeV})^4$ , preferred by the fit of $\Gamma(K^+ \rightarrow \pi^+\pi^0)$ . . . . .	128
7.3	Long distance and box contributions to $\Delta M$ , in units of $10^{-15} \text{ GeV}$ , for different values of the matching scale $\mu$ and $\Lambda_{\text{QCD}}^{(4)}$ in the $\chi$ QM. We take for the gluon condensate the value $\langle\alpha_s GG/\pi\rangle = (360 \text{ MeV})^4$ and for the quark condensate $\langle\bar{q}q\rangle = -(280 \text{ MeV})^3$ , which are the values preferred by the fit of the $\Delta I = 1/2$ selection rule at the same perturbative order. The box contribution is evaluated for a top quark pole mass of $180 \text{ GeV}$ . . . . .	136
B.1	Table of the numerical values of the input parameters used in this work. . . . .	147

## List of Figures

2.1	Schematic representation of a kaon decay into a couple of pions. . . . .	20
2.2	Feynman graph contributing to the transition represented in Fig. 2.1 . . . . .	21
2.3	New class of Feynman diagrams contributing to the transition $K \rightarrow \pi\pi$ . They appear when we switch on the strong interactions. . . . .	23
2.4	The Feynman diagrams originating penguin operators. Gluonic penguin graphs are represented in figure (A), while (B) gives the electroweak penguin operators. Note that in fig.(B) the gluon line has been substituted by a photon or a $Z$ . . . . .	24

4.1	The quark constituent loops for an arbitrary operator $Q_i$ . (A) is the un-factorized pattern, (B) the factorized one. The crossed circles represent operator and/or current insertions. . . . .	54
4.2	The constituent quark loops coupled to the mesons for an arbitrary operator. (A) is the unfactorized configuration, (B) the factorized one with the insertion of the gluon condensate. Meson and gluon lines must be attached in all possible ways. . . . .	55
4.3	The constituent quark loops coupled to $K$ and $\pi$ in the case of the insertion of the operator $Q_1$ , neglecting soft gluon corrections. (A) gives the leading $O(N_c^2)$ contribution of $Q_1$ to the chiral coefficient $G_{LL}^b$ , while (B) is the subleading $O(N_c)$ correction to $G_{LL}^a$ . The figure 3(C), instead, represents the contribution to the process $K^0 \rightarrow \pi^0$ coming from $\tilde{Q}_1$ , that is the Fierzed form of the operator $Q_1$ . . . . .	61
4.4	One-loop chiral renormalization of the the $K^0 \rightarrow \pi\pi$ amplitudes. The black box represents the insertion of the weak chiral lagrangian, whereas the black circle denotes the insertion of the $O(p^2)$ strong chiral lagrangian. For each chiral coefficient more than a hundred diagrams are generated by propagating in all allowed ways $K$ , $\pi$ and $\eta$ . . . . .	74
5.1	Dependence of $A_0$ and $A_2$ on $\langle\bar{q}q\rangle$ and $\langle GG\rangle$ for $\Lambda_{\text{QCD}}^{(4)} = 0.350$ GeV, $\mu = 0.8$ GeV, and $M = 180$ MeV. The black (grey) lines represent the HV (NDR) results for $\langle\bar{q}q\rangle$ in the range of eq. (5.45) and fixed $\langle\alpha_s GG/\pi\rangle$ . The vertical spread corresponds to varying $\langle\alpha_s GG/\pi\rangle$ in the range of eq. (5.44), with central lines corresponding to the central value of $\langle GG\rangle$ . The experimental values of $A_0$ and $A_2$ are given by the cross hairs. The small dependence of $A_2$ on the quark condensate is due to the the electroweak penguins $Q_{7,8}$ . . . . .	98
5.2	Same as in Fig. 1 for $M = 200$ MeV. . . . .	99
5.3	Same as in Fig.1 for $M = 220$ MeV. . . . .	99
5.4	Same as in Fig. 1 but for different values of the input parameters. $M = 200$ MeV and the quark and gluon condensates are given by eqs. (5.57)–(5.56). . . . .	100
5.5	The $\gamma_5$ -scheme dependence of $A_0$ is shown as a function of $M$ . The black (grey) line represent the HV (NDR) result. We use $\langle\alpha_s GG/\pi\rangle = (360 \text{ MeV})^4$ and $\langle\bar{q}q\rangle = -(220 \text{ MeV})^3$ . For this value of the quark condensate the stability appear between $M = 160$ and $M = 180$ MeV. . . . .	102

5.6	Same as in Fig.5 for $\langle \bar{q}q \rangle = -(280 \text{ MeV})^3$ . The stability is moved at about $M = 200 \text{ MeV}$ . . . . .	102
5.7	Same as in Fig. 6 for $A_2$ . There is no crossing of the HV and the NDR curves. Anyway the scheme dependence stays well below 20%. . . . .	103
5.8	The road to the $\Delta I = 1/2$ rule: 1) Effect of the W-induced current-current matrix elements ( $Q_{1,2}$ ) with the neglect of short-distance QCD renormalization; 2) $\langle Q_{1,2} \rangle$ with the inclusion of the NLO Wilson coefficients at $\mu = 0.8 \text{ GeV}$ . 3) inclusion of the gluon penguins ( $Q_{3-6}$ ); 4) inclusion of the electro-weak penguins ( $Q_{7-10}$ ); 5) inclusion of the $\pi^0 - \eta$ mixing; 6) inclusion of gluon condensate corrections; 7) meson-loop renormalization. The results shown are those of the HV scheme with the values $\langle \alpha_s GG/\pi \rangle = (360 \text{ MeV})^4$ and $\langle \bar{q}q \rangle = -(280 \text{ MeV})^3$ , for a matching scale $\mu = 0.8 \text{ GeV}$ and $M = 220 \text{ MeV}$ . The experimental values are given by the cross hairs. . . . .	108
7.1	The two configurations relevant to the determination of the chiral coefficient $C(Q_{S2})$ . . . . .	123
7.2	One-loop meson corrections to the kaon mass matrix. . . . .	124
7.3	The $\hat{B}_K$ parameter is shown as a function of the gluon condensate for $\Lambda_{\text{QCD}}^{(4)} = 350 \text{ MeV}$ and $\mu = 0.8 \text{ GeV}$ . We denote by $\langle GG \rangle$ the quantity $\langle \alpha_s GG/\pi \rangle^{1/4}$ in units of GeV. The dark and grey lines represent the HV and NDR results respectively. . . . .	129
7.4	Constraints on KM parameters from kaon physics. See the text for explanation. . . . .	132
7.5	Long-distance contributions to the $K^0 - \bar{K}^0$ mixing. The black box represents the insertion of the $\Delta S = 1$ weak hamiltonian. . . . .	135
7.6	The ratio $(\Delta M_{\text{box}} + \Delta M_{LD})/\Delta M_{LS}^{\text{exp}}$ is shown as a function of the gluon condensate for $\Lambda_{\text{QCD}}^{(4)} = 350 \text{ MeV}$ and $\mu = 0.8 \text{ GeV}$ . We denote by $\langle GG \rangle$ the quantity $\langle \alpha_s GG/\pi \rangle^{1/4}$ in units of GeV. The dark and grey lines represent the HV and NDR results results respectively. . . . .	138



## Acknowledgments

It is really difficult to express in a few words all my feelings in leaving Sissa. The three years I spent here have been for me a unique opportunity of human and scientific growing.

I had the possibility of knowing people coming from all over the world and I made friends with a lot of people. It is not possible to cite all of them here. Let me mention, in particular, E.I. Lashin, who has been not only a collaborator, but also a friend for me.

I am very grateful to my supervisors Dr. S. Bertolini and Dr. M. Fabbrichesi for many reasons. I would like to thank them especially for sharing with me the same enthusiasm about our research project and for teaching me the scientific insight and rigour which are essential elements of physics. I hope I would be able to benefit from their teachings also in my future career.

I also have found in Sissa a pleasant and stimulating scientific atmosphere. I am grateful for this reason to all Sissa Professors and Staff. I would like to thank in particular Prof. S. Pectov. It has been very important for me to have the possibility of interacting with him.

I am also glad to have the opportunity of thanking Prof. L. Trentadue for addressing me to the study of Elementary Particle Physics and for continuously advising and helping me.

Finally let me thank all the people that helped me during these years.

This thesis is dedicated to Barbara, who has continuously encouraged and supported me in the most difficult moments of my job.



# Chapter 1

## Introduction

Weak interactions can be considered the most complicated among the fundamental forces of nature and they represent probably the most interesting part of the Standard Model theory. We have in mind problems like the electroweak symmetry breaking and the explanation of the quark masses. Moreover, weak interactions (contrary to electromagnetic and strong ones) violate the discrete space time symmetries C, P, CP and T.

Weak meson decays are a typical example of weak processes, which are very important and at the same time very difficult to analyze. They present a rich phenomenology and therefore they can be used as an important test of the Standard Model consistency. As we will see, the main problem to address in the study of these processes is the fact that the fundamental forces of nature do not come in isolation. Therefore, to understand these decays, in which hadrons are involved, we have to consider the interplay between weak interactions and strong forces.

In this thesis we will focus our attention on the study of K meson physics and particularly of non leptonic weak processes which take place with variations of strangeness  $\Delta S = 1$  or  $\Delta S = 2$ .

These processes played a fundamental role in the development of our physical knowledge during the last thirty years, since the discovery [1] in 1964 by Christenson, Cronin, Fitch and Turlay of the decay of long-lived neutral K-mesons  $K_L$  into a CP even final state made by two pions. This was the first evidence for CP violation.

In principle there could be two different mechanisms responsible for this kind of decays. First of all we know that  $K_L$  is not a pure CP odd state, but it contains also a small fraction of CP even neutral kaons which can decay into two pions. In this case we speak of indirect CP violation. Then we can also consider a possible direct CP

violation, that is a transition between a CP odd state and a CP even one.

Nowadays we can measure with a good precision the parameter  $\varepsilon_K$  which characterizes the indirect violation of CP, but we are not yet able to draw a definite conclusion about the existence of direct CP violation. In fact this is one of the main topics on which the attention of both theoretical and experimental studies have been focused in the past twenty years. We will analyze this argument in a more detailed way in this dissertation, when we discuss the determination of the ratio  $\varepsilon'/\varepsilon$ .

Let us come back to our brief summary of the historical importance of K-meson physics. Another milestone in the development of Elementary Particle Physics was the study of the suppression of the decays involving flavor changing neutral currents. This experimental evidence was explained in a very brilliant way by Glashow, Iliopoulos and Maiani in 1970 with the introduction of the so called GIM mechanism based on the existence of a fourth quark, the quark charm [2]. Only a few years later, in 1974, Gaillard and Lee were able to predict the mass of the charm [3], starting from the analysis of  $K^0 - \bar{K}^0$  mixing and considering the dependence of  $\Delta S = 2$  transition on virtual charm mass. Their prediction was confirmed by the experiment and this calculation is also the prototype for present day analyses of virtual top contributions in  $B^0 - \bar{B}^0$  mixing, rare decays and CP violation.

Apart from its historical importance, K-meson physics has also a great relevance in our days. In fact there are still some important experimental evidences which are not explained in a complete and satisfactory way. A typical example is given by the  $\Delta I = 1/2$  selection rule [4], which has been a difficult theoretical puzzle since its discovery in the fifties (for a review see, for instance, ref. [5]).

This rule states that, in the weak non leptonic decays of kaons (as well as of hyperons), the amplitude in which the change in isospin between initial and final state is  $3/2$  is very much suppressed with respect to that in which the change is  $1/2$ . In the case of the kaon decay into two pions, the amplitude for transitions with total final isospin  $I = 0$  ( $\Delta I = 1/2$ ) is approximately 22 times larger than the one corresponding to transitions with total isospin of the final state  $I = 2$  ( $\Delta I = 3/2$ ).

This experimental result is very difficult to explain, as we can easily understand if we think that a naive Standard Model estimate, without considering the effect of strong interactions, would give more or less the same value for  $I = 0$  and  $I = 2$  amplitudes. We will treat this argument in a detailed way in chapter 5, where we will also try to explain how it is possible to account for this selection rule inside the model that we are going to develop [6].

Another reason that justifies our attention for kaon physics is the fact that it still presents a lot of important aspects which are not known and determined in a complete and satisfactory way. We can, for example, think of the problem of the determination of the ratio  $\varepsilon'/\varepsilon$  between the two parameters which characterize, respectively, direct and indirect CP violation.

A big experimental effort has been done to determine with the highest possible precision the value of this ratio. The results given by the two experimental collaborations NA31 at CERN [7] and E731 at Fermilab [8] are respectively:

$$\text{Re}\left(\frac{\varepsilon'}{\varepsilon}\right) = (23 \pm 7) \times 10^{-4}$$

and

$$\text{Re}\left(\frac{\varepsilon'}{\varepsilon}\right) = (7.4 \pm 6.0) \times 10^{-4}.$$

The discrepancy between these two values is quite big. In fact the result of the NA31 collaboration clearly indicates the existence of direct CP violation, while the Fermilab result can be compatible with the so called superweak theory [9], proposed by Wolfenstein in 1964, in which  $\varepsilon'/\varepsilon = 0$ . It is clear anyway that there is a need for new experimental devices which should be able to reduce the errors in a significant way.

In fact two new experiments are already working at CERN and Fermilab and another one, called DAΦNE, should start very soon in the INFN National Laboratories in Frascati (Italy). The data taking in DAΦNE is supposed to begin in 1997 and there is a big expectation for its results, even because this experiment is based on a different principle with respect to the other ones. It is clear that the possibility of having in future more and more precisely measured values of  $\varepsilon'/\varepsilon$  will require also a very accurate theoretical estimation of this quantity.

Another subject of great interest is the analysis of the mixing between the two flavor states of the neutral kaons,  $K^0$  and  $\bar{K}^0$ .

It would be very important, for instance, to give a consistent theoretical determination of the mass difference between  $K_L$  and  $K_S$  (the eigenstates of the weak hamiltonian) and to compare this estimate with the experimental result, that is known with a very good accuracy [10].

A complete analysis of  $K^0 - \bar{K}^0$  mixing processes is also fundamental for the exact determination of the parameters of the unitary  $3 \times 3$  Cabibbo-Kobayashi-Maskawa (CKM) matrix [11], describing the quark flavor mixing. As we will show, it is possible to obtain important constraints for the CKM matrix elements, and particularly for

its imaginary phase, from the value of the parameter  $\hat{B}_K$  (describing the transition amplitude between  $K^0$  and  $\bar{K}^0$ ) and from the experimental values of  $\varepsilon_K$  and  $m_t$ .

This kind of analysis is very important for different reasons. First of all, it can help us in the determination of some CKM matrix elements which are poorly known at present. Moreover, it is an essential test of consistency of the Standard Model of electroweak interactions. In fact the violation of CP in this model is supposed to arise from the single phase of Cabibbo-Kobayashi-Maskawa mixing matrix. It is also possible, in principle, that we will not be able to fit all the different observable with this single phase. In this case we should conclude the Standard Model is not able to justify the experimental results and we should consider some additional source of CP violation besides the usual one coming from the imaginary phase of CKM matrix. This would be of course an indication of new physics beyond the Standard Model. It is very important to underline the fact that the signals of new physics could come, not only from experiments involving very high energies, but also from the detailed analysis of this kind of low energy processes.

After having examined the historical role and the present relevance of kaon physics, it is important to stress which are the main difficulties that its study presents.

First of all we have to remember these processes usually involve very different energy scales, that may vary from the mass of the top quark, around 170 GeV, to a few hundreds of MeV (the typical scale of kaons and pions).

Usually the analysis is divided in two parts, called, respectively, short and long distances. This formal division is justified by the fact that in the operator product expansion (O.P.E.) formalism [12] we can write the amplitude  $A$  for a generic weak meson decay in the following way:

$$A = \langle H_{eff} \rangle = \sum_i C_i(\mu, M_W) \langle Q_i(\mu) \rangle. \quad (1.1)$$

In this way the amplitude is factorized in the product of the so called Wilson coefficients  $C_i$  (describing short distance physics) and of the matrix elements of local operators  $Q_i$ . These matrix elements represent the long distance contribution. The renormalization scale  $\mu$  which separates long and short distances is usually chosen to be around 1 GeV for kaon decays and a few GeV in the case of D and B mesons. The Wilson coefficients and the matrix elements separately exhibit a  $\mu$  dependence. When we match them, the  $\mu$  dependences should in principle cancel, in such a way to obtain a scale independent physical amplitude  $A$ .

Short distance analysis involves high energies. Hence it can be developed using well known field theoretical techniques, like perturbation theory, renormalization group [13]

and operator product expansion. In this sector fundamental progresses have been made in the last years, especially thanks to the work done by two groups in Munich and in Rome [15, 16]. Nowadays we know, for instance, the next to leading expression for the Wilson coefficients of all the operators appearing in the effective weak hamiltonian for  $\Delta S = 1$  and for  $\Delta S = 2$  weak non leptonic transitions.

On the other hand the analysis of the long distance (small energies) part of the interactions presents a lot of problems of difficult solution. This is the main reason for which we have essentially focused our attention on this part of the analysis. In fact we can say that there isn't a completely satisfactory and exhaustive description of all the aspects of long distance physics, even if it has been studied with a lot of different approaches, like lattice gauge theory [17],  $1/N_c$  expansion [18, 19] (where  $N_c$  is the number of colors), QCD effective action (see the first paper of ref. [20] and the last one of ref. [27]), QCD and hadronic sum rules [21], chiral perturbation theory [22].

The main difficulty is due to the fact that we have to face a highly non perturbative problem, because we want to describe processes taking place at typical scales of the order of 1 Gev or even less. The effect of strong interactions is certainly non negligible (as is shown very well for example in the case of the  $\Delta I = 1/2$  selection rule), but these scales are out of the range of validity of perturbative QCD. Hence we have to solve the problem of making a consistent analysis of hadronic interactions at low energies.

The natural theoretical framework in which we can work is chiral perturbation theory [23]. It enables us to describe these interactions just starting from the symmetry properties that the theory itself must satisfy.

In the case we want to study, that is  $\Delta S = 1$  and  $\Delta S = 2$  weak non leptonic decays, we can use a "bosonization" technique to write a complete chiral lagrangian [14, 24]. The different operators appearing in this chiral lagrangian contain only the degrees of freedom of the lighter octet of pseudoscalar mesons (kaons, pions and eta) and they have the same symmetry properties of the four quark operators of the original effective hamiltonian describing  $\Delta S = 1$  or  $\Delta S = 2$  weak interactions at low energies. The chiral lagrangian contains, of course, some unknown coefficients, which cannot be determined by symmetry requirements alone.

Since we do not know how to connect directly the degrees of freedom of the particles involved in our decays (pseudoscalar mesons) and those of the QCD lagrangian, that is quarks and gluons, the chiral lagrangian coefficients have to be recovered from the comparison with experimental results or with some phenomenological model.

To solve these problems we are forced to use some phenomenological model which

carries out the desired kind of interactions. We have based our analysis on the so called chiral quark model. This model, which resumes some of the ideas already proposed in [25] and [26], has been developed especially in [27]. It can also be seen as a mean field approximation of an extended Nambu-Jona-Lasinio model, mimicking QCD at intermediate energies [28].

The main feature of the chiral quark model is the presence in the lagrangian of a term which originates a spontaneous breaking of chiral symmetry and introduces an effective coupling between the mesons and the QCD degrees of freedom (quarks). This enables us to calculate explicitly the matrix elements, between initial and final meson states, of the quark operators appearing in the original effective hamiltonian.

Comparing the matrix elements calculated directly in the chiral quark model and the analogous results recovered from chiral perturbation theory, we can determine in an unique way all the unknown coefficients appearing in  $\Delta S = 1$  and  $\Delta S = 2$  weak chiral lagrangians.

This may be considered the most important result of our work. In fact in this way we have at our disposal a consistent phenomenological model and we can try to use it to give an explanation of some experimental results which have not been completely justified yet (like the  $\Delta I = 1/2$  rule) [6] and also to give predictions relative to processes of great present interest, like  $\varepsilon'/\varepsilon$  [29].

In the determination of the chiral lagrangian coefficients we have inserted the contributions of  $O(N_c^2)$ , which would be leading in the  $1/N_c$  expansion, the next to leading ones, and also terms of  $O(\alpha_S N_c)$ . This last kind of contributions is given by non perturbative gluonic corrections, which can be considered within our model. They are very important, because they contribute in an essential way to the exact determination of the physical results, as we will see later.

We can say that, for the way in which we have recovered it, by integrating out the light quark degrees of freedom, our chiral lagrangian is the effective theory of the chiral quark model at low energies.

There is another step that is essential in our approach, to obtain a correct evaluation of the hadronic matrix elements: we have to introduce the effect of the so called chiral loops.

In this kind of loops we consider the propagation of the only degrees of freedom still present in our low energy theory after the integration on the light quark degrees of freedom, that is the octet of pseudoscalar mesons. The insertion of these loop effects enables us to evaluate the hadronic matrix elements at energy scales near 1 GeV, at



which we can match them with the results of short distance analysis for the Wilson coefficients. In the loop computations some divergences arise and we have decided to regularize them by using the dimensional regularization technique, to be consistent with the way in which the short distance calculation of the Wilson coefficients is usually performed in literature.

The problem of the cancellation between the scale dependence introduced by chiral loops and the one coming from short distance analysis and also of the analogous scheme dependences has been faced by us and will be treated in a detailed way in this thesis.

We have organized this dissertation in the following way. In chapter 2 we discuss about the different kinds of K meson weak decays and we concentrate our attention on the  $\Delta S = 1$  weak non leptonic decays. We show how to recover the effective hamiltonian describing this kind of processes. As we have already said, the application of the O.P.E. formalism enables us to divide the study of the problem into short distance and long distance analysis. In this chapter we summarize the main steps of the calculation that one should perform to recover the short distance Wilson coefficients at the next to leading order. We close the second chapter with a brief discussion about the essential characteristics of some of the different techniques that can be used to compute hadronic matrix elements of the quark operators appearing in the  $\Delta S = 1$  effective hamiltonian. In the next chapters we show in a detailed way how these matrix elements can be evaluated within our model, which is essentially based on chiral perturbation theory and chiral quark model.

The third chapter is entirely devoted to these two theoretical tools. Of course, a complete and exhaustive description of all the different aspects of chiral perturbation theory and of its possible applications cannot be given in a few pages and it also would go beyond the scopes of this work. Anyhow we have reported the basic ideas on which chiral perturbation theory is founded and we have considered, in particular, the case of the strong chiral lagrangian up to  $O(p^4)$  in the momentum chiral expansion. The chiral quark model is the other essential ingredient on which we have based our analysis of kaon physics. In chapter three we present the main characteristic of this model and we also place it in a more general framework, which includes different models trying to mimic the mechanism of spontaneous chiral symmetry breaking that should take place in QCD. In particular we analyze the possible derivation of the chiral quark model as a mean field approximation of the extended Nambu-Jona-Lasinio model.

At this point we have all the ingredients we need to derive the chiral lagrangian for  $\Delta S = 1$  weak non leptonic processes. This derivation is performed in the fourth

chapter.

First of all we sketch the bosonization procedure that we follow to go from the four-quark operators  $Q_i$  of the  $\Delta S = 1$  effective hamiltonian to the bosonic operators appearing in the chiral lagrangian. Then we show how to use the chiral quark model, as a phenomenological reference model, to fix the originally unknown chiral lagrangian coefficients. We also stress some important aspects of the computation, like the introduction of gluonic corrections, the problem of fake anomalies cancellation in the t'Hooft-Veltman (HV) regularization scheme and that of the Fierzing properties of the operators. At the end of the chapter we introduce the last essential step for the hadronic matrix element computation, that is the calculation of mesonic chiral loop corrections.

The results obtained in chapter 4 are the basis for the analysis of the arguments treated in the next two chapters.

In chapter 5 we show how we can give a quite satisfactory justification of the famous experimental  $\Delta I = 1/2$  selection rule in the case of kaon decays in two pions.

In chapter 6, instead, we focus our attention on a problem of great present relevance, that is the determination of the ratio between the two CP violating parameters  $\varepsilon'$  and  $\varepsilon$ . We have said that a lot of experimental and theoretical work has been done and is still in progress on this subject. In this dissertation we just try to summarize briefly the physical relevance of the problem and the main results that can be found in literature. We also explain how to evaluate this quantity within our model.

In chapter 7 we switch to a new important subject, that is the  $\Delta S = 2$  processes and so the physics of  $K^0 - \bar{K}^0$  mixing. We apply the same formalism already used for  $\Delta S = 1$  physics, which here is made easier by the fact that we have to bosonize only one quark operator. Using the  $\Delta S = 2$  chiral lagrangian, we compute the value of the  $\hat{B}_K$  parameter, characterizing  $\Delta S = 2$  direct transition. We also analyze its phenomenological consequences, in particular for the determination of the Kobayashi-Maskawa mixing parameter  $\text{Im } \lambda_t$ . Besides the contribution to the mass difference between  $K_L$  and  $K_S$  ( $\Delta M_{LS}$ ) coming directly from box diagrams, we compute also the so called "long distance contribution". It is produced by a double insertion of  $\Delta S = 1$  weak lagrangian. In this way we can estimate the total mass difference and compare the obtained value with the experimental results.

Finally in the last chapter we try to make a critical analysis of our results and to see which could be the most interesting future applications and developments of our work.

# Chapter 2

## $\Delta S = 1$ Weak non Leptonic Interactions

### 2.1 Weak non Leptonic Decays of Kaons

#### 2.1.1 Classification of Weak Kaon Decays

Kaons are the lightest hadrons with strangeness quantum number different from zero. As we know that weak interactions can violate strangeness, contrary to strong and electromagnetic ones, it is clear that K mesons can only decay weakly into zero strangeness final states which can contain pions, photons and leptons. There are a lot of these possible decays and some of them have also very big decay rates [10].

The various decay modes are usually divided in three different groups :

-leptonic decays (in which only leptons appear);

-semileptonic decays (in this case both leptons and hadrons are present in the final state);

-non leptonic decays (in which there are no leptons between the decay products).

As we have already said, also photons can be produced in kaon decays and in this case we will speak naturally of radiative decays.

The simplest examples of leptonic decays are the ones usually denoted as  $K_{l2}$ . like, for instance,  $K^+ \rightarrow \mu^+ \nu_\mu$  or  $K^+ \rightarrow e^+ \nu_e$ . To study this kind of processes we always have to evaluate the matrix element of an axial current between a kaon state and the vacuum, which is given by the following relation :

$$\langle 0 | \bar{s} \gamma_\mu \gamma_5 u | K^+(k) \rangle = i\sqrt{2} f_K k_\mu. \quad (2.1)$$

This expression defines the kaon decay constant  $f_K$ .

Of course there are also more complex leptonic decays, like for example  $K^\pm \rightarrow l^\pm \nu_l l'^+ l'^-$  (where  $l$  and  $l'$  can denote either an electron or a muon), or  $K^\pm \rightarrow l^\pm \nu_l \nu_{\bar{l}}$ .

Among the semileptonic decays, we can remember, first of all, the beta decays of kaons, like  $K^+ \rightarrow \pi^0 l^+ \nu_l$ ,  $K^0 \rightarrow \pi^- l^+ \nu_l$  and so on. These processes, usually called  $K_{l3}^+$  and  $K_{l3}^0$ , are parametrized by two form factors ( $f_+$  and  $f_-$ ). They are defined by the following equations:

$$\langle \pi^0(p) | \bar{s} \gamma_\mu u | K^+(k) \rangle = - \frac{f_+^{K^+ \pi^0}(q^2)}{\sqrt{2}} (k+p)_\mu + \frac{f_-^{K^+ \pi^0}(q^2)}{\sqrt{2}} (k-p)_\mu \quad (2.2)$$

$$\langle \pi^-(p) | \bar{s} \gamma_\mu u | K^0(k) \rangle = -f_+^{K^0 \pi^-}(q^2) (k+p)_\mu + f_-^{K^0 \pi^-}(q^2) (k-p)_\mu. \quad (2.3)$$

In the limit in which  $SU(2)$  isospin invariance holds, we can introduce the following equalities:

$$f_\pm^{K^0 \pi^-}(q^2) = f_\pm^{K^+ \pi^0}(q^2) = f_\pm(q^2). \quad (2.4)$$

If we also assume  $SU(3)$  invariance, we can link the matrix element (2.2) to that of the decay  $\pi^+ \rightarrow \pi^0 l^+ \nu_l$ . In this limit we have  $f_-(0) = 0$  and  $f_+(0) = +1$ .

From a phenomenological point of view  $K_{l3}$  processes are very important, mainly because they can be used to extract the best evaluation of the element  $V_{us}$  of Cabibbo-Kobayashi-Maskawa mixing matrix.

Other important semileptonic processes are the so called  $K_{l4}$  decays, which typically have the form  $K^+ \rightarrow \pi \pi l^+ \nu_l$  or  $K_L \rightarrow \pi^0 \pi^\mp e^\pm \nu_e$ . They are characterized by small values of the branching ratios (usually of the order  $10^{-5} - 10^{-6}$ ). Nevertheless, they are quite important from a theoretical point of view. In fact they represent the only possible test for some relations between the different coefficients of chiral lagrangians that should hold in the  $1/N_c$  limit.

We will come back to the  $1/N_c$  expansion later in this thesis. For the time being let us just say that the basic idea of this expansion is that of considering, instead of the usual  $SU(3)$  of QCD, a generic gauge group  $SU(N_c)$  and to take the limit  $N_c \rightarrow \infty$ , while scaling the QCD coupling constant, so that  $g_s^2 N_c$  is kept fixed. It is possible, in this way, to organize the amplitudes as an expansion in powers of  $1/N_c$ .

Between the various semileptonic processes we can also mention the rare  $K_{l5}$  decays ( $K^+ \rightarrow \pi^+ \pi^- \pi^0 e^+ \nu_e$ ,  $K^+ \rightarrow \pi^0 \pi^0 \pi^0 e^+ \nu_e$  and the analogous ones for  $K^0$ ) and the radiative ones, like for instance  $K_{l2\gamma}$ ,  $K_{l3\gamma}$  and  $K_{l4\gamma}$ .

This brief survey of leptonic and semileptonic kaon decays is for sure incomplete. There are other decay modes besides the ones that we have mentioned and, moreover, there are a lot of other interesting remarks we could make for the processes we have considered. Anyway all these issues would be behind the main aim of this dissertation work. In fact we have decided to focus our attention on non leptonic decays of kaons and we will now begin to attach this wide and very interesting subject.

## 2.1.2 Non Leptonic Decays

We have already explained in the introduction the historical relevance and the present importance of non leptonic kaon decays.

We can remember first of all the discovery made by Christenson, Cronin, Fitch and Turlay in 1964 of the violation of CP parity [1].

This subject will be studied in chapter 6. We will analyze the problem of the definition of  $\varepsilon'$  and  $\varepsilon$  (the two parameters associated, respectively, to direct and indirect CP violation) and of the determination of the ratio  $\varepsilon'/\varepsilon$ . We will briefly report on the status of the experimental and theoretical knowledge of the value of  $\varepsilon'/\varepsilon$  and we will discuss how it is possible to obtain a theoretical estimate of it by studying the imaginary part of  $K \rightarrow \pi\pi$  amplitudes.

We would like to stress here that the determination of  $\varepsilon'/\varepsilon$  is not the only interesting open problem of  $\Delta S = 1$  non leptonic physics and also other very interesting subjects can be studied.

In chapter 5 we will attach, for instance, the problem of trying to give a satisfactory explanation of the  $\Delta I = 1/2$  selection rule. Despite the fact that this experimental rule was discovered a lot of years ago [4], in the fifties, we can say that until now it has not been completely justified from a theoretical point of view. As we will see any attempt to explain the origin of this selection rule has to take into consideration a lot of different effects and this issue can be considered a very good example of the complexity of  $\Delta S = 1$  weak non leptonic interactions.

## 2.1.3 Low Energies Effective Hamiltonian

In a Standard Model description the non leptonic weak interactions can be described, at lowest order in weak and zeroth order in strong interactions, by the product of two currents of left handed quarks, mediated by the exchange of a W boson. The weak

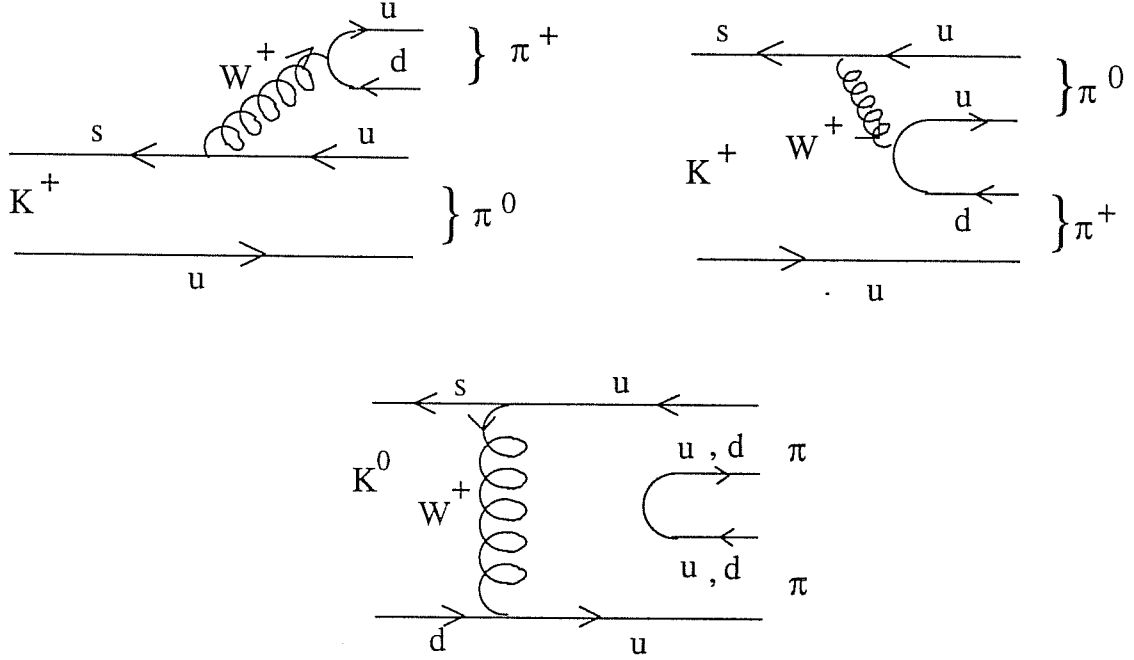


Figure 2.1: Schematic representation of a kaon decay into a couple of pions.

currents will have the following form :

$$J_{\mu}^{+}(x) = (\bar{u} \bar{c} \bar{t}) V \gamma_{\mu} (1 - \gamma_5) (d s b); \quad (2.5)$$

$$J_{\mu}^{-}(x) = (J_{\mu}^{+}(x))^{\dagger}. \quad (2.6)$$

In the previous formula  $V$  represents the Cabibbo-Kobayashi-Maskawa mixing matrix. In chapter 7 we will speak of the determination of some of its elements.

Let us consider, for instance, the case of a kaon decay into two pions, which can be represented schematically by the graphs in figure 1.

The Feynman diagrams contributing to this process are like the one of Fig. 2(A).

Neglecting (as usual for low energy processes) the momentum transfer dependence of the  $W$  boson propagator, we can represent the process as a local interaction, as it is shown in figure 2(B). In this way, we obtain the following  $(V-A) \times (V-A)$  structure for the weak non leptonic hamiltonian:

$$\mathcal{H}_{eff}(x) = \frac{g^2}{8M_W^2} J_{\mu}^{+}(x) J^{-\mu}(x) = \frac{G_F}{\sqrt{2}} J_{\mu}^{+}(x) J^{-\mu}(x), \quad (2.7)$$

where  $g$  and  $G_F$  are respectively the  $SU(2)$  weak and the Fermi coupling constant and  $M_W$  is the mass of the  $W$  boson.

The part of the effective weak hamiltonian which is involved in the kind of processes

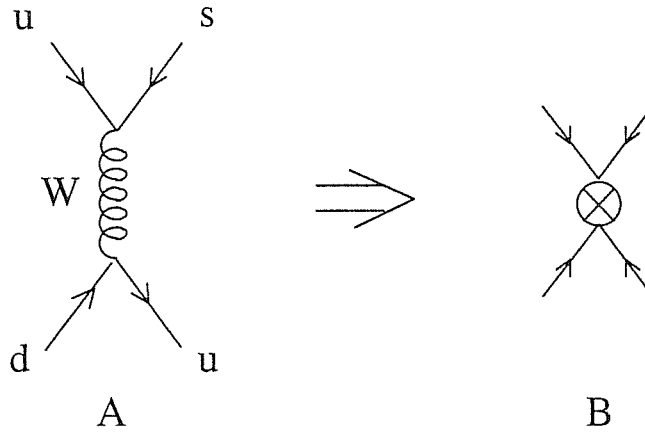


Figure 2.2: Feynman graph contributing to the transition represented in Fig. 2.1

we are describing ( $\Delta S = 1$ ,  $\Delta c = \Delta b = \Delta t = 0$ ) has the following form:

$$\mathcal{H}_{eff}^{\Delta S=1} = \frac{G_F}{\sqrt{2}} [V_{11}V_{12}^*(\bar{s}_\alpha u_\alpha)_{V-A}(\bar{u}_\beta d_\beta)_{V-A} + V_{21}V_{22}^*(\bar{s}_\alpha c_\alpha)_{V-A}(\bar{c}_\beta d_\beta)_{V-A} + V_{31}V_{32}^*(\bar{s}_\alpha t_\alpha)_{V-A}(\bar{t}_\beta d_\beta)_{V-A}], \quad (2.8)$$

where  $\alpha$  and  $\beta$  are the quark color indices and

$$V \pm A = \gamma_\mu (1 \pm \gamma_5). \quad (2.9)$$

The formal derivation of this effective hamiltonian is an example of application of the short distance operator product expansion (O.P.E.) formalism [12]. In our case, the convolution of the product of two local operators  $J_\mu^-(x)$  and  $J_\nu^+(y)$  with the massive W propagator can be expanded in a series of local operators. The dominant contributions in the short-distance expansion come from the lowest dimension operators, that in this case are the four fermion operators of the effective hamiltonian, which have dimension six.

It is important to notice that the approximation done in the application of the O.P.E. corresponds to neglecting contributions of the order  $\frac{k^2}{M_W^2}$ . So this technique gives us a convenient method to build up low energy effective theories for weak decays. The fact that the explicit dynamical degrees of freedom of the W boson are removed in the construction of the effective hamiltonian is usually expressed, in the path integral language, by saying that the W boson is “integrated out” of the theory.

In a similar way it is possible to consider lower scales of energy and to integrate out of the theory the degrees of freedom of the particles which can be considered heavy with respect to the scale at which we are working. To develop this procedure we have to write

new effective hamiltonians, which contain only the degrees of freedom of the particles which have not yet been integrated out. The new effective hamiltonian can be recovered from the previous one, by using renormalization group equations and requiring that the Green functions calculated in the new theory coincide with the previous ones. So we can start with an effective theory containing five quarks at scales  $\mu$  lower than  $M_W$  and integrate out, in different steps, the bottom and charm quark fields, until we are left, for scales lower than  $m_c$ , with an effective theory containing only the light quarks  $u$ ,  $d$  and  $s$ . We have to remember that, each time we integrate out of the theory a degree of freedom, the renormalization group equations change. In addition we have to impose some matching conditions.

Until now we haven't spoken explicitly of the strong interactions between the quarks, but, of course, they have to be included into our analysis. At short distances this effects can be studied in a perturbative way, due to the asymptotic freedom of QCD. Practically we will introduce the possibility of gluon exchanges and we will consider these effects as quantum corrections.

To understand the importance of strong interaction effects, we can consider the part of the hamiltonian of (2.8) corresponding to  $du \rightarrow us$  transitions. It is given by:

$$\mathcal{H}_{eff} = \frac{G_F}{\sqrt{2}} V_{us}^* V_{ud} (\bar{s}u)_{V-A} (\bar{u}d)_{V-A}, \quad (2.10)$$

where sums over repeated color indices are understood. If we turn on the strong interactions, we have to consider also Feynman diagrams like the one represented in figure 3, beside the one of Fig. 2 .

In this way we will find, instead of the expression of (2.10), the following one:

$$\mathcal{H}_{eff} = \frac{G_F}{\sqrt{2}} V_{us}^* V_{ud} (C_1 Q_1 + C_2 Q_2). \quad (2.11)$$

In the previous equation we have denoted with  $Q_1$  and  $Q_2$  the following four-quark operators:

$$\begin{aligned} Q_1 &= (\bar{s}_i u_j)_{V-A} (\bar{u}_j d_i)_{V-A} \\ Q_2 &= (\bar{s}_i u_i)_{V-A} (\bar{u}_j d_j)_{V-A}. \end{aligned} \quad (2.12)$$

We can see that, in addition to the original operator  $Q_2$ , a new operator  $Q_1$ , with the same flavor but different color structure arises. This is due to the fact that a gluon exchange between two color singlet weak current lines mixes the color indices.



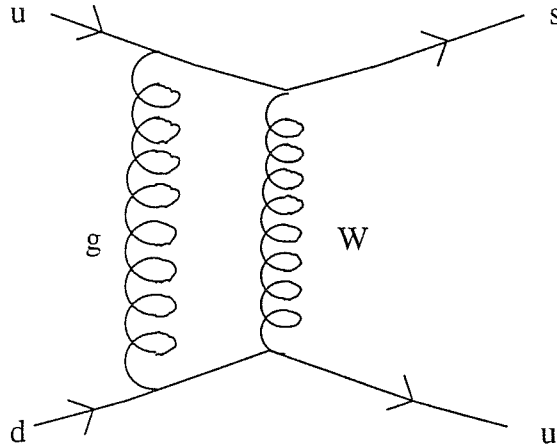


Figure 2.3: New class of Feynman diagrams contributing to the transition  $K \rightarrow \pi\pi$ . They appear when we switch on the strong interactions.

Another important effect of QCD interactions is the appearance of new operators, which have a structure different from that of the current-current operators  $Q_1$  and  $Q_2$ . These new operators are usually called gluonic penguins and they are generated by Feynman diagrams like the one of Fig. 4(A) .

They are usually denoted with the symbols  $Q_3 \dots Q_6$  and they are given by this set of equations:

$$\begin{aligned}
 Q_3 &= (\bar{s}_i d_i)_{V-A} \Sigma_q (\bar{q}_j q_j)_{V-A} \\
 Q_4 &= (\bar{s}_i d_j)_{V-A} \Sigma_q (\bar{q}_j q_i)_{V-A} \\
 Q_5 &= (\bar{s}_i d_i)_{V-A} \Sigma_q (\bar{q}_j q_j)_{V+A} \\
 Q_6 &= (\bar{s}_i d_j)_{V-A} \Sigma_q (\bar{q}_j q_i)_{V+A} .
 \end{aligned} \tag{2.13}$$

It is important to notice that here we can have, not only the usual structure of the product of two (V-A) currents, but also products of the kind (V-A)  $\times$  (V+A). The introduction of these new operators is fundamental, as was first understood by Shifman, Vainshtein and Zakharov [30]. This is due, essentially, to the fact that they contribute to the amplitude  $A_0$  (corresponding to decays with total final isospin  $I = 0$ ) while giving zero contribution to the  $A_2$  channel. Hence the presence of gluonic penguins (and especially of  $Q_6$ ) is very important in the explanation of the  $\Delta I = 1/2$  selection rule, as we will see in chapter 5.

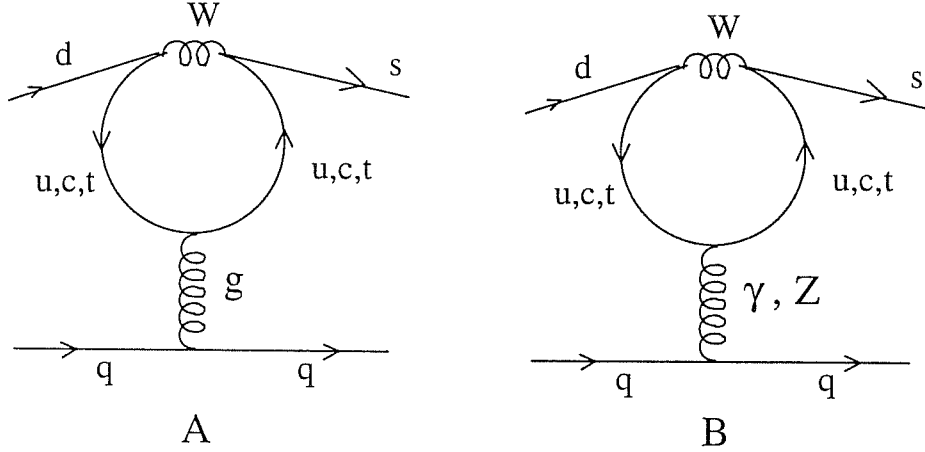


Figure 2.4: The Feynman diagrams originating penguin operators. Gluonic penguin graphs are represented in figure (A), while (B) gives the electroweak penguin operators. Note that in fig.(B) the gluon line has been substituted by a photon or a Z.

We still have to consider another kind of Feynman graphs, differing from the gluonic penguins only for the substitution of the gluonic line with a photon, as we can see in Fig. 4(B) .

Diagrams of this kind originate the so called electromagnetic penguins, which are defined as follows:

$$\begin{aligned}
 Q_7 &= \frac{3}{2}(\bar{s}_i d_i)_{V-A} \sum_q \hat{e}_q (\bar{q}_j q_j)_{V+A} \\
 Q_8 &= \frac{3}{2}(\bar{s}_i d_j)_{V-A} \sum_q \hat{e}_q (\bar{q}_j q_i)_{V+A} \\
 Q_9 &= \frac{3}{2}(\bar{s}_i d_i)_{V-A} \sum_q \hat{e}_q (\bar{q}_j q_j)_{V-A} \\
 Q_{10} &= \frac{3}{2}(\bar{s}_i d_j)_{V-A} \sum_q \hat{e}_q (\bar{q}_j q_i)_{V-A}, \tag{2.14}
 \end{aligned}$$

where  $\hat{e}_q$  are the quark charges ( $\hat{e}_d = \hat{e}_s = -1/3$  and  $\hat{e}_u = 2/3$ ).

We are not interested in reporting here the technical details of the derivation of the effective hamiltonian describing  $\Delta S = 1$  weak non leptonic interactions and we refer the interested reader to some beautiful works which can be find in literature, like the ones of ref. [31].

At last we are ready to write the complete expression for the effective hamiltonian at scales  $\mu < m_c$ :

$$\mathcal{H}_{eff}(\Delta S = 1) = \frac{G_F}{\sqrt{2}} V_{us}^* V_{ud} \sum_{i=1}^{10} C_i(\mu) Q_i(\mu). \tag{2.15}$$

In this expression  $Q_i$  are the ten four-quark operators that we have just introduced (current-current operators, gluonic and electromagnetic penguins) and  $C_i(\mu)$  are the so called Wilson coefficients associated to each operator.

In principle we should include in the effective hamiltonian two other possible operators  $Q_{11}$  and  $Q_{12}$ , which represent the dipole contributions of penguin operators.

As a matter of fact, these two operators would contribute only to the next order in chiral perturbation theory and turn out to be negligible, so we will not consider them in our analysis [32].

We would like to remark one of the beautiful aspects of the operator product expansion approach. It is clear from eq. (2.15) that the generic amplitude for the decay of the meson  $M$  into the final state  $F$  can be written in this way:

$$A(M \rightarrow F) = \langle F | \mathcal{H}_{eff} | M \rangle = \frac{G_F}{\sqrt{2}} V_{us}^* V_{ud} \sum_{i=1}^{10} C_i(\mu) \langle F | Q_i(\mu) | M \rangle. \quad (2.16)$$

Hence the scale  $\mu$ , that is the renormalization group scale at which the Wilson coefficients are evaluated, separates the physical contributions in two parts:

- the “short distance contributions” (corresponding to energies higher than  $\mu$ ) which are contained in the Wilson coefficients  $C_i(\mu)$ ;
- the “long distance contributions” (coming from scales lower than  $\mu$ ), contained in the matrix elements  $\langle F | Q_i(\mu) | M \rangle$ .

It is clear that this is only a formal separation and the choice of the scale  $\mu$  is arbitrary. Usually a scale around 1 GeV is chosen, as we will see better in the following chapters. This choice is motivated to find a compromise between two opposite requirements. We have to choose a scale that is not too low, otherwise the perturbative analysis of the Wilson coefficients would not be trustable anymore. At the same time, the matching scale cannot be too high, because we have to remain in the region of validity of the technique (chiral perturbation theory in our case) that we want to use to evaluate the long distance contributions.

Another obvious remark is that the physical result has, of course, to be scale independent. Hence the  $\mu$  dependence of the Wilson coefficients should, in principle, be compensated by the analogous dependence of the matrix elements. The scale dependence cancellation is an important problem for each model wanting to give a consistent description of  $\Delta S = 1$  weak non leptonic interactions. We will treat this subject in the case of the model that we are going to develop.

Let us now begin our analysis, starting from the problem of the determination of the Wilson coefficients.

### 2.1.4 The Wilson Coefficients

As we have already said, one of the good feature of the calculation of “short distance contributions” is that it can be performed in a perturbative way.

Anyway it is important to underline that ordinary perturbation theory is not sufficient by itself to compute the Wilson coefficients. In fact the expressions of these coefficients contain big logarithms (like  $\ln \frac{M_W^2}{\mu^2}$ ) multiplying  $\alpha_s(\mu)$  and, even if  $\alpha_s(\mu)$  could be a good perturbative expansion parameter down to scales of  $O(1 \text{ GeV})$ , it is no longer true for the product  $\alpha_s(\mu) \ln \frac{M_W^2}{\mu^2}$ .

This problem may be solved by using the methods of renormalization group. In fact the solutions of renormalization group equations in the so called leading logarithmic approximation sum up the terms  $\left(\frac{\alpha_s(\mu)}{4\pi} \ln \frac{M_W}{\mu}\right)^n$  to all orders in  $n$ .

If we consider the term  $\left(\alpha_s(\mu) \ln \frac{M_W}{\mu}\right)$  as a term of  $O(1)$  for values  $\mu \ll M_W$ , we can be interested also to  $O(\alpha_s)$  perturbative corrections, like the terms  $\alpha_s \left(\alpha_s(\mu) \ln \frac{M_W}{\mu}\right)^n$ .

The approximation consisting in taking not only the contributions of the type  $\left(\frac{\alpha_s(\mu)}{4\pi} \ln \frac{M_W}{\mu}\right)^n$  but also terms like  $\frac{\alpha_s(\mu)}{4\pi} \left(\frac{\alpha_s(\mu)}{4\pi} \ln \frac{M_W}{\mu}\right)^n$ , is called the next to leading logarithmic approximation.

To compute the Wilson coefficients at a given scale  $\mu$ , we have to solve the following renormalization group equation:

$$\frac{d}{d \ln \mu} \vec{C}(\mu) = \hat{\gamma}^T(g(\mu)) \vec{C}(\mu). \quad (2.17)$$

The solution of this equation can be written in the form :

$$\vec{C}(\mu) = \hat{U}(\mu, M_W) \vec{C}(M_W). \quad (2.18)$$

In the previous equations the component of the column vector  $\vec{C}$  are the ten Wilson coefficients  $C_i$  and  $\vec{C}(M_W)$  represents the initial conditions evaluated at the scale  $\mu = M_W$ . These initial conditions are determined by comparing the amputated Green functions in the full theory with the corresponding amplitudes obtained in the effective theory.

The evolution matrix  $\hat{U}$  can be obtained by solving the equation:

$$\hat{U}(\mu, M_W) = T_g \exp \left[ \int_{g(M_W)}^{g(\mu)} \frac{\hat{\gamma}^T(g')}{\beta(g')} dg' \right]. \quad (2.19)$$

In the previous formulas  $g$  denotes the QCD effective coupling constant ( $g^2 \equiv 4\pi\alpha_s$ ).  $\hat{\gamma}$  is the anomalous dimension matrix of the operators involved and the  $\beta$  function is

defined, as usual, by:

$$\beta(g(\mu)) = \frac{d}{d \ln \mu} g(\mu). \quad (2.20)$$

We have also introduced the symbol  $T_g$  denoting the so called g-ordered product, which is defined by :

$$T_g f(g_1) \dots f(g_n) = \sum_{perm} \Theta(g_{i_1} - g_{i_2}) \dots \Theta(g_{i_{n-1}} - g_{i_n}) f(g_{i_1}) \dots f(g_{i_n}). \quad (2.21)$$

In the previous expression the different factors  $f(g_i)$  are ordered in such a way that the corresponding coupling constants increase from right to left.

So, expanding explicitly the series of (2.19), we would obtain the following expression:

$$\hat{U}(\mu, M_W) = 1 + \int_{g(M_W)}^{g(\mu)} dg_1 \frac{\hat{\gamma}^T(g_1)}{\beta(g_1)} + \int_{g(M_W)}^{g(\mu)} dg_1 \int_{g(M_W)}^{g_1} dg_2 \frac{\hat{\gamma}^T(g_1)}{\beta(g_1)} \frac{\hat{\gamma}^T(g_2)}{\beta(g_2)} + \dots \quad (2.22)$$

An essential ingredient we still have to include into our analysis is the presence of threshold effects. As we have already explained, these effects are due to the fact that in the running of the renormalization group, when we reach a scale corresponding to the mass of a particle and we integrate out the degrees of freedom of this particle, we find ourselves in a new effective theory. Hence, also the form of the evolution matrix changes.

We have to require that the computation of the full physical amplitude in the old theory with  $f$  active flavors and in the new “(f-1)-flavor” theory gives the same result. So we have to impose the equation

$$\langle \vec{Q}_f(m) \rangle^T \vec{C}_f(m) = \langle \vec{Q}_{f-1}(m) \rangle^T \vec{C}_{f-1}(m) \quad (2.23)$$

It is possible to reexpress the Wilson coefficients of the new effective theory as functions of the previous ones in the following way

$$\vec{C}_{f-1}(m) = \hat{M}(m) \vec{C}_f(m). \quad (2.24)$$

The matching matrix  $\hat{M}$  has a non trivial form only at next to leading order, while at leading order  $\hat{M} = 1$ . To take into account these threshold effects, we have to substitute the simple equation (2.18) with the following one:

$$\vec{C}(\mu) = \hat{U}^{f=3}(\mu, \mu_c) \hat{M}(\mu_c) \hat{U}^{f=4}(\mu_c, \mu_b) \hat{M}(\mu_b) \hat{U}^{f=5}(\mu_b, \mu_W) \vec{C}(\mu_W). \quad (2.25)$$

The meaning of this formula is clear. We define the initial conditions at a scale  $\mu_W$  (near to  $M_W$ ) and start evolving the coefficients in an effective theory with five active

flavors ( $f=5$ ), until we reach the scale  $\mu_b \simeq m_b$ . Then we integrate out the degree of freedom of the bottom quark and we find ourselves in a theory with  $f=4$ , for values of  $\mu$  such that  $\mu_c < \mu < \mu_b$ . The scale  $\mu_c$  is the value of the energy at which we integrate out the charm quark and we remain with a three quark effective theory. Finally  $\mu$  is the scale at which the Wilson coefficients are evaluated, with  $\mu < \mu_c$ .

In addition we also have to require the continuity of QCD running coupling constant across the different thresholds, by imposing:

$$\alpha_{s,f=4}(\mu_b, \Lambda_{\text{QCD}}^{(4)}) = \alpha_{s,f=5}(\mu_b, \Lambda_{\text{QCD}}^{(5)}) \quad (2.26)$$

$$\alpha_{s,f=3}(\mu_c, \Lambda_{\text{QCD}}^{(3)}) = \alpha_{s,f=4}(\mu_c, \Lambda_{\text{QCD}}^{(4)}). \quad (2.27)$$

Coming back to the general expression for the evolution matrix, we can write:

$$\hat{U}(m_1, m_2, \alpha) = \hat{U}(m_1, m_2) + \frac{\alpha}{4\pi} \hat{R}(m_1, m_2), \quad (2.28)$$

where  $\hat{U}(m_1, m_2)$  describes pure QCD evolution and  $\hat{R}(m_1, m_2)$  the additional evolution in the presence of electromagnetic interactions.

For the pure QCD evolution we have the following equation

$$\hat{U}(m_1, m_2) = \left(1 + \frac{\alpha_s(m_1)}{4\pi} \hat{J}\right) \hat{U}^{(0)}(m_1, m_2) \left(1 - \frac{\alpha_s(m_2)}{4\pi} \hat{J}\right). \quad (2.29)$$

In (2.29)  $\hat{U}^{(0)}(m_1, m_2)$  denotes the evolution matrix evaluated in the leading logarithmic approximation, while  $\hat{J}$  summarizes the next to leading corrections to this evolution. The leading logarithmic result is given by

$$\hat{U}^{(0)}(m_1, m_2) = \hat{V} \left[ \left( \frac{\alpha_s(m_2)}{\alpha_s(m_1)} \right)^{\frac{\gamma_s^{(0)}}{2\beta_0}} \right] \hat{V}^{-1}, \quad (2.30)$$

where  $\hat{V}$  is the matrix diagonalizing the anomalous dimension matrix  $\hat{\gamma}$ .

Applying the formalism we have just discussed for the Wilson coefficients, it is possible to reexpress the formula (2.15) for  $\Delta S = 1$  transitions in the following way:

$$\mathcal{H}_{eff}(\Delta S = 1) = \frac{G_F}{\sqrt{2}} V_{ud} V_{us}^* \sum_{i=1}^{10} [z_i(\mu) + \tau y_i(\mu)] Q_i(\mu), \quad (2.31)$$

where  $V_{ij}$  are the Kobayashi-Maskawa (KM) matrix elements,  $\tau = -V_{td} V_{ts}^* / V_{ud} V_{us}^*$  and  $y_i(\mu) = v_i(\mu) - z_i(\mu)$ .

The coefficients  $z_i(\mu)$  and  $v_i(\mu)$  are given by

$$\vec{z}(\mu) = \hat{U}_3(\mu, m_c, \alpha) \vec{z}(m_c) \quad (2.32)$$

$$\vec{v}(\mu) = \hat{U}_3(\mu, m_c, \alpha) \hat{M}(m_c) \hat{U}_4(m_c, m_b, \alpha) \hat{M}(m_b) \hat{U}_5(m_b, M_W, \alpha) \vec{C}(M_W) \quad (2.33)$$

where the full evolution matrices  $\hat{U}_f(m_1, m_2, \alpha)$  are obtained from (2.28) and  $\hat{M}(m_i)$  is the matching matrix at the threshold  $m_i$ .

The explicit numerical values of  $z_i(\mu)$  and  $y_i(\mu)$  at two different scales ( $\mu = 0.8$  GeV and  $\mu = 1$  GeV) will be given in the following chapters, when we analyze two typical  $\Delta S = 1$  processes, that is the  $\Delta I = 1/2$  selection rule and  $\frac{\epsilon'}{\epsilon}$ .

### 2.1.5 Hadronic Matrix Elements

As we have seen, an essential ingredient of non leptonic kaon decay analysis is the calculation of the hadronic matrix elements of the operators  $Q_i$  appearing in the effective hamiltonian of (2.31), like for instance  $\langle \pi\pi | Q_i | K \rangle$ .

It is possible to find in literature a lot of attempts of calculating these matrix elements with different techniques. We can remember, among the others, the lattice computations [17], the  $1/N_c$  approach [18, 19], QCD and hadronic sum rules [21], effective QCD action (see ref. [20] and the last paper of ref. [27]), chiral perturbation theory [22] and vacuum insertion.

We will also see in this dissertation how to build a phenomenological model, based on chiral perturbation theory and chiral quark model, to evaluate the hadronic matrix elements.

Coming back to the other techniques we have mentioned, it can be noticed that only in the  $1/N_c$  expansion and in the vacuum insertion approach all the matrix elements have been calculated. The  $1/N_c$  approach also offers a quite good description of the CP conserving part of  $K \rightarrow \pi\pi$  amplitudes and it can give at least a qualitative understanding of the  $\Delta I = 1/2$  selection rule, even if it is not sufficient to obtain a complete quantitative explanation of this famous rule (as we will see in chapter 5). On the contrary, the vacuum saturation approximation misses completely the explanation of the  $\Delta I = 1/2$  rule.

In the  $1/N_c$  approach, the scale dependence of the hadronic matrix elements, which in principle should cancel the analogous dependence present in the Wilson coefficients, is given by mesonic loop effects [18]. For what concerns the renormalization scheme dependence, both the vacuum insertion and the  $1/N_c$  calculations seem to be insensitive

to the choice of the scheme. So in these two approaches there is no possibility of a scheme dependence cancellation in the matching with the Wilson coefficients.

In all the other methods we have mentioned only a subset of hadronic matrix elements have been calculated. Anyway we can remember, among the others, the effective QCD action approach (see ref. [20] and the last paper of ref. [27]) and the lattice approach [17]. An important qualitative feature of the lattice is that in this approach the scheme and scale dependences can in principle be calculated [33].

Generally speaking, we can say that all the different techniques considered can give important information on the non leptonic kaon decays, but none of them is sufficient by itself to give a complete and consistent description of this very complex phenomena.



## Chapter 3

# Chiral Perturbation Theory and Chiral Quark Model

### 3.1 Basics of Chiral Perturbation Theory

Chiral Perturbation Theory is an effective field theory which enables us to describe the hadronic interactions at low energies.

We use effective field theory when we are not able to give the exact laws ruling the evolution of a system, but we can describe it in an approximate way by restricting ourselves to consider only the degrees of freedom corresponding to energies lower than a fixed energy scale. The heavier degrees of freedom are integrated out of the theory and the informations about them are encoded in the couplings of the new effective low energy lagrangian.

We have seen in the previous chapter an example of application of this powerful theoretical tool, when we have shown how to construct an effective hamiltonian for  $\Delta S = 1$  weak non leptonic interactions, starting from a Standard Model description and integrating out of the theory the W boson and the heavy quarks.

Generally speaking, we can say there are two different typical situations in which effective field theories are usually applied. First of all we can have the case in which the complete underlying theory is unknown, but we are able to build an effective lagrangian by using the symmetry properties of the low energy states. This is the case, for instance, of the Standard Model itself, which can be seen as the effective theory at the electroweak scale of a more fundamental underlying unified theory.

There is also a second possible situation, in which we know the underlying theory,

but, for some reason, we cannot apply it in the low energy domain. This is the case, for instance, of the low energy hadronic interactions. In fact we know the complete theory, which is QCD, but we do not know how to solve the problem of confinement. So we have to face the following problem: QCD lagrangian is written in terms of quark and gluon fields, but these do not coincide with the asymptotic states of the theory, which are the hadron fields.

The basic idea of chiral perturbation theory is that of building an effective field theory for QCD starting from the symmetry properties that the theory itself should have and parametrizing the unknown dynamics in a few couplings.

In fact we know that, if we neglect an explicit mass term for the quarks, QCD is symmetric under transformations of the group  $SU(3)_L \times SU(3)_R$ . We can write the lagrangian in the following way

$$\mathcal{L}_{QCD}^0 = -\frac{1}{4} \sum_{a=1}^8 G_{\mu\nu}^{(a)} G^{(a)\mu\nu} + i\bar{q}_L \gamma^\mu D_\mu q_L + i\bar{q}_R \gamma^\mu D_\mu q_R, \quad (3.1)$$

where the column vector  $q$  denotes the generic quark field

$$q^T = (u, d, \dots). \quad (3.2)$$

In the previous formula the covariant derivative  $D_\mu$  is defined as

$$D_\mu = \partial_\mu + iG_\mu, \quad (3.3)$$

where  $G_\mu$  indicates the gluon field, which in the fundamental  $SU(3)_{colour}$  representation is given by

$$G_\mu \equiv g_s \sum_{a=1}^8 \frac{\lambda^{(a)}}{2} G_\mu^{(a)}(x) \quad (3.4)$$

$$\alpha_s = \frac{g_s^2}{4\pi}. \quad (3.5)$$

The gluon field strength tensor  $G_{\mu\nu}^{(a)}$  is given by

$$G_{\mu\nu}^{(a)} = \partial_\mu G_\nu^{(a)} - \partial_\nu G_\mu^{(a)} - g_s f_{abc} G_\mu^{(b)} G_\nu^{(c)}. \quad (3.6)$$

The lagrangian of (3.1) would have an  $U(N_f)_L \times U(N_f)_R$  symmetry, with  $N_f$  denoting the number of quark flavors, but we know that the  $U(1)_A$  part of the symmetry is broken by quantum effects (this is the well known  $U(1)$  axial anomaly). Moreover we can restrict ourselves to the case of only three light flavors (u,d,s), for which the chiral

symmetry is approximately good. In this case we are left with a global  $SU(3)_L \times SU(3)_R$  symmetry.

On the other hand, if we look at the low energy spectrum of the theory, we do not find particles which can be arranged in an axial octet, while we can classify hadrons in  $SU(3)$  vector multiplets of given spin and parity and degenerate in mass. This is an indication of a breaking of the original symmetry of the theory.

Chiral perturbation theory represents the result of the spontaneous symmetry breaking of the original  $SU(3)_L \times SU(3)_R$  down to a final  $SU(3)_V$  invariance. Goldstone theorem [34] tells us that, if we break spontaneously the symmetry with respect to  $n$  generators of the original symmetry group, an  $n$ -plet of massless particles, called Goldstone bosons, will appear in the new theory. In the case we are studying there is a mass gap in the spectrum of the theory, because the octet of pseudoscalar mesons (pions, kaons and eta) is much lighter than the other particles. So it is natural to consider the particles belonging to this pseudoscalar octet as the so called “Nambu - Goldstone bosons”, which are originated from the spontaneous symmetry breaking of the original theory.

As a matter of fact, these mesons have masses which are very small, but, in any case, different from zero. In fact we can think that their mass is due to the presence in the original lagrangian of a mass term, written in terms of the light quark fields, which breaks explicitly  $SU(3)_L \times SU(3)_R$  chiral symmetry. We will see in the following that we can link directly the mass of pions and of the other mesons of the octet to that of the light quarks (u,d,s).

It is also important to remember that the natural-order parameter of spontaneous chiral symmetry breaking in this case is given by the so called quark condensate, that is the following vacuum expectation value:  $\langle 0 | \bar{q}q | 0 \rangle \neq 0$ .

### 3.1.1 The Strong Chiral Lagrangian at $O(p^2)$

Let us start showing how to construct the strong chiral lagrangian.

Since there is a mass gap separating the pseudoscalar octet of mesons from the rest of the hadronic spectrum, we can write a lagrangian containing only these fields. We can write them in a compact way by using a  $3 \times 3$  matrix  $\Pi$ , which is a linear combination of the Gell-Mann matrices  $\lambda^a$  generators of  $SU(3)$  :

$$\Pi(x) = \sum_{a=1..8} \lambda_a \phi^a(x)/2. \quad (3.7)$$

The most economic way of writing the chiral lagrangian is that of using an exponential notation, introducing a matrix  $\Sigma$  defined in this way

$$\Sigma(\phi) \equiv \exp\left(\frac{2i}{f} \Pi(x)\right). \quad (3.8)$$

The  $\Sigma$  matrix transforms in this way

$$\Sigma(\phi) \rightarrow g_R \Sigma(\phi) g_L^\dagger, \quad (3.9)$$

where  $g_R$  and  $g_L$  are two global transformations belonging respectively to  $SU(3)_R$  and  $SU(3)_L$ .

We can write the most general lagrangian containing the matrix  $\Sigma(\phi)$  which is compatible with the chiral symmetry property requirements.

Effective field theories contain an infinite number of terms. Hence, strictly speaking, they are not renormalizable, but we can ask for an order-by-order renormalizability, because at each order the low energy theory is specified by a finite number of couplings.

A general feature of chiral perturbation theory is that we can organize the lagrangian as an expansion in powers of momenta of the meson fields or equivalently in terms of an increasing number of derivatives. We want to require parity conservation, so we have to consider only the terms containing an even number of derivatives and, due to the unitarity of  $\Sigma$  matrix, at least two derivatives are needed for a non trivial interaction. Since we are considering a low energy theory, it is also clear that the dominating terms will be the ones containing the lower number of derivatives. So let us start considering the  $O(p^2)$  expansion of the strong chiral lagrangian.

To be as general as possible, let us consider the case in which we add to the simple QCD lagrangian for three massless quarks some terms describing the interaction with any eventual external field. Hence we substitute the lagrangian of (3.1) with the following one

$$\mathcal{L}_{QCD} = \mathcal{L}_{QCD}^0 + \bar{q} \gamma^\mu (v_\mu + \gamma_5 a_\mu) q - \bar{q} (s - i\gamma_5 p) q, \quad (3.10)$$

where  $v_\mu, a_\mu, s$  and  $p$  represent generic vector, axial, scalar and pseudoscalar fields.

In this way we can, for instance, include in our discussion the effect of explicit

breaking of chiral symmetry, by taking

$$s = \mathcal{M} \equiv \begin{pmatrix} m_u & 0 & 0 \\ 0 & m_d & 0 \\ 0 & 0 & m_s \end{pmatrix} \quad (3.11)$$

$$p = 0 .$$

To build an effective lagrangian describing the Goldstone bosons in presence of external fields, we have to introduce the following covariant derivative

$$D_\mu \Sigma = \partial_\mu \Sigma - i r_\mu \Sigma + i \Sigma l_\mu , \quad (3.12)$$

with  $r_\mu \equiv v_\mu + a_\mu$  and  $l_\mu \equiv v_\mu - a_\mu$ .

Of course we also have to impose the transformation properties for the external fields, like the following one

$$(s + ip) \rightarrow g_R (s + ip) g_L^\dagger . \quad (3.13)$$

It can be proved that at  $O(p^2)$  the more general effective lagrangian consistent with Lorentz invariance and with our symmetry requirements has the following form [23]

$$\mathcal{L}_2 = \frac{f^2}{4} \text{Tr} \left[ D_\mu \Sigma^\dagger D^\mu \Sigma + \Sigma^\dagger \chi + \chi^\dagger \Sigma \right] , \quad (3.14)$$

where

$$\chi = 2B_0(s + ip) . \quad (3.15)$$

As usual in chiral perturbation theory, the two constants  $B_0$  and  $f$  are not fixed by symmetry requirements alone. Anyway, at this order of the chiral expansion, they can be connected respectively to the quark condensate and the pion decay constant, which is defined by

$$\langle 0 | \bar{u} \gamma^\mu \gamma_5 d | \pi^+(p) \rangle \equiv i\sqrt{2} f_\pi p^\mu . \quad (3.16)$$

We have

$$f = f_\pi \quad (3.17)$$

$$\langle 0 | \bar{q}^j q^i | 0 \rangle = -f^2 B_0 \delta^{ij} . \quad (3.18)$$

If we fix the external fields, for instance like in eq.(3.11), we can break explicitly the chiral symmetry, exactly in the same way as the fundamental lagrangian of (3.10) does.

Taking  $s = \mathcal{M}$  and  $p = 0$ , we obtain from (3.14) a quadratic pseudoscalar mass term plus additional interaction terms, all proportional to the quark masses.

In this way we can recover the following relations for the masses of the pseudoscalar mesons

$$\begin{aligned}
m_{\pi^\pm}^2 &= 2\bar{m}B_0, \\
m_{\pi^0}^2 &= 2\bar{m}B_0 + O(\epsilon), \\
m_{K^\pm}^2 &= (m_u + m_s)B_0, \\
m_{K^0}^2 &= (m_d + m_s)B_0, \\
m_\eta^2 &= \frac{2}{3}(\bar{m} + 2m_s)B_0 + O(\epsilon),
\end{aligned} \tag{3.19}$$

where

$$\begin{aligned}
\bar{m} &= \frac{m_u + m_d}{2}, \\
\epsilon &\propto B_0 \frac{(m_u - m_d)^2}{m_s - \bar{m}}.
\end{aligned} \tag{3.20}$$

If we neglect terms of  $O(m_u - m_d)$ , we can also verify the famous Gell-Mann-Okubo formula, linking the masses of the different pseudoscalar mesons

$$3m_\eta^2 = 4m_K^2 - m_\pi^2. \tag{3.21}$$

Using the relations (3.19) and the experimental values of the meson masses, we can find useful information about the ratios of masses of the three light quarks (u,d,s). The quark  $s$  results about 20 times heavier than the  $d$ , and the ratio  $m_u/m_d$  is about 1/2. Anyway, the isospin symmetry is a good symmetry (even if  $(m_d - m_u)$  is not small with respect to the single quark masses) and this is due to the fact that the  $SU(2)$  breaking effects are proportional to the following ratio

$$\frac{(m_d - m_u)}{m_s}$$

We can also see from (3.19) that the quark masses are linearly proportional to the square of the meson masses, so they are counted as  $O(p^2)$  in the chiral expansion.

Finally, by using the eqs. (3.19) and (3.18), we can obtain useful relations between the meson and quark masses and the quark condensate

$$\begin{aligned}
f_\pi^2 m_\pi^2 &= -\bar{m} \langle 0 | \bar{u}u + \bar{d}d | 0 \rangle, \\
f_K^2 m_K^2 &= -(m_s + m_d) \langle 0 | \bar{s}s | 0 \rangle,
\end{aligned} \tag{3.22}$$

where  $f_K$  is the kaon decay constant.

### 3.1.2 $O(p^4)$ Corrections to the Chiral Lagrangian

Going to the next order of chiral expansion, we have the following expression for the most general  $O(p^4)$  strong chiral lagrangian, which was recovered for the first time by Gasser and Leutwyler [23]:

$$\begin{aligned}
\mathcal{L}_4 = & L_1 \left[ \text{Tr} \left( D_\mu \Sigma^\dagger D^\mu \Sigma \right) \right]^2 + L_2 \text{Tr} \left( D_\mu \Sigma^\dagger D_\nu \Sigma \right) \text{Tr} \left( D^\mu \Sigma^\dagger D^\nu \Sigma \right) \\
& + L_3 \text{Tr} \left( D_\mu \Sigma^\dagger D^\mu \Sigma D_\nu \Sigma^\dagger D^\nu \Sigma \right) + L_4 \text{Tr} \left( D_\mu \Sigma^\dagger D^\mu \Sigma \right) \text{Tr} \left( \Sigma^\dagger \chi + \chi^\dagger \Sigma \right) \\
& + L_5 \text{Tr} \left[ D_\mu \Sigma^\dagger D^\mu \Sigma \left( \Sigma^\dagger \chi + \chi^\dagger \Sigma \right) \right] + L_6 \left[ \text{Tr} \left( \Sigma^\dagger \chi + \chi^\dagger \Sigma \right) \right]^2 \\
& + L_7 \left[ \text{Tr} \left( \Sigma^\dagger \chi - \chi^\dagger \Sigma \right) \right]^2 + L_8 \text{Tr} \left( \chi^\dagger \Sigma \chi^\dagger \Sigma + \Sigma^\dagger \chi \Sigma^\dagger \chi \right) \\
& - i L_9 \text{Tr} \left( F_R^{\mu\nu} D_\mu \Sigma D_\nu \Sigma^\dagger + F_L^{\mu\nu} D_\mu \Sigma^\dagger D_\nu \Sigma \right) + L_{10} \text{Tr} \left( \Sigma^\dagger F_R^{\mu\nu} \Sigma F_{L\mu\nu} \right) \\
& + H_1 \text{Tr} \left( F_{R\mu\nu} F_R^{\mu\nu} + F_{L\mu\nu} F_L^{\mu\nu} \right) + H_2 \text{Tr} \left( \chi^\dagger \chi \right) , \tag{3.23}
\end{aligned}$$

where

$$F_L^{\mu\nu} = \partial^\mu l^\nu - \partial^\nu l^\mu - i [l^\mu, l^\nu] , \tag{3.24}$$

and

$$F_R^{\mu\nu} = \partial^\mu r^\nu - \partial^\nu r^\mu - i [r^\mu, r^\nu] . \tag{3.25}$$

The last two terms of (3.23) account for the so called Wess-Zumino-Witten chiral anomaly; they do not contain the meson fields, so they are not directly measurable.

The ten  $L_i$  coefficients appearing in the expression of the chiral lagrangian parametrize our ignorance of the underlying QCD dynamics. As usual we cannot fix them only by using symmetry requirements, but it is possible to give a phenomenological determination of these coefficients considering the appropriate low energy experimental results [23, 35], as we will see later.

There is also another kind of  $O(p^4)$  chiral corrections we have to add to the ones coming from the lagrangian  $\mathcal{L}_4$ , that is the one-loop graph contributions obtained starting from the  $O(p^2)$  lagrangian  $\mathcal{L}_2$ . In this kind of diagrams we consider the propagation inside the loop of the mesons of the pseudoscalar octet. Each chiral loop adds two powers of momenta and this is the reason for which a one loop graph in which the vertices are recovered from the  $O(p^2)$  chiral lagrangian gives an  $O(p^4)$  contribution.

These meson loop corrections are divergent and we have to regularize them in a such a way to preserve the symmetry properties of the theory. We have already said that

chiral perturbation theory is renormalizable order-by-order, because at each order of the expansion in powers of momenta we only need a finite number of counterterms. All the  $O(p^4)$  counterterms needed to cancel the divergencies coming from meson loops must have the form of one of the terms of the  $\mathcal{L}_4$  lagrangian, because it contains all the possible  $O(p^4)$  contributions consistent with the symmetry properties of the theory. Hence, the effect of the introduction of chiral loops is that of renormalizing the  $L_i$  coefficients of the  $O(p^4)$  strong chiral lagrangian of (3.23). The scale dependence contained in the renormalized couplings  $L_i^R(\mu)$  cancels exactly the analogous dependence coming from the loops, so that the total physical results are scale independent.

It is important to stress here that we will take a different attitude in dealing with the renormalization prescriptions of the weak chiral lagrangian. In fact we will regularize the loop integrals by using dimensional regularization with modified minimal subtraction. Moreover, as we will see in the next chapter, the coefficients of our  $\Delta S = 1$  weak chiral lagrangian contain the explicit  $\mu$ -dependence originated from the short distance calculation of the Wilson coefficients. Our ansatz is that this scale dependence cancels the long distance  $\mu$ -dependence of the chiral loops. As a consequence we will assume that the  $O(p^4)$  tree level coefficients of the weak chiral lagrangian are scale independent.

The determination of the  $O(p^4)$  strong chiral lagrangian coefficients  $L_i$  is made easier by the fact that usually only some of them enter in the calculation of the observables relative to a specific physical process. For instance, in the case of processes (like  $\pi\pi$  and  $\pi K$  elastic scatterings) in which no external fields are involved, only the first three terms of the lagrangian of (3.23) survive and so only  $L_1$ ,  $L_2$  and  $L_3$  give contributions. The coefficients  $L_4$  and  $L_5$ , instead, introduce important mass corrections to the meson decay constants and induce mass dependent wave function renormalizations.

Hence the various  $L_i$  coefficients can be determined phenomenologically by considering a set of suitable processes and then their values can be used to study other processes. This has been done and the level of agreement with the experimental results can be considered one of the main results of chiral perturbation theory [23, 35].

The fact that we can determine the  $L_i$  coefficients at a good level of accuracy gives us an useful test to check the degree of reliability of each phenomenological model which tries to describe hadronic interactions at low energies (like we will see in the case of the chiral quark model). In fact each model mimicking low energy QCD shall be able to reproduce, up to an acceptable error, the values of the  $L_i$  determined from the experimental results.

Let us make some final remarks on the determination of the chiral coefficient  $f$ . We



have previously said that at lowest order of chiral perturbation theory we can identify it with the pion decay constant  $f_\pi$ , as it is usually done in literature. As a matter of fact, if we consider processes involving not only pions (like for instance  $K \rightarrow \pi\pi$  transitions or  $K^0 - \bar{K}^0$  mixing), it is clear that also another parameter  $f_K$  naturally enters into the game. The various meson decay constants ( $f_\pi$ ,  $f_K$  and  $f_\eta$ ) should be equal in the limit of  $SU(3)$  invariance, but, due to  $SU(3)$  breaking effects, their numerical values do not coincide, as we know from the experiments. So, if we stay at  $O(p^2)$  in the chiral expansion, we cannot determine in a unique way the coefficient  $f$ . If we go to  $O(p^4)$  in the meson decay constants calculation, the situation improves and we should be able to obtain the value of  $f$  starting from the experimental value of the meson decay constants and using the following formulas [101]

$$\begin{aligned} f_\pi &= f \left( 1 - 2\mu_\pi - \mu_K + \frac{4m_\pi^2}{f^2} L_5^R(\mu) + \frac{8m_K^2 + 4m_\pi^2}{f^2} L_4^R(\mu) \right), \\ f_K &= f \left( 1 - \frac{3}{4}\mu_\pi - \frac{3}{2}\mu_K - \frac{3}{4}\mu_\eta + 4\frac{m_K^2}{f^2} L_5^R(\mu) + \frac{8m_K^2 + 4m_\pi^2}{f^2} L_4^R(\mu) \right), \\ f_\eta &= f \left( 1 - 3\mu_K + \frac{4m_\eta^2}{f^2} L_5^R(\mu) + \frac{8m_K^2 + 4m_\pi^2}{f^2} L_4^R(\mu) \right), \end{aligned} \quad (3.26)$$

where we have denoted with  $\mu_P$  the following expression

$$\mu_P \equiv \frac{m_P^2}{32\pi^2 f^2} \log \left( \frac{m_P^2}{\mu^2} \right). \quad (3.27)$$

We can also see that we can fix  $L_5$  from the experimental value of  $f_K/f_\pi$ .

## 3.2 The Chiral Quark Model

In the previous section we have introduced chiral perturbation theory and we have seen that this theory enables us to describe the hadronic interactions at low energies, where simple perturbative QCD cannot anymore be applied. As we have said, chiral perturbation theory is a powerful theoretical tool and it showed a very satisfactory agreement with the experiment. On the other hand we have already seen, considering the  $O(p^4)$  lagrangian, that when we go to higher orders in the chiral expansion the number of unknown coefficients increases very much and their determination becomes a quite hard task.

We would like to be able to find a theory valid at low and intermediate regions, which creates a sort of link between the domains of validity of chiral perturbation theory and perturbative QCD and which, at the same time, permits us to obtain the

different coefficients of the chiral lagrangian directly from QCD properties. The symmetry requirements on which chiral perturbation theory is based are not sufficient by themselves to reach this aim; hence we have to make some additional assumptions.

Essentially we want to consider a model having a mechanism of spontaneous symmetry breaking which mimics the chiral symmetry breaking that shall be present in QCD.

In the literature there are different models of this type and we can divide them in two big categories, those including resonances higher than the pseudoscalar ones and remaining at the hadronic level, and those containing some kind of quarks. The models of these second class usually have the advantage of needing a lower number of parameters, but most of them do not include confinement.

We will focus our attention on the models in which the lagrangian contains meson and constituent quark fields together. In particular we will consider the so called “quark-loop models”, in which the interactions of mesons proceed only via quark loops. A particular example is given by the chiral quark model, that has the advantage of incorporating chiral symmetry in the correct way.

Before going on with its description, I would like to stress that the chiral quark model, like the other models about which we were discussing, is just a phenomenological model and not an exact theory. So it can try to mimic QCD, but it is not QCD itself and we can not even think to use it to solve QCD exactly. Nevertheless, we can hope it is able to reproduce the essential part of QCD behavior, in such a way to give us a consistent description of hadronic interactions at low and medium energies.

As already said, it is possible to find different works about the chiral quark model or, at least, containing some of its founding ideas [25, 26, 27]. We will consider essentially the version proposed by Georgi-Manohar and by Espriu-De Rafael-Taron in two of the papers of ref. [27]. In particular we will follow the idea, present in the work of Espriu-De Rafael-Taron, that the kinetic terms of mesons are not present in the initial lagrangian and they are generated by integration over the quark loops.

We will show later that the chiral quark model can be seen as a mean field approximation of a more general model, that is the extended Nambu-Jona-Lasinio (ENJL) model. The latter belongs to a class of models more general than the quark-loop ones, in which the original lagrangian contains only fermionic degrees of freedom and the hadronic fields are generated by the model itself. In the case of ENJL, four fermion interaction terms are added to the low energy QCD lagrangian and the model produces by itself a spontaneous breakdown of chiral symmetry. We will discuss later the ex-

tended Nambu-Jona-Lasinio model, but, for the time being, let us come back to the chiral quark model.

The main idea on which it is based is that of introducing in the low energy lagrangian a term that we will call  $\mathcal{L}_{\chi QM}$ , which couples the constituent light quarks to the Goldstone bosons in the following way:

$$\mathcal{L}_{\chi QM} = -M(\bar{q}_R \Sigma q_L + \bar{q}_L \Sigma^\dagger q_R), \quad (3.28)$$

where  $q$  and  $\Sigma$  are defined respectively by (3.2) and (3.8).

Under the action of the generators  $g_R$  and  $g_L$  of the chiral group  $SU(3)_R \times SU(3)_L$  the quark fields transform in the following way

$$\begin{aligned} q_L &\rightarrow g_L q_L, \\ q_R &\rightarrow g_R q_R, \end{aligned} \quad (3.29)$$

while the transformation properties of  $\Sigma$  are given by (3.9). So the term  $\mathcal{L}_{\chi QM}$  is invariant under the chiral transformations of  $SU(3)_L \times SU(3)_R$ , but for  $M \neq 0$  it introduces a mechanism of spontaneous symmetry breaking and the quark condensate acquires a non vanishing value.

We can also consider a ‘‘rotated picture’’, by defining the following rotated constituent quark fields  $Q_{L,R}$ :

$$\begin{aligned} Q_L &= \xi q_L \\ Q_R &= \xi^\dagger q_R, \end{aligned} \quad (3.30)$$

where

$$\begin{aligned} \xi \cdot \xi &= \Sigma, \\ (\xi^\dagger)^2 &= \Sigma^\dagger. \end{aligned} \quad (3.31)$$

In this way the term  $\mathcal{L}_{\chi QM}$  of eq. (3.28) is transformed into a pure mass term  $-M\bar{Q}Q$ .

Hence we could give a natural interpretation of the parameter  $M$ , characteristic of the chiral quark model, as a sort of constituent quark mass, which is generated in the spontaneous breaking of chiral symmetry. As a matter of fact, in our approach, in the study of  $\Delta S = 1$  physics, we will consider  $M$  as a free parameter and we will try to find the value of  $M$  which minimizes the regularization scheme dependence of our results. Then, in the case of  $\Delta S = 2$  processes, we will take for  $M$  the value obtained from the  $\Delta S = 1$  analysis.

For what concerns the gluons, the degrees of freedom corresponding to high energy gluons have already been integrated out of the theory, together with the heavy quarks, down to the scale  $\Lambda_\chi$  of spontaneous symmetry breaking. Anyway we still have to consider the effect of soft gluons. So we can think that quarks propagate in a background of soft gluons and the presence of such fields is treated in a non perturbative way within the model, as we will see in the next chapters. The fact that it can include non perturbative gluonic effects is one of the positive aspects of the chiral quark model. These effects will be very important for the correct determination of our final results, as we will see clearly, for instance, in the study of the  $\Delta I = 1/2$  selection rule and of  $\varepsilon'/\varepsilon$ .

Finally we would like to make some comments on the fact we have chosen this version of the chiral quark model and not more refined and complex versions, that can also be found in literature. Our choice is motivated by the fact that the chiral quark model, in the way in which we have taken it, has the advantage of being rather simple, but, at the same time, it contains already all the essential ingredients we need to give a consistent phenomenological description of hadronic interactions in an intermediate region of energies. In particular it reproduces quite well the values of the  $O(p^4)$  strong chiral lagrangian coefficients  $L_i$  and it is sensitive to the  $\gamma_5$  scheme dependence of dimensional regularization.

The domain of validity of chiral quark model is comprised between the two energy scales  $\Lambda_\chi$  and  $M$ . For the spontaneous symmetry breaking scale  $\Lambda_\chi$  we can take the value

$$\Lambda_\chi \equiv 2\pi \sqrt{\frac{6}{N_c}} f_\pi = 0.82 \text{ GeV} . \quad (3.32)$$

In the version of the chiral quark model we will use, the constituent quarks are the only dynamical degrees of freedom in the range between  $\Lambda_\chi$  and  $M$ , the Goldstone bosons do not propagate and they are considered external fields, like the soft gluons. We neglect heavier scalar, vector and axial meson multiplets. The fact that the degrees of freedom of the pseudoscalar mesons are frozen, allows us to deal with them in a separate step of the computation, as we will see in the next chapter. We will see also that the chiral quark model can be used to determine the coefficients of the  $\Delta S = 1$  and  $\Delta S = 2$  weak chiral lagrangians. So these lagrangians, obtained by integrating out of the theory the degrees of freedom of the constituent quarks, can be considered as the effective theory of the chiral quark model below the scale  $M$ .

In the strong sector, where the  $O(p^4)$  coefficients  $L_i$  are experimentally known, they can be used to compare the prediction of the model. These coefficients have

been computed in the last paper of ref. [27]. To the leading order in  $N_c$ ,  $L_i$  (except for  $L_5$  and  $L_8$ ) are purely geometrical factors that cannot be compared directly with experimental values, which have an explicit scale dependence. Only combinations of the same that have vanishing anomalous dimension can be compared. In this case the result is quite encouraging. See, for instance,  $L_3$ ,  $L_1 - L_2/2$  and  $L_9 + L_{10}$ . A more stringent comparison can only be made by including the heavier multiplets that are known to give rather large contributions to these coefficients. A recent computation shows an impressive agreement [28].

Let us now come back to the extended Nambu-Jona-Lasinio model and to its connections with the chiral quark model. A clear discussion about this point can be found, for instance, in the second paper of ref. [28]. Here we just want to report the main ideas. The original Nambu-Jona-Lasinio model [36] was introduced to understand the pions as Goldstone bosons arising from the spontaneous breaking of chiral symmetry, as suggested by Nambu. After the introduction of QCD there were many attempts to derive this model from QCD. Only in a second time (in the last paper of ref. [27]) it was extended to include gluonic effects.

To understand how this model works, let us start from the lagrangian of eq. (3.10), describing massless QCD in presence of external fields, and let us consider the generating functional of Green's functions of these external fields. In the path integral formalism, it is given by:

$$\begin{aligned} e^{i\Gamma(v,a,s,p)} &= \frac{1}{Z} \int DG_\mu D\bar{q} Dq \exp \left[ i \int d^4x \mathcal{L}_{QCD}(q, \bar{q}, G, v, a, s, p) \right] \\ &= \frac{1}{Z} \int D\Sigma \exp \left[ i \int d^4x \mathcal{L}_{ChPT} \right] \end{aligned} \quad (3.33)$$

The main idea is that of rewriting this generating functional in a form in which the degrees of freedom are still the quarks. This can be done integrating out of the theory the degrees of freedom of heavy quarks and gluons down to a scale  $\Lambda_\chi$  and expanding the resulting effective action in local fermionic operators, taking only the terms leading in  $N_c$  and dimensions. The resulting lagrangian  $\mathcal{L}_{ENJL}$  must satisfy the following relation

$$e^{i\Gamma(v,a,s,p)} = \frac{1}{Z} \int "DG''_\mu D\bar{q} Dq \exp \left[ i \int d^4x \mathcal{L}_{ENJL}(q, \bar{q}, G; v, a, s, p) \right], \quad (3.34)$$

where the quotation marks indicate that we still have to consider the effect of soft gluons below the scale  $\Lambda_\chi$ , but they have to be treated in a non perturbative way.

The form of the lagrangian in the ENJL model is the following

$$\mathcal{L}_{ENJL} = \mathcal{L}_{QCD}^{\Lambda_\chi} + \mathcal{L}_{NJL}^{S,P} + \mathcal{L}_{NJL}^{V,A} + O\left(\frac{1}{\Lambda_\chi^4}\right), \quad (3.35)$$

where

$$\mathcal{L}_{NJL}^{S,P} = 2g_S \sum_{a,b} (\bar{q}_R^a q_L^b) (\bar{q}_L^b q_R^a) \equiv \frac{8\pi^2 G_S(\Lambda_\chi)}{N_c \Lambda_\chi^2} \sum_{a,b} (\bar{q}_R^a q_L^b) (\bar{q}_L^b q_R^a) \quad (3.36)$$

and

$$\begin{aligned} \mathcal{L}_{NJL}^{V,A} &= -g_V \sum_{a,b} \left[ (\bar{q}_L^a \gamma^\mu q_L^b) (\bar{q}_L^b \gamma^\mu q_L^a) + (L \rightarrow R) \right] \\ &\equiv -\frac{8\pi^2 G_V(\Lambda_\chi)}{N_c \Lambda_\chi^2} \sum_{a,b} \left[ (\bar{q}_L^a \gamma^\mu q_L^b) (\bar{q}_L^b \gamma^\mu q_L^a) + (L \rightarrow R) \right]. \end{aligned} \quad (3.37)$$

As usual, the new couplings  $g_S$  and  $g_V$  appearing in the lagrangian must be determined empirically, due to our ignorance of the complete QCD dynamics.

Within this model the quark condensate obtains a value different from zero, which breaks spontaneously the chiral symmetry and causes the appearance of pseudoscalar Goldstone bosons. This is exactly the kind of scenario we wanted to reproduce.

To see which is the connection between the extended Nambu-Jona-Lasinio model and the chiral quark model, we have to reexpress the Nambu-Jona-Lasinio cut-off version of QCD lagrangian in a version which is only quadratic in the quark fields, by using auxiliary fields. This procedure will lead us to a lagrangian containing both fermionic and bosonic fields.

For simplicity, let us consider the case in which the lagrangian of the ENJL model contains only the scalar-pseudoscalar additional term and not the vector-axial one, that is  $g_V = 0$ . We will see that this level of approximation is enough to recover our version of the chiral quark model.

So let us introduce the  $3 \times 3$  auxiliary field matrix  $N(x)$ , with the following transformation property under  $SU(3)_L \times SU(3)_R$

$$N \rightarrow g_R N g_L^\dagger. \quad (3.38)$$

We can use this auxiliary field to reexpress the part of the lagrangian of (3.35) containing the scalar-pseudoscalar coupling, using the following relation

$$\exp \left[ i \int d^4x \mathcal{L}_{NJL}^{S,P}(x) \right] = \int DN \exp \left[ i \int d^4x \left[ -(\bar{q}_L N^\dagger q_R + \bar{q}_R N q_L) - \frac{1}{2g_S} \text{Tr} (N^\dagger N) \right] \right]. \quad (3.39)$$

We can introduce an hermitian matrix  $H$ , in such a way to have

$$N = \Sigma \tilde{H} = \xi H \xi, \quad (3.40)$$

with  $\Sigma$  and  $\xi$  given by eqs. (3.8) and (3.31).

So we have :

$$\exp \left[ i \int d^4x \mathcal{L}_{NJL}^{S,P}(x) \right] = \int D\xi DH \exp \left[ i \int d^4x \left[ - \left( \bar{q}_L \xi^\dagger H \xi^\dagger q_R + \bar{q}_R \xi H \xi q_L \right) - \frac{1}{2g_S} \text{Tr} H^2 \right] \right] \quad (3.41)$$

If we insert this relation in the expression  $e^{i\Gamma_{eff}}$  for the effective action  $\Gamma_{eff}(H, \xi; v, a, s, p)$  expressed in terms of the new auxiliary fields, we obtain an integrand which is quadratic in the fermionic fields and contains also bosonic fields. It is enough to fix  $H = \langle H \rangle = M$  and to remember that  $\xi \cdot \xi = \Sigma$ , to obtain our version of the chiral quark model as the mean field approximation of the extended Nambu-Jona-Lasinio model. The advantage of this more general approach is that in this way the mechanism of spontaneous breaking of chiral symmetry is generated naturally by the model, instead of being added by hand.





# Chapter 4

## Chiral Lagrangian for $\Delta S = 1$ non Leptonic Decays

### 4.1 The Model

In this chapter we will show how to construct a phenomenological model that enables us to calculate the hadronic matrix elements of the four-quark operators  $Q_i$  appearing in the effective hamiltonian of (2.31), in such a way to give a consistent description of  $\Delta S = 1$  weak non leptonic decays.

The essential ingredients we use to build up this model are chiral perturbation theory and the chiral quark model.

We will see that it is possible to bosonize the operators  $Q_i$ , that is to rewrite them in terms of the fields of the octet of pseudoscalar mesons containing pions and kaons. In this way we can write a chiral lagrangian containing different terms. These terms are characterized by specific properties of transformation under  $SU(3)_L \times SU(3)_R$ , which coincide with the transformation properties of the original operators  $Q_i$ . As usual in chiral perturbation theory, our  $\Delta S = 1$  chiral lagrangian contains some coefficients which are a priori unknown and can be determined only by comparison with experimental results or with some phenomenological model.

We have chosen as phenomenological model the chiral quark model. We have seen in the previous chapter that the chiral quark model lagrangian contains an explicit coupling between the pseudoscalar mesons and the light quarks (u,d,s). Therefore it is possible to compute the hadronic matrix elements in this model and to compare them with the results given by the chiral lagrangian. We have done explicitly this calculation

and, in this way, we have determined all the coefficients of the  $\Delta S = 1$  weak chiral lagrangian.

Our results contain the leading and the next to leading terms in the  $1/N_c$  expansion and also terms of  $O(\alpha_s \frac{1}{N_c})$ , which come out from non perturbative gluonic corrections and will be very important also from a numerical point of view (as we will see later studying the  $\Delta I = 1/2$  selection rule).

In this chapter we will explain the essential details of the calculation and we will also discuss about some technical but essential points, like the problem of the cancellation of fake anomalies in the t'Hooft-Veltman (HV) regularization scheme and that of the Fierz transformation properties of the operators. We will see that there are some differences between the HV results and the ones obtained in the naive dimensional regularization (NDR) scheme. We will also discuss about the possibility that these scheme dependence could cancel the analogous one present in the Wilson coefficients.

At the end of these calculations, we have reached the important aim of having at our disposal the complete  $\Delta S = 1$  weak chiral lagrangian at  $O(p^2)$ , to describe the non leptonic kaon decays. We will see in the next chapters our model at work in the case of the study of the  $\Delta I = 1/2$  selection rule and of the estimate of the ratio  $\varepsilon'/\varepsilon$ .

There is still the last, but not least, step we have to make in order to construct a consistent phenomenological model for the study of  $\Delta S = 1$  weak non leptonic processes. We have to introduce in our results a dependence on the matching scale  $\mu$ , that in principle should balance the  $\mu$  dependence of the Wilson coefficients.

In our model this is obtained by considering the  $O(p^4)$  corrections given by chiral loops. In this kind of loops we consider the propagation of the only degrees of freedom still present in the theory, which are the octet of pseudoscalar mesons. This is the reason for which we usually speak of meson loops. The addition of this chiral loop effects gives us expressions for the hadronic amplitudes at scales  $\mu$  which can be taken near to 1 GeV. Hence the hadronic matrix elements, calculated in this way, can be matched with the short distance results for the Wilson coefficients, in such a way to have a consistent expression for the physical amplitudes of  $\Delta S = 1$  weak non leptonic decays.

## 4.2 Bosonization

Let us start from the effective  $\Delta S = 1$  weak non leptonic lagrangian at scales  $\mu < m_c$  and try to bosonize it, that is to rewrite the different operators in terms of mesonic

fields.

As we have seen in the second chapter, the original lagrangian is the following [37, 15]:

$$\mathcal{L}_{\Delta S=1} = -\frac{G_F}{\sqrt{2}} V_{us}^* V_{ud} \sum_{i=1}^{10} [z_i(\mu) + \tau y_i(\mu)] Q_i(\mu) . \quad (4.1)$$

Following the standard parametrization of the KM matrix and considering that  $\text{Re } \tau$  is very small, we have that the  $z_i(\mu)$  control the CP conserving part of the amplitudes while the  $y_i(\mu)$  the CP violating one. The numerical value of the Wilson coefficients depends on the QCD coupling constant  $\alpha_s$ , the recent determination of which from NLO calculations on data taken at LEP and SLC gives [38]

$$\alpha_s(m_Z) = 0.119 \pm 0.006 , \quad (4.2)$$

which corresponds to

$$\Lambda_{QCD}^{(4)} = 350 \pm 100 \text{ MeV} . \quad (4.3)$$

This is the range of values we will use for our numerical estimates.

As a matter of fact, not all of these quark operators are independent (for instance  $Q_4 = Q_3 + Q_2 - Q_1$ ). Anyway this basis has become the standard one and it is the only one in which the Wilson coefficients have been estimated to the next to leading order.

Following a simple procedure we can find the bosonization of the four-quark operators  $Q_i$  appearing in (4.1). First of all we have to reproduce their  $SU(3)$  flavor structure, by using the appropriate combinations of Gell-Mann matrices acting on the quark flavor triplet  $q$ . For instance, left-handed current operators (like  $Q_1$  and  $Q_2$ ) can be written in the following way:

$$(\bar{q}_L \lambda_n^m \gamma^\mu q_L) (\bar{q}_L \lambda_q^p \gamma_\mu q_L) , \quad (4.4)$$

where  $\lambda_n^m$  ( $m, n = 1, 2, 3$ ) are the appropriate flavor projectors, obtained by combinations of  $SU(3)$  Gell-Mann matrices. They are defined by

$$(\lambda_n^m)_{lk} = \delta_{ml} \delta_{nk} . \quad (4.5)$$

In the case of  $Q_2$  we have, for instance,  $m = 3, n = 1, p = 1, q = 2$ .

The next step consists in performing a rotation on the quark multiplets as in eqs. (3.30)–(3.31). We have seen in the previous chapter that  $Q_{L,R}$  can be seen as the constituent quark fields and the rotation of eq. (3.30) is such as to transform the lagrangian of (3.28) into a pure mass term for the constituent quarks

$$-M (\bar{Q}_R Q_L + \bar{Q}_L Q_R) . \quad (4.6)$$

The quark coupling to the Goldstone bosons is transferred, instead, to the kinetic term in the QCD lagrangian. The same rotation, applied to the operators in (4.4), together with their Fierzed transformed expressions, yields

$$\bar{Q}_L \xi \lambda_n^m \gamma^\mu \xi^\dagger Q_L \quad \bar{Q}_L \xi \lambda_q^p \gamma_\mu \xi^\dagger Q_L \quad \text{and} \quad (n \leftrightarrow q) . \quad (4.7)$$

We want to integrate out the degrees of freedom of the rotated quark fields, by considering the constituent quark loops, in such a way to obtain the bosonized chiral lagrangian as the effective field theory of the chiral quark model. This integration is performed after having attached the axial fields [39, 82]

$$A_\mu = -\frac{i}{2} \xi (D_\mu \Sigma^\dagger) \xi = \frac{i}{2} \xi^\dagger (D_\mu \Sigma) \xi^\dagger \quad (4.8)$$

to the quark loops in all possible manners that are consistent with Lorentz invariance.

It can be proved that in the case of (4.7) the insertion of no axial fields (constant term) gives no contribution, since

$$\text{Tr} (\xi \lambda_n^m \xi^\dagger \xi \lambda_q^p \xi^\dagger) = \text{Tr} (\lambda_n^m \lambda_q^p) = 0 , \quad (4.9)$$

unless  $(p, q) = (n, m)$ . The first non-vanishing contributions are proportional to

$$\begin{aligned} \text{Tr} (\xi \lambda_n^m \xi^\dagger A^\mu \xi \lambda_q^p \xi^\dagger A_\mu) &\propto \text{Tr} (\lambda_n^m \Sigma^\dagger D_\mu \Sigma \lambda_q^p \Sigma^\dagger D_\mu \Sigma) \\ \text{Tr} (\xi \lambda_n^m \xi^\dagger \xi \lambda_q^p \xi^\dagger A_\mu A^\mu) &\propto \text{Tr} (\lambda_n^m \lambda_q^p \Sigma^\dagger D_\mu \Sigma \Sigma^\dagger D_\mu \Sigma) \\ \text{Tr} (\xi \lambda_n^m \xi^\dagger A^\mu A_\mu \xi \lambda_q^p \xi^\dagger) &\propto \text{Tr} (\lambda_q^p \lambda_n^m \Sigma^\dagger D_\mu \Sigma \Sigma^\dagger D_\mu \Sigma) \end{aligned} \quad (4.10)$$

which provide, together with the  $(n \leftrightarrow q)$  expressions, the  $O(p^2)$  chiral representation of the quark operator.

It is possible to rewrite the single trace of (4.10) as the product of two traces, by using the trace factorization properties. Given two complex  $3 \times 3$  matrices A and B, we have, for the cases of our interest,

$$\text{Tr} (\lambda_2^3 A \lambda_1^1 B) = \text{Tr} (\lambda_2^1 A) \text{Tr} (\lambda_1^3 B) \quad (4.11)$$

$$\text{Tr} (\lambda_1^3 A \lambda_2^1 B) = \text{Tr} (\lambda_1^1 A) \text{Tr} (\lambda_2^3 B) . \quad (4.12)$$

Using these relations, we can put the different bosonized expressions in a way in which the independent terms are more easily recognized.

The bosonization of operators involving also the right-handed currents proceeds along similar lines. Starting from the rotated operator

$$\bar{Q}_L \xi \lambda_n^m \gamma^\mu \xi^\dagger Q_L \quad \bar{Q}_R \xi^\dagger \lambda_q^p \gamma_\mu \xi Q_R , \quad (4.13)$$

or its Fierzed expression

$$\bar{Q}_L \xi \lambda_q^m \xi Q_R \quad \bar{Q}_R \xi^\dagger \lambda_n^p \xi^\dagger Q_L , \quad (4.14)$$

we obtain after the identification of equivalent terms

$$\begin{aligned} & \text{Tr} \left( \lambda_n^m \Sigma^\dagger \lambda_q^p \Sigma \right) , \\ & \text{Tr} \left( \lambda_n^m D_\mu \Sigma^\dagger \lambda_q^p D^\mu \Sigma \right) , \\ & \text{Tr} \left( \lambda_q^m \Sigma D_\mu \Sigma^\dagger \lambda_n^p \Sigma^\dagger D^\mu \Sigma \right) , \\ & \text{Tr} \left( \lambda_n^m \Sigma^\dagger \lambda_q^p D_\mu \Sigma D^\mu \Sigma^\dagger \Sigma \right) . \end{aligned} \quad (4.15)$$

Not all of these bosonizations are actually present for each operator. For instance, in the case of the gluonic penguins, the sum over the quark flavors together with unitarity make all but one of these terms vanish. It is only for some of the electroweak penguins that all contributions are actually there.

The contributions arising from the last term in (4.15) are usually not included in the literature.

As a matter of fact there is another different, but equivalent, bosonization procedure [41], in which one can consider the  $O(p^2)$  bosonization of the quark density in this way

$$\bar{q}_L q_R \rightarrow \frac{\langle \bar{q}q \rangle}{2} \left[ \Sigma - \frac{c_1}{\Lambda_\chi^2} D_\mu D^\mu \Sigma - \frac{c_2}{\Lambda_\chi^2} \Sigma D_\mu D^\mu \Sigma^\dagger \Sigma + c_3 D_\mu \Sigma D^\mu \Sigma^\dagger \Sigma \right] . \quad (4.16)$$

The last three terms are linearly dependent and so we can take just two of them. We can choose, for instance, to use the following expression

$$\bar{q}_L q_R \rightarrow \frac{\langle \bar{q}q \rangle}{2} \left[ \Sigma - \frac{c_1}{\Lambda_\chi^2} D_\mu D^\mu \Sigma - \frac{c_2}{\Lambda_\chi^2} \Sigma D_\mu D^\mu \Sigma^\dagger \Sigma \right] . \quad (4.17)$$

It can be proved that the neglect of the last term in (4.15) corresponds to discarding the second one of the two quadratic terms of (4.17).

In the first paper of ref. [41] the authors show that the constant  $c_2$  ( $c_1$ ) can be put to zero by a nonlinear transformation that preserves the unitarity of  $\Sigma$ , but not its unimodularity. To be exact we have to say that this is allowed only when a  $U(N_c)$  chiral limit can be invoked ( $N_c \rightarrow \infty$ ), so that  $\eta'$  is added to the octet of Goldstone bosons. While the applicability of such a transformation is immaterial in the case of the gluonic penguins, where all quadratic terms lead to the same bosonization (proportional

to the fixed combination  $c_1 + c_2$ ), it is of relevance in the electroweak sector, where non-equivalent bosonizations are generated by the two independent terms (see section 5.2).

We will see the effect of the introduction of this new bosonization term (corresponding to values of  $c_2 \neq 0$ ) when we study  $\varepsilon'/\varepsilon$ , because in that case the electroweak penguin operators will give a relevant contribution.

### 4.3 The Weak Chiral Lagrangian

We are now ready to write the weak chiral lagrangian describing  $\Delta S = 1$  flavor changing interactions. We can recover it by applying in a systematic way the bosonization procedure described in the previous section to the operators  $Q_i$  of (4.1). In this way we are led, after some algebraic manipulations, to the following  $O(p^2)$  chiral lagrangian:

$$\begin{aligned}
\mathcal{L}_{\Delta S=1}^{(2)} = & G^{(0)}(Q_{7,8}) \text{Tr} \left( \lambda_2^3 \Sigma^\dagger \lambda_1^1 \Sigma \right) \\
& + G_{\underline{8}}(Q_{3-10}) \text{Tr} \left( \lambda_2^3 D_\mu \Sigma^\dagger D^\mu \Sigma \right) \\
& + G_{LL}^a(Q_{1,2,9,10}) \text{Tr} \left( \lambda_1^3 \Sigma^\dagger D_\mu \Sigma \right) \text{Tr} \left( \lambda_2^1 \Sigma^\dagger D^\mu \Sigma \right) \\
& + G_{LL}^b(Q_{1,2,9,10}) \text{Tr} \left( \lambda_2^3 \Sigma^\dagger D_\mu \Sigma \right) \text{Tr} \left( \lambda_1^1 \Sigma^\dagger D^\mu \Sigma \right) \\
& + G_{LR}^a(Q_{7,8}) \text{Tr} \left( \lambda_1^3 D_\mu \Sigma \right) \text{Tr} \left( \lambda_2^1 D^\mu \Sigma^\dagger \right) \\
& + G_{LR}^b(Q_{7,8}) \text{Tr} \left( \lambda_2^3 \Sigma^\dagger D_\mu \Sigma \right) \text{Tr} \left( \lambda_1^1 \Sigma D^\mu \Sigma^\dagger \right) \\
& + G_{LR}^c(Q_{7,8}) \left[ \text{Tr} \left( \lambda_1^3 \Sigma \right) \text{Tr} \left( \lambda_2^1 D_\mu \Sigma^\dagger D^\mu \Sigma \Sigma^\dagger \right) \right. \\
& \quad \left. + \text{Tr} \left( \lambda_1^3 D_\mu \Sigma D^\mu \Sigma^\dagger \Sigma \right) \text{Tr} \left( \lambda_2^1 \Sigma^\dagger \right) \right], \quad (4.18)
\end{aligned}$$

where  $\lambda_j^i$  and  $\Sigma$  are defined respectively in eqs. (4.5) and (3.8). The covariant derivatives in (4.18) are taken with respect to the external gauge fields, whenever they are present.

The convenience of the non-standard form of (4.18) will become clear in the following. We have already said that in our approach the lagrangian (4.18) is the effective theory, generated by integration of the three light quarks of the  $\Delta S = 1$  quark lagrangian. Therefore the notation is such as to remind us the flavor and the chiral structure of the quark operators. In particular,  $G_{\underline{8}}$  represents the  $(\underline{8}_L \times \underline{1}_R)$  part of the interaction, as it is induced in QCD by the gluonic penguins, while the two terms proportional to  $G_{LL}^a$  and  $G_{LL}^b$  are admixtures of the  $(\underline{27}_L \times \underline{1}_R)$  and the  $(\underline{8}_L \times \underline{1}_R)$  part of the interaction, such as it is induced by left-handed current-current operators. The term proportional to  $G^{(0)}$  is the constant (non-derivative) part arising in the isospin violating and  $(\underline{8}_L \times \underline{8}_R)$  electroweak components, of which the terms proportional to  $G_{LR}^{a,b,c}$  represent the  $O(p^2)$  momentum corrections.

The terms proportional to  $G_{\mathfrak{g}}$ ,  $G_{LL}^a$  and  $G_{LL}^b$  have been already studied in the literature [26, 20, 42] in the framework of chiral perturbation theory. Those proportional to  $G_{LL}^a$  and  $G_{LL}^b$  are usually separated further into their isospin components as  $\mathcal{L}_{\underline{27}}$ , which is a  $(\underline{27}_L \times \underline{1}_R)$ , and  $\mathcal{L}_{\mathfrak{g}}$  which is a pure  $(\mathfrak{8}_L \times \underline{1}_R)$ . For more details about the relations between  $\mathcal{L}_{\underline{27},\mathfrak{g}}$  and  $G_{LL}^{a,b}$  we refer the interested reader to the ref. [14]. We prefer to keep the  $\Delta S = 1$  chiral Lagrangian in the form given in (4.18), which makes the bosonization of the various quark operators more transparent, and perform the isospin projections at the level of the matrix elements.

Concerning the  $(\mathfrak{8}_L \times \mathfrak{8}_R)$  part, the constant term was first considered in [43]: its momentum corrections are discussed here for the first time, as far as we know.

At the level of approximation at which we have decided to work in this dissertation we only need the weak chiral lagrangian to  $O(p^2)$ . The  $O(p^4)$  weak lagrangian is very complicated with thirty-seven [42] coefficients to be determined only in the  $(\mathfrak{8}_L \times \underline{1}_R)$  sector, and many more in the others.

Terms proportional to the current quark masses belong to such a higher-order lagrangian, except for a term  $O(m_q)$  for the operators  $Q_{7,8}$  :

$$G^{(m)}(Q_{7,8}) \left[ \text{Tr} \left( \lambda_2^3 \Sigma^\dagger \lambda_1^1 \Sigma \mathcal{M}^\dagger \Sigma \right) + \text{Tr} \left( \lambda_1^1 \Sigma \lambda_2^3 \Sigma^\dagger \mathcal{M} \Sigma^\dagger \right) \right], \quad (4.19)$$

whose contribution is anyway small compared to the leading constant term.

The weight of some of the next-to-leading order corrections on the physical amplitudes has been estimated in various models [42, 44] as well as in the  $\chi$ QM [45]. They range from 10 to 30% of the leading contributions, a potentially large effect that we should bear in mind when estimating the inherent uncertainty of our computation.

### 4.3.1 Determination of the $\Delta S = 1$ Chiral Lagrangian Coefficients

### 4.3.2 General outlines of the calculation

As we can see from (4.18), the weak chiral lagrangian still contains in front of each operator the unknown coefficients  $G_i$ , which have to be determined experimentally or by comparison with some phenomenological model. We have already said that we have determined these coefficients by calculating directly the hadronic matrix elements in the chiral quark model.

Within this model the computation is simply performed by applying the Feynman rules that are reported in the relative appendix. In figure 1 we have represented graph-

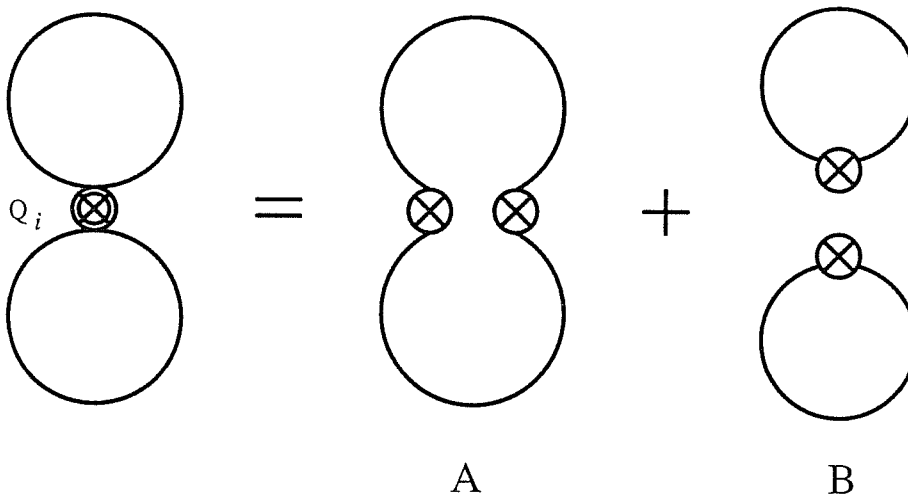


Figure 4.1: The quark constituent loops for an arbitrary operator  $Q_i$ . (A) is the unfactorized pattern, (B) the factorized one. The crossed circles represent operator and/or current insertions.

ically the calculation. In the loops we have the propagation of constituent quarks and the transition is made possible by the insertion of the  $Q_i$  operator. The mesons can appear only as external legs in the diagrams (like for example in Fig. 2(A)). For each operator we have to consider two different possible configurations, namely the “factorized” and the “unfactorized” one. In the case of an operator like  $Q_1$ , which is “color unsaturated”, (in the sense that the color indices are not directly saturated in the single quark current) the unfactorized configuration is of  $O(N_c^2)$  and so it is the leading one from the point of view of  $1/N_c$  expansion. The factorized configuration, instead, gives a contribution of  $O(N_c)$ . On the other hand, for a “color saturated” operator like  $Q_2$  we have the opposite situation and the leading configuration is the factorized one.

To determine the chiral lagrangian coefficients we have computed in the chiral quark model some easy reference processes, which are represented by two-meson diagrams, like the one of Fig. 2(A) and the corresponding factorized configuration. In the case of  $Q_1$ , for instance, we may use the transition  $K^0 \rightarrow \pi^0$  in order to fix uniquely  $G_{LL}^b(Q_1)$  and  $K^+ \rightarrow \pi^+$  to fix  $G_{LL}^a(Q_1)$ .

Once we have fixed the chiral lagrangian coefficients, the diagrams with three meson external lines, which are the relevant ones in the computation of the matrix elements for the processes we want to study, are generated by means of the chiral lagrangian in (4.18).



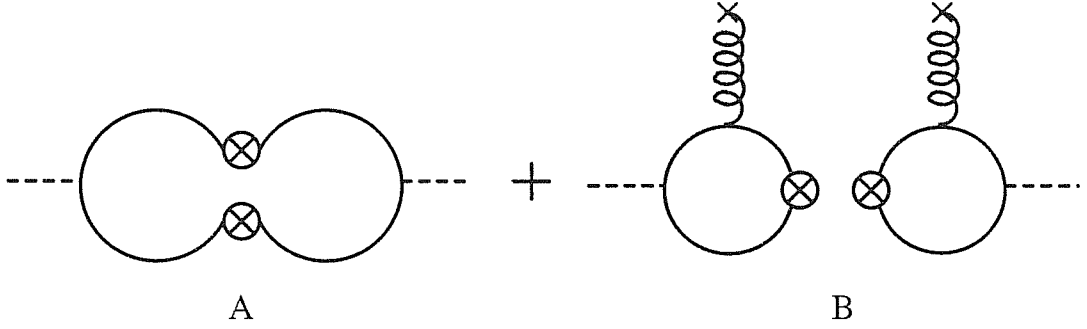


Figure 4.2: The constituent quark loops coupled to the mesons for an arbitrary operator. (A) is the unfactorized configuration, (B) the factorized one with the insertion of the gluon condensate. Meson and gluon lines must be attached in all possible ways.

### 4.3.3 Non Perturbative Gluonic Corrections

A very important part of the hadronic matrix elements calculation is represented by the insertion of non perturbative gluonic corrections. This kind of contributions can be evaluated in our model, as suggested in ref. [20], by considering graphs like the one of Fig 2(B).

As we can see from the figure, to perform the calculation we have to consider the internal quark line in the loop as dressed by external soft gluons. This corresponds to the substitution of the usual quark propagator  $S_0(p)$  with  $S_1(p)$ , where

$$S_0(p) = \frac{i}{\not{p} - M}, \quad (4.20)$$

(with  $\not{p} = \gamma \cdot p$ ) and

$$S_1(p) = -\frac{i}{4} g_s T^a G_{\mu\nu}^a \frac{\sigma^{\mu\nu}(\not{p} + M) + (\not{p} + M)\sigma^{\mu\nu}}{(p^2 - M^2)^2}. \quad (4.21)$$

In (4.21) we have  $\sigma_{\mu\nu} = (i/2) [\gamma_\mu, \gamma_\nu]$ , with

$$\sigma^{\mu\nu}\sigma_{\mu\nu} = 12 \mathbf{I}; \quad \sigma^{\mu\nu}\gamma_\rho\sigma_{\mu\nu} = 0. \quad (4.22)$$

Another important relation, which is relative to the  $SU(3)$  generators  $T^a$  is the following one :

$$\text{Tr}(T^a T^b) = \text{Tr}\left(\frac{\lambda^a \lambda^b}{4}\right) = \frac{\delta^{ab}}{2}. \quad (4.23)$$

The gluon correction is finite, so we can always compute it in the factorized form by means of a Fierz transformation in both the regularization schemes, HV and NDR, (as

we will see better in the next subsections). We also use the relation, valid for  $SU(N_c)$

$$\delta_{\alpha\beta}\delta_{\gamma\delta} = \frac{1}{N_c}\delta_{\alpha\delta}\delta_{\gamma\beta} + 2 T_{\alpha\delta}^a T_{\gamma\beta}^a. \quad (4.24)$$

In this way it is easier to single out those contributions that are non-vanishing in the presence of the external gluons.

The leading gluon condensate contribution is of  $O(1/N_c)$  and it is generated, as we have said, by diagrams of the type shown in Fig. 2(B). Only those configurations in which one external gluon field is attached to each quark loop are genuine corrections to the matrix element, since those in which both gluons are attached to the same quark loop are included in the renormalization of either the quark condensate or  $f_\pi$ , for which we take the physical values.

Gluonic contributions provide a sizable correction of order  $O(\alpha_s N_c)$  that we parameterize in terms of the leading gluon condensate  $\langle\alpha_s GG/\pi\rangle$  by introducing the quantity

$$\delta_{(GG)} = \frac{N_c \langle\alpha_s GG/\pi\rangle}{2 \cdot 16\pi^2 f^4}. \quad (4.25)$$

We will see in the study of the  $\Delta I = 1/2$  selection rule and in the determination of the  $B_K$  parameter of  $K^0 - \bar{K}^0$  mixing, that the introduction of the gluonic corrections is essential for an exact evaluation of the results.

### 4.3.4 Divergencies Regularization

Some of the constituent-quark loops are divergent. We use dimensional regularization (with the definition  $d = 4 - 2\epsilon$ ). The logarithmic divergencies of the loop integration (which appear for different kind of operators) and the quadratic ones (which are generated only in the case of gluonic and electroweak penguins) are identified with, respectively, the pion decay constant  $f_\pi$  and the quark condensate  $\langle\bar{q}q\rangle$ . We define the two quantities

$$f^{(0)} = \frac{M^2 N_c}{4\pi^2 f} \left( \frac{4\pi\mu^2}{M^2} \right)^\epsilon \Gamma(\epsilon), \quad (4.26)$$

$$\langle\bar{q}q\rangle^{(0)} = -\frac{M^3 N_c}{4\pi^2} \left( \frac{4\pi\mu^2}{M^2} \right)^\epsilon \Gamma(-1 + \epsilon), \quad (4.27)$$

and then identify  $f^{(0)} = f_\pi$  and  $\langle\bar{q}q\rangle^{(0)} = \langle\bar{q}q\rangle$  in the end of the computation. The latter are understood as the physical quantities, inclusive of gluon and mass corrections.

We use (4.26) and (4.27) as a convenient bookkeeping device for these input parameters, even if there is a certain degree of arbitrariness in these definitions inasmuch the two gamma functions go into each other up to a finite term by expanding around the pole.

Yet, for all practical purposes, keeping the two types of divergencies separated is a simple and effective way of singling out the different contributions.

Since the  $\mu$  dependence in Eqs. (4.26) and (4.27) is absorbed in the physical quantities  $f_\pi$  and  $\langle \bar{q}q \rangle^\dagger$ , there is no scale dependence induced by the  $\chi$ QM in the chiral coefficients. We will see later that the scale dependence, which must appear in the hadronic matrix elements in order to make physical quantities scale independent, will be inserted in our model in a second step, when we consider the effect of mesonic chiral loops.

As a matter of fact  $\chi$ QM can be thought as an effective QCD model, interpolating between the two scales  $\Lambda_\chi$  and  $M$ . In this sense, the most natural regularization scheme is a cut-off theory where no divergencies arise. In fact, one finds

$$f^{(0)} = \frac{M^2 N_c}{4\pi^2 f} \ln \frac{\Lambda_\chi^2}{M^2}, \quad (4.28)$$

$$\langle \bar{q}q \rangle^{(0)} = \frac{MN_c}{4\pi^2} \left( -\Lambda_\chi^2 + M^2 \ln \frac{\Lambda_\chi^2}{M^2} \right). \quad (4.29)$$

Eqs. (4.28) and (4.29) are finite (albeit cut-off dependent) quantities to be identified with  $f_\pi$  and  $\langle \bar{q}q \rangle$ , respectively.

Unfortunately, such a cut-off regularization of the hadronic matrix elements is not consistent with that of the Wilson coefficients, that are obtained by means of dimensional regularization. For this reason, we do not pursue this possibility further (see, however, refs. [28], where a matching of cut-off regularization and NDR was attempted).

### 4.3.5 Scheme Dependence and t'Hooft-Veltman Fake Anomalies

We have seen that to compute the matrix elements in the chiral quark model and to eliminate the divergencies appearing in this calculation we use dimensional regularization. Therefore we have to face the problem of dealing with the  $\gamma_5$  matrix in a generic dimension  $d$  with  $d \neq 4$ .

---

<sup>†</sup>The quark condensate has a perturbative scale dependence which originates in the short-distance computation; see the discussion of section 4

There are different possible regularization schemes which are characterized by different properties of the  $\gamma_5$  matrix, the most important schemes are the t'Hooft-Veltman (HV) and the naive dimensional regularization (NDR) scheme. We will analyze the main properties of HV and NDR in an apposite appendix. Here we just remember the main difference is that in the NDR scheme we have an anticommuting  $\gamma_5$  even in  $d$  dimension, while it is not true in the HV.

The Wilson coefficients have been computed separately in HV and in NDR. Hence we have to calculate also the hadronic matrix elements in both schemes, to match our results with the short distance calculation. We will also try to see if there is a  $\gamma_5$ -scheme dependence in the matrix elements and if it can compensate the analogous dependence present in the Wilson coefficients.

To give an idea of the calculation performed we can consider first the simple case of the evaluation of the matrix element of a current-current operator between a kaon and a pion (like for instance  $\langle \pi^+ | Q_2 | K^+ \rangle$ ). We have the following relation:

$$\langle \pi^+ | Q_2 | K^+ \rangle = \langle \pi^+ | (\bar{s}u)_{V-A} (\bar{u}d)_{V-A} | K^+ \rangle = \langle \pi^+ | \bar{u} \gamma_\mu \gamma_5 d | 0 \rangle \langle 0 | \bar{s} \gamma^\mu \gamma_5 u | K^+ \rangle. \quad (4.30)$$

When we consider the matrix elements of penguin operators we have also to take into account building blocks of quark densities (like for instance  $\langle \pi^+ | \bar{s}d | K^+ \rangle$ ) instead of quark currents.

Let us consider for the generic operator  $Q_i$  the building blocks out of which the matrix elements in the factorized form of Fig. 1(B) are made. These have an independent physical interpretation, as we shall see, and come in four kinds.

We consider first the results of the NDR scheme. There are two densities, that we need to  $O(p^2)$  (because this is the order at which we want to stop in the determination of the chiral lagrangian coefficients). For these kind of building blocks we obtain

$$\langle 0 | \bar{s} \gamma_5 u | K^+(k) \rangle_{\text{NDR}} = i\sqrt{2} \left[ \frac{\langle \bar{q}q \rangle^{(0)}}{f} - k^2 \frac{f^{(0)}}{2M} \right], \quad (4.31)$$

$$\begin{aligned} \langle \pi^+(p_+) | \bar{s}d | K^+(k) \rangle_{\text{NDR}} &= -\frac{\langle \bar{q}q \rangle^{(0)}}{f^2} + \frac{3M}{2\Lambda_x^2} P^2 \\ &+ \frac{q^2}{2M} \left( f_+^{\text{NDR}}(0) - 3 \frac{M^2}{\Lambda_x^2} \right). \end{aligned} \quad (4.32)$$

There are also two currents, that we only need to  $O(p)$ :

$$\langle 0 | \bar{s} \gamma^\mu \gamma_5 u | K^+(k) \rangle_{\text{NDR}} = i\sqrt{2} k^\mu f^{(0)} \quad (4.33)$$

$$\langle \pi^+(p_+) | \bar{s} \gamma^\mu d | K^+(k) \rangle_{\text{NDR}} = -f_+^{\text{NDR}}(q^2) P^\mu + f_-(q^2) q^\mu, \quad (4.34)$$

where  $q = k - p_+$  and  $P = k + p_+$ , while  $f_+^{\text{NDR}}(0) \equiv f^{(0)}/f$  is identified with the vector form factor at zero momentum transfer  $q$ .

In the NDR scheme we correctly find

$$f_+^{\text{NDR}}(0) = 1 \quad \text{and} \quad f_-(0) = 0. \quad (4.35)$$

This result holds in the limit of unbroken  $SU(3)$  symmetry, where

$$f_\pi = f_K \quad \text{and} \quad f_\pm^{K^0\pi^0}(0) = f_\pm^{K^+\pi^0}(0) = f_\pm(0). \quad (4.36)$$

In this limit, Eqs. (4.35) are in agreement with the experiments (deviations of  $f_\pm(0)$  from unity are of order  $m_s^2$  [46]) and we do not find any anomalous result in the NDR scheme.

Considering next the HV scheme, we find the following results for the current matrix elements

$$\langle 0 | \bar{s} \gamma^\mu \gamma_5 u | K^+(k) \rangle_{\text{HV}} = i\sqrt{2} k^\mu f^{(0)} \quad (4.37)$$

$$\langle \pi^+(p_+) | \bar{s} \gamma^\mu d | K^+(k) \rangle_{\text{HV}} = -f_+^{\text{HV}}(q^2) P^\mu + f_-(q^2) q^\mu, \quad (4.38)$$

where

$$f_+^{\text{HV}}(0) = 1 + 4 \frac{M^2}{\Lambda_\chi^2}. \quad (4.39)$$

Eq. (4.37) is the same as (4.33), so that  $f_\pi$  is defined identically in the two renormalization schemes. On the other hand, the vector form factor  $f_+(0)$  turns out to be different, and it happens also for the density matrix elements, that are now given by

$$\begin{aligned} \langle 0 | \bar{s} \gamma_5 u | K^+(k) \rangle_{\text{HV}} &= \langle 0 | \bar{s} \gamma_5 u | K^+(k) \rangle_{\text{NDR}} \\ &\quad + i\sqrt{2} f \left[ 12 \frac{M^3}{\Lambda_\chi^2} \left( 1 - \frac{k^2}{6M^2} \right) \right], \end{aligned} \quad (4.40)$$

$$\langle \pi^+(p_+) | \bar{s} d | K^+(k) \rangle_{\text{HV}} = \langle \pi^+(p_+) | \bar{s} d | K^+(k) \rangle_{\text{NDR}} + 24 \frac{M^3}{\Lambda_\chi^2}. \quad (4.41)$$

Even though  $f_+^{\text{HV}}(0) \neq 1$ , the vector current Ward identity is preserved also in the HV scheme. In fact, in the model the mesons propagate via quark loops, so that a simple calculation in the NDR case leads to

$$G_\Pi^{-1}(k) = k^2 f_+^{\text{NDR}}(0); \quad (4.42)$$

while in the HV we find

$$G_{\Pi}^{-1}(k) = k^2 f_+^{\text{HV}}(0) - 24 \frac{M^2}{\Lambda_\chi^2} M^2. \quad (4.43)$$

By looking at the term proportional to  $k^2$  we see by inspection that the same shift in  $f_+(0)$  is present in the propagator as well as in the vertex. Therefore the vector Ward identity

$$q^\mu \langle \pi^+(p_2) | \frac{2}{3} \bar{u} \gamma_\mu u - \frac{1}{3} \bar{d} \gamma_\mu d | \pi^+(p_1) \rangle = G_\pi^{-1}(p_2) - G_\pi^{-1}(p_1) \quad (4.44)$$

holds in both schemes, and one might think that a redefinition of  $f_+^{\text{HV}}(0)$  could solve all problems. Unfortunately, because  $f^{(0)}$  is the same in the two schemes, it is not possible to simply redefine  $f_+^{\text{HV}}(0)$  to be equal to 1, reabsorbing the HV shift in  $f_\pi$ . Moreover, (4.43) shows another problem: a mass term is generated in the HV case, thus leading to explicit breaking of chiral symmetry.

We therefore find that, in order to maintain the symmetries of the theory, we must subtract appropriate terms in the HV case. In particular, the mass term in (4.43) must be taken away. This subtraction leads to an analogous subtraction in the building blocks of (4.40) and (4.41), which become identical to the NDR results. Having fully subtracted the propagators, the Ward identity in (4.44) implies that also  $f_+^{\text{HV}}(0)$  in (4.38) becomes identical to the NDR result. The overall effect of the subtractions is to make the building blocks of the HV scheme identical to those of NDR, as given in (4.31-4.34).

These subtractions can be implemented in the strong sector by the addition of appropriate terms in the  $\chi$ QM one-loop chiral lagrangian. For more details about this point, we refer the interested reader to the ref. [14].

### 4.3.6 Fierz Transformation Properties of the Operators

Let us consider the operators  $Q_i$  written in the form of (2.12) and (2.13-2.14) and take, for instance, the operator  $Q_1$ . We can see from Fig. 3 that in the case of the matrix element  $\langle \pi^0 | Q_1 | K^0 \rangle$  we have to consider an unfactorized configuration (Fig. 3(A)), which will give a leading ( $O(N_c^2)$ ) contribution to the corresponding chiral lagrangian coefficient, while for  $\langle \pi^+ | Q_1 | K^+ \rangle$  we have the factorized pattern of Fig. 3(B) which is next to leading in  $1/N_c$ .

We can also perform a Fierz transformation on the operator  $Q_1$  and so we are lead to the following expression

$$Q_1 = (\bar{s}_\alpha u_\beta)_{V-A} (\bar{u}_\beta d_\alpha)_{V-A} = 4 (\bar{s}_{\alpha L} \gamma_\mu u_{\beta L}) (\bar{u}_{\beta L} \gamma^\mu d_{\alpha L}) =$$

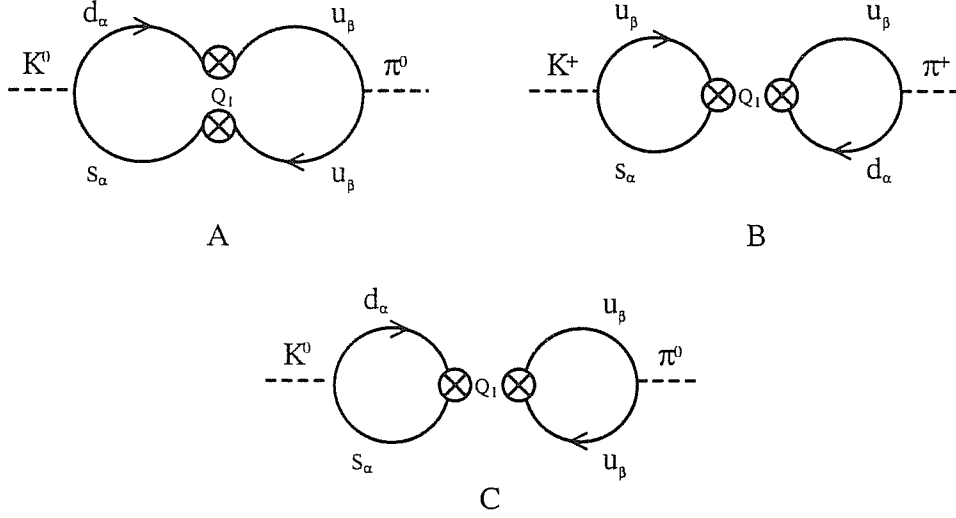


Figure 4.3: The constituent quark loops coupled to  $K$  and  $\pi$  in the case of the insertion of the operator  $Q_1$ , neglecting soft gluon corrections. (A) gives the leading  $O(N_c^2)$  contribution of  $Q_1$  to the chiral coefficient  $G_{LL}^b$ , while (B) is the subleading  $O(N_c)$  correction to  $G_{LL}^a$ . The figure 3(C), instead, represents the contribution to the process  $K^0 \rightarrow \pi^0$  coming from  $\tilde{Q}_1$ , that is the Fierzed form of the operator  $Q_1$ .

$$4(\bar{s}_L \gamma_\mu d_L)(\bar{u}_L \gamma^\mu u_L) = (\bar{s}d)_{V-A}(\bar{u}u)_{V-A} \equiv \tilde{Q}_1, \quad (4.45)$$

where  $q_{R,L} = \frac{1}{2}(1 \pm \gamma_5)q$ .

Writing  $Q_1$  in the form of the right hand side of (4.45) we see that also in the case of the matrix element  $\langle \pi^0 | Q_1 | K^0 \rangle$  we can obtain the leading contribution from a factorized configuration like the one of Fig. 3(C).

By performing similar Fierz transformations on the various operators it is possible to bring all matrix elements (leading as well as next to leading order in  $1/N_c$ ) to a factorized form.

It is important to notice that, applying a Fierz transformation on a  $(V-A) \times (V+A)$  operator, we pass from the product of two currents to the product of two densities. So, for example, we have for  $Q_6$ :

$$Q_6 = (\bar{s}_\alpha d_\beta)_{V-A} \sum_q (\bar{q}_\beta q_\alpha)_{V+A} = 4(\bar{s}_{\alpha L} \gamma_\mu d_{\beta L}) \sum_q (\bar{q}_{\beta R} \gamma^\mu q_{\alpha R}) =$$

$$-8 \sum_q (\bar{s}_L q_R) (\bar{q}_R d_L) \equiv \tilde{Q}_6, \quad (4.46)$$

where  $q$  denote the generic light quark field ( $q=u,d,s$ ).

We have shown in the previous subsection that the factorized building blocks (after making the appropriate subtraction for the HV results) are scheme independent. Therefore it would seem that there is no  $\gamma_5$ -scheme dependence at all in the hadronic matrix elements calculated in the chiral quark model. However this conclusion is not correct, because, while in the HV scheme it is possible to apply a Fierz transformation on the quark operators without changing the matrix element, this is not possible in the NDR scheme. In this scheme, in fact, operators related by a Fierz transformation lead to different matrix elements. This fact is at the origin of the  $\gamma_5$ -scheme dependence of the matrix elements.

As a first example, let us consider the contribution of  $Q_1$  to  $G_{LL}^b$ . A direct evaluation of the unfactorized diagram in Fig. 3(A) gives, in the HV scheme

$$G_{LL}^b(Q_1) = -f^2 (f^{(0)})^2. \quad (4.47)$$

The NDR result, instead, is more complicated and it is given by

$$G_{LL}^b(Q_1) = -f^2 (f^{(0)})^2 \left( 1 - 6 \frac{M^2}{\Lambda_x^2} \right). \quad (4.48)$$

It is important to notice the presence of the shift term  $6 \frac{M^2}{\Lambda_x^2}$ , which appears in the NDR results all the times that we consider an unfactorized configuration for a  $(V-A) \times (V-A)$  operator.

We could have performed the same computation by first Fierz transforming the operator  $Q_1$  like in (4.45) and in this case, by means of the building blocks in (4.33-4.34) (or the subtracted (4.37- 4.38)), we would have obtained the result in (4.47) in both the NDR and HV schemes. So we explicitly see that the Fierz related operators  $Q_1$  and  $\tilde{Q}_1$  could lead in NDR to different contributions to the chiral coefficients.

As a second, more complicated example, let us consider the case of a  $(V-A) \times (V+A)$  operator. We can study, for instance, the contribution of the gluonic penguin  $Q_6$  to  $G_{\underline{8}}$  and evaluate its bosonization directly in the form given in (2.13). By computing the two-loop unfactorized diagram in the NDR scheme we obtain

$$G_{\underline{8}}(Q_6) = 2 \frac{\langle \bar{q}q \rangle}{M} f^2 \left( f_+^{\text{NDR}} - 9 \frac{M^2}{\Lambda_x^2} \right). \quad (4.49)$$



By performing a Fierz transformation on the operator

$$\tilde{Q}_6 = -8 \sum_q (\bar{s}_L q_R)(\bar{q}_R d_L) \quad (4.50)$$

and using the density building blocks in (4.31-4.34) one obtains, in the NDR case,

$$G_{\underline{8}}(\tilde{Q}_6) = 2 \frac{\langle \bar{q}q \rangle}{M} f^2 \left( f_+^{\text{NDR}} - 6 \frac{M^2}{\Lambda_\chi^2} \right). \quad (4.51)$$

In the HV case instead both procedures lead to

$$G_{\underline{8}}(Q_6) = 2 \frac{\langle \bar{q}q \rangle}{M} f^2 \left( f_+^{\text{HV}} + 6 \frac{M^2}{\Lambda_\chi^2} \right). \quad (4.52)$$

Notice that (4.52) is not the correct result because of the necessary subtractions that must still be implemented in the HV scheme, as discussed in the previous subsection. After the subtraction we find the same result of (4.51).

Because a similar pattern holds for all ten operators, we have proved that a Fierz transformation preserves the  $\chi$ QM result in the HV scheme but not in the NDR one. This feature, which was already observed in short-distance calculations [15, 16], can be understood as a consequence of the prescription of symmetrization of the chiral vertices in the HV scheme, which is equivalent to considering the inserted operators as four dimensional objects, for which the usual Fierz transformation are allowed.

As a consequence of these results, when computing matrix elements in the HV scheme we will always resort to Fierzing the quark operators in such a way to exploit the simpler factorized form. Subtractions are then applied in order to satisfy the relevant Ward identities and equations of motion. On the contrary, we do not apply any Fierz transformation in the NDR case. We retain only terms up to order  $M^2/\Lambda_\chi^2$ . Ambiguities in the subtraction procedure—like those arising from the expansion of the gamma functions in the building blocks of Fig. 1(B)—can be shown to be of higher order.

A subtlety arises at this point. The NDR prescription of Refs. [15, 16] preserves the chiral properties of the operator ( $Q_1 - Q_2$ ) by means of a special choice of coefficients for the evanescent operators. Consistency with such a prescription suggests that we have to impose by an appropriate subtraction, that the operator  $Q_1 - Q_2$  (as well as  $Q_9 - Q_{10}$ ) remains a pure octet ( $\underline{8}_L \times \underline{1}_R$ ). As a consequence, the shift in Eq. (4.48) is cancelled and the matrix elements induced by  $Q_1$  and  $Q_2$  are the same in the two schemes.

### 4.3.7 HV Coefficients

In the previous subsections we have introduced all the ingredients needed to compute the contributions of the different  $Q_i$  operators of (4.1) to the seven coefficients of the weak chiral lagrangian (4.18) in both the HV and the NDR schemes. We just have to make a last technical remark. To evaluate the matrix elements of the electroweak operators it is convenient to rewrite them in the following way

$$\begin{aligned}
Q_7 &= \frac{3}{2}\hat{e}_d Q_5 + \frac{3}{2}(\hat{e}_u - \hat{e}_d)\Delta Q_7 \\
Q_8 &= \frac{3}{2}\hat{e}_d Q_6 + \frac{3}{2}(\hat{e}_u - \hat{e}_d)\Delta Q_8 \\
Q_9 &= \frac{3}{2}\hat{e}_d Q_3 + \frac{3}{2}(\hat{e}_u - \hat{e}_d)\Delta Q_9 \\
Q_{10} &= \frac{3}{2}\hat{e}_d Q_4 + \frac{3}{2}(\hat{e}_u - \hat{e}_d)\Delta Q_{10},
\end{aligned} \tag{4.53}$$

where

$$\begin{aligned}
\Delta Q_7 &= (\bar{s}d)_{V-A} (\bar{u}u)_{V+A} \\
\Delta Q_8 &= (\bar{s}_\alpha d_\beta)_{V-A} (\bar{u}_\beta u_\alpha)_{V+A} \\
\Delta Q_9 &= (\bar{s}d)_{V-A} (\bar{u}u)_{V-A} \\
\Delta Q_{10} &= (\bar{s}_\alpha d_\beta)_{V-A} (\bar{u}_\beta u_\alpha)_{V-A}.
\end{aligned} \tag{4.54}$$

We have included in our determination of the chiral lagrangian coefficients all the contributions of order  $O(N_c^2)$  and  $O(N_c)$  and also the ones  $O(\alpha_s N_c)$  coming from non perturbative gluonic corrections. Our result depends on the intrinsic  $\chi$ QM parameter  $M$  and on three input parameters:  $f_\pi$ ,  $\langle\alpha_s GG/\pi\rangle$  and the quark condensate  $\langle\bar{q}q\rangle$  which appears in the matrix elements of the penguin operators.

From now on, we identify  $f^{(0)} = f = f_\pi$ . We will see later, discussing  $\Delta S = 2$  physics that in that case we will have the problem of the distinction between  $f_\pi$  and  $f_K$ .

The inclusion in the chiral coefficients of the corresponding factors

$$-\frac{G_F}{\sqrt{2}}V_{ud}V_{us}^* [z_i(\mu) + \tau y_i(\mu)] \tag{4.55}$$

is understood.

Let us start giving the results for the chiral coefficients in the HV scheme.

For the pure  $(\underline{8}_L \times \underline{1}_R)$  term we include in the coefficient  $G_{\underline{8}}$  the contributions of the gluonic penguins, which are pure octets, as well as the gluon-penguin-like components of the electroweak penguins (4.53) (an octet component still remaining in the  $\Delta Q_i$ 's). In this way we find:

$$\begin{aligned}
G_{\underline{8}}(Q_3) &= f_\pi^4 \frac{1}{N_c} (1 - \delta_{(GG)}) \\
G_{\underline{8}}(Q_4) &= f_\pi^4 \\
G_{\underline{8}}(Q_5) &= \frac{2}{N_c} \frac{\langle \bar{q}q \rangle}{M} f_\pi^2 \left( 1 - 6 \frac{M^2}{\Lambda_\chi^2} \right) \\
G_{\underline{8}}(Q_6) &= 2 \frac{\langle \bar{q}q \rangle}{M} f_\pi^2 \left( 1 - 6 \frac{M^2}{\Lambda_\chi^2} \right) \\
G_{\underline{8}}(Q_7) &= 3 \hat{e}_d \frac{1}{N_c} \frac{\langle \bar{q}q \rangle}{M} f_\pi^2 \left( 1 - 6 \frac{M^2}{\Lambda_\chi^2} \right) \\
G_{\underline{8}}(Q_8) &= 3 \hat{e}_d \frac{\langle \bar{q}q \rangle}{M} f_\pi^2 \left( 1 - 6 \frac{M^2}{\Lambda_\chi^2} \right) \\
G_{\underline{8}}(Q_9) &= \frac{3}{2} \hat{e}_d \frac{1}{N_c} f_\pi^4 (1 - \delta_{(GG)}) \\
G_{\underline{8}}(Q_{10}) &= \frac{3}{2} \hat{e}_d f_\pi^4,
\end{aligned} \tag{4.56}$$

where  $\delta_{(GG)}$  is given by Eq. (4.25).

The  $(V - A) \otimes (V - A)$  operators  $Q_{1,2}$  and  $\Delta Q_{9,10}$  yield:

$$\begin{aligned}
G_{LL}^a(Q_1) &= -\frac{1}{N_c} f_\pi^4 (1 - \delta_{(GG)}) \\
G_{LL}^a(Q_2) &= -f_\pi^4 \\
G_{LL}^b(Q_1) &= -f_\pi^4 \\
G_{LL}^b(Q_2) &= -\frac{1}{N_c} f_\pi^4 (1 - \delta_{(GG)}) \\
G_{LL}^a(Q_9) &= -\frac{3}{2} (\hat{e}_u - \hat{e}_d) f_\pi^4 \frac{1}{N_c} (1 - \delta_{(GG)}) \\
G_{LL}^a(Q_{10}) &= -\frac{3}{2} (\hat{e}_u - \hat{e}_d) f_\pi^4 \\
G_{LL}^b(Q_9) &= -\frac{3}{2} (\hat{e}_u - \hat{e}_d) f_\pi^4 \\
G_{LL}^b(Q_{10}) &= -\frac{3}{2} (\hat{e}_u - \hat{e}_d) f_\pi^4 \frac{1}{N_c} (1 - \delta_{(GG)}) .
\end{aligned} \tag{4.57}$$

For the constant term which represents the leading contribution of  $Q_8$  and  $Q_7$ , we

find:

$$\begin{aligned} G^{(0)}(Q_7) &= -3 \frac{1}{N_c} (\hat{e}_u - \hat{e}_d) \langle \bar{q}q \rangle^2 \\ G^{(0)}(Q_8) &= -3 (\hat{e}_u - \hat{e}_d) \langle \bar{q}q \rangle^2, \end{aligned} \quad (4.58)$$

while, for their momentum corrections, we have:

$$\begin{aligned} G_{LR}^a(Q_7) &= 3(\hat{e}_u - \hat{e}_d) \frac{1}{N_c} \frac{f_\pi^2}{M} \langle \bar{q}q \rangle \\ G_{LR}^a(Q_8) &= 3(\hat{e}_u - \hat{e}_d) \frac{f_\pi^2}{M} \langle \bar{q}q \rangle \\ G_{LR}^b(Q_7) &= -\frac{3}{2} (\hat{e}_u - \hat{e}_d) f_\pi^4 \\ G_{LR}^b(Q_8) &= -\frac{3}{2} (\hat{e}_u - \hat{e}_d) f_\pi^4 \frac{1}{N_c} (1 + \delta_{\langle GG \rangle}) \\ G_{LR}^c(Q_7) &= -9 \frac{M^2}{\Lambda_\chi^2} (\hat{e}_u - \hat{e}_d) \frac{1}{N_c} \frac{f_\pi^2}{M} \langle \bar{q}q \rangle \\ G_{LR}^c(Q_8) &= -9 \frac{M^2}{\Lambda_\chi^2} (\hat{e}_u - \hat{e}_d) \frac{f_\pi^2}{M} \langle \bar{q}q \rangle. \end{aligned} \quad (4.59)$$

### 4.3.8 NDR Coefficients

Performing the same computation in the NDR scheme, we find a different determination of the coefficients because of the shifts discussed previously, like the one of the Eq. (4.48). In general, we can say that a shift is present whenever the determination of the coefficient requires the evaluation of the unfactorized configuration of Fig. 1(A). Anyway we will see in detail the single cases for the different coefficients.

We can start from the  $G_{\underline{8}}$  contributions which are now given by:

$$\begin{aligned} G_{\underline{8}}(Q_3) &= f_\pi^4 \frac{1}{N_c} \left( 1 - \delta_{\langle GG \rangle} - 6 \frac{M^2}{\Lambda_\chi^2} \right) \\ G_{\underline{8}}(Q_4) &= f_\pi^4 \left( 1 - 6 \frac{M^2}{\Lambda_\chi^2} \right) \\ G_{\underline{8}}(Q_5) &= \frac{2}{N_c} \frac{\langle \bar{q}q \rangle}{M} f_\pi^2 \left( 1 - 9 \frac{M^2}{\Lambda_\chi^2} \right) \\ G_{\underline{8}}(Q_6) &= 2 \frac{\langle \bar{q}q \rangle}{M} f_\pi^2 \left( 1 - 9 \frac{M^2}{\Lambda_\chi^2} \right) \\ G_{\underline{8}}(Q_7) &= 3 \hat{e}_d \frac{1}{N_c} \frac{\langle \bar{q}q \rangle}{M} f_\pi^2 \left( 1 - 9 \frac{M^2}{\Lambda_\chi^2} \right) \end{aligned}$$

$$\begin{aligned}
G_{\underline{8}}(Q_8) &= 3 \hat{e}_d \frac{\langle \bar{q}q \rangle}{M} f_\pi^2 \left( 1 - 9 \frac{M^2}{\Lambda_\chi^2} \right) \\
G_{\underline{8}}(Q_9) &= \frac{3}{2} \hat{e}_d f_\pi^4 \frac{1}{N_c} \left( 1 - \delta_{(GG)} - 6 \frac{M^2}{\Lambda_\chi^2} \right) \\
G_{\underline{8}}(Q_{10}) &= \frac{3}{2} \hat{e}_d f_\pi^4 \left( 1 - 6 \frac{M^2}{\Lambda_\chi^2} \right). \tag{4.60}
\end{aligned}$$

We can see that the characteristic shift term  $6 \frac{M^2}{\Lambda_\chi^2}$  is present in all the contributions coming from the  $(V - A) \times (V - A)$  operators  $Q_3, Q_4, Q_9, Q_{10}$ . This is due to the fact that for all of these operators we have to compute the unfactorized configuration, as we can see from the fact that the corresponding contributions to the chiral coefficients are  $O(N_c^2)$  for the ‘‘color unsaturated’’ operators ( $Q_4$  and  $Q_{10}$ ) and  $O(N_c)$  for the ‘‘color saturated’’ ones ( $Q_3$  and  $Q_9$ ).

We have a similar situation also for the  $(V - A) \times (V + A)$  operators  $Q_5 - Q_8$ . The only difference is that in this case the NDR term proportional to  $\frac{M^2}{\Lambda_\chi^2}$  is  $9 \frac{M^2}{\Lambda_\chi^2}$  (the corresponding HV coefficients contain the term  $6 \frac{M^2}{\Lambda_\chi^2}$ ).

For the  $(V - A) \times (V - A)$  operators  $Q_1, Q_2, Q_9, Q_{10}$  we have:

$$\begin{aligned}
G_{LL}^a(Q_1) &= -\frac{1}{N_c} f_\pi^4 \left( 1 - \delta_{(GG)} \right) \\
G_{LL}^a(Q_2) &= -f_\pi^4 \\
G_{LL}^b(Q_1) &= -f_\pi^4 \\
G_{LL}^b(Q_2) &= -\frac{1}{N_c} f_\pi^4 \left( 1 - \delta_{(GG)} \right) \\
G_{LL}^a(Q_9) &= -\frac{3}{2} (\hat{e}_u - \hat{e}_d) f_\pi^4 \frac{1}{N_c} \left( 1 - \delta_{(GG)} \right) \\
G_{LL}^a(Q_{10}) &= -\frac{3}{2} (\hat{e}_u - \hat{e}_d) f_\pi^4 \\
G_{LL}^b(Q_9) &= -\frac{3}{2} (\hat{e}_u - \hat{e}_d) f_\pi^4 \\
G_{LL}^b(Q_{10}) &= -\frac{3}{2} (\hat{e}_u - \hat{e}_d) f_\pi^4 \frac{1}{N_c} \left( 1 - \delta_{(GG)} \right). \tag{4.61}
\end{aligned}$$

These results coincide with the corresponding HV ones, because here the NDR shifts are eliminated if we choose the substitution imposed by the requirements of consistency with the choice of the coefficients for the evanescent operators, as we have already discussed.

For the constant term coming from the electroweak penguins we find:

$$G^{(0)}(Q_8) = -3(\hat{e}_u - \hat{e}_d) \langle \bar{q}q \rangle^2 \left( 1 - 3 \frac{M^3 f_\pi^2}{\langle \bar{q}q \rangle \Lambda_\chi^2} \right)$$

$$G^{(0)}(Q_7) = -3\frac{1}{N_c}(\hat{e}_u - \hat{e}_d) \langle \bar{q}q \rangle^2 \left( 1 - 3\frac{M^3 f_\pi^2}{\langle \bar{q}q \rangle \Lambda_\chi^2} \right) \quad (4.62)$$

with the corresponding momentum corrections:

$$\begin{aligned} G_{LR}^a(Q_7) &= 3(\hat{e}_u - \hat{e}_d) \frac{1}{N_c} \frac{f_\pi^2}{M} \langle \bar{q}q \rangle \left( 1 - 3\frac{M^2}{\Lambda_\chi^2} \right) \\ G_{LR}^a(Q_8) &= 3(\hat{e}_u - \hat{e}_d) \frac{f_\pi^2}{M} \langle \bar{q}q \rangle \left( 1 - 3\frac{M^2}{\Lambda_\chi^2} \right) \\ G_{LR}^b(Q_7) &= -\frac{3}{2}(\hat{e}_u - \hat{e}_d) f_\pi^4 \\ G_{LR}^b(Q_8) &= -\frac{3}{2}(\hat{e}_u - \hat{e}_d) f_\pi^4 \frac{1}{N_c} (1 + \delta_{(GG)}) \\ G_{LR}^c(Q_7) &= -9\frac{M^2}{\Lambda_\chi^2} (\hat{e}_u - \hat{e}_d) \frac{1}{N_c} \frac{f_\pi^2}{M} \langle \bar{q}q \rangle \\ G_{LR}^c(Q_8) &= -9\frac{M^2}{\Lambda_\chi^2} (\hat{e}_u - \hat{e}_d) \frac{f_\pi^2}{M} \langle \bar{q}q \rangle . \end{aligned} \quad (4.63)$$

We have the presence of NDR shift terms for  $G^{(0)}$  and  $G_{LR}^a$ ; on the contrary there are no shifts for  $G_{LR}^b$  and  $G_{LR}^c$ .

## 4.4 The Choice of the Input Parameters

We have seen that our results for the chiral lagrangian coefficients depend on some input parameters. They are the pion decay constant  $f_\pi$  (with which we have identified, at this stage, the chiral lagrangian parameter  $f$  and also  $f^{(0)}$ ), the quark and the gluon condensates, denoted respectively by  $\langle \bar{q}q \rangle$  and  $\langle \alpha_s GG/\pi \rangle$ . Moreover we have to consider the results dependence on the parameter  $M$ , which is characteristic of the chiral quark model.

For what concerns  $f_\pi$ , we know with a very good precision its experimental value (we take  $f_\pi = f_{\pi^+} = 92.4$  MeV). The situation is, instead, different for the two condensates, parametrizing the non perturbative part of the computation. We can try to give a phenomenological estimation of these two input parameters, by identifying them with the values of the condensates recovered in different models from the fitting of the experimental data. Of course we can not hope to obtain in this way an exact value for  $\langle \bar{q}q \rangle$  and  $\langle \alpha_s GG/\pi \rangle$ , but just to have a first rough estimation of the ranges of values that we can consider reasonable for these parameters.

In our numerical estimates in the next chapters we will vary the condensates within these ranges of values. We will see the final results are very sensitive functions of these input parameters. Fortunately we have at our disposal different processes to study and we can try to use them to restrict the range of values for the condensates and to investigate if for these choices of the parameters we are able to give a complete consistent description of kaon physics. In practice, as we will discuss in the following chapters, we can select a reasonable interval of values of  $\langle \bar{q}q \rangle$  and  $\langle \alpha_s GG/\pi \rangle$  for which we can fit in a satisfactory way the  $\Delta I = 1/2$  selection rule and we can use these values also for the determination of the ratio  $\varepsilon'/\varepsilon$  and the study of  $\Delta S = 2$  physics. In the case of  $\Delta S = 2$  processes, we can also see if the results obtained in this way for other observables (like the mass difference  $m_{K_L} - m_{K_S}$ ) are consistent with the experimental results.

Let us now start to consider separately the estimation of the quark and the gluon condensates.

#### 4.4.1 Gluon Condensate

For the gluon condensate, the most recent QCD-SR analysis [47], based on  $e^+e^-$  data, gives the scale independent result

$$\langle \frac{\alpha_s}{\pi} GG \rangle = (388 \pm 10 \text{ MeV})^4. \quad (4.64)$$

Such a value is consistent with older QCD-SR determinations [48] as well as with another recent one that finds [49]

$$\langle \frac{\alpha_s}{\pi} GG \rangle = (376 \pm 47 \text{ MeV})^4. \quad (4.65)$$

These values are systematically smaller than the central value of the lattice result [50]

$$\langle \frac{\alpha_s}{\pi} GG \rangle = (460 \pm 21 \text{ MeV})^4 \quad (4.66)$$

which however suffers of a systematic error that is difficult to evaluate. We will initially take (4.65) as the range to be explored in numerical estimates.

#### 4.4.2 Quark Condensate

The quark condensate is an important parameter in our computation, because it controls the size of the penguin contributions, in particular of the leading operator  $Q_6$ .

Unfortunately, the uncertainty about its value is large because of the sizable discrepancies among different estimates.

In the QCD-SR approach, the quark condensate can be determined from  $\Psi_5(q)$ , the two-point function of the hadronic axial current, as [51]

$$\begin{aligned}\Psi_5(0) &= -(m_u + m_d)\langle\bar{u}u + \bar{d}d\rangle \equiv 2f_\pi^2 m_\pi^2(1 - \delta_\pi) \\ &= (3.2 - 3.3) \times 10^8 \text{ MeV}^4.\end{aligned}\tag{4.67}$$

This estimate agrees with the most recent determination [52] of the parameter  $\delta_\pi$  that quantifies deviations from the PCAC result. Such deviations are of a few percents in (4.67) (but larger in the case of the strange-quark condensate).

These are scale independent values. To obtain the scale-dependent quark condensate, we use the renormalization-group running masses  $\bar{m}_u + \bar{m}_d$ , the value of which has been estimated at 1 GeV to be [52]

$$\bar{m}_u + \bar{m}_d = 12 \pm 2.5 \text{ MeV}\tag{4.68}$$

for  $\Lambda_{\text{QCD}}^{(3)} = 300 \pm 150 \text{ MeV}$ . The error in (4.68) reflects changes in the spectral functions. In our numerical estimates, we will take as input values the running masses at 1 GeV given by (4.68). Even though our preferred range of  $\Lambda_{\text{QCD}}^{(4)}$  (see eq. (4.3)) corresponds to  $\Lambda_{\text{QCD}}^{(3)} = 400 \pm 100 \text{ MeV}$ , we feel that we are not making too large an error, since this determination is not very sensitive to the choice of  $\Lambda_{\text{QCD}}$ .

By taking the value (4.68), we find for the scale-dependent (and normal-ordered) condensate

$$\langle\bar{q}q\rangle(\mu) = -\frac{f_\pi^2 m_\pi^2(1 - \delta_\pi)}{\bar{m}_u(\mu) + \bar{m}_d(\mu)},\tag{4.69}$$

the numerical values of

$$\langle\bar{q}q\rangle = -(238 \pm 19 \text{ MeV})^3\tag{4.70}$$

at  $\mu = 1 \text{ GeV}$  and

$$\langle\bar{q}q\rangle = -(222 \pm 19 \text{ MeV})^3\tag{4.71}$$

at 0.8 GeV. The error in Eqs. (4.70-4.71) is due to that in (4.68).

On the other hand, a recent determination of the quark condensate in lattice simulations with quenched Wilson fermions [53] finds a value of

$$\langle\bar{q}q\rangle = -(257 \pm 27 \text{ MeV})^3\tag{4.72}$$

at 1 GeV.



A similar simulation with dynamical staggered fermions [54] yields the rather large result

$$\langle \bar{q}q \rangle = -(380 \pm 7 \text{ MeV})^3, \quad (4.73)$$

which is probably an overestimate to be discarded for our purposes.

As we can see, while there is an overall consistency between QCD-SR and lattice simulations, the actual values for the quark condensate should be varied in the range

$$-(220 \text{ MeV})^3 \leq \langle \bar{q}q \rangle \leq -(280 \text{ MeV})^3 \quad (4.74)$$

in order to include QCD-SR and lattice estimates.

### 4.4.3 The parameter M

We have seen that, besides the quark and gluon condensates, our results still have a dependence on the value of M, which is the characteristic parameter of the chiral quark model.

This parameter appears in the term (3.28) of the chiral quark model lagrangian. We have seen that this term can be written in the form of a mass term for the rotated quark field Q. Therefore M may represent the mass of the constituent quark inside our Goldstone bosons. Considering this heuristic identification, we can expect to have the following order of magnitude for the parameter M :  $M \approx 200 \text{ MeV}$ , as consistently estimated in processes involving mesons. Such a value is smaller than the value  $M \simeq 330 \text{ MeV}$  often quoted, which originates from baryon physics.

As a matter of fact, in our numerical estimates we have taken M as a free parameter and we have tried to fit it, by minimizing the  $\gamma_5$  scheme dependence of our results. This is made possible by the fact that all the differences between the chiral lagrangian coefficients in HV and in NDR schemes are proportional to  $M^2/\Lambda_\chi^2$ . This way of proceeding will become clear when we analyze some specific physical process and in particular in the case of the study of the  $\Delta I = 1/2$  selection rule for  $K \rightarrow \pi\pi$  transitions and of  $\varepsilon'/\varepsilon$ .

## 4.5 Comments about the Results

We have seen in the previous sections that, by using the chiral quark model as a reference model, we have determined completely all the coefficients of the  $\Delta S = 1$  weak chiral lagrangian, both in NDR and in HV scheme. This, summarized in Eqs. (4.56-4.63), is one of the main results of this dissertation. In fact, in principle, it enables

us to compute in a quite easy way the amplitudes for each  $\Delta S = 1$  weak non leptonic process, independently from the number of particles which are involved. The power of this formalism will appear better in the next chapters, when we consider some specific applications. Anyway, let us discuss before the limits and the level of approximation of our results.

First of all we have to remember that our chiral lagrangian (4.18) is only given to the  $O(p^2)$  and any amplitude is expected to receive sizable corrections from higher order terms. In this work we have only added to the  $O(p^2)$  results for the amplitudes the  $O(p^4)$  corrections given from meson loop effects, as we will see in the next sections. Of course a complete analysis should include also other  $O(p^4)$  contributions, coming from the tree level lagrangian. These have been classified [42], but a direct computation of their coefficients, even in such a simple model as the  $\chi$ QM, is a rather formidable task. An estimate of the  $O(p^4)$  contributions to some matrix elements of  $Q_6$  has been given in ref. [45]. The NLO corrections vary from 10% to 30% depending on  $M$ . This is clearly a place where a future improvement is needed. This problem is already under our investigation, but it is really very complex and difficult to solve.

Another approximation we have made consists in keeping only the first term in the expansion in  $M^2/\Lambda_\chi^2$ , that is characteristic of the model.  $M^2/\Lambda_\chi^2$  is small enough to make us confident of our results. Anyway, insofar as the  $\chi$ QM is just a simple model, it is not clear whether going to the next order would result in a real improvement.

Finally, the chiral coefficients are given to  $O(1/N_c)$ . In this respect it is worth noticing that the quark operators  $Q_4$  and  $Q_6$  do not induce any  $O(1/N_c)$  correction to the coefficients. This happens because of kinematics and of the flavor singlet structure of the currents (which induces cancellations among  $u$  and  $d$  flavor exchange in the subleading configurations). As a consequence, gluonic corrections as well are absent for  $Q_4$  and  $Q_6$ , appearing first at  $O(1/N_c^2)$ . Similarly, no gluonic corrections appear for the operators  $Q_5$  and  $Q_7$  at  $O(1/N_c)$ , because of their color and chiral structures. Notice also that gluon corrections are in the form  $(1 - \delta_{(GG)})$  for  $LL$  operators and  $(1 + \delta_{(GG)})$  for those with  $LR$  current structure.

Let us come back to the results we have obtained. We can immediately apply them to the study of  $K \rightarrow \pi\pi$  transitions. This kind of process has a great physical relevance, as we will see in the next chapters, where we will study the  $\Delta I = 1/2$  rule and the determination of the ratio  $\varepsilon'/\varepsilon$ , which are related respectively to the real and the imaginary parts of these amplitudes.

To study these processes, we have to consider the amplitudes  $A_{00}$ ,  $A_{+-}$  and  $A_{+0}$ .

which are defined in the following way

$$A_{00} \equiv A(K^0 \rightarrow \pi^0 \pi^0), \quad A_{+-} \equiv A(K^0 \rightarrow \pi^+ \pi^-) \quad (4.75)$$

and

$$A_{+0} \equiv A(K^+ \rightarrow \pi^+ \pi^0). \quad (4.76)$$

These amplitudes can be related to the ones corresponding to a generic  $K \rightarrow \pi\pi$  transition with total final isospin  $I = 0$  or  $I = 2$  by using the appropriate  $SU(2)$  Clebsh-Gordan projections, given by

$$\begin{aligned} A_0 &= \sqrt{\frac{1}{6}}(A_{00} + 2A_{+-}) \\ A_2 &= \sqrt{\frac{1}{3}}(A_{+-} - A_{00}) = \frac{2}{\sqrt{3}}A_{+0}. \end{aligned} \quad (4.77)$$

Note that we will have to use  $A_0$  and  $A_2$  for the study of the  $\Delta I = 1/2$  rule.

We can notice that, up to this stage, we still have no scale dependence into our chiral lagrangian. On the other hand, we know the hadronic matrix elements should contain this  $\mu$  dependence, in such a way to compensate the analogous one present in the Wilson coefficients and to give scale independent results for the physical amplitudes. Within our model, we have chosen to introduce this  $\mu$  dependence by considering meson loop effects, following the idea proposed for the first time by Bardeen, Buras and Gérard [55, 18]. This step will be explained in the next section.

## 4.6 Meson Loop Corrections

As we have said, in our model the long-distance scale dependence of the hadronic matrix elements is contained, to this order, in the one-loop corrections induced by the propagation of mesons.

Until this point we have not considered this kind of contributions. In fact, recovering the coefficients of the chiral lagrangian with the chiral quark model calculation, we considered the propagation in the loop only of the constituent quark degrees of freedom. For this reason we have said that our  $\Delta S = 1$  weak chiral lagrangian can be seen as the effective theory of the chiral quark model after the integration of the quark degrees of freedom. As a consequence, the expressions we can obtain for the matrix elements by using the chiral lagrangian should be valid at a characteristic low scale (that we can identify for example with the parameter  $M$ ). To obtain the corresponding matrix

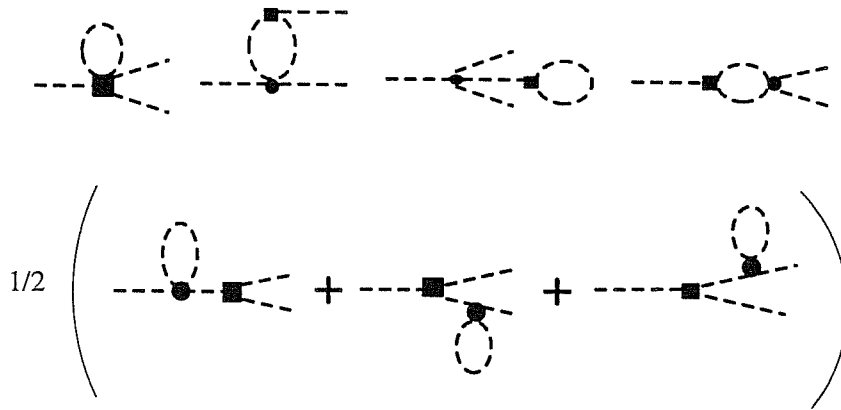


Figure 4.4: One-loop chiral renormalization of the the  $K^0 \rightarrow \pi\pi$  amplitudes. The black box represents the insertion of the weak chiral lagrangian, whereas the black circle denotes the insertion of the  $O(p^2)$  strong chiral lagrangian. For each chiral coefficient more than a hundred diagrams are generated by propagating in all allowed ways  $K$ ,  $\pi$  and  $\eta$ .

elements at a higher scale (typically around 1 GeV) at which we can match them with the short distance calculation, we have to include the corrections given by loop diagrams in which we consider the propagation of the only degrees of freedom left in the theory, that are the octet of pseudoscalar mesons. Their effect is important and moreover it is essential in the matching procedure between Wilson coefficients and matrix elements that is central in our approach.

The computation is rather involved because of the many terms that we have to consider. The diagrams (see Fig. 4) include the vertex as well as the wave-function one-loop renormalization (see Appendix C for the Feynman rules).

We give the final results for the meson loop renormalization of the matrix elements for the three processes in (4.75-4.76). We have formally factorized out the contribution to the tree-level amplitude of each term of the chiral lagrangian as a function of the input parameters, while the corresponding loop renormalization is given in the form of numerical coefficients. These numerical coefficients are complicated functions of the masses and the coupling constants. They are made of polynomial terms, generally of the order of

$$\frac{m^2}{(4\pi f)^2}, \quad (4.78)$$

and logarithmic terms of the order of

$$\frac{m^2}{(4\pi f)^2} \ln \frac{m_a^2}{m_b^2}, \quad (4.79)$$

where the masses can be any among  $m_\pi$ ,  $m_K$  and  $m_\eta$ . The values of the masses and other input variables are those given in table B.1 of appendix B.

Let us recall here that the leading-log approximation would be particularly crude in this case, since the large mass separation between  $m_\eta$  and  $m_\pi$  makes the renormalization group scale particularly uncertain. The resulting corrected amplitudes for  $K^0 \rightarrow \pi^0\pi^0$  and  $K^0 \rightarrow \pi^+\pi^-$  are given by:

$$\begin{aligned}
a_{00}(Q_i) = & -\frac{\sqrt{2}}{f^3} G_0(Q_i) (0.904 + 0.444 i + 0.255 \ln \mu^2) \\
& -\frac{\sqrt{2}}{f^3} (m_K^2 - m_\pi^2) \left[ G_{LL}^a(Q_i) (0.367 + 0.444 i + 0.0747 \ln \mu^2) \right. \\
& \quad - G_{LL}^b(Q_i) (1 + 0.349 + 0.0184 i + 0.135 \ln \mu^2) \\
& \quad - G_{\underline{8}}(Q_i) (1 + 0.716 + 0.463 i + 0.210 \ln \mu^2) \\
& \quad \left. + G_{LR}^b(Q_i) (1 + 0.349 + 0.0184 i + 0.135 \ln \mu^2) \right] \\
& -\frac{\sqrt{2}}{f^3} m_\pi^2 G_{LR}^a(Q_i) (0.868 + 0.444 i - 0.132 \ln \mu^2) \\
& +\frac{\sqrt{2}}{f^3} m_K^2 G_{LR}^c(Q_i) (0.719 + 0.444 i + 0.203 \ln \mu^2) \tag{4.80}
\end{aligned}$$

and

$$\begin{aligned}
a_{+-}(Q_i) = & -\frac{\sqrt{2}}{f^3} G_0(Q_i) (1 + 0.708 + 0.240 i + 0.203 \ln \mu^2) \\
& -\frac{\sqrt{2}}{f^3} (m_K^2 - m_\pi^2) \left[ G_{LL}^a(Q_i) (1 + 0.768 + 0.240 i + 0.278 \ln \mu^2) \right. \\
& \quad + G_{LL}^b(Q_i) (0.0525 - 0.222 i + 0.0688 \ln \mu^2) \\
& \quad - G_{\underline{8}}(Q_i) (1 + 0.716 + 0.463 i + 0.210 \ln \mu^2) \\
& \quad \left. - G_{LR}^b(Q_i) (0.000127 - 0.222 i + 0.0583 \ln \mu^2) \right] \\
& -\frac{\sqrt{2}}{f^3} m_\pi^2 G_{LR}^a(Q_i) (1 + 4.17 + 0.240 i + 1.29 \ln \mu^2) \\
& +\frac{\sqrt{2}}{f^3} m_K^2 G_{LR}^c(Q_i) (1 + 3.47 + 0.240 i + 1.40 \ln \mu^2) . \tag{4.81}
\end{aligned}$$

where all dimensionfull parameters must be taken in units of GeV.

The renormalization at any scale  $\mu$  can be readily obtained from Eqs. (4.80) and (4.81).

As a useful check we have also computed directly the meson loop renormalization for the amplitude  $K^+ \rightarrow \pi^+\pi^0$ , which is a pure  $\Delta I = 3/2$  transition:

$$\begin{aligned}
a_{+0}(Q_i) = & -\frac{1}{f^3} G_0(Q_i) \left(1 - 0.196 - 0.204 i - 0.0510 \ln \mu^2\right) \\
& -\frac{1}{f^3} (m_K^2 - m_\pi^2) \left[ G_{LL}^a(Q_i) \left(1 + 0.402 - 0.204 i + 0.204 \ln \mu^2\right) \right. \\
& \quad + G_{LL}^b(Q_i) \left(1 + 0.402 - 0.204 i + 0.204 \ln \mu^2\right) \\
& \quad \left. - G_{LR}^b(Q_i) \left(1 + 0.349 - 0.204 i + 0.193 \ln \mu^2\right) \right] \\
& -\frac{1}{f^3} m_\pi^2 G_{LR}^a(Q_i) \left(1 + 3.30 - 0.204 i + 1.42 \ln \mu^2\right) \\
& +\frac{1}{f^3} m_K^2 G_{LR}^c(Q_i) \left(1 + 2.75 - 0.204 i + 1.20 \ln \mu^2\right) . \tag{4.82}
\end{aligned}$$

This last equation is useful to verify that our result satisfies all the expected symmetry properties, that is

$$A_{+-} = A_{00} \tag{4.83}$$

for the octet amplitudes, and

$$A_{+0} = \frac{A_{+-} - A_{00}}{\sqrt{2}} \tag{4.84}$$

for the other parts. The fact that (4.83-4.84) are exactly satisfied for all coefficients makes us confident on our results.

Of course, the polynomial parts of these corrections receive contributions at the tree level from the next order terms in the chiral lagrangian. These are controlled by the two parameters  $K_1$  and  $K_4$  defined in reference [22], where they are estimated to be

$$\begin{aligned}
K_1 &= (0.4 \pm 1.2) \times 10^{-11} \\
K_4 &= (0.3 \pm 1.4) \times 10^{-12} . \tag{4.85}
\end{aligned}$$

A similar result was obtained for  $K_1$  in the framework of the  $\chi$ QM in [45].

These values correspond to a renormalization of the amplitudes  $A_0$  and  $A_2$  at the percent level, which is an order of magnitude smaller than the renormalization induced by chiral loops.

Let us remember that our approach differs from the one usually adopted in chiral perturbation theory (like for instance in the case of the strong chiral lagrangian), in the sense that we assume there is no scale dependence in the tree level  $O(p^4)$  terms of our chiral lagrangian. So, contrary to the usual treatment, in our approach these

next-to-leading-order contributions do not cancel the scale dependence of the chiral loops:

On top of this renormalization, we should also include the one-loop determination of  $f$  in terms of  $f_\pi$  and  $f_K$ . This is taken into account in our computation by replacing  $f$  by the one-loop renormalized value

$$f_1 = 0.087 \text{ GeV [23]} \quad (4.86)$$

in the tree level amplitudes.

Some of the loop renormalizations (the last two terms in (4.80-4.82)) appear to be large when compared to the partial tree level amplitudes we have factorized out. This is a notational artifact since anyway they remain always smaller than the leading tree level amplitude ( $\sim \sqrt{2}/f^3$ ). The overall renormalization is large but still under control. As a matter of fact, it is large in the  $I = 0$  channel and small in the  $I = 2$  one (except for the subleading  $LR$  momentum corrections), thus distributing itself in the right amount to bring the matrix elements of  $K \rightarrow \pi\pi$  transitions closer to their experimental values (as we will see in the next chapter).

In refs. [55, 18, 56] a similar computation was performed by means of a cut-off regularization, identifying then the cut-off with the dimensional regularization scale of the Wilson coefficients. The two approaches lead to different results. Among else, the meson loop renormalization of the amplitude  $A_2$  is strikingly different, being suppressed in [55, 18, 56], whereas it is slightly enhanced in our approach.

Our choice to use dimensional regularization in dealing with the divergent chiral loop integrals is motivated by the fact that this regularization technique is adopted in the short distance calculation of the Wilson coefficients.





# Chapter 5

## The $\Delta I = 1/2$ Selection Rule

### 5.1 Status of the $\Delta I = 1/2$ Rule

The chiral lagrangian we have derived in the last chapter can be used, in principle, to study any  $\Delta S = 1$  weak non leptonic process. As a first significative example, we consider the problem of giving a satisfactory theoretical explanation of the so called  $\Delta I = 1/2$  selection rule.

This very famous rule was discovered more than forty years ago [4], by studying the kaon decays into pions. It was observed that the decay rate of the process  $K^+ \rightarrow \pi^+\pi^0$  was highly suppressed with respect to that of  $K_S^0 \rightarrow \pi\pi$ . The decay  $K^+ \rightarrow \pi^+\pi^0$  is a pure  $\Delta I = 3/2$  transition (where  $\Delta I$  is the difference between the total isospins of the final and the initial states). The decays  $K_S^0 \rightarrow \pi\pi$ , instead, contain both the  $\Delta I = 3/2$  and the  $\Delta I = 1/2$  components. Hence the experimental result was a clear indication of the suppression of the  $\Delta I = 3/2$  channel in these weak non-leptonic decays of kaons.

According to the last edition of the Particle Data Book [10], the experimental amplitude for the decay of a kaon into two pions in which the two pions are in the isospin state  $I = 0$  (and  $\Delta I = 1/2$ ) is:

$$\text{Re } A_0(K^0 \rightarrow 2\pi) = 3.33 \times 10^{-7} \text{ GeV}. \quad (5.1)$$

It is approximately 22 times larger than the amplitude in which the pions are in the state  $I = 2$  (and  $\Delta I = 3/2$ ):

$$\text{Re } A_2(K^0 \rightarrow 2\pi) = 1.50 \times 10^{-8} \text{ GeV}. \quad (5.2)$$

This  $\Delta I = 1/2$  enhancement is also present in  $K \rightarrow 3\pi$  and non leptonic hyperon decays, but it is not always effective in other processes. This effect does not appear, for

instance, in the  $K \rightarrow \pi l^+ l^-$  transition and in the radiative decay  $K^+ \rightarrow \pi^+ \pi^0 \gamma$ , which can have a  $\Delta I = 1/2$  component (because here, due to the presence of the photon,  $\pi^+ \pi^0$  can be also in the  $I = 1$  isospin state). This observation suggests that the  $\Delta I = 1/2$  rule in kaon decays is most likely of dynamical origin, rather than a consequence of the intrinsic structure of the  $\Delta S = 1$  weak hamiltonian.

It is important to remember that a simple computation in the Standard Model, in the absence of QCD corrections, gives two results for the  $\Delta I = 1/2$  and the  $\Delta I = 3/2$  amplitudes ( $A_0$  and  $A_2$ ) which are comparable in size. So we can easily understand that the explanation of this selection rule has been a standing enigma, the solution of which has attracted a great deal of theoretical work over the past 40 years (for a review see, for instance, ref. [5]).

We can mention, without any pretense of completeness, some of the most important steps that have been historically done towards a better understanding of this rule.

Wilson was the first to suggest [57] that the introduction of short distance strong interaction corrections could enhance the  $\Delta I = 1/2$  amplitude. The following important works of Gaillard–Lee [58] and Altarelli–Maiani [59] showed the perturbative QCD effect is in the right direction, even if it is not at all sufficient to explain the total  $\Delta I = 1/2$  enhancement. Later, Vainshtein, Zakharov and Shifman [30] suggested the very important idea that the gluon penguin operators could be a source of enhancement of  $A_0$  with respect to  $A_2$ . This fundamental idea was improved by the work of various authors [60] who correctly estimated the size of this contribution.

At the same time, a parallel development took place, as Cohen–Manohar [63] first pointed out the relevance for the selection rule of meson-loop corrections in a chiral quark model computation. This loop effect was estimated by Bardeen–Buras–Gerard [18, 55] in a different approach, based on the  $1/N_c$  expansion, with the meson loops regularized by a cutoff, and, more recently, by Kambor–Missimer–Wyler [22] in chiral perturbation theory.

All these improvements can be considered milestones in the way toward a better theoretical understanding of the  $\Delta I = 1/2$  rule. Nevertheless we can say that they are still far to be sufficient for a complete comprehension of the origin of this rule, as we will see in the last section of this chapter.

To summarize the present status of our knowledge we can divide, as usual, the analysis in two parts : the perturbative short distance problem of the Wilson coefficients determination and the long distance part of the analysis, that is the hadronic matrix elements computation. For what concerns the Wilson coefficients, the existing results

are already satisfactory and we have only updated the existing analyses, by including next-to-leading order results (see ref. [16] and the last paper of ref. [15]) and evaluating the Wilson coefficients at various hadronic scales for the updated range of  $\Lambda_{\text{QCD}}^{(4)}$  that we have quoted in eq. (4.3). Therefore, it is clear the main uncertainty resides in the second ingredient: the evaluation of hadronic matrix elements. The vacuum saturation approximation (VSA) is not sufficient, because non-factorizable and non-perturbative effects are essential in a dynamical explanation of the rule, and a model for QCD at low energies is called for in order to make progress in this direction.

In this chapter we will use our  $\Delta S = 1$  chiral lagrangian to try to solve this problem and we will show that it is possible to explain the  $\Delta I = 1/2$  selection rule in a quite satisfactory way, within the Standard Model and by our present understanding of its non perturbative aspects.

We will see that there are essentially two points in which our model differs from the VSA and both of them are fundamental to reach a better agreement between the theoretical prediction and the experimental results. We refer to the insertion of non perturbative gluonic effects and of meson-loop renormalization. The effect of the non factorizable gluonic corrections is basically that of giving the desired suppression of the  $A_2$  amplitude. The addition of mesonic chiral loops, instead, causes the needed enhancement of the  $A_0$  amplitude, while little affecting  $A_2$ . It also introduces in the matrix elements a scale dependence, which is requested to make the matching with the Wilson coefficients consistent, as we have already explained.

At the end of this chapter we will discuss in the details the way in which all these cumulative effects combine to give the final results for the physical amplitude. Let us now start the analysis of the  $\Delta I = 1/2$  rule, by reporting the relevant hadronic matrix elements for the transition  $K \rightarrow \pi\pi$ , which we have recovered [14] by using our  $\Delta S = 1$  chiral lagrangian, as explained in the previous chapter.

## 5.2 Hadronic Matrix Elements for $K \rightarrow \pi\pi$ in the Chiral Quark Model

To analyze the transition  $K \rightarrow \pi\pi$  we have to start from the effective  $\Delta S = 1$  quark lagrangian at a scale  $\mu < m_c$ , which is given by eq. (4.1). The four-quark  $Q_i$  operators are given by the eqs. (2.12), (2.13) and (2.14). We report here the results obtained in our model for the matrix elements of these operators, by writing directly the expressions

for the two isospin states

$$\langle Q_i \rangle_{0,2} \equiv \langle 2\pi, I = 0, 2 | Q_i | K^0 \rangle. \quad (5.3)$$

They include all contributions of order  $O(N_c^2)$ ,  $O(N_c)$  and also the gluonic contributions, which are  $O(\alpha_s N_c)$ . As already said, we have used dimensional regularization and, in dealing with the  $\gamma_5$  matrices, we have worked in both the HV and the NDR schemes. To these matrix elements we have already added the corresponding one-loop meson corrections, denoted by  $a_{0,2}(Q_i)$ , which can be obtained from eqs. (4.80)–(4.82), by using the Clebsh-Gordan coefficients for the isospin projections of eq. (4.77).

### 5.2.1 HV Results

We recall that in the HV scheme one may rely on Fierz transformations and use the factorized building blocks when computing the chiral coefficients. Fake HV anomalies must then be subtracted according to the discussion in chapter 4.

So in the t'Hooft-Veltman scheme we obtain the following expressions for the hadronic matrix elements:

$$\langle Q_1 \rangle_0 = \frac{1}{3}X \left[ -1 + \frac{2}{N_c} (1 - \delta_{GG}) \right] + a_0(Q_1) \quad (5.4)$$

$$\langle Q_1 \rangle_2 = \frac{\sqrt{2}}{3}X \left[ 1 + \frac{1}{N_c} (1 - \delta_{GG}) \right] + a_2(Q_1) \quad (5.5)$$

$$\langle Q_2 \rangle_0 = \frac{1}{3}X \left[ 2 - \frac{1}{N_c} (1 - \delta_{GG}) \right] + a_0(Q_2) \quad (5.6)$$

$$\langle Q_2 \rangle_2 = \frac{\sqrt{2}}{3}X \left[ 1 + \frac{1}{N_c} (1 - \delta_{GG}) \right] + a_2(Q_2) \quad (5.7)$$

$$\langle Q_3 \rangle_0 = \frac{1}{N_c}X (1 - \delta_{GG}) + a_0(Q_3) \quad (5.8)$$

$$\langle Q_4 \rangle_0 = X + a_0(Q_4) \quad (5.9)$$

$$\langle Q_5 \rangle_0 = \frac{2}{N_c} \frac{\langle \bar{q}q \rangle}{M f_\pi^2} X' + a_0(Q_5) \quad (5.10)$$

$$\langle Q_6 \rangle_0 = 2 \frac{\langle \bar{q}q \rangle}{M f_\pi^2} X' + a_0(Q_6) \quad (5.11)$$

$$\begin{aligned} \langle Q_7 \rangle_0 &= \frac{2\sqrt{3}}{N_c} \frac{\langle \bar{q}q \rangle^2}{f_\pi^3} - \frac{1}{N_c} \frac{\langle \bar{q}q \rangle}{M f_\pi^2} X' \\ &\quad - \frac{2}{N_c} \frac{\langle \bar{q}q \rangle}{M f_\pi^2} Y + \frac{1}{2}X + a_0(Q_7) \end{aligned} \quad (5.12)$$

$$\langle Q_7 \rangle_2 = \sqrt{6} \frac{\langle \bar{q}q \rangle^2}{f_\pi^3} \frac{1}{N_c} - \frac{\sqrt{2} \langle \bar{q}q \rangle}{N_c M f_\pi^2} Y - \frac{\sqrt{2}}{2} X + a_2(Q_7) \quad (5.13)$$

$$\begin{aligned} \langle Q_8 \rangle_0 &= 2\sqrt{3} \frac{\langle \bar{q}q \rangle^2}{f_\pi^3} - \frac{\langle \bar{q}q \rangle}{M f_\pi^2} X' \\ &\quad - 2 \frac{\langle \bar{q}q \rangle}{M f_\pi^2} Y + \frac{1}{2N_c} X (1 + \delta_{(GG)}) + a_0(Q_8) \end{aligned} \quad (5.14)$$

$$\langle Q_8 \rangle_2 = \sqrt{6} \frac{\langle \bar{q}q \rangle^2}{f_\pi^3} - \sqrt{2} \frac{\langle \bar{q}q \rangle}{M f_\pi^2} Y - \frac{\sqrt{2}}{2N_c} X (1 + \delta_{(GG)}) + a_2(Q_8) \quad (5.15)$$

$$\langle Q_9 \rangle_0 = -\frac{1}{2} X \left[ 1 - \frac{1}{N_c} (1 - \delta_{(GG)}) \right] + a_0(Q_9) \quad (5.16)$$

$$\langle Q_9 \rangle_2 = \frac{\sqrt{2}}{2} X \left[ 1 + \frac{1}{N_c} (1 - \delta_{(GG)}) \right] + a_2(Q_9) \quad (5.17)$$

$$\langle Q_{10} \rangle_0 = \frac{1}{2} X \left[ 1 - \frac{1}{N_c} (1 - \delta_{(GG)}) \right] + a_0(Q_{10}) \quad (5.18)$$

$$\langle Q_{10} \rangle_2 = \frac{\sqrt{2}}{2} X \left[ 1 + \frac{1}{N_c} (1 - \delta_{(GG)}) \right] + a_2(Q_{10}). \quad (5.19)$$

where

$$X \equiv \sqrt{3} f_\pi (m_K^2 - m_\pi^2), \quad X' = X \left( 1 - 6 \frac{M^2}{\Lambda_X^2} \right) \quad (5.20)$$

and

$$Y \equiv \sqrt{3} f_\pi \left[ m_\pi^2 + 3 m_K^2 \frac{M^2}{\Lambda_X^2} \right]; \quad (5.21)$$

$\delta_{(GG)}$  is given by (4.25).

## 5.2.2 NDR Results

In the naive dimensional regularization scheme we are not allowed to Fierz transform the quark operators, and we must resort to the direct computation of the unfactorized two-loop diagrams. On the other hand, we need not worry about chiral anomalies as in the HV scheme and no subtraction is required. We thus find:

$$\langle Q_1 \rangle_0 = \frac{1}{3} X \left[ -1 + \frac{2}{N_c} (1 - \delta_{(GG)}) \right] + a_0(Q_1) \quad (5.22)$$

$$\langle Q_1 \rangle_2 = \frac{\sqrt{2}}{3} X \left[ 1 + \frac{1}{N_c} (1 - \delta_{(GG)}) \right] + a_2(Q_1) \quad (5.23)$$

$$\langle Q_2 \rangle_0 = \frac{1}{3} X \left[ 2 - \frac{1}{N_c} (1 - \delta_{(GG)}) \right] + a_0(Q_2) \quad (5.24)$$

$$\langle Q_2 \rangle_2 = \frac{\sqrt{2}}{3} X \left[ 1 + \frac{1}{N_c} (1 - \delta_{(GG)}) \right] + a_2(Q_2) \quad (5.25)$$

$$\langle Q_3 \rangle_0 = \frac{1}{N_c} (X' - \delta_{(GG)} X) + a_0(Q_3) \quad (5.26)$$

$$\langle Q_4 \rangle_0 = X' + a_0(Q_4) \quad (5.27)$$

$$\langle Q_5 \rangle_0 = \frac{2}{N_c} \frac{\langle \bar{q}q \rangle}{M f_\pi^2} X'' + a_0(Q_5) \quad (5.28)$$

$$\langle Q_6 \rangle_0 = 2 \frac{\langle \bar{q}q \rangle}{M f_\pi^2} X'' + a_0(Q_6) \quad (5.29)$$

$$\begin{aligned} \langle Q_7 \rangle_0 &= \frac{2\sqrt{3}}{N_c} \frac{\langle \bar{q}q \rangle^2}{f_\pi^3} \left( 1 - 3 \frac{M^3 f_\pi^2}{\langle \bar{q}q \rangle \Lambda_\chi^2} \right) - \frac{1}{N_c} \frac{\langle \bar{q}q \rangle}{M f_\pi^2} X'' \\ &\quad - \frac{2}{N_c} \frac{\langle \bar{q}q \rangle}{M f_\pi^2} Y' + \frac{1}{2} X + a_0(Q_7) \end{aligned} \quad (5.30)$$

$$\begin{aligned} \langle Q_7 \rangle_2 &= \frac{1}{N_c} \sqrt{6} \frac{\langle \bar{q}q \rangle^2}{f_\pi^3} \left( 1 - 3 \frac{M^3 f_\pi^2}{\langle \bar{q}q \rangle \Lambda_\chi^2} \right) \\ &\quad - \frac{\sqrt{2}}{N_c} \frac{\langle \bar{q}q \rangle}{M f_\pi^2} Y' - \frac{\sqrt{2}}{2} X + a_2(Q_7) \end{aligned} \quad (5.31)$$

$$\begin{aligned} \langle Q_8 \rangle_0 &= 2\sqrt{3} \frac{\langle \bar{q}q \rangle^2}{f_\pi^3} \left( 1 - 3 \frac{M^3 f_\pi^2}{\langle \bar{q}q \rangle \Lambda_\chi^2} \right) - \frac{\langle \bar{q}q \rangle}{M f_\pi^2} X'' \\ &\quad - 2 \frac{\langle \bar{q}q \rangle}{M f_\pi^2} Y' + \frac{1}{2N_c} X (1 + \delta_{(GG)}) + a_0(Q_8) \end{aligned} \quad (5.32)$$

$$\begin{aligned} \langle Q_8 \rangle_2 &= \sqrt{6} \frac{\langle \bar{q}q \rangle^2}{f_\pi^3} \left( 1 - 3 \frac{M^3 f_\pi^2}{\langle \bar{q}q \rangle \Lambda_\chi^2} \right) \\ &\quad - \sqrt{2} \frac{\langle \bar{q}q \rangle}{M f_\pi^2} Y' - \frac{\sqrt{2}}{2N_c} X (1 + \delta_{(GG)}) + a_2(Q_8) \end{aligned} \quad (5.33)$$

$$\langle Q_9 \rangle_0 = -\frac{1}{2} \left[ X - \frac{1}{N_c} (2X - X' - \delta_{(GG)} X) \right] + a_0(Q_9) \quad (5.34)$$

$$\langle Q_9 \rangle_2 = \frac{\sqrt{2}}{2} X \left[ 1 + \frac{1}{N_c} (1 - \delta_{(GG)}) \right] + a_2(Q_9) \quad (5.35)$$

$$\langle Q_{10} \rangle_0 = \frac{1}{2} \left[ 2X - X' - \frac{1}{N_c} (1 - \delta_{(GG)}) X \right] + a_0(Q_{10}) \quad (5.36)$$

$$\langle Q_{10} \rangle_2 = \frac{\sqrt{2}}{2} X \left[ 1 + \frac{1}{N_c} (1 - \delta_{(GG)}) \right] + a_2(Q_{10}), \quad (5.37)$$

where

$$X'' = X \left( 1 - 9 \frac{M^2}{\Lambda_\chi^2} \right), \quad Y' \equiv \sqrt{3} f_\pi \left[ m_\pi^2 + 3 (m_K^2 - m_\pi^2) \frac{M^2}{\Lambda_\chi^2} \right]. \quad (5.38)$$

$\langle Q_i \rangle_2 = 0$  for  $i = 3, 4, 5, 6$  in both schemes.

The equations above show the importance of the corrections of  $O(\alpha_s N_c)$  (parameterized by the value of the gluonic condensate) as well as of the meson-loop renormal-

izations. In the limit  $\delta_{(GG)} \rightarrow 0$  and zero meson-loop renormalization, the HV hadronic matrix elements are the same as those found in the  $1/N_c$  approach, except for the  $(V - A) \times (V + A)$  operators  $Q_5$ ,  $Q_6$ ,  $Q_7$  and  $Q_8$ , for which the detailed form of the matrix elements is characteristic of the model employed. For instance, by means of eq. (4.17), we find

$$\langle Q_6 \rangle_0 = -4 \frac{\langle \bar{q}q \rangle^2}{f_\pi^4 \Lambda_\chi^2} X \quad (5.39)$$

in the  $1/N_c$  computation, where we used

$$c_1 + c_2 = \left( \frac{f_K}{f_\pi} - 1 \right) \frac{\Lambda_\chi^2}{m_K^2 - m_\pi^2} \quad (5.40)$$

as determined from  $\mathcal{A}(K^+ \rightarrow \mu^+ \nu_\mu) / \mathcal{A}(\pi^+ \rightarrow \mu^+ \nu_\mu)$  [41, 61, 62]. Eq. (5.39) shows the quadratic dependence on the quark condensate which is distinctive of such an approach.

To our knowledge the terms proportional to  $Y$  and  $Y'$  in the matrix elements of  $Q_7$  and  $Q_8$  have been neglected so far. As an example, in the  $1/N_c$  framework we find for the matrix element  $\langle Q_8 \rangle_2$ :

$$\langle Q_8 \rangle_2 = \sqrt{6} \frac{\langle \bar{q}q \rangle^2}{f_\pi^3} + 2\sqrt{6} \frac{\langle \bar{q}q \rangle^2}{f_\pi^3 \Lambda_\chi^2} [(c_1 - c_2) m_\pi^2 - c_2 m_K^2] - \frac{\sqrt{2}}{2N_c} X, \quad (5.41)$$

where the absolute values of  $c_1$  and  $c_2$  remain undetermined (only their sum is determined by eq. (5.40)). Analogous contributions appear in the matrix elements of  $Q_7$ . The matrix element (5.41) corresponds to the  $1/N_c$  determination of the chiral coefficients

$$G_{LR}^a = -6 \frac{\langle \bar{q}q \rangle^2}{\Lambda_\chi^2} (c_1 - c_2) \quad \text{and} \quad G_{LR}^c = -6 \frac{\langle \bar{q}q \rangle^2}{\Lambda_\chi^2} c_2, \quad (5.42)$$

to be contrasted to that of the  $\chi$ QM in eqs. (4.59) and (4.63). In particular, the  $\chi$ QM determination of  $G_{LR}^a$  and  $G_{LR}^c$  gives  $c_2 / (c_1 - c_2) \sim O(M^2 / \Lambda_\chi^2)$ , thus making the term proportional to  $m_K^2$  of the same order of magnitude of that proportional to  $m_\pi^2$ .

These additional contributions do not affect the estimate of the  $\Delta I = 1/2$  rule, which is little sensitive to the electroweak penguin operators  $Q_{7-10}$  (due to the smallness of their Wilson coefficients), anyway they have an impact on the determination of  $\varepsilon' / \varepsilon$  [29].

We have said the most relevant operators for the analysis of the  $\Delta I = 1/2$  rule are  $Q_1$ ,  $Q_2$  and the gluonic penguins (especially  $Q_6$ ). So, by a simple inspection of the formulas that we have given for the matrix elements in both schemes, we can have an immediate confirmation of the fact that the gluonic correction determine an important suppression of the  $A_2$  amplitude. In fact we have

$$A_2 \approx (z_1 + z_2) \left[ 1 + \frac{1}{N_c} (1 - \delta_{(GG)}) \right] \quad (5.43)$$

and by taking  $\delta_{\langle GG \rangle} \simeq 3$ , that is what we obtain for the central value of the gluon condensate (see eq. (5.44) below), the correction is large enough to revert the sign of the  $1/N_c$  term and thus suppress the amplitude.

For what concerns  $A_0$ , a relevant contribution to this amplitude arises from the gluonic penguins  $Q_{5,6}$ , whose matrix elements are directly proportional to the value of  $\langle \bar{q}q \rangle$  and are controlled by  $M$ , through the suppression factors in (5.20) and (5.38), that make their matrix elements larger for smaller values of  $M$ .

### 5.3 Wilson Coefficients

In this section we simply report the values of the functions  $z_i(\mu)$  and  $y_i(\mu)$ , which are the Wilson coefficients of the quark operators  $Q_i$  of the effective  $\Delta S = 1$  lagrangian of eq. (4.1). Of course, the numerical value of these Wilson coefficients depends on  $\alpha_s$ , and we have considered for the QCD coupling constant the range of values given by eqs. (4.2)–(4.3).

In tables 1 and 2 we give explicitly the Wilson coefficients of the ten operators at the scale  $\mu = 0.8$  GeV in the naive dimensional regularization (NDR) and 't Hooft-Veltman (HV)  $\gamma_5$ -scheme, respectively. Tables 3 and 4 are identical to the previous ones, apart from the fact that they are obtained for  $\mu = 1$  GeV, instead of  $\mu = 0.8$  GeV. Since  $\text{Re} \tau = O(10^{-3})$ , the  $CP$ -conserving  $\Delta S = 1$  transitions are controlled by the coefficients  $z_i$ , which do not depend on  $m_t$ .



$\Lambda_{QCD}^{(4)}$	250 MeV		350 MeV		450 MeV	
$\alpha_s(m_Z)_{\overline{MS}}$	0.113		0.119		0.125	
$z_1$	(0.0503)	-0.524	(0.0533)	-0.663	(0.0557)	-0.781
$z_2$	(0.982)	1.29	(0.981)	1.39	(0.980)	1.48
$z_3$		0.0180		0.0360		0.0870
$z_4$		-0.0471		-0.0852		-0.182
$z_5$		0.0085		0.0077		-0.0129
$z_6$		-0.0495		-0.0947		-0.226
$z_7/\alpha$		0.0073		0.0204		0.0366
$z_8/\alpha$		0.0280		0.0589		0.143
$z_9/\alpha$		0.0206		0.0441		0.0779
$z_{10}/\alpha$		-0.0159		-0.0267		-0.0438
$y_3$	(0.0017)	0.0294	(0.0018)	0.0373	(0.0018)	0.0422
$y_4$	(-0.0019)	-0.0493	(-0.0021)	-0.0569	(-0.0022)	-0.0603
$y_5$	(0.0007)	-0.0014	(0.0007)	-0.0167	(0.0007)	-0.0708
$y_6$	(-0.0019)	-0.104	(-0.0021)	-0.171	(-0.0022)	-0.353
$y_7/\alpha$	(0.149)	-0.0138	(0.149)	-0.0156	(0.149)	-0.0274
$y_8/\alpha$	(0)	0.189	(0)	0.294	(0)	0.511
$y_9/\alpha$	(-1.22)	-1.81	(-1.22)	-2.03	(-1.22)	-2.42
$y_{10}/\alpha$	(0)	0.819	(0)	1.11	(0)	1.60

Table 5.1: NLO Wilson coefficients at  $\mu = 0.8$  GeV in the NDR scheme for  $\bar{m}_t(m_W) = 183$  GeV, which corresponds to  $m_t^{pole} = 180$  GeV. The corresponding values at  $\mu = m_W$  are given in parenthesis ( $\alpha = 1/128$ ). In addition one has  $y_{1,2}(\mu) = 0$ . The coefficients  $z_i(\mu)$  do not depend on  $m_t$ .

$\Lambda_{QCD}^{(4)}$	250 MeV		350 MeV		450 MeV	
$\alpha_s(m_Z)_{\overline{MS}}$	0.113		0.119		0.125	
$z_1$	(0.0320)	-0.657	(0.0339)	-0.910	(0.0355)	-1.36
$z_2$	(0.988)	1.38	(0.987)	1.58	(0.987)	1.96
$z_3$		0.0137		0.0301		0.0798
$z_4$		-0.0292		-0.0540		-0.115
$z_5$		0.0070		0.0100		0.0123
$z_6$		-0.0275		-0.0515		-0.112
$z_7/\alpha$		-0.0055		-0.0030		-0.0065
$z_8/\alpha$		0.0198		0.0379		0.0827
$z_9/\alpha$		0.0070		0.0203		0.0415
$z_{10}/\alpha$		-0.0181		-0.0330		-0.0644
$y_3$	(0.0007)	0.0338	(0.0007)	0.0456	(0.0007)	0.0602
$y_4$	(0.0011)	-0.0522	(0.0012)	-0.0626	(0.0012)	-0.0741
$y_5$	(-0.0004)	0.0140	(-0.0004)	0.0192	(-0.0004)	0.0397
$y_6$	(0.0011)	-0.0904	(0.0012)	-0.137	(0.0012)	-0.242
$y_7/\alpha$	(0.172)	-0.0131	(0.172)	-0.0111	(0.172)	-0.0039
$y_8/\alpha$	(0)	0.209	(0)	0.327	(0)	0.583
$y_9/\alpha$	(-1.19)	-1.82	(-1.19)	-2.04	(-1.19)	-2.45
$y_{10}/\alpha$	(0)	0.835	(0)	1.14	(0)	1.66

Table 5.2: Same as in table 1 in the HV scheme.

$\Lambda_{QCD}^{(4)}$	250 MeV		350 MeV		450 MeV	
$\alpha_s(m_Z)_{\overline{MS}}$	0.113		0.119		0.125	
$z_1$	(0.0503)	-0.440	(0.0533)	-0.535	(0.0557)	-0.644
$z_2$	(0.982)	1.23	(0.981)	1.30	(0.980)	1.37
$z_3$		0.00995		0.0161		0.0283
$z_4$		-0.0281		-0.0432		-0.0703
$z_5$		0.00667		0.0083		0.0088
$z_6$		-0.0281		-0.0438		-0.0730
$z_7/\alpha$		0.0039		0.0122		0.0218
$z_8/\alpha$		0.0120		0.0208		0.0378
$z_9/\alpha$		0.0102		0.0223		0.0382
$z_{10}/\alpha$		-0.0076		-0.0116		-0.0180
$y_3$	(0.0017)	0.0268	(0.0018)	0.0336	(0.0018)	0.0416
$y_4$	(-0.0019)	-0.0491	(-0.0021)	-0.0574	(-0.0022)	-0.0660
$y_5$	(0.0007)	0.0031	(0.0007)	-0.0028	(0.0007)	-0.0165
$y_6$	(-0.0019)	-0.0849	(-0.0021)	-0.119	(-0.0022)	-0.178
$y_7/\alpha$	(0.149)	-0.0119	(0.149)	-0.0118	(0.136)	-0.0127
$y_8/\alpha$	(0)	0.153	(0)	0.212	(0)	0.304
$y_9/\alpha$	(-1.22)	-1.71	(-1.22)	-1.83	(-1.22)	-1.99
$y_{10}/\alpha$	(0)	0.674	(0)	0.843	(0)	1.07

Table 5.3: Same as in table 1 for  $\mu = 1$  GeV.

$\Lambda_{QCD}^{(4)}$	250 MeV		350 MeV		450 MeV	
$\alpha_s(m_Z)_{\overline{MS}}$	0.113		0.119		0.125	
$z_1$	(0.0320)	-0.539	(0.0339)	-0.683	(0.0355)	-0.884
$z_2$	(0.988)	1.30	(0.987)	1.40	(0.987)	1.56
$z_3$		0.0060		0.0108		0.0210
$z_4$		-0.0142		-0.0230		-0.0389
$z_5$		0.0037		0.0052		0.0068
$z_6$		-0.0128		-0.0204		-0.0341
$z_7/\alpha$		-0.0041		-0.0024		-0.0012
$z_8/\alpha$		0.0087		0.0140		0.0234
$z_9/\alpha$		0.0016		0.0068		0.0140
$z_{10}/\alpha$		-0.0084		-0.0135		-0.0223
$y_3$	(0.0007)	0.0301	(0.0007)	0.0390	(0.0007)	0.0509
$y_4$	(0.0011)	-0.0513	(0.0012)	-0.0610	(0.0012)	-0.0723
$y_5$	(-0.0004)	0.0137	(-0.0004)	0.0163	(-0.0004)	0.0209
$y_6$	(0.0011)	-0.0766	(0.0012)	-0.103	(0.0012)	-0.144
$y_7/\alpha$	(0.172)	-0.0115	(0.172)	-0.0103	(0.172)	-0.0083
$y_8/\alpha$	(0)	0.167	(0)	0.230	(0)	0.328
$y_9/\alpha$	(-1.19)	-1.71	(-1.19)	-1.83	(-1.19)	-2.00
$y_{10}/\alpha$	(0)	0.750	(0)	0.859	(0)	1.10

Table 5.4: Same as in table 2 for  $\mu = 1$  GeV

## 5.4 Choice of the Input Parameters

As we have seen in the last chapter, our results depend upon the values we choose for the two quantities parametrizing the genuine non-perturbative part of the computation, that is the quark and the gluon condensates. We have already discussed the problem of their phenomenological determination, which is not easy because the literature offers different estimates. We have also seen that, if we suppose to identify the condensates entering our computation with those obtained by fitting the experimental data, by means of the QCD sum rules (QCD-SR) or lattice computations, we can have an idea of the range of reasonable values we can span for these two input parameters. Here we only report the ranges that we will explore in our numerical analysis.

For the gluon condensate, we take the scale independent range

$$\left\langle \frac{\alpha_s}{\pi} GG \right\rangle = (376 \pm 47 \text{ MeV})^4, \quad (5.44)$$

which encompasses the results of recent QCD-SR analyses [47, 49, 48].

For the quark condensate, we consider the range

$$-(220 \text{ MeV})^3 \leq \langle \bar{q}q \rangle \leq -(280 \text{ MeV})^3 \quad (5.45)$$

in order to include QCD-SR [51] and lattice estimates [53].

In discussing the scale dependence of our results, it is necessary to include the perturbative running of the quark condensate. This can be done in the QCD-SR approach by using the renormalization-group running masses  $\bar{m}_u + \bar{m}_d$ , the value of which is estimated at  $\mu = 1 \text{ GeV}$  to be [52]

$$\bar{m}_u + \bar{m}_d = 12 \pm 2.5 \text{ MeV} \quad (5.46)$$

for  $\Lambda_{\text{QCD}}^{(3)} = 300 \pm 150 \text{ MeV}$ . The error in (5.46) reflects changes in the spectral functions.

By taking the value (5.46), we find for the scale-dependent (and normal-ordered) condensate

$$\langle \bar{q}q \rangle (\mu) = -\frac{f_\pi^2 m_\pi^2 (1 - \delta_\pi)}{\bar{m}_u(\mu) + \bar{m}_d(\mu)}, \quad (5.47)$$

corresponding ( $\delta_\pi$  is a few percents) to the numerical values of

$$\langle \bar{q}q \rangle = -(238 \pm 19 \text{ MeV})^3 \quad (5.48)$$

at 1 GeV and

$$\langle \bar{q}q \rangle = -(222 \pm 19 \text{ MeV})^3 \quad (5.49)$$

at 0.8 GeV. The error in eqs. (5.48)–(5.49) corresponds to that in (5.46). The central values in eqs. (5.48)–(5.49) are in the lower half of the range (5.45).

There is also another important input parameter appearing in our results, that is  $M$ , the characteristic parameter of the chiral quark model. As already said, we will not fix it and we will analyze for which values of  $M$  the  $\gamma_5$ -scheme dependence of our results is minimized. Anyway, this point will become clear when we analyze our numerical results.

## 5.5 Results of Other Approaches

To understand which are the improvements that can be obtained with our model, it can be useful to compare our results for the two amplitudes  $A_0$  and  $A_2$ , with the ones already existing in literature. In particular we will consider, as a reference, the results one would obtain by using the same short distance analysis that we have done, but computing the hadronic matrix elements in the vacuum saturation approximation (VSA). These results are reported in Table 5.

Let us compare the results of table 5 with the experimental values of  $A_0$  and  $A_2$ , given in eqs. (5.1)–(5.2). The value of  $A_0$  is smaller than it should be, at least, by a factor three and, at the same time, the result reported for the amplitude  $A_2$  is almost twice bigger than the experimental value. We can focus our attention, for instance, on the values obtained for  $\mu = 0.8$  GeV, which can be considered our preferred matching scale, as we will explain later. If we define the parameter

$$\omega^{-1} \equiv \text{Re } A_0 / \text{Re } A_2, \quad (5.50)$$

we find  $\omega^{-1} \simeq 3.4$  in the HV and  $\omega^{-1} \simeq 3.7$  in the NDR scheme, which is about a factor of six smaller than the experimental value  $\omega^{-1} = 22.2$ .

The situation could improve if we would take for the quark condensate a larger value, instead of the PCAC expression given by eq. (5.47). In fact we will see later that, taking higher values for  $\langle \bar{q}q \rangle$ , we enhance the amplitude  $A_0$ . We could use, for instance, the quite popular value

$$(\langle \bar{q}q \rangle)^{1/3} (1\text{GeV}) = \left( -\frac{m_K^2 f_K^2}{m_s(1\text{GeV})} \right)^{1/3} \simeq -260 \text{ MeV}. \quad (5.51)$$

Anyway, also in this case we would find values for  $A_0$  and  $A_2$  which are quite far from the experimental results.

	$\mu = 0.8 \text{ GeV}$		$\mu = 0.9 \text{ GeV}$		$\mu = 1 \text{ GeV}$	
	NDR	HV	NDR	HV	NDR	HV
$A_0$	1.11	0.93	0.89	0.77	0.75	0.67
$A_2$	3.00	2.76	3.07	2.87	3.13	2.95
$\Delta_{\gamma_5} A_0$	18%		15%		12%	
$\Delta_{\gamma_5} A_2$	8%		7%		6%	
$\Delta_{\mu} A_0$	39% – 33%					
$\Delta_{\mu} A_2$	4% – 7%					

Table 5.5: Matching scale and  $\gamma_5$  scheme dependence of  $A_0$  (in units of  $10^{-7}$  GeV) and  $A_2$  (in units of  $10^{-8}$  GeV) in the VSA approach with NLO Wilson coefficients. The amplitudes are computed for  $\Lambda_{\text{QCD}}^{(4)} = 350 \text{ MeV}$  and  $\langle \bar{q}q \rangle$  given in eq. (5.47). The two values quoted for the  $\mu$ -dependence of the amplitudes correspond to the NDR and HV scheme results in the range between 0.8 and 1.0 GeV.

In Table 5 we have also analyzed the scale and the  $\gamma_5$ -scheme dependence of the results, by introducing the following two quantities:

$$\Delta_\mu A_i \equiv 2 \left| \frac{A_i(0.8 \text{ GeV}) - A_i(1.0 \text{ GeV})}{A_i(0.8 \text{ GeV}) + A_i(1.0 \text{ GeV})} \right| \quad (5.52)$$

and

$$\Delta_{\gamma_5} A_i \equiv 2 \left| \frac{A_i^{\text{NDR}} - A_i^{\text{HV}}}{A_i^{\text{NDR}} + A_i^{\text{HV}}} \right|. \quad (5.53)$$

The scale dependence of  $A_0$  is rather large, with  $\Delta_\mu A_0$  almost 40% in the NDR scheme, while the  $A_2$ 's scale dependence remains within 10%. The  $\gamma_5$ -scheme dependence, instead, is not too large for the two amplitudes  $A_0$  and  $A_2$ , remaining below 20%. We would like to stress that these scale and scheme dependences of the amplitudes are due to those of the Wilson coefficients, because the VSA hadronic matrix elements depend neither on the  $\gamma_5$ -scheme, nor on the scale (except for the perturbative running of the quark condensate). Therefore these values of  $\Delta_\mu A_i$  and  $\Delta_{\gamma_5} A_i$  can be useful for a comparison with the results we will obtain with our chiral quark model computation.

It is clear, from all these remarks, that the results obtained in the VSA are still far from the experimental ones. This is true despite the fact that we have already inserted the effects due to the next to leading order corrections of the Wilson coefficients and to the presence of penguin operators, which historically have been considered the main responsible of the  $\Delta I = 1/2$  rule. Hence, to understand completely this selection rule, we have to introduce other effects. We will see in the next sections that the results we can obtain in our model are nearer to the experimental values of  $A_0$  and  $A_2$ . The main sources of improvement are the gluonic contributions and the chiral loop corrections, as we have already said. Let us remember that the literature also offers determinations of the selection rule in which the matching between Wilson coefficients and hadronic matrix elements is done without meson-loop renormalization, but at a much lower values of the matching scale (at about 300 MeV, for instance). Such a procedure is no longer justifiable in view of the NLO determination of the Wilson coefficients that shows, for such a low-energy matching, the breaking down of the perturbative expansion.

We now turn to the  $\chi$ QM model determination of the selection rule.

## 5.6 Numerical Results in the Chiral Quark Model

To analyze the chiral quark model results, let us start to report in a table the values of the two isospin amplitudes that we have obtained for a representative set of input



parameters, as we have done before for the VSA results. In this way we can have a first idea of the scheme and the scale dependence of our results.

We can see from Table 6 that the scale dependence of our results is below 20% (except for the case of the HV scheme at  $\Lambda_{\text{QCD}}^{(4)}=450$  MeV). This is an important improvement with respect to the VSA results, where the scale dependence for the amplitude  $A_0$  is between 30% and 40%. Thanks to our satisfactory scale independence, we can take the matching at any values between 0.8 and 1 GeV. Yet it is useful to bear in mind that any number quoted in what follows suffers of an intrinsic uncertainty of at least 20% because of the residual scale dependence in the matching itself. We privilege the matching at 0.8 GeV as the best compromise between the range of validity of the perturbative regime and that of chiral perturbation theory.

We have also verified the consistency of the perturbative expansion in the short-distance regime by comparing leading order and the NLO results for  $A_0$  and  $A_2$  at  $\mu = 0.8$  GeV. The change in  $A_0$  turns out to be of about 10% and similarly for  $A_2$ . These values confirm that the choice of matching at  $\mu = 0.8$  GeV is well within the perturbative regime of the QCD corrections.

Also the  $\gamma_5$  scheme dependence of our results seems to be under control. In fact, for  $\Lambda_{\text{QCD}}^{(4)} \leq 350$  MeV, it is well below the 20%. Both the scale and the scheme dependence are stronger for larger values of  $\Lambda_{\text{QCD}}^{(4)}$ . In the following we will take the central value, at  $\Lambda_{\text{QCD}}^{(4)} = 350$  MeV, as our reference value for the discussion.

We will discuss in a more detailed way the dependence on the regularization scheme in the subsection 5.6.2, where we will consider different values of the parameter  $M$ .

Of course, it is not so important to compare directly to the experimental values the values for  $A_0$  and  $A_2$  in table 6, because they correspond to a specific choice for the quark and gluon condensates, as well as of  $M$ . A more complete discussion of these input parameters is presented in a specific subsection. Anyway, we can notice from Table 6 that we are going in the right direction; in fact we have a significant increasing of  $A_0$  and reduction of  $A_2$ , with respect to the VSA results of Table 5. Here we have used for the quark condensate the formula (5.47), to be consistent with what we have done in the case of the VSA, and we have taken the central value of the interval of (5.44) for the gluon condensate. We will see in the next subsections that we could obtain a further enhancement of the amplitude  $A_0$ , by taking higher values of  $\langle \bar{q}q \rangle$  without going out of the range given in (5.45). At the same time we could choose slightly smaller values for the gluon condensate, in such a way to reduce the gluonic suppression of the amplitude  $A_2$ , and to reproduce almost exactly the experimental value.

$\Lambda_{\text{QCD}}^{(4)} = 250 \text{ MeV}$						
	$\mu = 0.8 \text{ GeV}$		$\mu = 0.9 \text{ GeV}$		$\mu = 1 \text{ GeV}$	
	NDR	HV	NDR	HV	NDR	HV
$A_0$	2.11	2.29	2.05	2.20	2.02	2.14
$A_2$	1.20	1.12	1.27	1.20	1.34	1.27
$\Delta_{\gamma_5} A_0$	8%		7%		6%	
$\Delta_{\gamma_5} A_2$	7%		6%		5%	
$\Delta_{\mu} A_0$	4% – 7%					
$\Delta_{\mu} A_2$	11% – 13%					
$\Lambda_{\text{QCD}}^{(4)} = 350 \text{ MeV}$						
	$\mu = 0.8 \text{ GeV}$		$\mu = 0.9 \text{ GeV}$		$\mu = 1 \text{ GeV}$	
	NDR	HV	NDR	HV	NDR	HV
$A_0$	2.52	2.85	2.37	2.61	2.27	2.45
$A_2$	1.15	1.03	1.23	1.12	1.29	1.20
$\Delta_{\gamma_5} A_0$	12%		10%		8%	
$\Delta_{\gamma_5} A_2$	11%		9%		7%	
$\Delta_{\mu} A_0$	10% – 15%					
$\Delta_{\mu} A_2$	11% – 15%					
$\Lambda_{\text{QCD}}^{(4)} = 450 \text{ MeV}$						
	$\mu = 0.8 \text{ GeV}$		$\mu = 0.9 \text{ GeV}$		$\mu = 1 \text{ GeV}$	
	NDR	HV	NDR	HV	NDR	HV
$A_0$	3.13	3.90	2.84	3.29	2.63	2.94
$A_2$	1.13	0.93	1.19	1.04	1.26	1.13
$\Delta_{\gamma_5} A_0$	22%		15%		11%	
$\Delta_{\gamma_5} A_2$	19%		13%		11%	
$\Delta_{\mu} A_0$	17% – 28%					
$\Delta_{\mu} A_2$	11% – 19%					

Table 5.6: Same as in table 5 in the  $\chi$ QM approach, for different values of  $\Lambda_{\text{QCD}}^{(4)}$ . We take for the gluon condensate the central value  $\langle \alpha_s GG/\pi \rangle = (376 \text{ MeV})^4$  and for the quark condensate  $\langle \bar{q}q \rangle$  eq. (5.47). For the chiral quark model parameter we choose  $M = 220 \text{ MeV}$ .

### 5.6.1 Dependence on the Input Parameters

Let us study the dependence of  $A_0$  and  $A_2$  on the values of the quark and gluon condensates. To make this analysis, we fix  $\Lambda_{\text{QCD}}^{(4)} = 350$  MeV and  $\mu = 0.8$  GeV and we vary the condensates inside the ranges of (5.44) and (5.45), looking at the corresponding values of  $A_0$  and  $A_2$ . Figs. 1, 2 and 3 show such a dependence for three representative values of  $M$ .

Each figure contains the HV result (black lines) as well as the NDR one (grey lines). The spread between these two determinations is mostly due to  $A_2$  that contains an irreducible  $\gamma_5$ -scheme dependence, as we will explain later.

We can notice that in each figure there are three horizontal bands, which correspond to three different values of the gluon condensate. The central one is obtained for the central value given in eq. (5.44), while the other two correspond to one standard deviation. A larger gluon condensate leads to lower values of  $A_2$ . The dependence on the quark condensate, instead, is represented by the points on a given line. The initial and final point of each line correspond, respectively, to the minimum and the maximum value of the range given in eq. (5.45).

Larger values of  $A_0$  are obtained for larger values of the quark condensate and smaller values of  $M$ . This is due to the fact that  $A_0$  is, almost completely, dominated by the contributions of the gluon penguin operators  $Q_5$  and  $Q_6$ , whose matrix elements are proportional to the factor

$$\langle \bar{q}q \rangle \left( 1 - 6 \frac{M^2}{\Lambda_\chi^2} \right) \quad (5.54)$$

in the HV scheme, and similarly (with 6 being replaced by 9) in the NDR scheme.

The amplitude  $A_2$ , instead is almost independent on the value of the quark condensate ( $\langle \bar{q}q \rangle$  enters in the determination of  $A_2$  only through the small contribution coming from the electroweak penguins). On the other hand, its size is a very sensitive function of the gluon condensate.

By looking at Figs. 1,2,3 and extending our analysis at other values of the parameter  $M$ , we can have an idea of the validity of our results. For any choice of  $M$  in the range

$$M = 140 - 220 \text{ MeV} \quad (5.55)$$

our computation can reproduce exactly the experimental values of  $A_0$  and  $A_2$  (or at least values which are very near to the experimental ones) by different choices of the input parameters  $\langle \bar{q}q \rangle$  and  $\langle GG \rangle$ , that, however, remain within the ranges given in (5.45) and (5.44). The suppression of the gluon penguin contributions as we increase

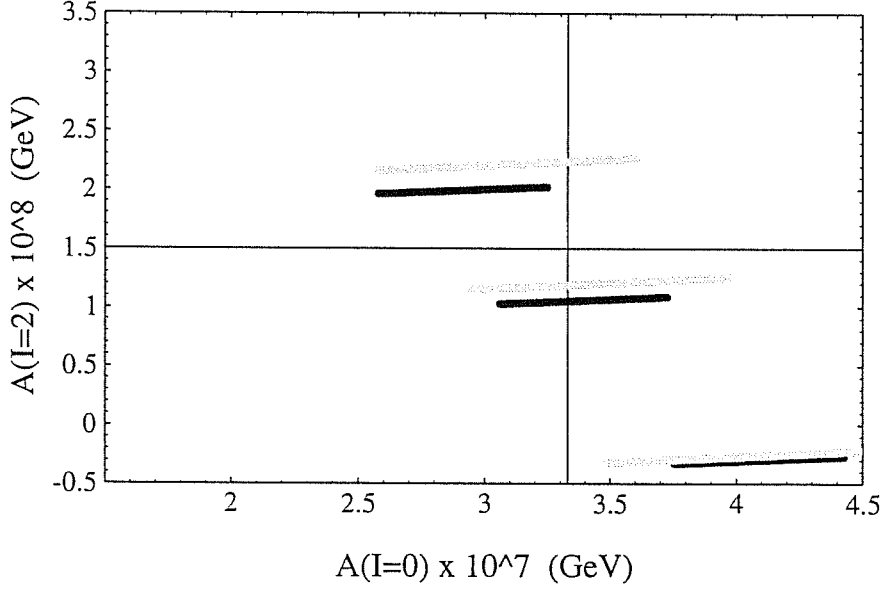


Figure 5.1: Dependence of  $A_0$  and  $A_2$  on  $\langle \bar{q}q \rangle$  and  $\langle GG \rangle$  for  $\Lambda_{\text{QCD}}^{(4)} = 0.350$  GeV,  $\mu = 0.8$  GeV, and  $M = 180$  MeV. The black (grey) lines represent the HV (NDR) results for  $\langle \bar{q}q \rangle$  in the range of eq. (5.45) and fixed  $\langle \alpha_s GG/\pi \rangle$ . The vertical spread corresponds to varying  $\langle \alpha_s GG/\pi \rangle$  in the range of eq. (5.44), with central lines corresponding to the central value of  $\langle GG \rangle$ . The experimental values of  $A_0$  and  $A_2$  are given by the cross hairs. The small dependence of  $A_2$  on the quark condensate is due to the the electroweak penguins  $Q_{7,8}$ .

$M$  above 220 MeV would force us to values for the quark condensate outside the range (5.45) in order to remain close to the experimental value for  $A_0$ .

It is clear, from Figs. 1,2,3, that we can span a quite large interval of values for  $A_0$  and  $A_2$ , by varying the two condensates inside the ranges of (5.45) and (5.44). However these two intervals of values for  $\langle \bar{q}q \rangle$  and  $\langle \alpha_s GG/\pi \rangle$  are rather conservative and, what is more important, we have quoted them only to give an idea of the values we could consider the reasonable ones for the condensates. It can be more interesting to restrict the ranges of these input parameters in such a way to obtain values of  $A_0$  and  $A_2$  which are very near to the experimental ones. In Fig. 4 we have represented  $A_0$  and  $A_2$  like in the previous three figures, but for the following “restricted” range of values for the gluon and the quark condensates:

$$\left\langle \frac{\alpha_s}{\pi} GG \right\rangle = (360 \pm 15 \text{ MeV})^4, \quad (5.56)$$

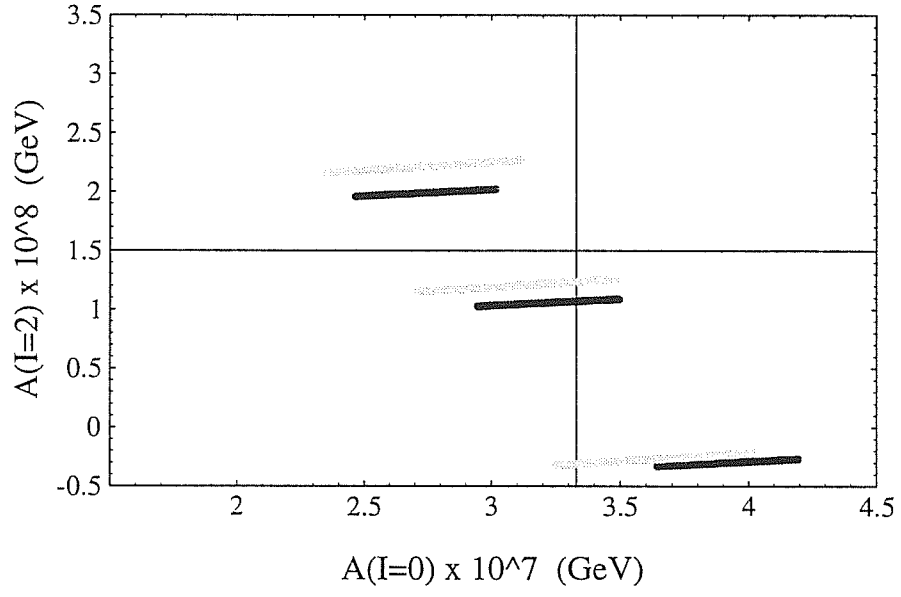


Figure 5.2: Same as in Fig. 1 for  $M = 200$  MeV.

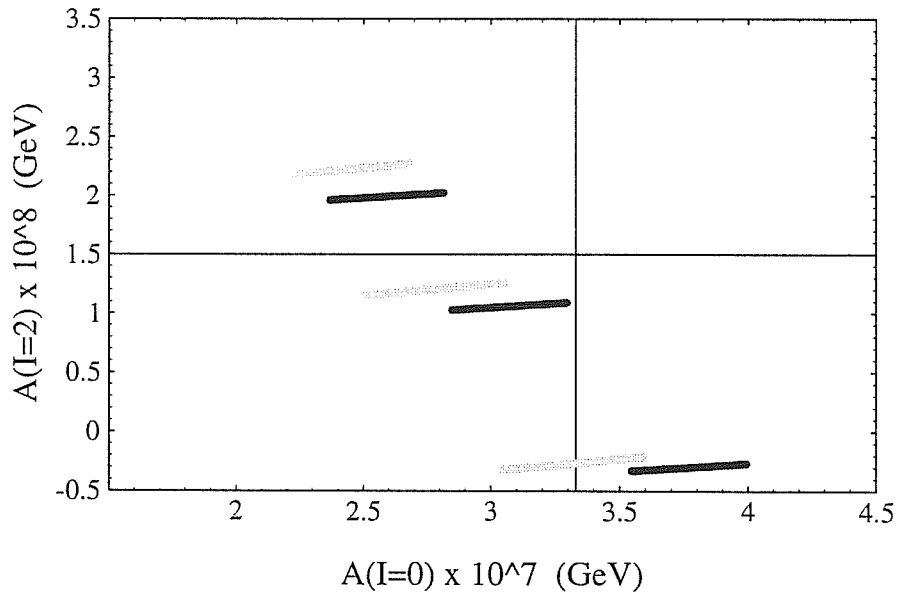


Figure 5.3: Same as in Fig.1 for  $M = 220$  MeV.

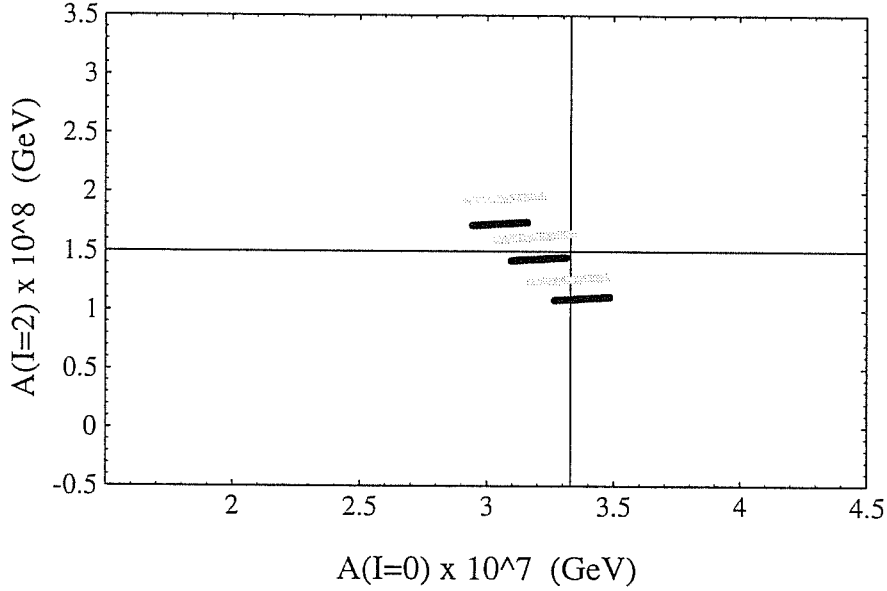


Figure 5.4: Same as in Fig. 1 but for different values of the input parameters.  $M = 200$  MeV and the quark and gluon condensates are given by eqs. (5.57)–(5.56).

$$-(260 \text{ MeV})^3 \leq \langle \bar{q}q \rangle \leq -(280 \text{ MeV})^3. \quad (5.57)$$

In figure 4 we have taken  $M = 200$  MeV.

Now that we have selected the values of the condensates giving us the best fit for the  $\Delta I = 1/2$  rule, we can use the same values to analyze other processes. In this way we can see if we are able to give a consistent description of kaon physics. For instance, in the study of  $\Delta S = 2$  physics we will use the range of eq. (5.56) for the gluon condensate and we will take  $\langle \bar{q}q \rangle = -(280 \text{ MeV})^3$ .

### 5.6.2 $\gamma_5$ -scheme Independence

In this subsection we discuss the residual scheme dependence of our results and the way in which we can try to minimize it by choosing an appropriate value of the parameter  $M$ .

The Wilson coefficients in eq. (4.1) depend at the NLO on the  $\gamma_5$ -scheme employed [15, 16]. On the other hand, we have seen that in the  $\chi$ QM also the hadronic matrix elements depend on the  $\gamma_5$ -scheme used in computing them. We would like that these two dependences compensate each other in such a way to give a  $\gamma_5$ -scheme independent result. This requirement can be used in order to restrict the allowed val-

ues for the characteristic chiral quark model parameter  $M$ , that until now we have considered as a free parameter.

The scheme dependence of the amplitudes  $A_0$  and  $A_2$  is not strong, as we have shown in our previous analysis. So, in this case, we can only restrict a range of values of  $M$  for which it is reasonably under control, but nothing more. The situation is, however, different when we examine other observables with a stronger scheme dependence as, for instance,  $\varepsilon'/\varepsilon$  [29]. In that case we can find a substantial reduction of the scheme dependence for values of  $M$  that are still within the range determined by means of  $A_0$  and  $A_2$ . A consistent picture for the whole of kaon physics emerge in this way, with different observables concurring in the determination of the free parameter  $M$  as well as the range of the input parameters. We will come back on this point in chapter 6.

Let us analyze separately the scheme dependence of  $A_0$  and  $A_2$ .

In our estimate of the hadronic matrix elements, the  $\gamma_5$ -scheme independence of  $A_0$  turns out to be controlled by the gluonic penguins. In fact, the Wilson coefficients  $z_{3-6}$  are systematically larger in the NDR scheme than in the HV scheme. On the other hand, in the NDR scheme the matrix elements of the gluonic penguins decrease with increasing  $M$  faster than in the HV scheme. As a consequence, it always exists a value of  $M$  for which the  $\gamma_5$ -scheme independence is achieved.

Larger values of the quark condensate gives stability for larger values of  $M$ . From Fig. 5 and 6 one can readily see that the difference between the two schemes remains below 10% for a large range of values of  $M$  between 160 and 220 MeV.

The situation is different for the amplitude  $A_2$ , which is dominated by the contributions coming from the current-current operators  $Q_1$  and  $Q_2$ . We have already explained that we have to take the same expressions for the matrix elements of these operators in the two different schemes HV and NDR. Hence, in this case, there is no hope of cancelling the scheme dependence of the Wilson coefficients and we have a residual scheme dependence for  $A_2$  independently from the value of the parameter  $M$ . Anyway, as we can see from Fig. 7, the  $\gamma_5$ -scheme dependence can be considered under control also in this case. In fact it is around 10%.

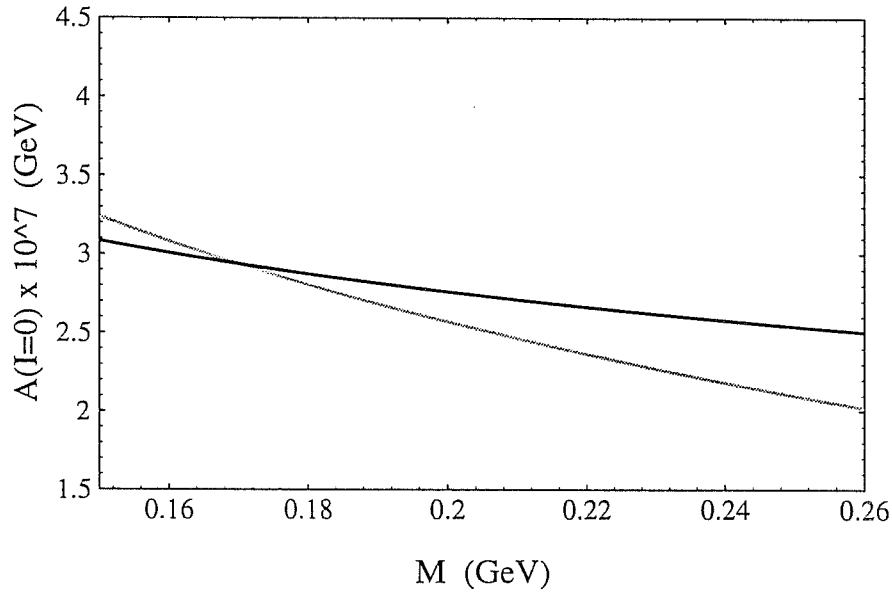


Figure 5.5: The  $\gamma_5$ -scheme dependence of  $A_0$  is shown as a function of  $M$ . The black (grey) line represent the HV (NDR) result. We use  $\langle\alpha_s GG/\pi\rangle = (360 \text{ MeV})^4$  and  $\langle\bar{q}q\rangle = -(220 \text{ MeV})^3$ . For this value of the quark condensate the stability appear between  $M = 160$  and  $M = 180 \text{ MeV}$ .

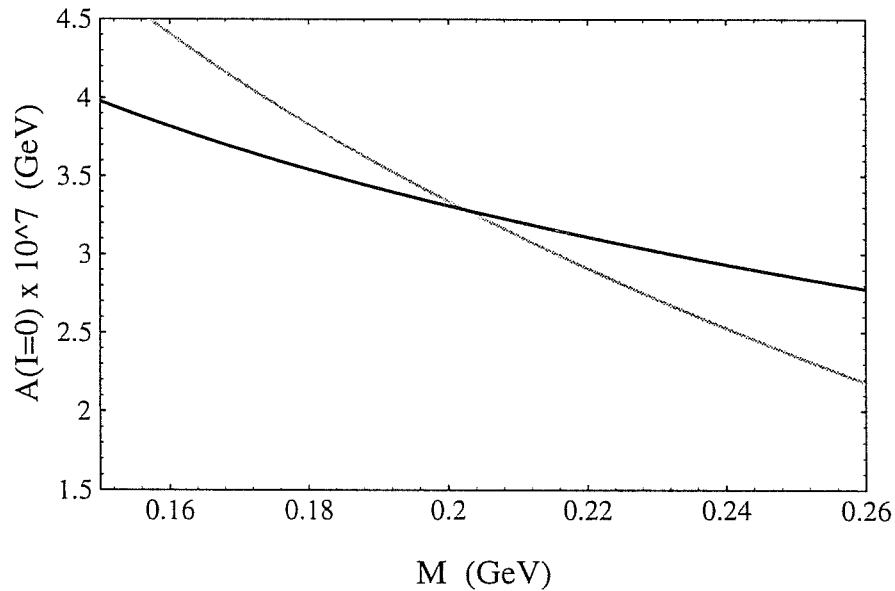


Figure 5.6: Same as in Fig.5 for  $\langle\bar{q}q\rangle = -(280 \text{ MeV})^3$ . The stability is moved at about  $M = 200 \text{ MeV}$ .



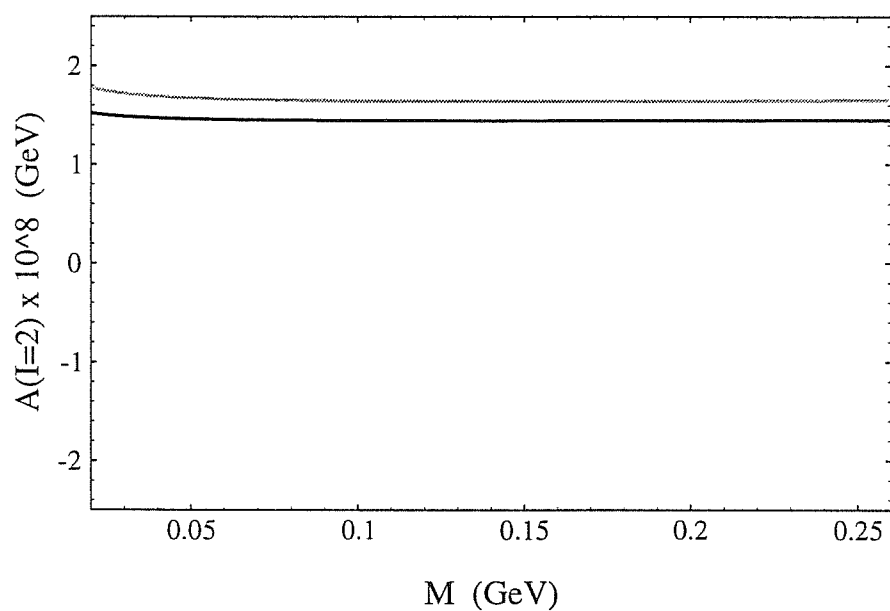


Figure 5.7: Same as in Fig. 6 for  $A_2$ . There is no crossing of the HV and the NDR curves. Anywhere the scheme dependence stays well below 20%.

## 5.7 Comments about our Results

In the previous section we have shown that, by using the  $\Delta S = 1$  weak chiral lagrangian. we can account for the  $\Delta I = 1/2$  rule in a quite satisfactory way. It can be interesting to isolate the single contributions to  $A_0$  and  $A_2$ , in such a way to identify the main sources of improvement with respect to the results already existing in literature.

We will use again, for a comparison, the results obtained in the VSA. Hence we can start our analysis introducing the  $B_i$  factors, which are defined in the following way

$$B_i^{(0,2)} \equiv \frac{\langle Q_i \rangle_{0,2}^{\chi QM}}{\langle Q_i \rangle_{0,2}^{VSA}}. \quad (5.58)$$

These factors tell us which is the ratio between the hadronic matrix element of the operator  $Q_i$  in the isospin channel  $I = 0$  or  $I = 2$  computed in the chiral quark model and the same matrix element evaluated in the vacuum saturation approximation.

In Table 7, we collect the  $B_i$  factors for all the operators  $Q_i$  ( $i=1..10$ ). In this table we take for the gluon condensate the central value of  $eq.$  (5.56) and  $M = 220$  MeV. This is our preferred value of  $M$ . as we have partially explained in the previous section and will become more clear in the next chapter. We choose the central value for the QCD scale parameter,  $\Lambda_{QCD}^{(4)} = 350$  MeV, and we consider two different matching scales ( $\mu = 0.8$  GeV and  $\mu = 1$  GeV). We also consider two different values for the quark condensate, to show explicitly the dependences of some penguin operators on this input parameter.

Table 7 shows us, in a very clear way that the main difference between our results and the ones of VSA is due to the matrix elements of the current-current operators  $Q_1$  and  $Q_2$ . In fact, after the introduction in the  $\chi QM$  results of gluonic contributions and chiral loop corrections,  $\langle Q_1 \rangle_0$  and  $\langle Q_2 \rangle_0$  are, respectively 8 and 2-3 times bigger than the corresponding matrix elements in the VSA. At the same time the matrix elements of these two operators in the isospin channel  $I = 2$ , that is  $\langle Q_1 \rangle_2$  and  $\langle Q_2 \rangle_2$  are about two times smaller in the  $\chi QM$  than in the VSA. These two results are almost enough to explain the enhancement of  $A_0$  and the suppression of  $A_2$  that we find in the  $\chi QM$  results with respect to the VSA ones. For a comparison with other results that can be found in literature, let us remember that in the  $1/N_c$  approach of ref. [18, 55]. the inclusion of meson-loop renormalization through a cutoff regularization, leads . at

	HV		NDR	
	$\mu = 0.8 \text{ GeV}$	$\mu = 1 \text{ GeV}$	$\mu = 0.8 \text{ GeV}$	$\mu = 1 \text{ GeV}$
$B_1^{(0)}$	7.7	8.1	7.7	8.1
$B_2^{(0)}$	2.4	2.6	2.4	2.6
$B_1^{(2)} = B_2^{(2)}$	0.57	0.61	0.57	0.61
$B_3$	-1.9	-2.0	-2.5	-2.7
$B_4$	1.6	1.7	0.9	0.94
$B_5 = B_6$	1.1 - 0.53	1.2 - 0.56	0.68 - 0.33	0.72 - 0.35
$B_7^{(0)}$	2.5 - 2.0	2.7 - 2.2	2.4 - 1.9	2.6 - 2.1
$B_8^{(0)}$	2.6 - 2.0	2.9 - 2.2	2.5 - 2.0	2.7 - 2.1
$B_7^{(2)}$	1.8 - 1.2	1.9 - 1.2	1.7 - 1.2	1.8 - 1.2
$B_8^{(2)}$	1.6 - 1.2	1.7 - 1.2	1.6 - 1.2	1.7 - 1.2
$B_9^{(0)}$	2.9	3.0	2.6	2.7
$B_{10}^{(0)}$	3.6	3.9	4.6	5.0
$B_9^{(2)}$	0.57	0.61	0.57	0.61
$B_{10}^{(2)}$	0.57	0.61	0.57	0.61

Table 5.7: The  $B_i$  factors in the  $\chi$ QM (including meson-loop renormalizations) for all the ten operators  $Q_i$ , at two different scales:  $\mu = 0.8$  and  $1.0 \text{ GeV}$ . We have taken the gluon condensate at the central value of eq. (5.56), while the range given for  $B_{5,6}$  corresponds to varying the quark condensate according to eq. (5.45). The results shown are given in both schemes for  $M = 220 \text{ MeV}$ .

the scale of 1 GeV, to  $B_1^{(0)} = 5.2$ ,  $B_2^{(0)} = 2.2$  and  $B_1^{(2)} = B_2^{(2)} = 0.55$  (see the second paper of ref. [62]), a result that is not sufficient to reproduce the  $\Delta I = 1/2$  rule. The value  $B_1^{(2)} = B_2^{(2)} \simeq 0.50 - 0.60$  in both the  $\chi QM$  (table 7) and the  $1/N_c$  approaches is remarkable, and yet a numerical coincidence, since the suppression originates from gluon condensate corrections in the  $\chi QM$ , whereas it is the effect of the meson loop renormalization (regularized via explicit cut-off) in ref. [18, 55].

The other two operators that are relevant for the explanation of the  $\Delta I = 1/2$  rule are the gluonic penguins  $Q_5$  and  $Q_6$ , which contribute only to the amplitude  $A_0$ . The factors  $B_5$  and  $B_6$  are very sensitive functions of the quark condensate. This is due to the fact that these matrix elements depend linearly on the quark condensate in the chiral quark model, while the analogous dependence in the VSA is quadratic. Anyway the values of  $B_5$  and  $B_6$  in the HV scheme are not far from 1 and so they are consistent with the results of the VSA and of the  $1/N_c$  approach. Let us also remember that the lattice estimation for this operators is  $B_5 = B_6 = 1.0 \pm 0.2$  (see the first two papers of ref. [17] and the last one of ref. [16]). The further reduction of  $B_{5,6}$  in the NDR scheme is due to the fact that in front of the factor proportional to  $M^2/\Lambda_\chi^2$ , which suppresses the matrix elements of  $Q_{5,6}$ , we have a coefficient 9 in the NDR and only 6 in the HV scheme. It is clear that we could also obtain higher values of  $B_{5,6}$  by taking smaller values for the parameter  $M$ . For instance, for  $M=180$  MeV  $\mu = 1\text{GeV}$  and  $\langle \bar{q}q \rangle = -(220 \text{ MeV})^3$  we have  $B_5 = B_6 = 1.8$  in the HV and  $B_5 = B_6 = 1.4$  in the NDR scheme.

The  $B_i$  factors are bigger than one for almost all of the other penguin operators and it is interesting to notice that in the case of  $Q_3$ , the  $\chi QM$  result has the opposite sign of the VSA result and  $B_3$  is negative. This is the effect of the large non-perturbative gluon correction. This fact is not relevant for the study of the  $\Delta I = 1/2$  rule, but it has a certain importance for the evaluation of  $\varepsilon'/\varepsilon$  [29].

An instructive way of analyzing the relevance of the various contributions to the  $\Delta I = 1/2$  rule is obtained by turning on in our computation each of them as we follow the historical steps that led to the present understanding of the rule (Fig. 8).

We can start from the theoretical predictions for  $A_0$  and  $A_2$  one would obtain by considering the pure VSA matrix elements of  $Q_1$  and  $Q_2$ , without the short distance renormalization of the corresponding Wilson coefficients. They represent the coordinates of the point labelled by (1) in Fig. 8.

The next step is the inclusion of the NLO renormalized Wilson coefficients, matched to the hadronic matrix elements at the scale  $\mu = 0.8$  GeV, which is our preferred scale

for the reasons already explained. As we can see from point (2) the insertion of these corrections enhances  $A_0$ , while reducing  $A_2$ . So it goes in the right direction. but the value for  $A_0$  is far too small and that of  $A_2$  too large by almost a factor of two.

Point (3) corresponds to the introduction of gluonic penguin operators. They increase  $A_0$ , but leave  $A_2$  unchanged. Their effect on  $A_0$  is very important but, at least in the  $\chi$ QM, it is not as crucial as often claimed. In fact we can see from the figure that at this stage, for the values chosen of the input parameters,  $A_0$  is still about three times smaller than the experimental result.

The introduction of the electroweak penguins ( $Q_{7-10}$ ) little affects the  $CP$  conserving amplitudes (point (4)), being suppressed by the smallness of their Wilson coefficients. Another isospin breaking contribution to the amplitude  $A_2$  comes from a long-distance effect, namely the mixing between  $\pi^0$  and  $\eta$  particles. This contribution is evaluated to be

$$A_2^{iso-brk} \simeq -\frac{1}{3\sqrt{2}} \frac{m_d - m_u}{m_s} A_0. \quad (5.59)$$

Accordingly, we have a reduction of the amplitude  $A_2$  represented by point (5) which compensates for the effect of the electroweak penguins.

There are still the last two contributions we have to add: the non perturbative gluonic corrections and the meson loop renormalization. They are essential to reproduce the experimental result, as we have repeated a lot of times and as we can see in a very clear way from Fig. 8. The introduction of non-factorizable gluonic corrections bring us from point (5) to point (6). This genuine non-perturbative part of the computation increases  $A_0$  and, what is more important, it improves dramatically  $A_2$ , that becomes very close to its experimental value.

The meson-loop renormalization provides, in our approach, the final step toward the experimental results. The size of the relative renormalizations of  $A_0$  and  $A_2$  goes in the right direction. In fact it is large for  $A_0$  and small for  $A_2$ .

As point (7) of Fig. 8 shows, the  $\Delta I = 1/2$  selection rule is well reproduced in the  $\chi$ QM. We have already seen that this model provides not only values for the amplitudes  $A_0$  and  $A_2$  close to the experimental ones but also a satisfactory scale and  $\gamma_5$ -scheme independence of the estimate.

This said, a word of caution is perhaps advisable. Various uncertainties related to the input parameters are necessarily present in our computation as we have discussed in this chapter. In addition, we have to consider the approximations inherent to our approach. In particular, higher-order terms  $O(p^4)$  in the chiral expansion may cause a 20-30% correction [45]. This is the systematic uncertainty we ascribe to our results.

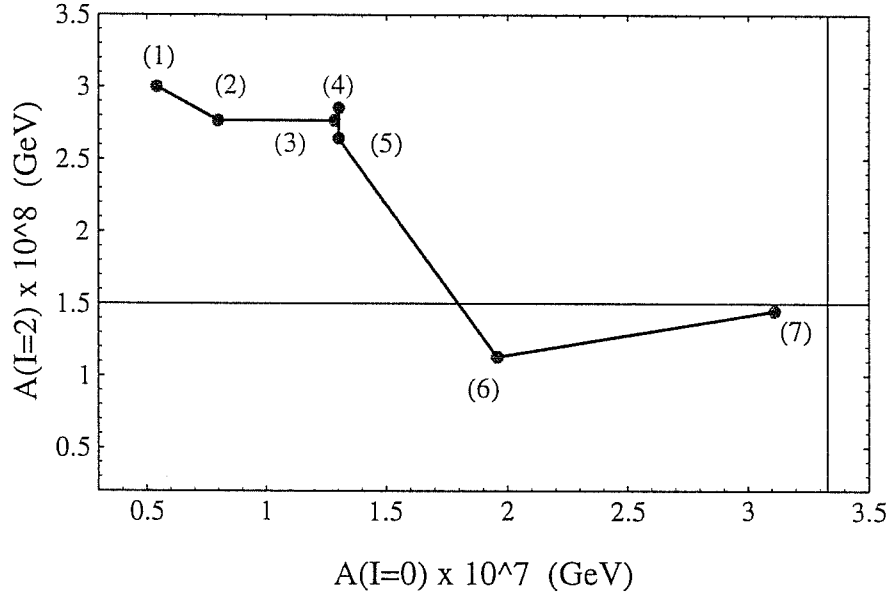


Figure 5.8: The road to the  $\Delta I = 1/2$  rule: 1) Effect of the W-induced current-current matrix elements ( $Q_{1,2}$ ) with the neglect of short-distance QCD renormalization; 2)  $\langle Q_{1,2} \rangle$  with the inclusion of the NLO Wilson coefficients at  $\mu = 0.8$  GeV. 3) inclusion of the gluon penguins ( $Q_{3-6}$ ); 4) inclusion of the electro-weak penguins ( $Q_{7-10}$ ); 5) inclusion of the  $\pi^0 - \eta$  mixing; 6) inclusion of gluon condensate corrections; 7) meson-loop renormalization. The results shown are those of the HV scheme with the values  $\langle \alpha_s GG/\pi \rangle = (360 \text{ MeV})^4$  and  $\langle \bar{q}q \rangle = -(280 \text{ MeV})^3$ , for a matching scale  $\mu = 0.8$  GeV and  $M = 220$  MeV. The experimental values are given by the cross hairs.

# Chapter 6

## CP Violation in Kaon Systems

### 6.1 The Ratio $\varepsilon'/\varepsilon$

In this chapter we would like to recall the main ideas about CP violation in the Standard Model and about  $K^0 - \bar{K}^0$  mixing. These theoretical subjects are wide and here we do not claim at all to treat them in an exhaustive way. Our aim is just that of introducing the basic concepts and definitions we will use in our analysis of the ratio  $\varepsilon'/\varepsilon$  and of  $K^0 - \bar{K}^0$  mixing. Anyway a lot of interesting books and reviews on these subjects can be found in literature [64]. We refer the interested reader to these works for a more detailed and complete analysis.

It is well known, since the work of Lee and Yang [65] and the subsequent experiments [66], that elementary processes are not invariant under the application of discrete transformations, like the parity operation P (which is a reflection in space) or the charge conjugation C and the time reversal T. On the other hand, according to the CPT theorem of Lueders and Pauli [67], there is a connection among these transformations. Under rather weak assumptions, in a local field theory all processes are invariant under the combined operation C P T.

For a certain period also CP was considered a good symmetry [68]. If this postulate were true, there should be two neutral particles ( $K_+^0$  and  $K_-^0$ ) of definite CP parity, which would be mixtures of the two strangeness eigenstates  $K^0$  ( $S=+1$ ) and  $\bar{K}^0$  ( $S=-1$ ). The following relations should hold <sup>†</sup>

$$CP |K_+^0\rangle = CP \left[ \frac{|K^0\rangle + |\bar{K}^0\rangle}{\sqrt{2}} \right] = |K_+^0\rangle$$

---

<sup>†</sup>We adopt the phase convention:  $CP K^0 = +\bar{K}^0$  ;  $CP \bar{K}^0 = +K^0$

$$CP|K_-^0\rangle = CP\left[\frac{|K^0\rangle - |\bar{K}^0\rangle}{\sqrt{2}}\right] = -|K_-^0\rangle. \quad (6.1)$$

A final state made by two pions with zero angular momentum has CP parity +1. Hence it is clear that, if CP were conserved even in the weak interactions, only  $K_+^0$  could decay in two pions, while the same decay would be forbidden for  $K_-^0$ . As a consequence  $K_-^0$  would have a longer lifetime. The discovery of a second neutral kaon state with a lifetime longer than the one already known [69] seemed to be a confirmation of this idea.

In 1964, however, Christenson, Cronin, Fitch and Turlay discovered that also the long-lived neutral kaon can decay into a couple  $\pi^+\pi^-$  [1], with a branching ratio of the order of  $2 \times 10^{-3}$ . It was a clear evidence that weak decays violate CP and the two eigenstates of the hamiltonian, called  $K_L$  and  $K_S$ , do not coincide with the two CP eigenstates  $K_+^0$  and  $K_-^0$ . The violation of CP was also confirmed in the following years by the discovery of the decays  $K_L \rightarrow \pi^0\pi^0$  and by the presence of charge asymmetries in semileptonic decays of  $K_L$ .

Let us now study briefly a system of neutral kaons. We know the two eigenstates of strangeness  $K^0$  and  $\bar{K}^0$  can mix, by means of weak transitions, because weak interactions do not conserve strangeness. We can write the generic neutral kaon state in the following way:

$$\psi(t) = \begin{pmatrix} a(t) \\ b(t) \end{pmatrix} = a(t)|K^0\rangle + b(t)|\bar{K}^0\rangle. \quad (6.2)$$

This state must satisfy the Schroedinger equation:

$$i\frac{d}{dt} \begin{pmatrix} a(t) \\ b(t) \end{pmatrix} = H \begin{pmatrix} a(t) \\ b(t) \end{pmatrix}, \quad (6.3)$$

where  $H = M - \frac{i}{2}\Gamma$  and the two hermitian matrices M and  $\Gamma$  are called, respectively, mass and decay matrix. We have

$$\left[M - \frac{i}{2}\Gamma\right]_{ij} \equiv \frac{\langle K_i^0 | \mathcal{H}_{eff} | K_j^0 \rangle}{2m_K}. \quad (6.4)$$

In the previous equation we have denoted by  $K_{i,j}^0$  the two neutral kaons  $K^0$  and  $\bar{K}^0$ .

The invariance under CPT implies  $H_{11} = H_{22}$ . Moreover  $M_{21} = M_{12}^*$  and  $\Gamma_{21} = \Gamma_{12}^*$ , because M and  $\Gamma$  are hermitian. If CP invariance were valid, we would also have



$\langle K^0 | \mathcal{H}_{eff} | \bar{K}^0 \rangle = \langle \bar{K}^0 | \mathcal{H}_{eff} | K^0 \rangle$  and so  $M$  and  $\Gamma$  would be real. We know, instead, that CP is violated. Hence  $M$  and  $\Gamma$  are not real and the two eigenstates of the mass matrix have the form:

$$|K_{S,L}\rangle = \frac{1}{\sqrt{|p|^2 + |q|^2}} \left[ p |K^0\rangle \pm q |\bar{K}^0\rangle \right], \quad (6.5)$$

with

$$\frac{p}{q} = \sqrt{\frac{M_{12} - \frac{i}{2}\Gamma_{12}}{M_{12}^* - \frac{i}{2}\Gamma_{12}^*}}. \quad (6.6)$$

The corresponding eigenvalues are:

$$M_L = m_L - i \frac{\Gamma_L}{2} \quad (6.7)$$

and

$$M_S = m_S - i \frac{\Gamma_S}{2}. \quad (6.8)$$

The subscripts in  $K_L$  and  $K_S$  stand for “long” and “short” and they are due to the fact there is a big difference between the lifetimes of these two states. If CP were conserved ( $p = q$ ), these two states would also become eigenstates of CP and they would coincide with the states we have previously denoted by  $K_-^0$  and  $K_+^0$ . In this limit, which is not true but approximates well reality,  $K_S$  would decay to CP-even final states (like  $\pi\pi$ ).  $K_L$ , instead, would decay only to CP-odd final states. The phase space for states like  $\pi\pi$  is much bigger than the one for CP-odd final states. So it is clear why the lifetime of  $K_S$  is much shorter than the one of  $K_L$ .

To study CP violation, it can be useful to introduce a parameter  $\bar{\varepsilon}$ , which is defined in the following way:

$$\bar{\varepsilon} = \frac{p - q}{p + q} \quad (6.9)$$

We have:

$$\bar{\varepsilon} \simeq \frac{\text{Im } \Gamma_{12}/2 + i \text{Im } M_{12}}{m_L - m_S - \frac{i}{2}(\Gamma_L - \Gamma_S)}. \quad (6.10)$$

The two states  $K_L$  and  $K_S$  can be rewritten, by using  $\bar{\varepsilon}$ , in the following way:

$$\begin{aligned} |K_L\rangle &= \frac{1}{\sqrt{1+|\bar{\varepsilon}|^2}} \left( |K_-^0\rangle + \bar{\varepsilon} |K_+^0\rangle \right) = \frac{1}{\sqrt{2(1+|\bar{\varepsilon}|^2)}} \left[ |K^0\rangle (1 + \bar{\varepsilon}) - |\bar{K}^0\rangle (1 - \bar{\varepsilon}) \right] \\ |K_S\rangle &= \frac{1}{\sqrt{1+|\bar{\varepsilon}|^2}} \left( |K_+^0\rangle + \bar{\varepsilon} |K_-^0\rangle \right) = \frac{1}{\sqrt{2(1+|\bar{\varepsilon}|^2)}} \left[ |K^0\rangle (1 + \bar{\varepsilon}) + |\bar{K}^0\rangle (1 - \bar{\varepsilon}) \right]. \end{aligned} \quad (6.11)$$

Hence we see that CP violation in the decay matrix or in the mass matrix ( $\text{Im } \Gamma_{12} \neq 0$  or  $\text{Im } M_{12} \neq 0$ ) implies a CP impurity in the physical states, which can be measured by the parameter  $\bar{\varepsilon}$ .

We denote, as usual, by  $A_0$  and  $A_2$  the two following amplitudes

$$A_0 = A(K^0 \rightarrow 2\pi, I = 0) \quad (6.12)$$

$$A_2 = A(K_0 \rightarrow 2\pi, I = 2). \quad (6.13)$$

With a suitable choice for the phase of  $A_0$ , we can take for this amplitude a real expression, except for the final state pion - pion interaction, leading to a phase shift  $\delta_0$ . Hence we have:

$$A_0 = \text{Re } A_0 e^{i\delta_0}. \quad (6.14)$$

We also introduce two quantities  $\eta_{+-}$  and  $\eta_{00}$ , defined in this way:

$$\eta_{+-} = \frac{A(K_L \rightarrow \pi^+\pi^-)}{A(K_S \rightarrow \pi^+\pi^-)}; \quad (6.15)$$

$$\eta_{00} = \frac{A(K_L \rightarrow \pi^0\pi^0)}{A(K_S \rightarrow \pi^0\pi^0)}. \quad (6.16)$$

It is possible to express these experimentally observable quantities as functions of the CP violating parameters. We have:

$$\eta_{+-} = \varepsilon + \varepsilon', \quad (6.17)$$

$$\eta_{00} = \varepsilon - 2\varepsilon'. \quad (6.18)$$

In the previous formulas  $\varepsilon$  coincide with  $\bar{\varepsilon}$ . We have also introduced the new parameter  $\varepsilon'$ , which is defined in the following way:

$$\varepsilon' = ie^{i(\delta_2 - \delta_0)} \frac{\omega}{\sqrt{2}} \left[ \frac{\text{Im } A_2}{\text{Re } A_2} \right], \quad (6.19)$$

with  $\omega = \frac{\text{Re } A_2}{\text{Re } A_0} \simeq \frac{1}{22}$ .

The parameter  $\varepsilon$  (which coincide with  $\bar{\varepsilon}$ ) is related to the CP violation in the matrix  $M - \frac{i}{2}\Gamma$ , as we can see from eqs. (6.10)-(6.11). The mechanism of mixing of the CP eigenstates is the first possible source of CP violation, which is usually called "indirect" CP violation. The parameter  $\varepsilon'$ , instead, is linked to "direct"  $\Delta S = 1$  CP violation. We speak of direct CP violation when we have a transition of the CP odd eigenstate  $K_-^0$  to two pions.

### 6.1.1 The Present Status of Experimental and Theoretical Knowledge

The value of the parameter  $\varepsilon$  is known with a quite good accuracy. We have [10]:  
 $|\varepsilon| = (2.266 \pm 0.023) \times 10^{-3}$ .

The situation is different, instead, for what concerns the determination of the ratio  $\frac{\varepsilon'}{\varepsilon}$ . This quantity is very important, because the real part of  $\frac{\varepsilon'}{\varepsilon}$  measures direct CP violation in the decay of a neutral kaon in two pions.

The two main experiments measuring this quantity gave contradictory results. In fact the result of the collaboration NA31 at CERN is [7]:

$$\operatorname{Re} \frac{\varepsilon'}{\varepsilon} = (23 \pm 7) \times 10^{-4}, \quad (6.20)$$

while the Fermilab (E731) result is [8]:

$$\operatorname{Re} \frac{\varepsilon'}{\varepsilon} = (7.4 \pm 6.0) \times 10^{-4}. \quad (6.21)$$

The result of the E731 collaboration is compatible also with the so called superweak theory. This theory predicts that the violation of CP is present only in the mass matrix and not in the direct kaon decay. Hence in this superweak scenario there would be only the CP violation parameter  $\varepsilon$  and, of course, the ratio  $\frac{\varepsilon'}{\varepsilon}$  would be equal to zero. The CERN result is different from the one of Fermilab and, in particular, it is not consistent with the superweak theory.

It is clear that there is a need for new and more precise results.

New experiments are already working at CERN and Fermilab. Another one called DAΦNE should become operative very soon at the INFN National Laboratories in Frascati. DAΦNE is a so called  $\Phi$ -factory, that is an  $e^+e^-$  collider optimized for operation at a total energy of 1020 MeV, corresponding to the mass of the  $\Phi$  meson. The  $\Phi$  particles produced in the collider decay mainly into a pair of neutral kaons which can then decay into different final states  $f_1$  and  $f_2$ . A whole spectrum of “kaon interferometry” experiments can be performed at DAΦNE with an appropriate choice of  $f_1$  and  $f_2$ .

For more details and informations about DaΦne we refer the interested reader to the ref. [73].

All these new experiments should improve the sensitiveness to  $1 \times 10^{-4}$  and there is the hope they can give a definite result.

Also from a theoretical point of view the determination of  $\operatorname{Re} \frac{\varepsilon'}{\varepsilon}$  is a very difficult task and we do not have a definite answer at our disposal, although a lot of work has been done in the last years.

The short distance part of the calculation is well known. The Wilson coefficients of all the  $Q_i$  operators of the lagrangian of eq. (4.1) have been calculated to the next to leading order by the Rome [16] and Munich [15] groups. Here, differently from what we have seen in the case of the  $\Delta I = 1/2$  rule, we only need the  $y_i(\mu)$ , which control the CP violating part of the amplitudes.

The main source of theoretical uncertainty is, also in this case, the long distance computation of the hadronic matrix elements of the quark operators. There are two complete estimates of these matrix elements, made by the two groups of Rome and Munich and recently updated [70, 71]. The lattice result is:

$$\text{Re} \frac{\varepsilon'}{\varepsilon} = (3.1 \pm 2.5 \pm 0.3) \times 10^{-4}, \quad (6.22)$$

while the  $1/N_c$  approach (improved by fitting the  $\Delta I = 1/2$  rule) gives

$$-2.5 \times 10^{-4} \leq \text{Re} \frac{\varepsilon'}{\varepsilon} \leq 13.7 \times 10^{-4}. \quad (6.23)$$

The results of both groups seem to indicate it would be difficult to justify, within the Standard Model a value substantially larger than  $1 \times 10^{-3}$ . This small value is mainly due to the cancellation between gluon and electroweak penguin operators [72].

### 6.1.2 $\varepsilon'/\varepsilon$ in the Chiral Quark Model

It is also possible to estimate the ratio  $\frac{\varepsilon'}{\varepsilon}$  within our model. In fact the  $\Delta S = 1$  chiral lagrangian we have recovered in chapter 4 enables us to compute the matrix elements of all the  $Q_i$  operators. This estimate of  $\frac{\varepsilon'}{\varepsilon}$  has been done and can be found in ref. [29]. Here we just limit ourselves to report and comment the main results of this analysis.

Some new elements have been introduced in this determination of  $\frac{\varepsilon'}{\varepsilon}$ .

We can remember, among the others, the inclusion of non perturbative gluon condensate effects and of meson loop renormalization, which introduces a scale dependence for the matrix elements. These two kinds of contributions are essential to achieve consistency with the  $\Delta I = 1/2$  selection rule, as we have seen in chapter 5. Another important novelty of the analysis of [29] is the introduction of the complete  $O(p^2)$  bosonization of the operators  $Q_7$  and  $Q_8$ , including some terms which had been neglected in the previous determinations.

The final result for  $\text{Re} \frac{\varepsilon'}{\varepsilon}$  depends on a lot of input parameters and mainly on the values of the mixing parameter  $\text{Im} \lambda_t$  and of the quark condensate  $\langle \bar{q}q \rangle$ .

To have a first idea of the possible values for  $\frac{\varepsilon'}{\varepsilon}$ , we can try to vary all the input parameters inside their ranges of allowed values and to take this large range of values for the quark condensate:

$$(-200\text{MeV})^3 \leq \langle \bar{q}q \rangle \leq (-280\text{MeV})^3. \quad (6.24)$$

In this way we find the very conservative estimate:

$$-5.0 \times 10^{-3} \leq \frac{\varepsilon'}{\varepsilon} \leq 1.4 \times 10^{-3} \quad (6.25)$$

It can be more interesting to give also a less conservative, “biased” estimate, obtained restricting the range of values of some input parameters. First of all we can fix the QCD scale parameter to its central value,  $\Lambda_{QCD}^{(4)} = 350 \text{ MeV}$ . For the quark condensate we can use the improved PCAC value given by eqs. (4.69)-(4.71). In this way we have

$$\frac{\varepsilon'}{\varepsilon} = (4 \pm 5) \times 10^{-4}. \quad (6.26)$$

It is clear that the final result is a very sensitive function of the value chosen for the quark condensate. Moreover it is the result of the cancellation between two quantities which are almost equal but have the opposite sign (the contributions of  $Q_6$  and  $Q_8$ ). Hence, even a small uncertainty can be amplified and we can say that only the order of magnitude can be predicted with a good degree of reliability.

Anyway, apart from the exact value of  $\varepsilon'/\varepsilon$ , the chiral quark model result is consistent with the conclusion of ref. [70], that it would be very difficult to explain, within the Standard Model, a value for this ratio bigger than  $10^{-3}$ . The introduction in our model of terms coming from the bosonization of the electroweak penguins, which had always been neglected in the VSA estimate of matrix elements, enhances the contribution coming from these operators. Hence the cancellation between the contributions of the gluonic and the electroweak penguins takes place also for the present values of  $m_t$ . This cancellation is more effective for larger values of the quark condensates, while at smaller values the gluonic penguin contribution exceeds the electroweak one.

The role of meson loop renormalization is that of bringing back the central value of  $\varepsilon'/\varepsilon$  towards positive numbers.

Finally let us discuss the scheme dependence and the problem of the determination of the parameter  $M$ . In chapter 5, studying the  $\Delta I = 1/2$  rule, we have selected a range of values for this input parameter between 160 and 220 MeV, by requiring the minimization of the  $\gamma_5$ -scheme dependence.

A similar analysis in the case of the estimate of  $\varepsilon'/\varepsilon$  gives a value of  $M \simeq 215 - 220$  MeV, which is inside the interval mentioned before. This value is quite stable with respect to the choice made for the matching scale, the quark and gluon condensate and  $m_t$ . Let us notice that  $\varepsilon'/\varepsilon$  is a very sensitive decreasing function of  $M$ .

The fact that, choosing an appropriate value for  $M$ , one can reduce very much the  $\gamma_5$ -scheme dependence of the result is very important. In fact the scheme dependence induced by the Wilson coefficients determines a 80% uncertainty when using the  $1/N_c$  matrix elements (see for example the last paper of ref. [15]), which are the same in both schemes.

From now on we will fix  $M = 220$  MeV.

# Chapter 7

## $\Delta S = 2$ Processes

### 7.1 Analysis of $K^0 - \bar{K}^0$ Mixing

Until now we have considered  $\Delta S = 1$  physics. We have developed a formalism, based on chiral perturbation theory and chiral quark model, which enables us to study the weak non leptonic decays of kaons. We have also seen our model at work in the analysis of the  $\Delta I = 1/2$  selection rule and in the estimate of  $\varepsilon'/\varepsilon$ .

In this chapter we want to extend this formalism to  $\Delta S = 2$  physics, in such a way to study the  $K^0 - \bar{K}^0$  mixing.

We have seen in the previous chapter that the neutral kaon system is particularly interesting. In fact the analysis of  $K^0 - \bar{K}^0$  mixing is the easiest way to study CP violation in the Standard Model. From the results of this analysis we can recover important information about the elements of the CKM mixing matrix and especially about its imaginary phase, which is important, as we have seen, for the estimate of  $\varepsilon'/\varepsilon$ .

There are also other important phenomenological parameters that can be studied, like, for instance, the mass difference  $\Delta M_{LS}$  between  $K_L$  and  $K_S$ . This quantity is known quite well from the experiments. Hence it can be interesting to compare the experimental result with the theoretical prediction.

The mixing in the neutral kaon system is determined by the weak effective hamiltonian, through the matrix element

$$\langle \bar{K}^0 | \mathcal{H}_{eff} | K^0 \rangle. \quad (7.1)$$

The imaginary and the real part of this matrix element are related, respectively, to the CP violating quantity  $\varepsilon$  and the mass difference  $\Delta M_{LS}$ .

We can split, as usual, the analysis into short distance effects (which are included in the Wilson coefficients) and long distance effects.

For what concerns the last ones, we still have to distinguish between two different kinds of contributions. First of all there are the ones usually denoted as “short distance” contributions. We prefer not to adopt this notation, which could be misleading. Therefore we will call them “box diagram contributions”, because they are originated by the so called box Feynman diagrams. They correspond to a direct  $\Delta S = 2$  transition  $K^0 \rightarrow \bar{K}^0$ .

The second kind of contributions we have to consider is that of the usually called “long distance” contributions. They correspond to a double insertion of  $\Delta S = 1$  hamiltonian. So, in this case, the  $K^0 - \bar{K}^0$  mixing proceeds through the insertion of intermediate states made of one or more particles.

The long distance contribution is practically irrelevant for the determination of the parameter  $\varepsilon$ , but it cannot be neglected in the analysis of the mass difference.

### 7.1.1 Effective Lagrangian for $\Delta S = 2$ Transitions

Let us start our analysis from the box diagram contribution. It leads to the following effective  $\Delta S = 2$  quark lagrangian at scales  $\mu < m_c$

$$\mathcal{L}_{\Delta S=2} = -\frac{G_F^2 M_W^2}{4\pi^2} \left[ \lambda_c^2 \eta_1 S(x_c) + \lambda_t^2 \eta_2 S(x_t) + 2\lambda_c \lambda_t \eta_3 S(x_c, x_t) \right] b(\mu) Q_{S2}(\mu), \quad (7.2)$$

where  $G_F$  is the Fermi constant,  $M_W$  is the  $W$  boson mass,  $x_i = m_i^2/M_W^2$ , and  $\mu$  is the renormalization scale. The parameters  $\lambda_j = V_{jd}V_{js}^*$  represent the relevant combinations of Kobayashi-Maskawa (KM) matrix elements ( $j = u, c, t$ ). We have denoted by  $Q_{S2}$  the  $\Delta S = 2$  local four quark operator

$$Q_{S2} = (\bar{s}_L \gamma^\mu d_L)(\bar{s}_L \gamma_\mu d_L). \quad (7.3)$$

Finally, the Inami-Lim functions [74]  $S(x)$  and  $S(x_c, x_t)$  are defined as follows

$$S(x) = x \left[ \frac{1}{4} + \frac{9}{4} \frac{1}{1-x} - \frac{3}{2} \frac{1}{(1-x)^2} \right] - \frac{3}{2} \left[ \frac{x}{1-x} \right]^3 \ln x, \quad (7.4)$$

$$S(x_c, x_t) = -x_c \ln x_c + x_c \left[ \frac{x_t^2 - 8x_t + 4}{4(1-x_t)^2} \ln x_t + \frac{3}{4} \frac{x_t}{x_t - 1} \right]. \quad (7.5)$$



These functions, which depend on the masses of the charm and top quarks, are generated by the integration of the electroweak loops. They describe the  $\Delta S = 2$  transition amplitude in the absence of strong interactions.

The short distance QCD corrections are encoded in the coefficients  $\eta_1$ ,  $\eta_2$  and  $\eta_3$ , with a common scale-dependent factor  $b(\mu)$  factorized out. They are functions of the heavy quarks masses and of the scale parameter  $\Lambda_{\text{QCD}}$ . These QCD corrections are available to NLO [76, 75, 77] in the strong and electromagnetic couplings.

The scale-dependent common factor of the short-distance corrections is given by

$$b(\mu) = [\alpha_s(\mu)]^{-2/9} \left( 1 - J_3 \frac{\alpha_s(\mu)}{4\pi} \right), \quad (7.6)$$

where  $J_3$  depends on the  $\gamma_5$ -scheme used in the regularization. The NDR gives

$$J_3^{\text{NDR}} = -\frac{307}{162}, \quad (7.7)$$

while in the HV scheme one finds

$$J_3^{\text{HV}} = -\frac{91}{162}. \quad (7.8)$$

For the running QCD coupling we take, as usual, the values given by eqs. (4.2)–(4.3).

Let us note that the GIM mechanism is at work in the derivation of the lagrangian of (7.2). In fact the contributions of the u, c, t intermediate states would exactly cancel each other if their masses were equal. The mass of the u quark has been neglected with respect to heavy quark masses.

The box diagram contributions are usually expressed in terms of the renormalization group-invariant parameter  $\widehat{B}_K$ . We have, first of all, to introduce the scale-dependent parameter  $B_K(\mu)$ , which is defined by the following equation:

$$\langle \bar{K}^0 | Q_{S2}(\mu) | K^0 \rangle = \frac{4}{3} f_K^2 m_K^2 B_K(\mu), \quad (7.9)$$

where  $f_K$  and  $m_K$  are, respectively, the kaon decay constant and mass (see table B.1 of appendix B for their numerical values).

The value of  $B_K(\mu)$  measures the deviation of the matrix element from the result obtained in the vacuum saturation approximation, used in the original work of Gaillard and Lee [3], namely  $B_K(\mu) = 1$ . The physically relevant parameter  $\widehat{B}_K$ , is defined by the relation:

$$\widehat{B}_K = B_K(\mu) b(\mu). \quad (7.10)$$

$\hat{B}_K$	Method	Reference
3/4	Leading $1/N_c$	[80]
0.37	Lowest-Order Chiral Perturbation Theory	[81]
$0.70 \pm 0.10$	Next-to-Leading $1/N_c$ Estimate	[84]
$0.4 \pm 0.2$	Next-to-Leading $1/N_c$ Estimate, $O(p^2)$	[20]
0.6 – 0.8	NJL Model with Spin 1 Interactions	[82]
$0.42 \pm 0.06$	$O(p^4)$ CHPT + $1/N_c$ Estimate	[83]
$0.39 \pm 0.10$	QCD-Hadronic Duality	[85, 86]
$0.5 \pm 0.1 \pm 0.2$	QCD Sum Rules (3-Point Functions)	[87]
$0.90 \pm 0.03 \pm 0.14$	Lattice	[88]

Table 7.1: Values of  $\hat{B}_K$  obtained in different approaches.

This quantity should be in principle scale independent. As we include the perturbative NLO determination of the Wilson coefficient, we shall also discuss the  $\gamma_5$ -scheme dependence of our result.

An useful summary of various determinations of this parameter is given in Table 1, which is an up-to-date version of a table taken from ref. [79].

We can have a first model independent estimate of  $\hat{B}_K$ , by using chiral symmetry arguments. In fact the  $\Delta S = 2$  matrix element can be related via chiral symmetry to that of the  $\Delta S = 1$  and  $\Delta I = 3/2$  amplitude  $\mathcal{A}(K^+ \rightarrow \pi^+\pi^0)$ [81]. Neglecting the  $SU(3)$  breaking effects related to the chiral loop corrections to the matrix element, the electromagnetic contributions and the  $\pi - \eta$  mixing, we obtain the relation

$$\frac{4}{3}f_K^2 m_K^2 \hat{B}_K = \frac{\sqrt{2}}{G_F} \frac{f_\pi}{V_{us}^* V_{ud}} \frac{m_K^2}{m_K^2 - m_\pi^2} \frac{b(\mu)}{z_1(\mu) + z_2(\mu)} \mathcal{A}(K^+ \rightarrow \pi^+\pi^0). \quad (7.11)$$

In the previous equation, we can notice the presence of the  $\Delta S = 2$  Wilson coefficient  $b(\mu)$ , given by (7.6), and of  $z_1(\mu)$  and  $z_2(\mu)$ , the real parts of the Wilson coefficients for the two  $\Delta S = 1$  operators  $Q_1$  and  $Q_2$  which dominate the  $K^+ \rightarrow \pi^+\pi^0$  transition.

By inputting the experimental value  $\mathcal{A}(K^+ \rightarrow \pi^+\pi^0) = 1.84 \times 10^{-8}$  GeV and the NLO results for the Wilson coefficients (the ratio  $b(\mu)/(z_1(\mu) + z_2(\mu))$  is to a large extent  $\mu$  and  $\gamma_5$ -scheme independent) we find the model independent estimate

$$\hat{B}_K = 0.40. \quad (7.12)$$

This number updates the value  $\hat{B}_K = 0.33$  given in ref. [81].

On the other hand, having a model, like ours, that reproduces the experimental result, in order to apply correctly eq. (7.11) we must subtract in  $\mathcal{A}(K^+ \rightarrow \pi^+\pi^0)$  all the chiral symmetry breaking corrections due to chiral loops, electroweak penguins and  $\pi - \eta$  mixing [6].

In this way we obtain in the  $\chi$ QM approach, on the basis of chiral symmetry arguments alone, the following  $O(p^2)$  prediction:

$$\hat{B}_K = \frac{3}{4}b(\mu) \frac{f_\pi f}{f_K^2} \left[ 1 + \frac{1}{N_c} (1 - \delta_{(GG)}) \right]. \quad (7.13)$$

In considering eq. (7.13), it is important to remember that the factor  $f_\pi$  comes out from the soft pion theorem, while  $f$  is the chiral lagrangian parameter appearing in the calculation of the amplitude  $\mathcal{A}(K^+ \rightarrow \pi^+\pi^0)$ . At the tree level  $f = f_\pi$ .

The spurious  $\mu$  dependence present in eq. (7.13) should be cancelled by that of the hadronic matrix elements, which is absent at the lowest order in the chiral expansion.

If we choose for the gluon condensate the value  $\langle \frac{\alpha_s}{\pi} GG \rangle = (360 \text{ MeV})^4$  (which gives the best fit of  $\mathcal{A}(K^+ \rightarrow \pi^+\pi^0)$ ), we obtain at  $\mu = 0.8 \text{ GeV}$

$$\widehat{B}_K \simeq 0.33. \quad (7.14)$$

This value includes the non-factorizable effects of gluon condensate corrections, which play a crucial role in the fit of the  $\Delta I = 3/2$  amplitude in  $K \rightarrow \pi\pi$  decays.

The value in eq. (7.14) represents the starting point for our analysis, to which we will add the effects of chiral loop contributions, which are characteristic of the  $\Delta S = 2$  matrix element.

Let us show how we can compute the  $\widehat{B}_K$  parameter by using the chiral quark model to construct the  $\Delta S = 2$  chiral lagrangian, as we have done in the case of  $\Delta S = 1$  physics.

### 7.1.2 The $\Delta S = 2$ Weak Chiral Lagrangian

In the case we are studying, it is quite easy to derive the weak chiral lagrangian. In fact we have to bosonize only one quark operator, that is the operator  $Q_{S2}$  of eq. (7.3). At the leading  $O(p^2)$  order in the chiral expansion, the  $\Delta S = 2$  weak chiral lagrangian is given by:

$$\mathcal{L}_{\Delta S=2}^{(2)} = C(Q_{S2}) \text{Tr} \left( \lambda_2^3 \Sigma D_\mu \Sigma^\dagger \right) \text{Tr} \left( \lambda_2^3 \Sigma D_\mu \Sigma^\dagger \right). \quad (7.15)$$

In eq. (7.15)  $\Sigma$  and  $\lambda_2^3$  are given, as usual, by eq. (3.8) and eq. (4.5) and the meaning of the notations is the same we have followed in all the previous chapters.

To determine the coefficient of bosonization  $C(Q_{S2})$  we have to consider the two configurations represented in Fig. 1.

As discussed in chapter 4 in the case of the operators  $Q_1$  and  $Q_2$ , the consistency with the normalization prescription adopted for the evanescent operators makes also the matrix elements of  $Q_{S2}$  the same in HV and NDR schemes. Hence, in both schemes we find

$$C(Q_{S2}) = -\frac{f^4}{4} \left( 1 + \frac{1}{N_c} \right). \quad (7.16)$$

We still have to add to this expression the contribution coming from non perturbative gluonic corrections. We have already shown the importance of these corrections in the study of  $\Delta I = 1/2$  rule. Including this contribution, the coefficient of bosonization becomes

$$C(Q_{S2}) = -\frac{f^4}{4} \left[ 1 + \frac{1}{N_c} \left( 1 - \delta_{(GG)} \right) \right], \quad (7.17)$$

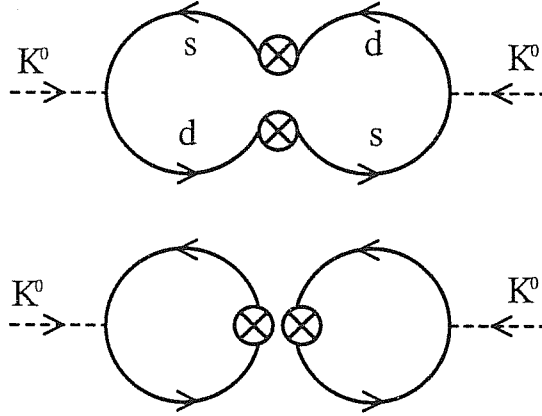


Figure 7.1: The two configurations relevant to the determination of the chiral coefficient  $C(Q_{S2})$ .

where  $\delta_{(GG)}$  is given by eq. (4.25).

By using the definition given in eq. (7.9) and computing at leading order the matrix element  $\langle \bar{K}^0 | Q_{S2} | K^0 \rangle$ , we obtain the following expression for  $B_K(\mu)$ :

$$B_K(\mu) = \frac{3}{4} \left[ 1 + \frac{1}{N_c} (1 - \delta_{(GG)}) \right] \frac{f^2}{f_K^2}. \quad (7.18)$$

At this stage of the computation,  $B_K(\mu)$  does not exhibit yet an explicit dependence on  $\mu$ . In our approach the scale dependence arises from meson-loop corrections.

If we take  $f = f_\pi$  in eq. (7.18) we recover eq. (7.14), as it should be.

Taking  $f = f_K$  and  $\delta_{(GG)} = 0$ , eq. (7.18) reproduces the result obtained in the  $1/N_c$ -approach.

We have already discussed in chapter 3 about the fact that it is not possible to give a unique determination of the chiral lagrangian parameter  $f$  at the leading order and about the way in which this ambiguity can be solved going to the next to leading order in chiral perturbation theory and considering the meson decay constant renormalization.

### 7.1.3 Meson Loop Corrections

Let us introduce in our estimation the contributions coming from the mesonic chiral loops.

Here we proceed as in the case of  $\Delta S = 1$  chiral lagrangian. We assume that the tree level  $O(p^4)$  terms of the chiral lagrangian are  $\mu$  independent. Hence the scale dependence introduced in the hadronic matrix element via the meson loops, evaluated in

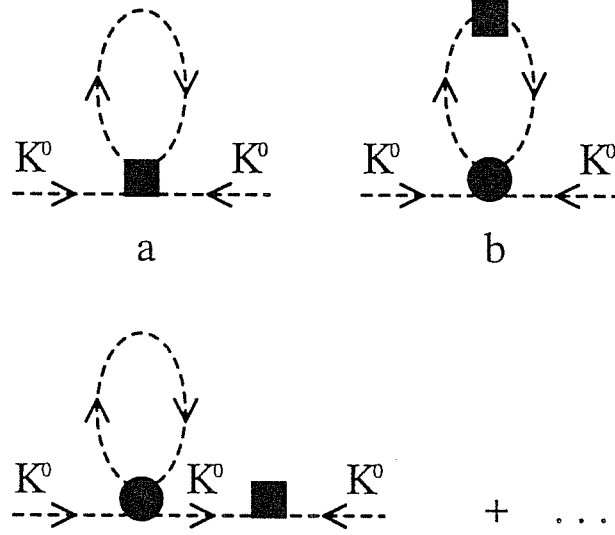


Figure 7.2: One-loop meson corrections to the kaon mass matrix.

dimensional regularization with the standard minimal subtraction, should be matched by the scale dependence of the Wilson coefficient.

The diagrams relevant to the present case are depicted in Fig. 2. The diagram in Fig. 2(a) contains only a four-meson weak vertex of the  $\Delta S = 2$  chiral Lagrangian. The diagram in Fig. 2(b), instead, contains two vertices, one of which is a four-meson strong vertex and the other is a two-meson weak vertex. Another class of diagrams, which are induced by wave function renormalization, is shown below 3(a,b).

A direct calculation yields:

$$\langle \bar{K}^0 | Q_{S2}(\mu) | K^0 \rangle_{tree} = C(Q_{S2}) \left( \frac{-4m_K^2}{f^2} \right) \quad (7.19)$$

$$\begin{aligned} \langle \bar{K}^0 | Q_{S2}(\mu) | K^0 \rangle_{1a} &= i C(Q_{S2}) \frac{1}{f^4} \left[ 3I_4(m_\eta^2) + I_4(m_\pi^2) + 7m_K^2 I_2(m_\eta^2) \right. \\ &\quad \left. + \frac{7}{3}m_K^2 I_2(m_\pi^2) + \frac{8}{3}m_K^2 [I_2(m_\pi^2) + I_2(m_K^2)] \right] \end{aligned} \quad (7.20)$$

$$\begin{aligned} \langle \bar{K}^0 | Q_{S2}(\mu) | K^0 \rangle_{1b} &= \frac{4}{3}i C(Q_{S2}) \frac{1}{f^4} \left[ I_4(m_K^2) + 3m_K^2 I_2(m_K^2) \right. \\ &\quad \left. + 3m_K^4 I_3(m_K^2) \right] \end{aligned} \quad (7.21)$$

$$\begin{aligned} \langle \bar{K}^0 | Q_{S2}(\mu) | K^0 \rangle_{wf} &= -4i C(Q_{S2}) \frac{m_K^2}{f^4} \left[ \frac{1}{4}I_2(m_\pi^2) + \frac{1}{4}I_2(m_\eta^2) \right. \\ &\quad \left. + \frac{1}{2}I_2(m_K^2) \right], \end{aligned} \quad (7.22)$$

where  $C(Q_{S2})$  is the coefficient of bosonization as given by eq. (7.17), and

$$I_2(m_i^2) = \frac{1}{(2\pi)^4} \int \frac{1}{(q^2 - m_i^2)} d^4q = \frac{i}{(16\pi^2)} m_i^2 \left(1 - \ln \frac{m_i^2}{\mu^2}\right) \quad (7.23)$$

$$I_3(m_i^2) = \frac{1}{(2\pi)^4} \int \frac{1}{(q^2 - m_i^2)^2} d^4q = -\frac{i}{(16\pi^2)} \ln \left(\frac{m_i^2}{\mu^2}\right) \quad (7.24)$$

$$I_4(m_i^2) = \frac{1}{(2\pi)^4} \int \frac{q^2}{(q^2 - m_i^2)} d^4q = \frac{i}{(16\pi^2)} m_i^4 \left(1 - \ln \frac{m_i^2}{\mu^2}\right). \quad (7.25)$$

We also have to consider the meson decay constant renormalization, that is the one-loop determination of  $f$  in terms of  $f_K$ . This renormalization introduces chiral corrections which cancel some of the contributions coming from meson loops. The chiral loops coming from the kaon decay constant renormalization cancel exactly those coming from the wave function renormalization and part of the ones produced by the diagrams of Fig. 2(a).

Denoting by  $\langle \bar{K}^0 | Q_{S2}(\mu) | K^0 \rangle|_{1aNF}$  the chiral corrections coming from the diagrams of Fig. 2(a) that remain after the kaon decay constant renormalization, we have:

$$\begin{aligned} \langle \bar{K}^0 | Q_{S2}(\mu) | K^0 \rangle|_{1aNF} &= 4i C(Q_{S2}) \frac{1}{f^4} \left[ -\frac{4}{3} I_4(m_K^2) + \frac{3}{4} I_4(m_\eta^2) \right. \\ &\quad \left. + \frac{1}{4} I_4(m_\pi^2) + \frac{1}{4} m_K^2 [I_2(m_\pi^2) + 3I_2(m_\eta^2)] \right]. \end{aligned} \quad (7.26)$$

The expression for the amplitude, comprehensive of meson loops, wave function and kaon decay constant renormalization can be written as

$$\begin{aligned} \langle \bar{K}^0 | Q_{S2}(\mu) | K^0 \rangle &= \langle \bar{K}^0 | Q_{S2}(\mu) | K^0 \rangle|_{tree} + \langle \bar{K}^0 | Q_{S2}(\mu) | K^0 \rangle|_{1b} + \\ &\quad + \langle \bar{K}^0 | Q_{S2}(\mu) | K^0 \rangle|_{1aNF}, \end{aligned} \quad (7.27)$$

where the contribution  $\langle \bar{K}^0 | Q_{S2}(\mu) | K^0 \rangle|_{tree}$  must be evaluated identifying the chiral lagrangian coefficient  $f$  with  $f_K$ .

In order to show the impact of chiral loops on the  $K^0 - \bar{K}^0$  amplitude, we find convenient to factorize formally the tree level contribution in terms of the input parameters, while giving the corresponding loops renormalization as a numerical coefficient with an explicit  $\mu$  dependence, as we have already done in the case of  $\Delta S = 1$ . The values of the masses and other input variables are those (central values) given in Table B.1 of appendix B.

We thus find:

$$\langle \bar{K}^0 | Q_{S2}(\mu) | K^0 \rangle = m_K^2 f_K^2 \left[ 1 + \frac{1}{N_c} (1 - \delta_{GG}) \right] (1 + 0.728 + 0.372 \ln \mu^2). \quad (7.28)$$

From eq. (7.28) we obtain the final result for  $B_K(\mu)$ , inclusive of the effects of meson loops, wave function and kaon decay constant renormalization:

$$B_K(\mu) = \frac{3}{4} \left[ 1 + \frac{1}{N_c} (1 - \delta_{(GG)}) \right] (1 + 0.728 + 0.372 \ln \mu^2) . \quad (7.29)$$

The scale dependence of the hadronic matrix element interferes constructively with that of  $b(\mu)$ , instead of cancelling. Nevertheless, the overall scale dependence remains below 20% in the range between 0.8 and 1 GeV.

An approach similar to the one that we are adopting here has been followed in ref. [84] in the framework of a cut-off regularization of the chiral loops. In that way the scale dependence of the hadronic matrix element partially compensates the one of the Wilson coefficient, leading to a reduction of the total  $\mu$  dependence of the physical amplitude.

Anyway, it is important to remember that here we have chosen to regularize the divergent integrals appearing in the meson loops by using dimensional regularization (as we have already done in the previous chapters), to be consistent with the short distance calculation of the Wilson coefficients, which is performed using the same regularization.

## 7.2 The $\widehat{B}_K$ Parameter

We now have at our disposal all the ingredients needed to analyze the values of the parameter  $\widehat{B}_K$ , where  $B_K(\mu)$  and  $b(\mu)$  are given by eq. (7.29) and eq. (7.6), respectively. Let us start from the choice of the input parameters entering in the determination of our final result.

### 7.2.1 Input Parameters

A relevant input parameter in our present analysis is the gluon condensate, which determines the size of the gluon corrections to  $B_K(\mu)$ .

As already said, we are trying to construct a phenomenological model which can permit us to obtain consistent estimations of different observables of kaon physics for a given set of input parameters. Therefore we have chosen for the gluon condensate the value that gives the best fit of the  $\Delta I = 1/2$  selection rule. We have seen in chapter 5 that we obtain the best fit of the  $\Delta I = 1/2$  rule for the value of the gluon condensate  $\langle \frac{\alpha_s}{\pi} GG \rangle = (360 \text{ MeV})^4$ .

By requiring that the  $\Delta I = 3/2$   $K^+ \rightarrow \pi^+ \pi^0$  amplitude is reproduced within a 30%



error, we obtain

$$\left\langle \frac{\alpha_S}{\pi} GG \right\rangle = (360 \pm 15 \text{ MeV})^4 . \quad (7.30)$$

In our numerical analysis we will vary the value of the gluon condensate inside this interval, to have an idea of the way in which  $B_K$  depends on it.

There is also another input parameter which is important for the determination of  $\widehat{B}_K$ . It is the QCD running coupling constant  $\alpha_s$ , entering in the computation of the short distance factor  $b(\mu)$ . In our numerical estimates we use for  $\alpha_s$  the range of eq.(4.2), corresponding to the values of  $\Lambda_{\text{QCD}}^{(4)}$  given by eq.(4.3).

Our results depend very mildly on the quark condensate that we keep fixed at the value  $\langle \bar{q}q \rangle = -(280 \text{ MeV})^3$ , which gives the best fit of the  $\Delta I = 1/2 K^0 \rightarrow \pi\pi$  amplitude.

### 7.2.2 Numerical Results for $\widehat{B}_K$

At last we are ready to give a numerical estimate of the parameter  $\widehat{B}_K$ .

We have summarized our results in Tab.2 In this table we have fixed the gluon condensate to the central value of the range given in eq. (7.30) and we have considered two different values of the matching scale ( $\mu = 0.8 \text{ GeV}$  and  $\mu = 1 \text{ GeV}$ ) in both schemes HV and NDR.

In this way we can have also an idea of the  $\gamma_5$ -scheme and of the scale dependence of our results. These dependences are expressed, as usual, by means of the two following quantities:

$$\Delta_{\gamma_5} \widehat{B}_K = 2 \left| \frac{\widehat{B}_K|_{HV} - \widehat{B}_K|_{NDR}}{\widehat{B}_K|_{HV} + \widehat{B}_K|_{NDR}} \right| \quad (7.31)$$

$$\Delta_{\mu} \widehat{B}_K = 2 \left| \frac{\widehat{B}_K(1\text{GeV}) - \widehat{B}_K(0.8\text{GeV})}{\widehat{B}_K(1\text{GeV}) + \widehat{B}_K(0.8\text{GeV})} \right|. \quad (7.32)$$

The three parts of the table correspond to three different values of  $\Lambda_{\text{QCD}}^{(4)}$ , in such a way to recover information about the result dependence on this parameter.

From table 2 we obtain the ranges  $0.79 \leq \widehat{B}_K \leq 1.01$  in NDR and  $0.69 \leq \widehat{B}_K \leq 0.97$  in HV scheme.

The scale dependence  $\Delta_{\mu} \widehat{B}_K$  is near to 20% in both schemes. As a matter of fact, the final  $\mu$  dependence is about 10% larger than the one originally present in the coefficient  $b(\mu)$ . We have already discussed this point in the previous section. The desired cancellation of the scale dependences doesn't take place, if we regularize the meson loops with dimensional regularization, but we have to use this regularization technique to be consistent with the Wilson coefficient calculation.

$\Lambda_{\text{QCD}}^{(4)} = 250 \text{ MeV}$				
	$\mu = 0.8 \text{ GeV}$		$\mu = 1 \text{ GeV}$	
	NDR	HV	NDR	HV
$b(\mu)$	1.25	1.19	1.30	1.24
$\widehat{B}_K$	0.88	0.84	1.01	0.97
$\Delta_{\gamma_5} \widehat{B}_K$	5.2%		4.2%	
$\Delta_\mu \widehat{B}_K$	14% – 15%			
$\Delta_\mu b(\mu)$	4% – 5%			
$\Lambda_{\text{QCD}}^{(4)} = 350 \text{ MeV}$				
	$\mu = 0.8 \text{ GeV}$		$\mu = 1 \text{ GeV}$	
	NDR	HV	NDR	HV
$b(\mu)$	1.17	1.08	1.23	1.17
$\widehat{B}_K$	0.83	0.77	0.96	0.91
$\Delta_{\gamma_5} \widehat{B}_K$	8%		5.7%	
$\Delta_\mu \widehat{B}_K$	15% – 17%			
$\Delta_\mu b(\mu)$	5% – 7%			
$\Lambda_{\text{QCD}}^{(4)} = 450 \text{ MeV}$				
	$\mu = 0.8 \text{ GeV}$		$\mu = 1 \text{ GeV}$	
	NDR	HV	NDR	HV
$b(\mu)$	1.12	0.97	1.18	1.09
$\widehat{B}_K$	0.79	0.69	0.92	0.85
$\Delta_{\gamma_5} \widehat{B}_K$	14.1%		7.9%	
$\Delta_\mu \widehat{B}_K$	15% – 21%			
$\Delta_\mu b(\mu)$	5% – 11%			

Table 7.2: Matching scale and  $\gamma_5$  scheme dependence of  $\widehat{B}_K$  in the  $\chi$ QM with NLO Wilson coefficient, for three different values of  $\Lambda_{\text{QCD}}^{(4)}$ . We take for the gluon condensate the value  $\langle \alpha_s GG/\pi \rangle = (360 \text{ MeV})^4$ , preferred by the fit of  $\Gamma(K^+ \rightarrow \pi^+ \pi^0)$ .

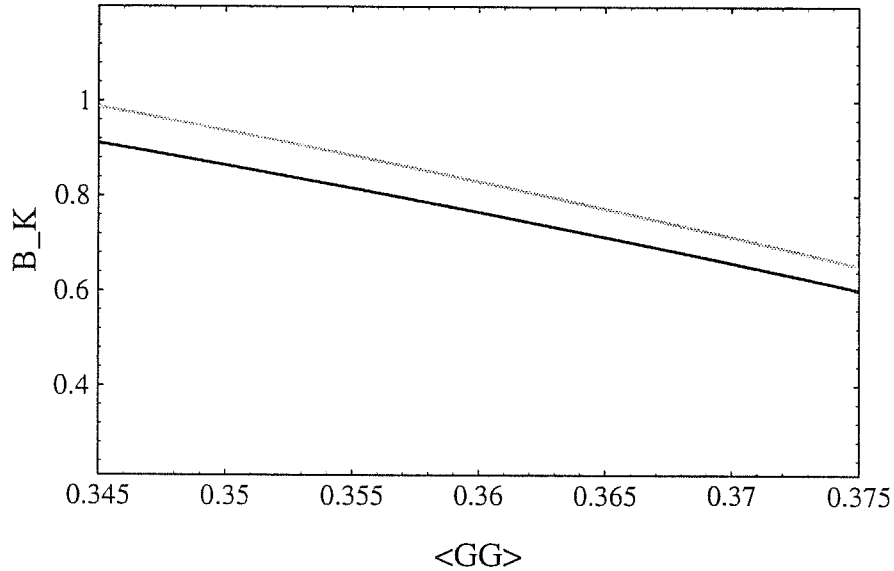


Figure 7.3: The  $\hat{B}_K$  parameter is shown as a function of the gluon condensate for  $\Lambda_{\text{QCD}}^{(4)} = 350$  MeV and  $\mu = 0.8$  GeV. We denote by  $\langle GG \rangle$  the quantity  $\langle \alpha_s GG / \pi \rangle^{1/4}$  in units of GeV. The dark and grey lines represent the HV and NDR results respectively.

Nevertheless, the fact that the scale dependence is at most 20% makes us confident on the stability of our results and allows us to choose, as usual,  $\mu = 0.8$  GeV as our preferred matching scale.

The scheme dependence of our result is entirely due to  $b(\mu)$ , since the hadronic matrix element does not exhibit any scheme dependence for the reasons we have already explained. At any rate  $\Delta_{\gamma_5} \hat{B}_K$  is below 10% for all values of  $\mu$  in the given range (apart from the case  $\mu = 0.8$  GeV and  $\Lambda_{\text{QCD}}^{(4)} = 450$  MeV).

For what concerns the dependence of the results on the QCD scale parameter, we have smaller values of  $\hat{B}_K$  for higher values of  $\Lambda_{\text{QCD}}^{(4)}$ . We can also notice that the scheme and the scale dependences are reduced if we take smaller values of  $\Lambda_{\text{QCD}}^{(4)}$ . Anyway, from this point of view, there are only small differences between  $\Lambda_{\text{QCD}}^{(4)} = 250$  MeV and  $\Lambda_{\text{QCD}}^{(4)} = 350$  MeV.

Finally, let us consider the dependence of our results on the value chosen for the gluon condensate. In Fig. 3 we show  $\hat{B}_K$  as a function of the gluon condensate, for our preferred matching scale  $\mu = 0.8$  GeV, and for the central value  $\Lambda_{\text{QCD}}^{(4)} = 350$  MeV. It appears that  $\hat{B}_K$  is a sensitive decreasing function of the gluon condensate.

This can be simply understood, by looking at eq. (7.29) which gives  $B_K(\mu)$ . In fact,

for our values of the gluon condensate, the term  $\delta_{(GG)}$  appearing in eq. (7.29) is greater than 1, thus changing the sign of the  $1/N_c$  contribution and determining a reduction of the final result for  $\widehat{B}_K$ . This non perturbative gluonic effect is larger for higher values of the gluon condensate.

We see in Fig. 3 that, by spanning the whole range of eq. (7.30) and considering both HV and NDR scheme, but fixing  $\alpha_s$  to its central value, we obtain a sizable range of values for  $\widehat{B}_K$ :

$0.6 \leq \widehat{B}_K \leq 1.0$ . By varying also the value of  $\Lambda_{\text{QCD}}^{(4)}$  in the interval of eq. (4.3) we obtain the overall range

$$0.54 \leq \widehat{B}_K \leq 1.2, \quad (7.33)$$

which represents our conservative prediction for  $B_K$ . The value  $\widehat{B}_K = 0.87 \pm 0.10$  is obtained by taking  $\Lambda_{\text{QCD}}^{(4)}$  and the gluon condensate at their central values, varying  $\mu$  between 0.8 and 1 GeV and considering both HV and NDR schemes. This value represents a large renormalization with respect to the initial value given by eq. (7.14). In this respect improving to  $O(p^4)$  the chiral expansion, albeit challenging, might be needed in order to assess the degree of stability of the result.

### 7.2.3 Next to Leading Order $\eta$ Factors

The  $\Delta S = 2$  Wilson coefficients can be splitted into a common scale dependent factor  $b(\mu)$  and three coefficients denoted by  $\eta_1$ ,  $\eta_2$  and  $\eta_3$  (see eq. (7.2)).

The  $\eta$ -coefficients have been already calculated at the leading-logarithmic approximation by Gilman and Wise [97] in the case of a light top quark. The corresponding results for a heavy top have been recovered in [98].

Anyway, this level of approximation is not enough and one has to go to next to leading order results. This is true for many reasons, but mainly because in this way there is a significant reduction of the artificial dependence of the  $\eta$ -coefficients on the various renormalization scales introduced by the threshold effects.

The NLO calculations of  $\eta_1$  and  $\eta_2$  can be found in refs. [75] and [76] respectively, while the analogous calculation for  $\eta_3$ , which is particularly challenging, has been performed only recently by the authors of ref. [77]. We have taken their results and evaluated the QCD factors for our choice of parameters.

As an example, for  $\Lambda_{\text{QCD}}^{(4)} = 350$  MeV and  $m_t^{(pole)} = 180$  GeV, at  $\mu = m_c$  we find

$$\eta_1 = 1.36 \quad \eta_2 = 0.51 \quad \eta_3 = 0.45. \quad (7.34)$$

### 7.2.4 The Mixing Parameter $\text{Im } \lambda_t$

There are two important parameters related to the  $K^0$ - $\bar{K}^0$  mixing: the  $CP$  violating quantity  $\varepsilon$ , which is proportional to the imaginary part of the mass matrix, and the mass difference  $\Delta M_{LS}$ .

We will discuss separately, in the next section, about  $\Delta M_{LS}$ , because its analysis requires also the estimate of the “long distance” contribution that we have not introduced yet.

Let us concentrate, for the time being, on the parameter  $\varepsilon$ , which is fully dominated by the “box diagram” contribution.

The observed value for this quantity is [10]:

$$|\varepsilon| = (2.266 \pm 0.023) \times 10^{-3}. \quad (7.35)$$

Knowing  $\varepsilon$ , we can determine the KM parameter  $\text{Im } \lambda_t$ , as we are going to discuss.

A range for  $\text{Im } \lambda_t$ , which is relevant for the  $CP$  violating observables, can be determined from the experimental value of  $\varepsilon$  as a function of  $\hat{B}_K$ ,  $m_t$  and the other relevant parameters involved in the theoretical estimate.

Given  $m_t$ ,  $m_c$  and the KM parameters [10]

$$|V_{us}| = 0.2205 \pm 0.0018 \quad (7.36)$$

$$|V_{cb}| = 0.041 \pm 0.003 \quad (7.37)$$

$$|V_{ub}/V_{cb}| = 0.08 \pm 0.02, \quad (7.38)$$

we can solve the two equations

$$\varepsilon_{th}(\hat{B}_K, |V_{cb}|, |V_{us}|, \Lambda_{\text{QCD}}^{(4)}, m_t, m_c, \eta, \rho) = \varepsilon \quad (7.39)$$

$$\eta^2 + \rho^2 = \frac{1}{|V_{us}|^2} \left| \frac{V_{ub}}{V_{cb}} \right|^2 \quad (7.40)$$

to find the allowed values of the two parameters  $\eta$  and  $\rho$  appearing in the Wolfenstein parametrization of KM mixing matrix.

We include in this analysis the interval of values for  $\Lambda_{\text{QCD}}^{(4)}$  in eq. (4.3) and for the gluon condensate the range in eq. (7.30). The matching scale  $\mu$  is varied between 0.8 and 1 GeV, while  $\hat{B}_K$  is varied according to the range obtained in the previous sections. The results for  $m_t^{\text{pole}} = 180$  GeV are represented graphically in Fig. 4 .

We can see that the equations (7.39) and (7.40) define two families of curves (respectively hyperbola and circles) in the  $(\rho$ - $\eta)$  plane. The allowed values of the two

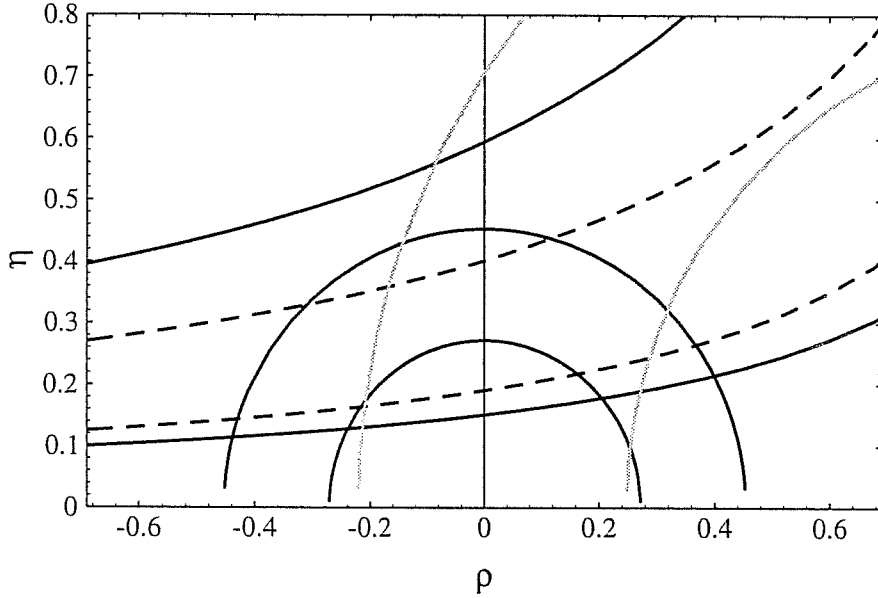


Figure 7.4: Constraints on KM parameters from kaon physics. See the text for explanation.

parameters correspond to the region delimited by the intersections between the two families of curves. The area enclosed by the two solid line hyperbolae corresponds to our most conservative range  $0.54 < \hat{B}_K < 1.2$ .

This procedure gives two possible ranges for  $\eta$  and consequently for  $\text{Im } \lambda_t \simeq \eta |V_{us}| |V_{cb}|^2$ , which correspond to having the KM phase in the I or II quadrant ( $\rho$  positive or negative, respectively). For the central value of the top mass ( $\overline{m}_t(m_W) \simeq 183$  GeV) we find

$$0.67 \times 10^{-4} \leq \text{Im } \lambda_t \leq 1.7 \times 10^{-4} \quad (7.41)$$

in the first quadrant and

$$0.41 \times 10^{-4} \leq \text{Im } \lambda_t \leq 1.7 \times 10^{-4} \quad (7.42)$$

in the second quadrant.

We also consider a “biased” estimate of  $\text{Im } \lambda_t$ , obtained by fixing the gluon condensate and  $\Lambda_{\text{QCD}}^{(4)}$  to their central values and varying the matching scale  $\mu$  between 0.8 and 1 GeV. In this way we are spanning the following range for the renormalization group invariant parameter  $\hat{B}_K$  :

$$\hat{B}_K = 0.87 \pm 0.10, \quad (7.43)$$

This choice of the input parameters restricts the hyperbolic band to the area enclosed by the dashed lines in Fig. 4. The overlap with the constraint of eq. (7.40) leads to the following ranges of allowed values for  $\text{Im } \lambda_t$

$$0.81 \times 10^{-4} \leq \text{Im } \lambda_t \leq 1.6 \times 10^{-4} \quad (7.44)$$

in the first quadrant and

$$0.52 \times 10^{-4} \leq \text{Im } \lambda_t \leq 1.5 \times 10^{-4} \quad (7.45)$$

in the second quadrant.

Varying  $m_t$  in the range  $m_t^{pole} = 180 \pm 12$  GeV affects very little the quoted lower bounds on  $\text{Im } \lambda_t$  while the upper bounds are changed by less than 20% (decreasing  $m_t$  corresponds to increasing the upper limits). On the other hand, the upper bound on  $\text{Im } \lambda_t$  remains stable, being bounded by the maximum value of  $\eta$  obtained from eq. (7.40) ( $\rho = 0$ ).

We do not discuss here details of the bounds provided by  $\Delta M_{B_d}$  which are represented, for the central value of  $m_t$ , by the area delimited by the grey lines in Fig. 4. The constraints of  $B_d - \bar{B}_d$  mixing have a marginal impact in the determination of the overall range of  $\eta$ . As the example in the figure shows, only the lower bound of  $\text{Im } \lambda_t$  in the second quadrant is affected by such an inclusion and raised to  $0.6 \times 10^{-4}$ .

### 7.3 The $K_L - K_S$ Mass Difference

Let us now study the mass difference  $\Delta M_{LS} \equiv m_L - m_S$  between the two eigenstates of the weak hamiltonian  $K_L$  and  $K_S$ . The expressions of  $K_L$  and  $K_S$  are given by eq. (6.11). The observed value of  $\Delta M_{LS}$  is [10]

$$\Delta M_{LS} = (3.510 \pm 0.018) \times 10^{-15} \text{ GeV}. \quad (7.46)$$

In the limit of small CP violation, we have

$$\Delta M_{LS} = \frac{1}{m_K} \text{Re} \left[ \langle K^0 | \mathcal{H}_{eff} | \bar{K}^0 \rangle \right]. \quad (7.47)$$

To estimate this quantity we have to evaluate, in addition to the box diagram contribution, coming from the  $\Delta S = 2$  effective lagrangian of eq. (7.2), the ‘‘long distance’’ contribution coming from the double insertion of  $\Delta S = 1$  weak chiral lagrangian. Therefore we can formally split the full  $\Delta M_{LS}$  in this way:

$$\Delta M_{LS} = \Delta M_{box} + \Delta M_{LD} \quad (7.48)$$

The interesting question is whether the interplay between  $\Delta M_{box}$  and  $\Delta M_{LD}$  reproduces the observed value  $\Delta M_{exp}$ .

### 7.3.1 Calculation of Long Distance Contribution

Let us start evaluating the purely long distance contribution  $\Delta M_{LD}$ . Many attempts have been made to estimate this contribution [89]–[96], by means of various techniques like chiral symmetry, dispersion relation with experimental data of  $s$ -wave  $\pi\pi$  scattering. They led to a variety of numerical results.

We want to give a consistent estimate of  $\Delta M_{LD}$  based on the  $\chi$ QM approach. As already mentioned, the long distance contribution to  $K^0 - \bar{K}^0$  mass difference is produced by the exchange of the  $SU(3)$  meson field octet (we leave aside in this analysis the contribution of  $\eta'$ ) via the double insertion of the  $\Delta S = 1$  chiral vertices. The relevant diagrams are those with one particle intermediate state and two particle intermediate states (three-particle intermediate states do not give significant contributions, as explained, for instance, in ref. [91]).

In the previous chapters we have derived and already used the  $\Delta S = 1$  chiral lagrangian, at the order  $O(p^2)$ . It is given by eq. (4.18). The electroweak penguin operators  $Q_{7-10}$  give a negligible contribution (of the order of 1%) to  $\Delta M_{LD}$ , due the smallness of their Wilson coefficients. Therefore we can limit ourselves to consider the operators  $Q_{1-6}$ , which turn out to be relevant for the present calculation. In this way we will use, instead of the complete  $\Delta S = 1$  chiral lagrangian of eq. (4.18), the following simpler expression:

$$\begin{aligned} \mathcal{L}_{\Delta S=1}^{(2)} = & G_{\underline{8}}(Q_{3-6}) \text{Tr} \left( \lambda_2^3 D_\mu \Sigma^\dagger D^\mu \Sigma \right) + \\ & G_{LL}^a(Q_{1,2}) \text{Tr} \left( \lambda_1^3 \Sigma^\dagger D_\mu \Sigma \right) \text{Tr} \left( \lambda_2^1 \Sigma^\dagger D^\mu \Sigma \right) + \\ & G_{LL}^b(Q_{1,2}) \text{Tr} \left( \lambda_2^3 \Sigma^\dagger D_\mu \Sigma \right) \text{Tr} \left( \lambda_1^1 \Sigma^\dagger D^\mu \Sigma \right), \end{aligned} \quad (7.49)$$

where the notations are obviously the same adopted in eq. (4.18).

The expressions in the HV and the NDR schemes of the different coefficients of bosonization appearing in (7.49) are given by eqs. (4.56)–(4.57) and eqs. (4.60)–(4.61). For the parameter  $M$ , appearing in these coefficients, we use the value 220 MeV, consistently with previous analysis.

The relevant diagrams contain two weak vertices, among those proportional to  $G_{\underline{8}}$ ,  $G_{LL}^a$  and  $G_{LL}^b$ . Therefore we have to consider all the possible combinations:  $G_{LL}^a G_{LL}^a$ ,  $G_{LL}^b G_{LL}^b$ ,  $G_{\underline{8}} G_{\underline{8}}$ ,  $G_{LL}^a G_{LL}^b$ ,  $G_{\underline{8}} G_{LL}^a$ ,  $G_{\underline{8}} G_{LL}^b$ .



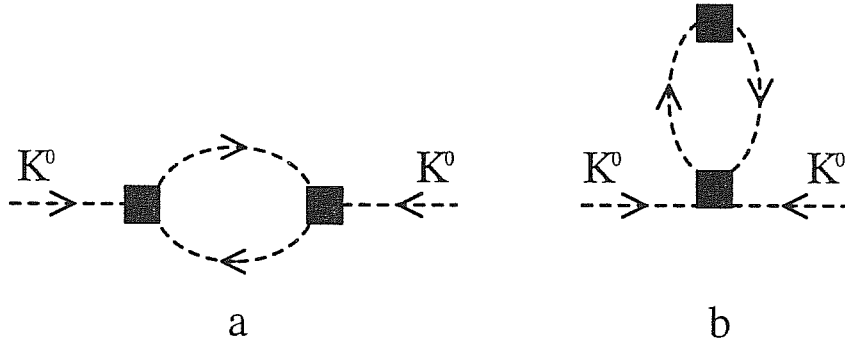


Figure 7.5: Long-distance contributions to the  $K^0 - \bar{K}^0$  mixing. The black box represents the insertion of the  $\Delta S = 1$  weak hamiltonian.

To compute all these contributions we have to use the Feynman rules presented in the relative appendix.

The single particle intermediate state contribution gives a result  $\propto (4m_K^2 - m_\pi^2 - 3m_\eta^2)$ , which vanishes by using Gell-mann-Okubo relation [89].

A non-vanishing contribution, instead, is obtained from the two particle intermediate states, which correspond to the double insertion of the  $\Delta S = 1$  chiral lagrangian as depicted in Fig. 5(a). Another class of diagrams called tadpole diagrams is shown in Fig. 5(b); to our knowledge, they were first pointed out in ref. [95].

In evaluating the diagrams of Fig. 5, we use dimensional regularization and modified minimal subtraction, as we have done in the case of  $\Delta S = 1$  processes.

### 7.3.2 The Wilson Coefficients

The chiral coefficients of the  $\Delta S = 1$  lagrangian include the Wilson coefficients of the original effective quark lagrangian.

In chapter 5 we have reported the Wilson coefficients of all the  $Q_i$  operators at the scales  $\mu = 0.8$  GeV and  $\mu = 1$  GeV in both the NDR and HV  $\gamma_5$ -schemes.

Since  $\text{Re } \tau$  in eq. (4.1) is of  $O(10^{-3})$ , the  $K^0 \leftrightarrow \bar{K}^0$  transition is controlled by the coefficients  $z_i$ , which do not depend on  $m_t$ .

We have already discussed about the Wilson coefficients of the  $\Delta S = 2$  effective four quark operator in the previous section.

### 7.3.3 Numerical Analysis

Following Wolfenstein notation [99], we define the parameter  $D$  which characterizes

$\Lambda_{\text{QCD}}^{(4)} = 250 \text{ MeV}$				
	$\mu = 0.8 \text{ GeV}$		$\mu = 1 \text{ GeV}$	
	NDR	HV	NDR	HV
$\Delta M_{\text{box}}$	2.55	2.42	2.92	2.80
$\Delta M_{LD}$	-0.34	-0.38	-0.35	-0.38
$D$	-0.10	-0.11	-0.10	-0.11
$\Delta M^{th}/\Delta M^{exp}$	0.63	0.58	0.73	0.69
$\Lambda_{\text{QCD}}^{(4)} = 350 \text{ MeV}$				
	$\mu = 0.8 \text{ GeV}$		$\mu = 1 \text{ GeV}$	
	NDR	HV	NDR	HV
$\Delta M_{\text{box}}$	3.07	2.83	3.56	3.37
$\Delta M_{LD}$	-0.54	-0.65	-0.46	-0.51
$D$	-0.15	-0.18	-0.13	-0.14
$\Delta M^{th}/\Delta M^{exp}$	0.72	0.62	0.88	0.81
$\Lambda_{\text{QCD}}^{(4)} = 450 \text{ MeV}$				
	$\mu = 0.8 \text{ GeV}$		$\mu = 1 \text{ GeV}$	
	NDR	HV	NDR	HV
$\Delta M_{\text{box}}$	3.91	3.40	4.55	4.20
$\Delta M_{LD}$	-1.18	-1.50	-0.65	-0.75
$D$	-0.34	-0.43	-0.18	-0.21
$\Delta M^{th}/\Delta M^{exp}$	0.77	0.54	1.11	0.98

Table 7.3: Long distance and box contributions to  $\Delta M$ , in units of  $10^{-15}$  GeV, for different values of the matching scale  $\mu$  and  $\Lambda_{\text{QCD}}^{(4)}$  in the  $\chi$ QM. We take for the gluon condensate the value  $\langle\alpha_s GG/\pi\rangle = (360 \text{ MeV})^4$  and for the quark condensate  $\langle\bar{q}q\rangle = -(280 \text{ MeV})^3$ , which are the values preferred by the fit of the  $\Delta I = 1/2$  selection rule at the same perturbative order. The box contribution is evaluated for a top quark pole mass of 180 GeV.

the long distance contribution

$$D = \frac{\Delta M_{LD}}{\Delta M_{LS}^{exp}}. \quad (7.50)$$

Numerical estimates of  $D$ ,  $\Delta M_{LD}$  and  $\Delta M_{box}$  for different values of  $\Lambda_{\text{QCD}}^{(4)}$  and of the matching scale  $\mu$  are given in Table 3. In this table we have fixed the gluon condensate to our central value  $\langle \frac{\alpha_s}{\pi} GG \rangle = (360 \text{ MeV})^4$  and we have chosen for the quark condensate the value  $\langle \bar{q}q \rangle = -(280 \text{ MeV})^3$  which gives us the best fit of the  $\Delta I = 1/2$  selection rule. The ranges thus obtained are  $0.63 \leq \Delta M^{th}/\Delta M^{exp} \leq 1.11$  in the NDR and  $0.54 \leq \Delta M^{th}/\Delta M^{exp} \leq 0.98$  in the HV. If we let the value of the gluon condensate vary in the range of eq. (7.30), as we did in determining  $\hat{B}_K$ , we obtain the overall range

$$0.42 \leq \Delta M^{th}/\Delta M^{exp} \leq 1.40 \quad (7.51)$$

which represents our most conservative result.

A few comments are in order. Among the diagrams of Fig. 5(a), those containing two intermediate pion states dominate over kaon and eta exchange by about a factor of two. The diagrams of Fig. 5(b) (tadpole diagrams) give a contribution comparable in size with those of Fig. 5(a) but of the opposite sign, leading as a net result to a small and negative  $\Delta M_{LD}$  in the most part of the parameter space.

Although the relevance of the tadpole diagrams has been pointed out in ref. [95], we disagree in the details of the calculation and on the relevant interactions. In particular, the author of ref. [95] seems to neglect some contributions coming from the insertion of the operator  $Q_2$ , which are among the leading contributions according to our computation.

Our result depends on the value of the gluon condensate. Fig. 6 shows the typical behavior. The ratio  $(\Delta M_{box} + \Delta M_{LD})/\Delta M_{LS}^{exp}$  is a decreasing function of the value of the gluon condensate, as we have already seen for the values of  $\hat{B}_K$ , which parametrizes the box diagram contribution.

The scheme dependences of the results is satisfactory. In fact it is always below 20% for  $\Lambda_{\text{QCD}}^{(4)} \leq 350 \text{ MeV}$ .

Less satisfactory is the renormalization scale dependence.  $\Delta M_{box}$  is an increasing function of  $\mu$  and the enhancement of the box diagram contribution is not compensated by a corresponding decrease of the  $D$  parameter. Anyway the scale dependence is lower than 30% for  $\Lambda_{\text{QCD}}^{(4)} \leq 350 \text{ MeV}$ . These results may indicate the need to extend the analysis to  $O(p^4)$  in the chiral lagrangian expansion. An improved chiral quark model calculation of the  $\Delta S = 1$  and  $\Delta S = 2$  chiral coefficients at  $O(p^4)$  is under way.

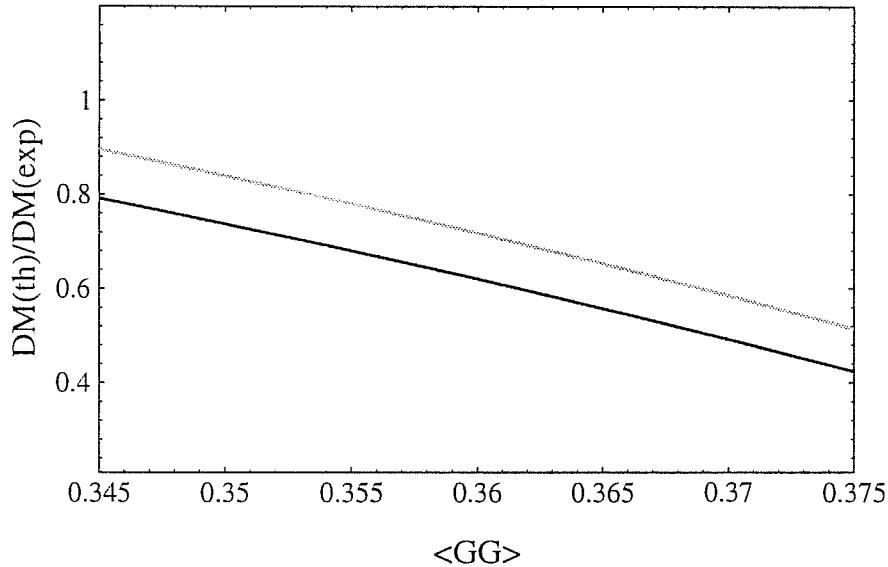


Figure 7.6: The ratio  $(\Delta M_{box} + \Delta M_{LD})/\Delta M_{LS}^{exp}$  is shown as a function of the gluon condensate for  $\Lambda_{\text{QCD}}^{(4)} = 350$  MeV and  $\mu = 0.8$  GeV. We denote by  $\langle GG \rangle$  the quantity  $\langle \alpha_s GG/\pi \rangle^{1/4}$  in units of GeV. The dark and grey lines represent the HV and NDR results respectively.

A final comment about the width difference  $\Delta\Gamma_{LS}$  is necessary. A direct calculation of the absorptive component of Fig. 5(a) gives about 1/6 of the experimental result. The reason is that the tree-level  $K \rightarrow \pi\pi$  decay amplitudes do not reproduce the measured ones. Only by replacing in the vertices of Fig. 5(a) the one-loop results obtained in [6], we obtain the agreement with the experimental  $\Delta\Gamma_{LS}$ . This is equivalent to computing directly the absorptive part of Fig.5(a) up to three loops.

## Chapter 8

# Conclusions and Overview of Future Perspectives

Let us finish this dissertation with a brief critical analysis of the main results obtained. We will also give a look at future possible improvements and applications of this work.

The topic we have considered is wide and it is interesting, not only for historical reasons, but also for its present relevance. On the other hand, to study this subject we had to face difficult problems.

The main difficulty is due to the fact we want to study weak processes in which the strong interactions play a relevant role. Hence we have to face the problem of studying the interplay between weak and strong forces and giving a consistent description of hadronic interactions at low energies.

Adopting the formal distinction between short and long distance analysis, we can say that the short distance component has not been the object of study of this dissertation. For this part of the physical analysis we have reproduced the next to leading order results obtained by the Rome and the Munich groups [16, 15] and updated them for our values of the input parameters.

Instead, we have focused our attention on the analysis of the long distance part of the problem. We have tried to develop a formalism which enables us to give a consistent description of different physical observables for a fixed set of input parameters.

I would say the main result of this work is the derivation of the complete  $O(p^2)$  weak chiral lagrangians for  $\Delta S = 1$  and  $\Delta S = 2$  non leptonic processes and the determination of all the chiral lagrangian coefficients.

This provides us with a powerful theoretical tool that we can use in principle to study a lot of physical processes.

The first direct application of this result is the calculation of the hadronic matrix elements of the  $K \rightarrow \pi\pi$  transitions for all the four quark operators of the  $\Delta S = 1$  effective hamiltonian. We have seen this computation enables us to give a quite satisfactory explanation of the famous  $\Delta I = 1/2$  selection rule.

I would like to spend a few words on this subject. The main result of our analysis, besides the fact that we can reproduce the  $\Delta I = 1/2$  rule for a particular choice of the input parameters, is that the values of the amplitudes  $A_0$  and  $A_2$  stay close to the experimental ones when we vary the inputs inside a range of reasonable values. Moreover, we can say that the scheme and scale dependences of our results is under control.

Another important aspect is that we have included in our  $\Delta S = 1$  chiral lagrangian also some  $O(p^2)$  contributions which, up to our knowledge, had never been studied before. These terms, coming from the bosonization of the electroweak operators, are practically irrelevant for the analysis of the  $\Delta I = 1/2$  rule, but they cannot be neglected in the estimate of the ratio  $\varepsilon'/\varepsilon$ .

The study of  $K^0 - \bar{K}^0$  mixing has been also a useful check of the consistency of our approach. In fact it is encouraging that, with the same choice of the input parameters giving us the best fit of the  $\Delta I = 1/2$  rule, we obtain reasonable values of the parameter  $\hat{B}_K$  and of  $\Delta M_{LS}$ .

The main limit of our analysis is that we have considered the  $\Delta S = 1$  and  $\Delta S = 2$  chiral lagrangians only up to the order  $O(p^2)$  in the momentum expansion. We have also added the very important  $O(p^4)$  corrections, coming from chiral loops, but we have not yet evaluated the complete  $O(p^4)$  chiral lagrangian.

This approximation introduces an overall uncertainty in our results, as we have already discussed in the previous chapters.

Another objection one could make is linked to the physical interpretation of the gluon and the quark condensates entering in our results. The relation of these quantities, parametrizing the non perturbative part of our computation, with those derived with other methods (like QCD sum rules and lattice) is not clear. Moreover it is not possible to recover a unique determination of these parameters from the literature.

Anyway we have taken the attitude to consider them as phenomenological parameters which could vary inside a range of values determined by comparison with the existing analysis. Then we have determined them by requiring the best fit of the  $\Delta I = 1/2$  rule and we have consistently used these values in the study of the  $\Delta S = 2$  physics.

Another possible objection could be considered more philosophic. It is related to the limit of validity of the chiral quark model, on which we have based, together with chiral perturbation theory, the derivation of our formalism. A few remarks on this point are in order.

The chiral quark model is a simple, but effective, model which enables us to give a consistent and quite satisfactory description of low energy hadron physics. It can also be derived by more general models, like the extended Nambu-Jona-Lasinio model, as we tried to show briefly.

Anyway one has to bear in mind that it is just a model. We do not want to claim that the model solves QCD. We are just trying to see whether it is able to reproduce some of the essential features of QCD, in such a way to describe consistently the processes we are studying.

Let us make some comments about the future perspectives.

The first natural extension of our work is the inclusion of the  $O(p^4)$  counterterms in the  $\Delta S = 1$  and  $\Delta S = 2$  chiral lagrangians. This improvement could in principle reduce in a significant way the overall uncertainty of our results. We already started the study of this problem and we hope to reach definite results in the near future. However, we have to say this is a challenging issue, mainly, but not only, for technical reasons.

The formalism we have developed can be applied, with little modifications, to a variety of physical processes. One could think, for instance, to the extension of our analysis of  $K \rightarrow 2\pi$  decays to the case of  $K \rightarrow 3\pi$  decays.

The semileptonic and the radiative kaon decays are other examples of processes which can be studied in a way similar to what we have done for  $\Delta S = 1$  non leptonic decays.

It is also important to remember that the DaΦne experiment in Frascati should become operative very soon. It is expected to give important results about CP violation and kaon physics in general. Therefore we can think that these topics will receive significant attention also in the near future.





# Appendix A

## Chiral Quark Model

### A.1 Feynman Rules

The relevant meson–quark interactions are derived from the lagrangian of eq. (3.28), which we write here as

$$\begin{aligned} \mathcal{L}_{\text{xQM}} = & -M\bar{q}q + 2i \frac{M}{f} \bar{q}\gamma_5 \Pi q + 2 \frac{M}{f^2} \bar{q} \Pi^2 q \\ & + \frac{4}{3} i \frac{M}{f^3} \bar{q}\gamma_5 \Pi^3 q + O(1/f^4), \end{aligned} \quad (\text{A.1})$$

where

$$\Pi = \frac{1}{2} \sum_a \lambda^a \pi^a = \frac{1}{\sqrt{2}} \begin{bmatrix} \tilde{\pi}^0 & \pi^+ & K^+ \\ \pi^- & -\tilde{\pi}^0 & K^0 \\ K^- & \bar{K}^0 & \tilde{\pi}^8 \end{bmatrix}, \quad (\text{A.2})$$

and

$$\tilde{\pi}^0 = \frac{1}{\sqrt{2}}\pi^0 + \frac{1}{\sqrt{6}}\eta_8, \quad \bar{\pi}^0 = \frac{1}{\sqrt{2}}\pi^0 - \frac{1}{\sqrt{6}}\eta_8, \quad \tilde{\pi}^8 = -\frac{2}{\sqrt{6}}\eta_8. \quad (\text{A.3})$$

In the case of a single meson interactions one obtains

$$\bar{q}\gamma_5 \Pi q = \frac{1}{\sqrt{2}} \left( \bar{u}\gamma_5 u \tilde{\pi}^0 - \bar{d}\gamma_5 d \bar{\pi}^0 + \bar{d}\gamma_5 s K^0 + \bar{u}\gamma_5 d \pi^+ + \dots \right). \quad (\text{A.4})$$

The relevant Feynman rules are therefore given by:

$$K^0 \bar{d}\gamma_5 s = K^+ \bar{u}\gamma_5 s = \pi^+ \bar{u}\gamma_5 d - \text{coupling:} \quad -\frac{M\sqrt{2}}{f}\gamma_5$$

$$\begin{aligned}
\pi^0 \bar{d}\gamma_5 d - \text{coupling:} & \quad +\frac{M}{f}\gamma_5 \\
\pi^0 \bar{u}\gamma_5 u - \text{coupling:} & \quad -\frac{M}{f}\gamma_5 \\
K^0 \pi^0 \bar{d}s - \text{coupling:} & \quad -i\frac{M}{f^2\sqrt{2}} \\
K^+ \pi^- \bar{d}s = K^+ K^- \bar{u}u = K^0 \pi^+ \bar{u}s - \text{coupling:} & \quad +i\frac{M}{f^2} \\
K^+ K^- \bar{s}s = \pi^+ \pi^- \bar{u}u = \pi^+ \pi^- \bar{d}d - \text{coupling:} & \quad +i\frac{M}{f^2} \\
K^+ \pi^0 \bar{u}s = \pi^+ \pi^0 \bar{u}d - \text{coupling:} & \quad +i\frac{M}{f^2\sqrt{2}} \\
\pi^0 \pi^0 \bar{u}u = \pi^0 \pi^0 \bar{d}d - \text{coupling:} & \quad +i\frac{M}{2f^2}
\end{aligned} \tag{A.5}$$

All meson fields are entering the vertex. The same rules hold for the conjugated couplings.

## A.2 Fierz Transformations and Clebsh-Gordan Coefficients

The relevant Fierz transformations (for anti-commuting fields) are the following:

$$\begin{aligned}
\bar{a}_\alpha \gamma_\mu (1 \pm \gamma_5) b_\beta \bar{c}_\beta \gamma^\mu (1 \mp \gamma_5) d_\alpha & = -2 \bar{a}_\alpha (1 \mp \gamma_5) d_\alpha \bar{c}_\beta (1 \pm \gamma_5) b_\beta \\
\bar{a}_\alpha \gamma_\mu (1 \pm \gamma_5) b_\beta \bar{c}_\beta \gamma^\mu (1 \pm \gamma_5) d_\alpha & = \bar{a}_\alpha \gamma_\mu (1 \pm \gamma_5) d_\alpha \bar{c}_\beta \gamma^\mu (1 \pm \gamma_5) b_\beta.
\end{aligned} \tag{A.6}$$

We also have for  $SU(N_c)$

$$\delta_{\alpha\beta} \delta_{\gamma\delta} = \frac{1}{N_c} \delta_{\alpha\delta} \delta_{\gamma\beta} + 2 T_{\alpha\delta}^a T_{\gamma\beta}^a. \tag{A.7}$$

The  $SU(2)$  Clebsh-Gordan projections are as given by

$$\begin{aligned}
A_0 & = \sqrt{\frac{1}{6}} (A_{00} + 2A_{+-}) \\
A_2 & = \sqrt{\frac{1}{3}} (A_{+-} - A_{00}) = \frac{2}{\sqrt{3}} A_{+0}.
\end{aligned} \tag{A.8}$$

The  $SU(3)$  projections are [100]

$$|\mathbb{8}, \frac{1}{2}\rangle = \text{Tr} (\lambda_2^1 \Sigma^\dagger D_\mu \Sigma) \text{Tr} (\lambda_1^3 \Sigma^\dagger D^\mu \Sigma)$$

$$\begin{aligned}
& - \text{Tr} \left( \lambda_2^3 \Sigma^\dagger D_\mu \Sigma \right) \text{Tr} \left( \lambda_1^1 \Sigma^\dagger D^\mu \Sigma \right) \\
|27, \frac{1}{2}\rangle &= \text{Tr} \left( \lambda_2^1 \Sigma^\dagger D_\mu \Sigma \right) \text{Tr} \left( \lambda_1^3 \Sigma^\dagger D^\mu \Sigma \right) \\
& + 4 \text{Tr} \left( \lambda_2^3 \Sigma^\dagger D_\mu \Sigma \right) \text{Tr} \left( \lambda_1^1 \Sigma^\dagger D^\mu \Sigma \right) \\
& + 5 \text{Tr} \left( \lambda_2^3 \Sigma^\dagger D_\mu \Sigma \right) \text{Tr} \left( \lambda_2^2 \Sigma^\dagger D^\mu \Sigma \right) \\
|27, \frac{3}{2}\rangle &= \text{Tr} \left( \lambda_2^1 \Sigma^\dagger D_\mu \Sigma \right) \text{Tr} \left( \lambda_1^3 \Sigma^\dagger D^\mu \Sigma \right) \\
& + \text{Tr} \left( \lambda_2^3 \Sigma^\dagger D_\mu \Sigma \right) \text{Tr} \left( \lambda_1^1 \Sigma^\dagger D^\mu \Sigma \right) \\
& - \text{Tr} \left( \lambda_2^3 \Sigma^\dagger D_\mu \Sigma \right) \text{Tr} \left( \lambda_2^2 \Sigma^\dagger D^\mu \Sigma \right) .
\end{aligned} \tag{A.9}$$

Therefore, we have

$$\begin{aligned}
|27\rangle &= \frac{5}{9} |27, \frac{3}{2}\rangle + \frac{1}{9} |27, \frac{1}{2}\rangle \\
&= \frac{2}{3} \text{Tr} \left( \lambda_2^1 \Sigma^\dagger D_\mu \Sigma \right) \text{Tr} \left( \lambda_1^3 \Sigma^\dagger D^\mu \Sigma \right) \\
& + \text{Tr} \left( \lambda_2^3 \Sigma^\dagger D_\mu \Sigma \right) \text{Tr} \left( \lambda_1^1 \Sigma^\dagger D^\mu \Sigma \right) .
\end{aligned} \tag{A.10}$$

### A.3 Dimensional Regularization

We work in the  $\overline{\text{MS}}$  scheme. In the naive dimensional regularization (NDR) everything is continued to  $d$  dimensions and the same four-dimensional rules applied. We therefore have that

$$\{\gamma_\mu, \gamma_\nu\} = 2g_{\mu\nu} \tag{A.11}$$

and

$$g_\mu^\mu = d. \tag{A.12}$$

The  $\gamma_5$  matrix is defined so as to anti-commute in any dimensions as

$$\{\gamma_\mu, \gamma_5\} = 0. \tag{A.13}$$

The term naive refers to the fact that such a prescription leads to manifest algebraic inconsistencies.

In the 't Hooft-Veltman regularization (HV) the Dirac matrices are separately considered in 4 (tilded quantities) and  $d - 4$  (hatted quantities) dimensions so that

$$\gamma_\mu = \tilde{\gamma}_\mu + \hat{\gamma}_\mu. \tag{A.14}$$

The two sub-spaces are orthogonal to each other:

$$\{\tilde{\gamma}_\mu, \tilde{\gamma}_\nu\} = 2\tilde{g}_{\mu\nu} \quad \{\hat{\gamma}_\mu, \hat{\gamma}_\nu\} = 2\hat{g}_{\mu\nu} \quad \{\hat{\gamma}_\mu, \tilde{\gamma}_\nu\} = 0, \tag{A.15}$$

and

$$\hat{g}_\mu^\mu = d - 4 \quad \tilde{g}_\mu^\mu = 4 \quad \text{and} \quad \hat{g}_\alpha^\mu \tilde{g}_\nu^\alpha = 0. \quad (\text{A.16})$$

The  $\gamma_5$  matrix is defined as anti-commuting in 4 dimensions and commuting in  $d-4$ : therefore

$$\{\hat{\gamma}_\mu, \gamma_5\} = 0 \quad [\hat{\gamma}_\mu, \gamma_5] = 0. \quad (\text{A.17})$$

The rules above lead to

$$\{\gamma^\mu, \gamma_5\} = 2 \gamma_5 \hat{\gamma}^\mu. \quad (\text{A.18})$$

In both schemes the external momenta are kept in four dimensions. Chiral currents must be symmetrized in order to have a unique definition. This is immaterial in the NDR case but gives

$$\frac{1}{2}(1 + \gamma_5)\gamma_\mu(1 - \gamma_5) = \tilde{\gamma}_\mu(1 - \gamma_5) \quad (\text{A.19})$$

in the HV case.

# Appendix B

## Table of Input Parameters

parameter	value
$V_{ud}$	0.9753
$V_{us}$	0.221
$\sin^2 \theta_W$	0.2247
$m_Z$	91.187 GeV
$m_W$	80.22 GeV
$m_b$	4.8 GeV
$m_c$	1.4 GeV
$f_\pi = f_{\pi^+}$	92.4 MeV
$f_K = f_{K^+}$	113 MeV
$m_\pi = (m_{\pi^+} + m_{\pi^0})/2$	138 MeV
$m_K = m_{K^0}$	498 MeV
$m_\eta$	548 MeV
$\Lambda_\chi$	$2\sqrt{2}\pi f_\pi$
$\Lambda_{QCD}^{(4)}$	$350 \pm 100$ MeV
$\bar{m}_u + \bar{m}_d$ (1 GeV)	$12 \pm 2.5$ MeV

Table B.1: Table of the numerical values of the input parameters used in this work.



# Appendix C

## Feynman Rules for the Chiral Loops

We report the Feynman rules which are relevant for the computation of the chiral loop corrections to the processes we have studied. We include all the strong, the  $\Delta S = 1$  and the  $\Delta S = 2$  chiral vertices that we need.

The total number of relevant vertices is huge and this makes the computation quite cumbersome.

### C.1 Feynman Rules for the Strong Chiral Lagrangian

In writing Feynman rule for the strong interaction, it is convenient to define the following functions

$$\begin{aligned} A(p_1, p_2, p_3, p_4) &= \frac{1}{2}(p_1 + p_2) \cdot (p_3 + p_4) - p_1 \cdot p_2 - p_4 \cdot p_3 \\ B(p_1, p_2, p_3, p_4) &= \frac{1}{2}(p_1 + p_4) \cdot (p_2 + p_3) - p_1 \cdot p_4 - p_2 \cdot p_3 \\ C(p_1, p_2, p_3, p_4) &= (p_4 - p_3) \cdot (p_2 - p_1) \\ D(p_1, p_2, p_3, p_4) &= \frac{1}{2}(p_1 + p_3) \cdot (p_2 + p_4) - p_1 \cdot p_3 - p_2 \cdot p_4 \end{aligned}$$

The relevant strong vertices are:

$$\begin{aligned} \pi^-(p_1)\pi^+(p_2)\pi^+(p_3)\pi^-(p_4) & \quad \frac{i}{6f^2}B \\ K^-(p_1)K^+(p_2)\pi^+(p_3)\pi^-(p_4) & \quad \frac{i}{3f^2}B \\ \pi^-(p_1)\pi^+(p_2)\pi^0(p_3)\pi^0(p_4) & \quad -\frac{i}{3f^2}A \end{aligned}$$

$$\begin{aligned}
K^-(p_1)K^+(p_2)\pi^0(p_3)\pi^0(p_4) & -\frac{i}{12f^2}A \\
\bar{K}^0(p_1)K^0(p_2)\pi^+(p_3)\pi^-(p_4) & \frac{i}{3f^2}D \\
\bar{K}^0(p_1)K^0(p_2)\pi^0(p_3)\pi^0(p_4) & -\frac{i}{12f^2}A \\
K^-(p_1)K^0(p_2)\pi^0(p_3)\pi^+(p_4) & \frac{i}{2\sqrt{2}f^2}C \\
\bar{K}^0(p_1)K^0(p_2)\eta(p_3)\pi^0(p_4) & \frac{i}{2\sqrt{3}f^2}A \\
K^-(p_1)K^0(p_2)\eta(p_3)\pi^+(p_4) & -\frac{i}{\sqrt{6}f^2}A \\
\bar{K}^0(p_1)K^0(p_2)\eta(p_3)\eta(p_4) & -\frac{i}{4f^2}A \\
K^-(p_1)K^+(p_2)\eta(p_3)\eta(p_4) & -\frac{i}{4f^2}A \\
\bar{K}^0(p_1)K^0(p_2)K^0(p_3)\bar{K}^0(p_4) & \frac{i}{6f^2}B \\
K^-(p_1)K^+(p_2)K^+(p_3)K^-(p_4) & \frac{i}{6f^2}B \\
\bar{K}^0(p_1)K^0(p_2)K^+(p_3)K^-(p_4) & \frac{i}{3f^2}B \\
K^-(p_1)K^+(p_2)\eta(p_3)\eta(p_4) & -\frac{i}{4f^2}A \\
K^+(p_1)\bar{K}^0(p_2)\pi^0(p_3)\pi^-(p_4) & \frac{i}{2\sqrt{2}f^2}C \\
K^+(p_1)\bar{K}^0(p_2)\eta(p_3)\pi^-(p_4) & -\frac{i}{\sqrt{6}f^2}A \\
K^-(p_1)K^+(p_2)\eta(p_3)\pi^0(p_4) & -\frac{i}{2\sqrt{3}f^2}A
\end{aligned} \tag{C.1}$$

The relevant vertices coming from the mass term in the strong lagragian are:

$$\begin{aligned}
\pi^- \pi^- \pi^+ \pi^+ & i \frac{m_\pi^2}{6f^2} \\
\pi^+ \pi^- \pi^0 \pi^0 & i \frac{m_\pi^2}{6f^2} \\
\pi^0 \pi^0 \pi^0 \pi^0 & i \frac{m_\pi^2}{24f^2}
\end{aligned}$$



$$\begin{aligned}
\eta \eta \pi^+ \pi^- & i \frac{m_\pi^2}{6f^2} \\
\eta \eta \pi^0 \pi^0 & i \frac{m_\pi^2}{12f^2} \\
K^+ K^- \pi^+ \pi^- & i \frac{(m_\pi^2 + m_K^2)}{6f^2} \\
K^+ K^- \pi^0 \pi^0 & i \frac{(m_\pi^2 + m_K^2)}{12f^2} \\
K^0 \bar{K}^0 \pi^+ \pi^- & i \frac{(m_\pi^2 + m_K^2)}{6f^2} \\
K^0 \bar{K}^0 \pi^0 \pi^0 & i \frac{(m_\pi^2 + m_K^2)}{12f^2} \\
K^0 \bar{K}^0 \bar{K}^0 K^0 & i \frac{m_K^2}{6f^2} \\
K^0 K^- \pi^+ \eta & -\frac{1}{\sqrt{6}} i \frac{m_K^2 - m_\pi^2}{3f^2} \\
K^0 \bar{K}^0 \pi^0 \eta & \frac{1}{\sqrt{3}} i \frac{m_K^2 - m_\pi^2}{6f^2} \\
K^- K^+ \pi^0 \eta & \frac{1}{\sqrt{3}} i \frac{-m_K^2 + m_\pi^2}{6f^2}
\end{aligned} \tag{C.2}$$

## C.2 Feynman Rules for the $\Delta S = 1$ Chiral Lagrangian

$G_{LL}^a$

$$\begin{aligned}
K^+(p_1)\pi^-(p_2) & \frac{2i}{f^2} p_1 \cdot p_2 \\
K^0(p_1)\pi^+(p_2)\pi^-(p_3) & -\frac{\sqrt{2}}{f^3} p_3 \cdot (p_2 - p_1) \\
K^+(p_1)\pi^-(p_2)\pi^0(p_3) & -\frac{1}{f^3} [p_1 \cdot (p_2 - 2p_3) + p_2 \cdot p_3] \\
K^0(p_1)K^+(p_2)K^-(p_3) & -\frac{\sqrt{2}}{f^3} p_2 \cdot (p_1 - p_3) \\
K^+(p_1)\pi^-(p_2)\eta(p_3) & -\frac{\sqrt{3}}{f^3} (p_3 - p_1) \cdot p_2 \\
K^0(p_1)K^0(p_2)\pi^+(p_3)K^-(p_4) & \frac{i}{f^4} \left[ p_1 \cdot p_2 - \frac{p_1 + p_2}{2} \cdot (p_3 + p_4) + p_3 \cdot p_4 \right]
\end{aligned}$$

$$\begin{aligned}
K^0(p_1)\pi^0(p_2)\pi^0(p_3)\pi^+(p_4)\pi^-(p_5) & -\frac{1}{3\sqrt{2}f^5} \left[ \frac{9}{2}p_1 \cdot p_5 + (p_2 + p_3) \cdot (-2p_1 - \frac{3}{2}p_5 - p_4) \right. \\
& \left. + 6p_2 \cdot p_3 - \frac{3}{2}p_4 \cdot p_5 \right] \\
K^0(p_1)\pi^0(p_2)\pi^0(p_3)K^+(p_4)K^-(p_5) & -\frac{1}{3\sqrt{2}f^5} \left[ -\frac{3}{2}p_1 \cdot p_4 + \frac{3}{2}p_4 \cdot p_5 + (p_2 + p_3) \cdot (p_5 - p_1) \right] \\
K^+(p_1)\pi^-(p_2)\pi^0(p_3)\bar{K}^0(p_4)K^0(p_5) & \frac{1}{6f^5} [p_1 \cdot (p_4 + p_5 + 3p_2 - 9p_3) \\
& + 2p_2 \cdot (-p_4 + 2p_5) - 2p_3 \cdot (p_5 - 2p_4)] \\
K^+(p_1)K^+(p_2)\pi^-(p_3)\pi^0(p_4)K^-(p_5) & -\frac{1}{6f^5} \left[ -p_5 \cdot \frac{p_1 + p_2}{2} - p_1 \cdot p_2 + 8p_5 \cdot p_3 \right. \\
& \left. - 7\frac{p_1 + p_2}{2} \cdot p_3 - 10p_5 \cdot p_4 + 17\frac{p_1 + p_2}{2} \cdot p_4 - 6p_3 \cdot p_4 \right] \\
K^+(p_1)\pi^-(p_2)\pi^-(p_3)\pi^+(p_4)\pi^0(p_5) & -\frac{1}{6f^5} \left[ \frac{p_2 + p_3}{2} \cdot (-7p_1 - 19p_5 - p_4) + 11p_2 \cdot p_3 \right. \\
& \left. + 12p_1 \cdot p_5 - 4p_1 \cdot p_4 + 8p_5 \cdot p_4 \right] \\
K^+(p_1)\eta(p_2)\eta(p_3)\pi^-(p_4)\pi^0(p_5) & -\frac{1}{4f^5} [(p_2 + p_3) \cdot (p_4 - 2p_5) - p_1 \cdot (p_4 - 4p_5) - p_4 \cdot p_5] \\
K^+(p_1)\pi^-(p_2)\pi^0(p_3)\pi^0(p_4)\pi^0(p_5) & -\frac{1}{12f^5} \left[ -3p_1 \cdot p_2 + \frac{4}{3}p_1 \cdot (p_3 + p_4 + p_5) \right. \\
& \left. - \frac{5}{3}p_2 \cdot (p_3 + p_4 + p_5) + \frac{4}{3}(p_3 \cdot p_4 + p_3 \cdot p_5 + p_4 \cdot p_5) \right] \\
K^0(p_1)\pi^+(p_2)\pi^-(p_3)\eta(p_4)\eta(p_5) & -\frac{1}{\sqrt{2}f^5} \frac{1}{f^5} \left( -\frac{1}{2}p_2 \cdot p_3 + \frac{3}{2}p_1 \cdot p_3 - \frac{1}{2}p_3 \cdot (p_4 + p_5) \right) \\
K^0(p_1)\pi^+(p_2)\pi^-(p_3)\bar{K}^0(p_4)K^0(p_5) & -\sqrt{2}\frac{1}{3f^5} \left[ -p_4 \cdot (p_1 + p_5) + p_1 \cdot p_5 - \frac{3}{2}p_3 \cdot p_4 + \frac{3}{2}p_3 \cdot (p_1 + p_5) \right. \\
& \left. + 2p_2 \cdot p_4 - \frac{1}{2}p_2 \cdot (p_1 + p_5) - \frac{3}{2}p_2 \cdot p_3 \right] \\
K^0(p_1)\pi^+(p_2)\pi^-(p_3)\pi^+(p_4)\pi^-(p_5) & -\sqrt{2}\frac{1}{3f^5} \left[ \frac{5}{4}p_1 \cdot (p_3 + p_5) + \frac{3}{2}p_3 \cdot p_5 - p_1 \cdot (p_2 + p_4) \right. \\
& \left. - (p_3 + p_5) \cdot (p_2 + p_4) + 2p_2 \cdot p_4 \right] \\
K^0(p_1)\pi^+(p_2)\pi^-(p_3)K^+(p_4)K^-(p_5) & -\sqrt{2}\frac{1}{3f^5} [p_1 \cdot p_5 - 5p_1 \cdot p_4 + 3p_4 \cdot p_5 + 5p_1 \cdot p_3 - 2p_5 \cdot p_3 \\
& - p_1 \cdot p_2 + 2p_4 \cdot p_2 - 3p_2 \cdot p_3]
\end{aligned} \tag{C.}$$

 $G_{LL}^b$ 

$$K^0(p_1)\pi^0(p_2) \quad \frac{i\sqrt{2}}{f^2} p_1 \cdot p_2$$

$$\begin{aligned}
K^0(p_1)\eta(p_2) & \frac{i}{f^2}\sqrt{\frac{2}{3}}p_1 \cdot p_2 \\
K^0(p_1)\pi^0(p_2)\pi^0(p_3) & -\frac{1}{\sqrt{2}f^3}\left[p_1 \cdot \left(\frac{p_2+p_3}{2}\right) - p_2 \cdot p_3\right] \\
K^0(p_1)\eta(p_2)\eta(p_3) & -\frac{1}{\sqrt{2}f^3}\left[p_2 \cdot p_3 - p_1 \cdot \left(\frac{p_2+p_3}{2}\right)\right] \\
K^0(p_1)K^+(p_2)K^-(p_3) & -\frac{\sqrt{2}}{f^3}(-p_1 \cdot p_3 + p_1 \cdot p_2) \\
K^0(p_1)\pi^+(p_2)\pi^-(p_3) & -\frac{\sqrt{2}}{f^3}(-p_1 \cdot p_3 + p_1 \cdot p_2) \\
K^0(p_1)\eta(p_2)\pi^0(p_3) & -\frac{1}{\sqrt{6}f^3}(+p_1 \cdot p_2 + 2p_2 \cdot p_3 - 3p_1 \cdot p_3) \\
K^+(p_1)\pi^-(p_2)\pi^0(p_3) & -\frac{1}{f^3}[p_3 \cdot (p_2 - p_1)] \\
K^+(p_1)\eta(p_2)\pi^-(p_3) & -\frac{1}{\sqrt{3}f^3}[p_2 \cdot (p_3 - p_1)] \\
K^0(p_1)K^0(p_2)\bar{K}^0(p_3)\pi^0(p_4) & \frac{2\sqrt{2}}{3}\frac{i}{f^4}\left[+p_3 \cdot p_4 - \left(\frac{p_1+p_2}{2}\right) \cdot p_4\right] \\
K^0(p_1)K^0(p_2)\pi^+(p_3)K^-(p_4) & \frac{i}{3f^4}\left[4p_1 \cdot p_2 - 2\left(\frac{p_1+p_2}{2}\right) \cdot (p_4+p_3)\right] \\
K^0(p_1)K^0(p_2)\bar{K}^0(p_3)\eta(p_4) & \frac{2}{3}\sqrt{\frac{2}{3}}\frac{i}{f^4}\left[p_3 \cdot p_4 - \left(\frac{p_1+p_2}{2}\right) \cdot p_4\right] \\
K^0(p_1)\pi^+(p_2)\pi^-(p_3)\bar{K}^0(p_4)K^0(p_5) & -\frac{\sqrt{2}}{3f^5}\left[\frac{p_1+p_5}{4} \cdot (-5p_2+5p_3-3p_4) + \frac{3}{2}p_1 \cdot p_5\right. \\
& \left.- 2p_3 \cdot p_4 + 2p_2 \cdot p_4\right] \\
K^0(p_1)\pi^0(p_2)\pi^0(p_3)\pi^0(p_4)\pi^0(p_5) & -\frac{1}{12\sqrt{2}f^5}\left[-p_1 \cdot \frac{p_2+p_3+p_4+p_5}{4} + \frac{1}{6}(p_2 \cdot p_3)\right. \\
& \left.+ \frac{1}{6}(p_2 \cdot p_4 + p_2 \cdot p_5 + p_3 \cdot p_4 + p_3 \cdot p_5 + p_4 \cdot p_5)\right] \\
K^0(p_1)\pi^+(p_2)\pi^-(p_3)\pi^+(p_4)\pi^-(p_5) & -\frac{\sqrt{2}}{3f^5}\left[\frac{3}{2}p_1 \cdot (p_3+p_5) + 2p_2 \cdot p_4\right. \\
& \left.- \frac{3}{2}(p_2+p_4) \cdot \left(p_1 + \frac{p_3+p_5}{2}\right) + p_3 \cdot p_5\right] \\
K^0(p_1)\pi^0(p_2)\pi^0(p_3)K^+(p_4)K^-(p_5) & -\frac{1}{6\sqrt{2}f^5}\left[p_1 \cdot (-4p_2-4p_3-p_4+5p_5)\right. \\
& \left.+ p_5 \cdot (p_2+p_3) + 2p_2 \cdot p_3\right] \\
K^0(p_1)\pi^0(p_2)\pi^0(p_3)\pi^+(p_4)\pi^-(p_5) & -\frac{1}{3\sqrt{2}f^5}\left[\frac{p_2+p_3}{4} \cdot (-9p_1-5p_4-9p_5) - p_1 \cdot p_4\right]
\end{aligned}$$

$$\begin{aligned}
& +5p_1 \cdot p_5 + \frac{15}{2}p_2 \cdot p_3] \\
K^0(p_1)\pi^+(p_2)\pi^-(p_3)K^+(p_4)K^-(p_5) & -\frac{\sqrt{2}}{3f^5} [p_1 \cdot (-3p_2 + 5p_3 - 5p_4 + 3p_5) - p_2 \cdot p_3 \\
& +2p_2 \cdot p_4 - 2p_3 \cdot p_5 + p_4 \cdot p_5] \\
K^+(p_1)K^+(p_2)\pi^-(p_3)\pi^0(p_4)K^-(p_5) & -\frac{1}{6f^5} [(p_1 + p_2) \cdot (-2p_3 + 7p_4 - p_5) \\
& -2p_1 \cdot p_2 + 8p_3 \cdot p_5 - 5p_3 \cdot p_4 - 9p_4p_5] \\
K^+(p_1)\pi^-(p_2)\pi^-(p_3)\pi^+(p_4)\pi^0(p_5) & -\frac{1}{6f^5} [(p_2 + p_3) \cdot (-2p_1 - p_4 - 9p_5) \\
& +9p_1 \cdot p_5 + 10p_2 \cdot p_3 - 4p_1 \cdot p_4 + 9p_4 \cdot p_5] \\
K^+(p_1)\pi^-(p_2)\pi^0(p_3)\pi^0(p_4)\pi^0(p_5) & -\frac{1}{12f^5} \left[ \frac{p_3 + p_4 + p_5}{3} \cdot (p_1 - 7p_2) \right. \\
& \left. +2(p_3 \cdot p_4 + p_3 \cdot p_5 + p_4 \cdot p_5) \right] \\
K^+(p_1)\eta(p_2)\eta(p_3)\pi^-(p_4)\pi^0(p_5) & -\frac{1}{6f^5} \left[ (p_2 + p_3) \cdot \left( p_4 - \frac{5}{2}p_5 \right) + \frac{9}{2}p_1 \cdot p_5 \right. \\
& \left. -\frac{3}{2}p_4 \cdot p_5 \right] \\
K^+(p_1)\pi^-(p_2)\pi^0(p_3)\bar{K}^0(p_4)K^0(p_5) & -\frac{1}{6f^5} [p_4 \cdot p_5 + p_5 \cdot p_1 - 5p_5 \cdot p_2 - 4p_4 \cdot p_3 + 3p_3 \cdot p_5 \\
& +6p_1 \cdot p_3 - 2p_2 \cdot p_3] \\
K^0(p_1)\pi^+(p_2)\pi^-(p_3)\eta(p_4)\eta(p_5) & -\frac{1}{6\sqrt{2}f^5} \left[ -p_4 \cdot p_5 + \frac{3}{2}p_1 \cdot (p_4 + p_5) - \frac{5}{2}p_3 \cdot (p_4 + p_5) \right. \\
& \left. +6p_1 \cdot p_3 + \frac{3}{2}p_2 \cdot (p_4 + p_5) - 6p_1 \cdot p_2 \right] \\
K^0(p_1)\pi^0(p_2)\pi^0(p_3)\eta(p_4)\eta(p_5) & -\frac{1}{12\sqrt{2}f^5} \left[ -p_4 \cdot p_5 + \frac{3}{2}p_1 \cdot (p_4 + p_5) + (p_4 + p_5) \cdot (p_2 + p_3) \right. \\
& \left. -\frac{9}{2}p_1 \cdot (p_2 + p_3) + 3p_2 \cdot p_3 \right]
\end{aligned}$$

$G_{\underline{8}}$

$$\begin{aligned}
K^0(p_1)\pi^0(p_2) & \frac{i\sqrt{2}}{f^2} p_1 \cdot p_2 \\
K^0(p_1)\eta(p_2) & \frac{i}{f^2} \sqrt{\frac{2}{3}} p_1 \cdot p_2 \\
K^+(p_1)\pi^-(p_2) & -\frac{2i}{f^2} p_1 \cdot p_2 \\
K^0(p_1)\pi^0(p_2)\pi^0(p_3) & \frac{1}{2\sqrt{2}f^3} [-p_3 \cdot (p_1 - p_2) - p_2 \cdot (p_1 - p_3)]
\end{aligned}$$

$$\begin{aligned}
K^0(p_1)\pi^0(p_2)\eta(p_3) & -\frac{1}{\sqrt{6}f^3}(p_1 \cdot p_3 + 2p_2 \cdot p_3 - 3p_1 \cdot p_2) \\
K^0(p_1)\eta(p_2)\eta(p_3) & -\frac{1}{\sqrt{2}f^3}\left[p_2 \cdot p_3 - p_1 \cdot \left(\frac{p_2 + p_3}{2}\right)\right] \\
K^0(p_1)K^+(p_2)K^-(p_3) & -\frac{\sqrt{2}}{f^3}p_3 \cdot (p_2 - p_1) \\
K^0(p_1)\pi^+(p_2)\pi^-(p_3) & -\frac{\sqrt{2}}{f^3}p_2 \cdot (p_1 - p_3) \\
K^+(p_1)\pi^0(p_2)\pi^-(p_3) & -\frac{1}{f^3}p_1 \cdot (p_2 - p_3) \\
K^+(p_1)\eta(p_2)\pi^-(p_3) & \frac{1}{\sqrt{3}f^3}(p_1 \cdot p_2 + 2p_2 \cdot p_3 - 3p_1 \cdot p_3) \\
K^0(p_1)K^0(p_2)\bar{K}^0(p_3)\pi^0(p_4) & \frac{2\sqrt{2}}{3}\frac{i}{f^4}\left[+p_3 \cdot p_4 - \left(\frac{p_1 + p_2}{2}\right) \cdot p_4\right] \\
K^0(p_1)K^0(p_2)\pi^+(p_3)K^-(p_4) & \frac{i}{3f^4}\left[p_1 \cdot p_2 + (p_4 + p_3)\left(\frac{p_1 + p_2}{2}\right) - 3p_3 \cdot p_4\right] \\
K^0(p_1)K^0(p_2)\bar{K}^0(p_3)\eta(p_4) & \frac{2}{3}\sqrt{\frac{2}{3}}\frac{i}{f^4}\left[+p_3 \cdot p_4 - \left(\frac{p_1 + p_2}{2}\right) \cdot p_4\right] \\
K^0(p_1)\pi^-(p_2)\pi^+(p_3)\pi^0(p_4)\pi^0(p_5) & -\frac{1}{6\sqrt{2}f^5}\left[p_1 \cdot p_2 - (p_1 + 3p_2 + p_3) \cdot \frac{p_4 + p_5}{2} + 3p_4 \cdot p_5\right. \\
& \left. - 2p_1 \cdot p_3 + 3p_2 \cdot p_3\right] \\
K^0(p_1)\pi^-(p_2)\pi^+(p_3)\pi^+(p_4)\pi^-(p_5) & -\frac{1}{3\sqrt{2}f^5}\left[\frac{p_2 + p_5}{2} \cdot (p_1 + p_3 + p_4) - p_2 \cdot p_5\right. \\
& \left. - p_1 \cdot (p_3 + p_4)\right] \\
K^0(p_1)\pi^0(p_2)\pi^0(p_3)\pi^0(p_4)\pi^0(p_5) & -\frac{1}{12\sqrt{2}f^5}\left[-p_1 \cdot \frac{p_2 + p_3 + p_4 + p_5}{4} + \frac{1}{6}(p_2 \cdot p_3 + p_2 \cdot p_4)\right. \\
& \left. + \frac{1}{6}(p_2 \cdot p_5 + p_3 \cdot p_4 + p_3 \cdot p_5 + p_4 \cdot p_5)\right] \\
K^0(p_1)\pi^-(p_2)\pi^+(p_3)K^+(p_4)K^-(p_5) & -2\sqrt{2}\frac{1}{3f^5}(p_1 \cdot p_5 - p_5 \cdot p_4 - p_1 \cdot p_3 + p_2 \cdot p_3) \\
K^0(p_1)\pi^0(p_2)\pi^0(p_3)K^+(p_4)K^-(p_5) & -\frac{1}{6\sqrt{2}f^5}\left[5p_1 \cdot p_5 + 2p_1 \cdot p_4 - 3p_4 \cdot p_5 - 2p_1 \cdot (p_2 + p_3)\right. \\
& \left. - p_5 \cdot (p_2 + p_3) + 2p_2 \cdot p_3\right] \\
K^0(p_1)\pi^-(p_2)\pi^+(p_3)\eta(p_4)\eta(p_5) & -\frac{1}{6\sqrt{2}f^5}\left[-p_4 \cdot p_5 + \frac{3}{2}p_1 \cdot (p_4 + p_5) + \frac{1}{2}p_2 \cdot (p_4 + p_5)\right. \\
& \left. - 3p_1 \cdot p_2 + \frac{3}{2}p_3 \cdot (p_4 + p_5) - 6p_1 \cdot p_3 + 3p_2 \cdot p_3\right]
\end{aligned}$$

$$\begin{aligned}
K^0(p_1)\pi^0(p_2)\pi^0(p_3)\eta(p_4)\eta(p_5) &= -\frac{1}{12\sqrt{2}f^5} \left[ -p_4 \cdot p_5 + \frac{3}{2}p_1 \cdot (p_4 + p_5) \right. \\
&\quad \left. + (p_4 + p_5) \cdot (p_2 + p_3) - \frac{9}{2}p_1 \cdot (p_2 + p_3) + 3p_2 \cdot p_3 \right] \\
K^0(p_1)\pi^0(p_2)\pi^0(p_3)K^0(p_4)\bar{K}^0(p_5) &= -\sqrt{2}\frac{1}{3f^5} \left[ -\frac{1}{4}(p_1 + p_4) \cdot (p_2 + p_3) + p_2 \cdot p_3 \right] \\
K^0(p_1)\pi^-(p_2)\pi^+(p_3)K^0(p_4)\bar{K}^0(p_5) &= -\frac{1}{3\sqrt{2}f^5} \left[ \frac{1}{2}p_5 \cdot (p_1 + p_4) + p_1 \cdot p_4 - p_2 \cdot p_5 \right. \\
&\quad \left. - \frac{1}{2}p_2 \cdot (p_1 + p_4) - \frac{3}{2}p_3 \cdot (p_1 + p_4) + 3p_2 \cdot p_3 \right]
\end{aligned} \tag{C.4}$$

$G^{(0)}$

$$\begin{aligned}
K^+\pi^- &= \frac{2i}{f^2} \\
K^0\pi^-\pi^+ &= \frac{-\sqrt{2}}{f^3} \\
K^+\pi^-\pi^0 &= \frac{-1}{f^3} \\
K^0K^+K^- &= \frac{\sqrt{2}}{f^3} \\
K^+\pi^-\eta &= \frac{\sqrt{3}}{f^3} \\
K^0\pi^0\pi^0\pi^-\pi^+ &= \frac{1}{2\sqrt{2}f^5} \\
K^0\pi^0\pi^0K^-K^+ &= \frac{-1}{2\sqrt{2}f^5} \\
K^0\pi^-\pi^+\pi^-\pi^+ &= \frac{1}{\sqrt{2}f^5} \\
K^0\pi^-\pi^+\eta\eta &= \frac{1}{2\sqrt{2}f^5} \\
K^0\pi^-\pi^+K^0\bar{K}^0 &= \frac{1}{\sqrt{2}f^5} \\
K^+\pi^-\pi^0\pi^-\pi^+ &= \frac{1}{2f^5} \\
K^+\pi^-\pi^0\pi^0\pi^0 &= \frac{1}{4f^5} \\
K^+\pi^-\pi^0\pi^0\pi^0 &= \frac{1}{4f^5}
\end{aligned}$$

$$\begin{aligned}
K^+ \pi^- \pi^0 K^- K^+ & \frac{1}{2f^5} \\
K^+ \pi^- \pi^0 \pi^0 \eta & -\frac{\sqrt{3}}{4f^5} \\
K^+ \pi^- \pi^0 K^0 \bar{K}^0 & \frac{1}{2f^5}
\end{aligned} \tag{C.5}$$

$G_{LR}^a$

$$\begin{aligned}
K^+(p_1)\pi^-(p_2) & -\frac{2i}{f^2}p_1 \cdot p_2 \\
K^+(p_1)\pi^0(p_2)\pi^-(p_3) & \frac{1}{f^3}p_3 \cdot (p_1 + p_2) \\
K^+(p_1)\eta(p_2)\pi^-(p_3) & -\frac{1}{\sqrt{3}f^3} [2p_1 \cdot p_2 + p_2 \cdot p_3 + 3p_1 \cdot p_3] \\
K^0(p_1)K^-(p_2)K^+(p_3) & -\frac{\sqrt{2}}{f^3}p_3 \cdot (p_1 + p_2) \\
K^0(p_1)\pi^+(p_2)\pi^-(p_3) & \frac{\sqrt{2}}{f^3}p_3 \cdot (p_1 + p_2) \\
K^+(p_1)\pi^-(p_2)\pi^0(p_3)K^+(p_4)K^-(p_5) & -\frac{1}{12f^5} [p_5 \cdot (p_1 + p_4) + 2p_1 \cdot p_4 + 4p_5 \cdot p_2 \\
& + 5p_2 \cdot (p_1 + p_4) + 4p_5 \cdot p_3 \\
& + p_3 \cdot (p_1 + p_4) + 8p_2 \cdot p_3] \\
K^+(p_1)\pi^-(p_2)\pi^0(p_3)\pi^0(p_4)\pi^0(p_5) & -\frac{1}{36f^5} [9p_1 \cdot p_2 + 4p_1 \cdot (p_3 + p_4 + p_5) + \\
& 5p_2 \cdot (p_3 + p_4 + p_5) + 4(p_3 \cdot p_4 + p_5 \cdot p_3 + p_4 \cdot p_5)] \\
K^+(p_1)\pi^-(p_2)\pi^0(p_3)\pi^+(p_4)\pi^-(p_5) & -\frac{1}{12f^5} [5p_1 \cdot (p_2 + p_5) + 2p_2 \cdot p_5 + 5p_3 \cdot (p_2 + p_5) \\
& + 4p_1 \cdot p_4 + p_4 \cdot (p_2 + p_5) + 4p_3 \cdot p_4] \\
K^+(p_1)\pi^-(p_2)\pi^0(p_3)\eta(p_4)\eta(p_5) & -\frac{1}{24f^5} [4p_1 \cdot (p_4 + p_5) + 2p_2 \cdot (p_4 + p_5) + 6p_1 \cdot p_2 \\
& + 4p_3 \cdot (p_4 + p_5) + 6p_2 \cdot p_3] \\
K^+(p_1)\pi^-(p_2)\pi^0(p_3)K^0(p_4)\bar{K}^0(p_5) & -\frac{1}{6f^5} [3p_1 \cdot (p_2 + p_4 + p_5) + 2p_3 \cdot (p_2 + p_4 + p_5) + \\
& p_1 \cdot p_3] \\
K^0(p_1)\pi^-(p_2)\pi^+(p_3)K^0(p_4)\bar{K}^0(p_5) & -\frac{\sqrt{2}}{6f^5} [p_5 \cdot (p_1 + p_4) + 2p_1 \cdot p_4 + p_5 \cdot p_2 + \\
& 2p_2 \cdot (p_1 + p_4) + 2p_5 \cdot p_3 + p_3 \cdot (p_1 + p_4) + 3p_2 \cdot p_3]
\end{aligned}$$

$$\begin{aligned}
K^0(p_1)\pi^-(p_2)\pi^+(p_3)\eta(p_4)\eta(p_5) & -\frac{\sqrt{2}}{24f^5} [2(p_4 + p_5) \cdot (2p_1 + p_2 + 2p_3) + 6p_2 \cdot (p_1 + p_3)] \\
K^0(p_1)\pi^-(p_2)\pi^+(p_3)\pi^+(p_4)\pi^-(p_5) & -\frac{\sqrt{2}}{12f^5} [(p_2 + p_5) \cdot (5p_1 + 3p_3 + 3p_4) + 2p_1 \cdot (p_3 + p_4) + \\
& 2p_2 \cdot p_5 + 4p_3 \cdot p_4] \\
K^0(p_1)\pi^-(p_2)\pi^+(p_3)K^+(p_4)K^-(p_5) & -\frac{\sqrt{2}}{3f^5} [p_1 \cdot (p_5 - p_4 + p_2 - p_3) - 2p_5 \cdot p_4 + \\
& 2p_2 \cdot p_3] \\
K^0(p_1)\pi^0(p_2)\pi^0(p_3)\pi^+(p_4)\pi^-(p_5) & -\frac{\sqrt{2}}{12f^5} [(p_2 + p_3) \cdot (2p_1 + p_5 + 2p_4) + 3p_5 \cdot (p_1 + p_4)] \\
K^0(p_1)\pi^0(p_2)\pi^0(p_3)K^+(p_4)K^-(p_5) & \frac{\sqrt{2}}{12f^5} [(p_2 + p_3) \cdot (2p_1 + 2p_5 + p_4) + 3p_4 \cdot (p_1 + p_5)]
\end{aligned} \tag{C.6}$$

 $G_{LR}^b$ 

$$\begin{aligned}
K^0(p_1)\eta(p_2) & -\sqrt{\frac{2}{3}} \frac{i}{f^2} p_1 \cdot p_2 \\
K^0(p_1)\pi^0(p_2) & -\frac{\sqrt{2}i}{f^2} p_1 \cdot p_2 \\
K^+(p_1)\pi^-(p_2)\pi^0(p_3) & -\frac{1}{f^3} p_3 \cdot (p_1 - p_2) \\
K^0(p_1)\eta(p_2)\eta(p_3) & -\frac{1}{2\sqrt{2}f^3} [-2p_2 \cdot p_3 + p_1 \cdot (p_2 + p_3)] \\
K^0(p_1)\pi^0(p_2)\pi^0(p_3) & -\frac{1}{2\sqrt{2}f^3} [2p_2 \cdot p_3 - p_1 \cdot (p_2 + p_3)] \\
K^0(p_1)K^-(p_2)K^+(p_3) & -\frac{\sqrt{2}}{f^3} p_1 \cdot (p_3 - p_2) \\
K^0(p_1)\pi^-(p_2)\pi^+(p_3) & -\frac{\sqrt{2}}{f^3} p_1 \cdot (p_3 - p_2) \\
K^+(p_1)\pi^-(p_2)\eta(p_3) & -\frac{1}{\sqrt{3}f^3} p_3 \cdot (p_1 - p_2) \\
K^0(p_1)\pi^0(p_2)\eta(p_3) & -\frac{1}{\sqrt{6}f^3} [-p_1 \cdot p_3 - 2p_3 \cdot p_2 + 3p_1 \cdot p_2] \\
K^+(p_1)\pi^-(p_2)\pi^0(p_3)K^+(p_4)K^-(p_5) & -\frac{1}{6f^5} [p_5 \cdot (p_1 + p_4) + 2p_1 \cdot p_4 + 4p_5 \cdot p_2 \\
& -4p_2 \cdot (p_1 + p_4) - 3p_5 \cdot p_3 - p_3 \cdot (p_1 + p_4) + 5p_2 \cdot p_3]
\end{aligned}$$



$$\begin{aligned}
K^+(p_1)\pi^-(p_2)\pi^0(p_3)\pi^0(p_4)\pi^0(p_5) & -\frac{1}{36f^5}[-p_1 \cdot (p_3 + p_4 + p_5) + \\
& 7p_2 \cdot (p_3 + p_4 + p_5) - \\
& 6(p_3 \cdot p_4 + p_3 \cdot p_5 + p_4 \cdot p_5)] \\
K^+(p_1)\pi^-(p_2)\pi^0(p_3)\pi^+(p_4)\pi^-(p_5) & -\frac{1}{6f^5}[2p_1 \cdot (p_2 + p_5) + 2p_2 \cdot p_5 + 3p_3 \cdot (p_2 + p_5) \\
& + 4p_1 \cdot p_4 - 5p_4 \cdot (p_2 + p_5) + 3p_3 \cdot p_4 - 9p_1 \cdot p_3] \\
K^+(p_1)\pi^-(p_2)\pi^0(p_3)\eta(p_4)\eta(p_5) & -\frac{1}{12f^5}[-2p_2 \cdot (p_4 + p_5) + 5p_3 \cdot (p_4 + p_5) - \\
& -9p_1 \cdot p_3 + 3p_2 \cdot p_3] \\
K^+(p_1)\pi^-(p_2)\pi^0(p_3)K^0(p_4)\bar{K}^0(p_5) & -\frac{1}{6f^5}[p_4 \cdot (-7p_5 + 5p_1 - p_2 + 3p_3) \\
& p_3 \cdot (4p_5 - 6p_1 + 2p_2)] \\
K^0(p_1)\pi^0(p_2)\pi^0(p_3)\eta(p_4)\eta(p_5) & -\frac{1}{12\sqrt{2}f^5}\left[p_5 \cdot p_4 - \frac{3}{2}p_1 \cdot (p_4 + p_5) - (p_4 + p_5) \cdot (p_2 + p_3) \right. \\
& \left. + \frac{9}{2}p_1 \cdot (p_2 + p_3) - 3p_2 \cdot p_3\right] \\
K^0(p_1)\pi^-(p_2)\pi^+(p_3)\eta(p_4)\eta(p_5) & -\frac{1}{12\sqrt{2}f^5}[2p_4 \cdot p_5 - 3p_1 \cdot (p_4 + p_5) \\
& -7p_2 \cdot (p_4 + p_5) + \\
& 12p_1 \cdot p_2 + 9p_3 \cdot (p_4 + p_5) - 12p_1 \cdot p_3] \\
K^0(p_1)\pi^0(p_2)\pi^0(p_3)K^0(p_4)\bar{K}^0(p_5) & -\frac{1}{6\sqrt{2}f^5}[(p_1 + p_4) \cdot (p_2 + p_3) - 4p_2 \cdot p_3] \\
K^0(p_1)\pi^0(p_2)\pi^0(p_3)\pi^0(p_4)\pi^0(p_5) & -\frac{1}{12\sqrt{2}f^5}\left[\frac{1}{4}p_1 \cdot (p_2 + p_3 + p_4 + p_5) \right. \\
& -\frac{1}{6}(p_2 \cdot p_3 + p_2 \cdot p_4 + p_2 \cdot p_5 \\
& \left. + p_3 \cdot p_4 + p_3 \cdot p_5 + p_4 \cdot p_5)\right] \\
K^0(p_1)\pi^-(p_2)\pi^+(p_3)K^0(p_4)\bar{K}^0(p_5) & -\frac{1}{6\sqrt{2}f^5}[-3p_5 \cdot (p_1 + p_4) + 6p_1 \cdot p_4 - 8p_5 \cdot p_2 \\
& + 5p_2 \cdot (p_1 + p_4) + 8p_5 \cdot p_2 - 5p_3 \cdot (p_1 + p_4)] \\
K^0(p_1)\pi^-(p_2)\pi^+(p_3)\pi^+(p_4)\pi^-(p_5) & -\frac{1}{12\sqrt{2}f^5}[12p_1 \cdot (p_2 + p_5) + 8p_2 \cdot p_5 - 12p_1 \cdot (p_3 + p_4) - \\
& 6(p_2 + p_5) \cdot (p_3 + p_4) + 16p_3 \cdot p_4] \\
K^0(p_1)\pi^0(p_2)\pi^0(p_3)K^+(p_4)K^-(p_5) & -\frac{1}{6\sqrt{2}f^5}[(p_2 + p_3) \cdot (4p_1 - 3p_5 + 2p_4) + p_1 \cdot p_5 - \\
& 5p_1 \cdot p_4 - 2p_2 \cdot p_3]
\end{aligned}$$

$$\begin{aligned}
K^0(p_1)\pi^-(p_2)\pi^+(p_3)K^+(p_4)K^+(p_5) & -\frac{\sqrt{2}}{3f^5} [3p_1 \cdot p_5 - p_1 \cdot p_4 - p_5 \cdot p_4 + \\
& p_1 \cdot p_2 - 3p_1 \cdot p_3 + p_2 \cdot p_3] \\
K^0(p_1)\pi^0(p_2)\pi^0(p_3)\pi^+(p_4)\pi^-(p_5) & -\frac{1}{12\sqrt{2}f^5} [4p_1 \cdot p_5 + 9p_1 \cdot (p_2 + p_3) + 5p_5 \cdot (p_2 + p_3) - \\
& 30p_2 \cdot p_3 - 20p_1 \cdot p_4 + 9p_4 \cdot (p_2 + p_3)]
\end{aligned} \tag{C.7}$$

 $G_{LR}^c$ 

$$\begin{aligned}
K^+(p_1)\pi^-(p_2)\pi^0(p_3) & -\frac{2}{f^3}p_1 \cdot p_2 \\
K^+(p_1)\eta(p_2)\pi^-(p_3) & \frac{2}{\sqrt{3}f^3} [p_1 \cdot p_2 + 2p_2 \cdot p_3] \\
K^0(p_1)K^+(p_2)K^-(p_3) & \frac{2\sqrt{2}}{f^3}p_1 \cdot p_3 \\
K^0(p_1)\pi^+(p_2)\pi^-(p_3) & -\frac{2\sqrt{2}}{f^3}p_1 \cdot p_2 \\
K^+(p_1)\pi^-(p_2)\pi^0(p_3)K^+(p_4)K^-(p_5) & -\frac{1}{6f^5} [-6p_5 \cdot (p_1 + p_4) + 2p_5 \cdot p_2 - 5p_2 \cdot (p_1 + p_4) \\
& -4p_5 \cdot p_3 - 3p_3 \cdot (p_1 + p_4) + 2p_2 \cdot p_3] \\
K^+(p_1)\pi^-(p_2)\pi^0(p_3)\pi^0(p_4)\pi^0(p_5) & \frac{1}{9f^5} [2p_1 \cdot (p_3 + p_4 + p_5) + \\
& 5(p_3 \cdot p_4 + p_3 \cdot p_5 + p_4 \cdot p_5)] \\
K^+(p_1)\pi^-(p_2)\pi^0(p_3)\pi^+(p_4)\pi^-(p_5) & -\frac{1}{6f^5} [(p_2 + p_5) \cdot (p_1 + p_3 - 12p_4) - 12p_1 \cdot p_3 \\
& + 2p_4 \cdot (p_1 + p_3)] \\
K^+(p_1)\pi^-(p_2)\pi^0(p_3)\eta(p_4)\eta(p_5) & -\frac{1}{6f^5} [-6p_5 \cdot p_4 - 6p_3 \cdot p_1 + (p_4 + p_5) \cdot (2p_3 - p_1 - 2p_2)] \\
K^+(p_1)\pi^-(p_2)\pi^0(p_3)K^0(p_4)\bar{K}^0(p_5) & -\frac{1}{3f^5} [p_5 \cdot (-9p_4 - p_1 - p_2 + p_3) - p_2 \cdot p_3 + \\
& p_4 \cdot (2p_1 - p_2 + p_3) - 5p_1 \cdot p_3] \\
K^0(p_1)\pi^-(p_2)\pi^+(p_3)\eta(p_4)\eta(p_5) & -\frac{\sqrt{2}}{6f^5} [(p_5 + p_4) \cdot (-p_1 - 2p_2 + 2p_3) \\
& - 6p_4 \cdot p_5 - 6p_1 \cdot p_3] \\
K^0(p_1)\pi^-(p_2)\pi^+(p_3)K^0(p_4)\bar{K}^0(p_5) & -\frac{\sqrt{2}}{6f^5} [(p_1 + p_4) \cdot (-8p_5 - 5p_3)
\end{aligned}$$

$$\begin{aligned}
& K^0(p_1)\pi^-(p_2)\pi^+(p_3)\pi^+(p_4)\pi^-(p_5) && +2p_1 \cdot p_4 - 6p_5 \cdot p_2 + 2p_5 \cdot p_3] \\
& && -\frac{\sqrt{2}}{12f^5} [2p_1 \cdot (p_2 + p_5) - 10p_1 \cdot (p_3 + p_4) \\
& && -11(p_2 + p_5) \cdot (p_3 + p_4) + 4p_3 \cdot p_4] \\
& K^0(p_1)\pi^-(p_2)\pi^+(p_3)K^+(p_4)K^-(p_5) && -\frac{\sqrt{2}}{3f^5} [4p_5 \cdot p_1 - 7p_5 \cdot p_4 - 4p_1 \cdot p_3 + 7p_2 \cdot p_3] \\
& K^0(p_1)\pi^-(p_2)\pi^+(p_3)\pi^0(p_4)\pi^0(p_5) && -\frac{\sqrt{2}}{6f^5} [p_1 \cdot (p_4 + p_5) - 12p_5 \cdot p_4 - 6p_1 \cdot p_3 + \\
& && p_3 \cdot (p_4 + p_5)] \\
& K^0(p_1)\pi^0(p_2)\pi^0(p_3)K^+(p_4)K^-(p_5) && \frac{\sqrt{2}}{24f^5} [(p_2 + p_3) \cdot (-4p_5 + 8p_1 + 6p_4) \\
& && +12p_5 \cdot p_1 + 24p_2 \cdot p_3]
\end{aligned}$$

(C.8)

### C.3 Feynman Rules for the $\Delta S = 2$ Chiral Lagrangian

The relevant vertices for the  $\Delta S = 2$  term, proportional to  $C(Q_{S2})$  are :

$$\begin{aligned}
K^0(p_1)K^0(p_2) & \frac{2i}{f^2}p_1 \cdot p_2 \\
K^0(p_1)K^0(p_2)\eta(p_3)\eta(p_4) & \frac{i}{2f^4} \left[ \frac{5}{2}(p_1 + p_2) \cdot (p_3 + p_4) - 7p_1 \cdot p_2 - 3p_3 \cdot p_4 \right] \\
K^0(p_1)K^0(p_2)K^+(p_3)K^-(p_4) & \frac{i}{3f^4} [(p_1 + p_2) \cdot (4p_4 - 2p_3) - 4p_1 \cdot p_2] \\
K^0(p_1)K^0(p_2)\pi^0(p_3)\pi^0(p_4) & \frac{i}{f^4} \left[ -\frac{1}{2}p_3 \cdot p_4 - \frac{7}{6}p_1 \cdot p_2 + \frac{5}{12}(p_1 + p_2) \cdot (p_3 + p_4) \right] \\
K^0(p_1)K^0(p_2)\pi^+(p_3)\pi^-(p_4) & \frac{i}{3f^4} [-4p_1 \cdot p_2 - 2p_4 \cdot (p_1 + p_2) + 4p_3 \cdot (p_1 + p_2)] \\
K^0(p_1)K^0(p_2)K^0(p_3)\bar{K}^0(p_4) & \frac{8i}{9f^4} [p_4 \cdot (p_1 + p_2 + p_3) - (p_1 \cdot p_2 + p_1 \cdot p_3 + p_2 \cdot p_3)]
\end{aligned} \tag{C.9}$$

# Bibliography

- [1] J.H. Christenson, J.W. Cronin, V.L. Fitch and R. Turlay, *Phys. Rev. Lett.* **13** (1964) 138.
- [2] S.L. Glashow, J. Iliopoulos and L. Maiani, *Phys. Rev. D* **2** (1970) 1285.
- [3] M.K. Gaillard and B.W. Lee, *Phys. Rev. D* **10** (1974) 897.
- [4] M. Gell-Mann and A. Pais, *Proc. Glasgow Conf. 1954*, p. 342 (Pergamon, London, 1955).
- [5] H.-Y. Cheng, *Int. J. Mod. Phys. A* **4** (1989) 495.
- [6] V. Antonelli, S. Bertolini, M. Fabbrichesi and E.I. Lashin, *Nucl. Phys. B* **469** (1996) 181.
- [7] G.D. Barr *et al.*(Na31 Coll.), *Phys. Lett. B* **317** (1993) 233.
- [8] L.K. Gibbons *et al.*(E731 Coll.), *Phys. Rev. Lett.* **70** (1993) 1203.
- [9] L. Wolfenstein, *Phys. Rev. Lett.* **13** (1964) 562.
- [10] See for instance: Particle Data Group, *Phys. Rev. D* **50** (1994) 1173.
- [11] N. Cabibbo, *Phys. Rev. Lett.* **10** (1963) 531;  
M. Kobayashi and T. Maskawa, *Prog. Theor. Phys.* **49** (1973) 652.
- [12] K. G. Wilson and W. Zimmermann, *Comm. Math. Phys.* **24** (1972) 87.
- [13] E.C.G. Stueckelberg and A. Petermann, *Helv. Phys. Acta* **26** (1953) 499;  
M. Gell-Mann and F.E. Low *Phys. Rev.* **95** (1954) 1300;  
K. Symanzik, *Comm. Math. Phys.* **18** (1970) 227;  
C.G. Callan Jr. *Phys. Rev. D* **2** (1970) 1541;  
G. 't Hooft, *Nucl. Phys. B* **61** (1973) 455;  
S. Weinberg, *Phys. Rev. D* **8** (1973) 3497.
- [14] V. Antonelli, S. Bertolini, J.O. Eeg, M. Fabbrichesi and E.I. Lashin, *Nucl. Phys. B* **469** (1996) 143.

- [15] A.J. Buras, M. Jamin, M.E. Lautenbacher and P.H. Weisz, *Nucl. Phys. B* **370** (1992) 69, [Addendum: *B375* (1992) 501];  
 A.J. Buras, M. Jamin, M.E. Lautenbacher and P.H. Weisz, *Nucl. Phys. B* **400** (1993) 37;  
 A.J. Buras, M. Jamin and M.E. Lautenbacher, *Nucl. Phys. B* **400** (1993) 75; *Nucl. Phys. B* **408** (1993) 209.
- [16] M. Ciuchini, E. Franco, G. Martinelli and L. Reina, *Nucl. Phys. B* **415** (1994) 403; *Phys. Lett. B* **301** (1993) 263.
- [17] See for instance:  
 S. Sharpe, *Nucl. Phys. B* **20** (1991) 429 (*Proc. Suppl.*);  
 G.W. Kilcupp, *Nucl. Phys. B* **20** (1991) 417 (*Proc. Suppl.*);  
 C. Bernard *et al.*, *Nucl. Phys.* **17** (1990) 495 (*Proc. Suppl.*);  
 M.B. Gavela *et al.*, *Nucl. Phys. B* **306** (1988) 677.
- [18] W.A. Bardeen A.J. Buras and J.-M. Gérard, *Phys. Lett. B* **192** (1987) 138.
- [19] W.A. Bardeen A.J. Buras and J.-M. Gérard, *Phys. Lett. B* **180** (1986) 133.
- [20] A. Pich and E. de Rafael, *Nucl. Phys. B* **358** (1991) 311;  
 see, also: E. De Rafael, *Chiral Lagrangians and Kaon CP-violation*, Lecture at TASI 1994, J.F. Donoghue, ed. (World Scientific, Singapore 1995).
- [21] M. A. Shifman, *QCD Sum Rules: The Second Decade*, hep-ph/9304253, published in Aachen QCD Wkshp.1992:775-794(QCD161:W586:1992);  
 N. Bilic and B. Guberina, *Z. Physik C* **27** (1985) 399;  
 R. Decker, . *Nucl. Phys. Proc. Suppl.* **7A** :180,1989.
- [22] J. Kambor, J. Missimer and D. Wyler, *Nucl. Phys. B* **346** (1990) 17 and *Phys. Lett. B* **261** (1991) 496.
- [23] J. Gasser and H. Leutwyler. *Ann. Phys. (NY)* **158** (1984) 142; *Nucl. Phys. B* **250** (1985) 465, 517, 539.
- [24] V. Antonelli, S. Bertolini, M. Fabbrichesi and E.I. Lashin, *The Physics of  $K^0 - \bar{K}^0$  Mixing:  $\hat{B}_K$  and  $\Delta M_{LS}$  in the Chiral Quark Model*, preprint SISSA 20/96/EP and hep-ph/9610230, submitted for publication to Nuclear Physics B .
- [25] K. Nishijima, *Nuovo Cim.* **11** (1959) 698;  
 F. Gursey, *Nuovo Cim.* **16** (1960) 230 and *Ann. Phys. (NY)* **12** (1961) 91.
- [26] J.A. Cronin, *Phys. Rev.* **161** (1967) 1483.
- [27] S. Weinberg, *Physica* **96A** (1979) 327;  
 A. Manohar and H. Georgi, *Nucl. Phys. B* **234** (1984) 189;  
 A. Manohar and G. Moore, *Nucl. Phys. B* **243** (1984) 55;  
 D. Espriu, E. De Rafael and J. Taron, *Nucl. Phys. B* **345** (1990) 22.

- [28] J. Bijnens, C. Bruno and E. de Rafael, *Nucl. Phys. B* **390** (1993) 501;  
J. Bijnens, *Phys. Rep.* **265** (1996) 369.
- [29] S. Bertolini, J.O. Eeg and M. Fabbrichesi, *Nucl. Phys. B* **476** (1996) 225.
- [30] M.A. Shifman, A.I. Vainshtein and V.I. Zakharov, *Nucl. Phys. B* **120** (1977) 316;  
*JETP Lett.* **22** (1975) 55;  
A.I. Vainshtein, V.I. Zakharov and M.A. Shifman, *Sov. Phys. JETP* **45** (1977) 670.
- [31] Among all the works about the derivation of  $\Delta S = 1$  effective hamiltonian, I consider particularly instructive the following one:  
F. J. Gilman and M. B. Wise *Phys. Rev. D* **20** N.9 (1979) 2392.  
An useful review containing also this subject is:  
G. Buchalla, A.J. Buras and M.E. Lautenbacher, *Weak Decays beyond Leading Logarithms*, SLAC-PUB-95-7009, Nov. 1995 and hep-ph/9512380, to appear in *Rev. Mod. Phys.* .
- [32] About the relevance of the operator  $Q_{11}$  see the discussion in the paper ref. [45] and in:  
S. Bertolini, M. Fabbrichesi and E. Gabrielli, *Phys. Lett. B* **327** (1994) 136.
- [33] See for instance:  
G. Martinelli, *Phys. Lett. B* **141** (1984) 395;  
D. Daniel and S. Sheard, *Nucl. Phys. B* **302** (1988) 471;  
S. Sheard, *Nucl. Phys. B* **314** (1989) 238;  
G. Curci, E. Franco, L. Maiani and G. Martinelli, *Phys. Lett. B* **202** (1988) 363.
- [34] J. Goldstone, *Nuovo Cim.* **19** (1961) 154.
- [35] See for instance:  
J. Bijnens, G.Ecker and J. Gasser, *Chiral Perturbation Theory*, in *The Second DAΦNE Physics Handbook*, eds. L. Maiani, G. Pancheri and N. Paver, (Frascati,1995). Vol.1 pag.125 and the references inside.
- [36] Y. Nambu and G. Jona-Lasinio, *Phys. Rev.* **122** (1961) 345.
- [37] M.A. Shifman, A.I. Vainshtein and V.I. Zakharov, *Nucl. Phys. B* **120** (1977) 316;  
F.J. Gilman and M.B. Wise, *Phys. Rev. D* **20** (1979) 2392;  
J. Bijnens and M.B. Wise, *Phys. Lett. B* **137** (1984) 245;  
M. Lusignoli, *Nucl. Phys. B* **325** (1989) 33.
- [38] L3 Coll., *Phys. Lett. B* **248** (1990) 464, *Phys. Lett. B* **257** (1991) 469;  
ALEPH Coll., *Phys. Lett. B* **255** (1991) 623, *Phys. Lett. B* **257** (1991) 479;  
DELPHI Coll., *Z. Physik C* **54** (1992) 55;  
OPAL Coll., *Z. Physik C* **55** (1992) 1;  
Mark-II Coll., *Phys. Rev. Lett.* **64** (1990) 987;  
SLD Coll., *Phys. Rev. Lett.* **71** (1993) 2528.
- [39] J. Bijnens, *Int. J. Mod. Phys. A* **8** (1993) 3045.

- [40] C. Bruno and J. Prades, *Z. Physik C* **57** (1993) 585.
- [41] R.S. Chivukula, J.M. Flynn and H. Georgi, *Phys. Lett. B* **171** (1986) 453;  
See also the paper of ref. [18].
- [42] G. Ecker, J. Kambor and D. Wyler, *Nucl. Phys. B* **394** (1993) 101.
- [43] J. Bijnens and M.B. Wise, *Phys. Lett. B* **137** (1984) 245.
- [44] S. Fajfer, *Phys. Rev. D* **49** (1994) 5840.
- [45] S. Bertolini, J.O. Eeg and M. Fabbrichesi, *Nucl. Phys. B* **449** (1995) 197.
- [46] M. Ademollo, R. Gatto, *Phys. Rev. Lett.* **13** (1964) 264.
- [47] S. Narison, *Phys. Lett. B* **361** (1995) 121.
- [48] R.A. Bertlmann *et al.*, *Z. Physik C* **39** (1988) 231.
- [49] E. Braaten, S. Narison and A. Pich, *Nucl. Phys. B* **373** (1992) 581
- [50] A. Di Giacomo, H. Panagopoulos and E. Vicari, *Nucl. Phys. B* **338** (1990) 294.
- [51] C.A. Domínguez and E. de Rafael, *Ann. Phys. (NY)* **174** (1987) 372.
- [52] J. Bijnens, J. Prades and E. de Rafael, *Phys. Lett. B* **348** (1995) 226.
- [53] D. Daniel *et al.*, *Phys. Rev. D* **46** (1992) 3130;  
D. Weingarten, *Nucl. Phys. B* **34** (1994) 29 (*Proc. Suppl.*).
- [54] M. Fukugita *et al.*, *Phys. Rev. D* **47** (1993) 4739.
- [55] W.A. Bardeen, A.J. Buras and J.-M. Gérard, *Nucl. Phys. B* **293** (1987) 787.
- [56] J. Heinrich *et al.*, *Phys. Lett. B* **279** (1992) 140.
- [57] K.G. Wilson, *Phys. Rev.* **179** (1969) 1499.
- [58] M.K. Gaillard and B.W. Lee, *Phys. Rev. Lett.* **33** (1974) 108.
- [59] G. Altarelli and L. Maiani, *Phys. Lett. B* **52** (1974) 351.
- [60] Y. Dupont and T.N. Pham, *Phys. Rev. D* **29** (1984) 1368;  
J.F. Donoghue, *Phys. Rev. D* **30** (1984) 1499;  
M.B. Gavela *et al.*, *Phys. Lett. B* **148** (1984) 225;  
R.S. Chivukula, J.M. Flynn and H. Georgi, *Phys. Lett. B* **171** (1986) 453.
- [61] A.J. Buras and J.-M. Gérard, *Nucl. Phys. B* **264** (1986) 371.
- [62] A.J. Buras, J.-M. Gérard and R. Rückl, *Nucl. Phys. B* **268** (1986) 16.  
See also:  
G. Buchalla, A.J. Buras and K. Harlander, *Nucl. Phys. B* **337** (1990) 313.



- [63] A.G. Cohen and A. Manohar, *Phys. Lett. B* **143** (1984) 481.
- [64] See for instance:  
*CP Violation*, Advanced Series on Directions in High Energy Physics-Vol. 3. Editor C.Jarlskog;  
 J.F. Donoghue, E. Golowich and B.R. Holstein, *Dynamics of the Standard Model*. Cambridge monographs on particle physics, nuclear physics and cosmology;  
 L. Maiani, *CP and CPT Violation in neutral Kaon Decays*, in *The Second DAΦNE Physics Handbook* -Vol. I. eds. L. Maiani, G. Pancheri and N. Paver, (Frascati. 1995).
- [65] T.D. Lee and C.N.Yang, *Phys. Rev.* **104** (1956) 254.
- [66] C.S. Wu *et al.*, *Phys. Rev.* **105** (1957) 1413;  
 R.L. Garwin, L.M. Lederman and M. Weinrich, *Phys. Rev.* **105** (1957) 1415;  
 J.I. Friedman, V.L. Telegdi, *Phys. Rev.* **105** (1957) 1681 .
- [67] G. Lueders, *Kgl.Danske Videnskab. Selskab. Matfys. Medd.* **28** (5) (1954) 1:  
 W. Pauli, in *Niels Bohr and the Development of Physics*, ed. W. Pauli. p.30. Oxford. Pergamon 2.nd ed.(1955).
- [68] L.D. Landau, *Nucl. Phys.***3** (1957) 127.
- [69] M. Bardon *et al.*, *Ann. Phys. (NY)* **5** (1958) 156;  
 D. Neagu *et al.*, *Phys. Rev. Lett.* **6** (1961) 552.
- [70] M. Ciuchini, E. Franco, G. Martinelli and L. Reina, *Estimates of  $\epsilon'/\epsilon$* , in *The Second DAΦNE Physics Handbook*, eds. L. Maiani, G. Pancheri and N. Paver, (Frascati. 1995): *Z. Physik C* **68** (1995) 239.
- [71] A.J. Buras, *Theoretical Progress in K and B Decays*, hep-ph/9504269, published in *Tokio INS Sympos.1995:39-60 QCD162* : 121
- [72] J. Flynn and R.Randall, *Phys. Lett. B* **224** (1989) 221; Erratum *Phys. Lett. B* **235** (1990) 412;  
 M. Lusignoli, *Nucl. Phys. B* **325** (1989) 33;  
 G. Buchalla, A.J. Buras and M.K. Harlander, *Nucl. Phys. B* **337** (1990) 313.
- [73] *The Second DAΦNE Physics Handbook*, Vol.1 and Vol.2, eds. L. Maiani, G. Pancheri and N. Paver, (Frascati, 1995).  
 See also: *LNF Spring School in Nuclear and Subnuclear Physics*, LNF-96/030 (IR). 28 June 1996(Frascati).
- [74] T. Inami and C.S. Lim, *Prog. Theor. Phys.* **65** (1981) 297.
- [75] S. Herrlich and U. Nierste, *Nucl. Phys. B* **419** (1994) 292.
- [76] A.J. Buras, M. Jamin and P. H. Weisz, *Nucl. Phys. B* **347** (1990) 491.
- [77] S. Herrlich and U. Nierste, hep-ph/9604330, (April 1996).

- [78] A.J. Buras and P. H. Weisz, *Nucl. Phys. B* **333** (1990) 66;  
S. Herrlich and U. Nierste, *Nucl. Phys. B* **455** (1995) 39 and DESY preprint, DESY 96-048 (1996).
- [79] A. Pich and J. Prades, *Phys. Lett. B* **346** (1995) 342.
- [80] B. D. Gaiser, T. Tsao and M. B. Wise, *Ann. Phys. (NY)* **132** (1981) 66;  
A. J. Buras and J. -M. Gérard, *Nucl. Phys. B* **264** (1986) 371.
- [81] J. F. Donoghue, E. Golowich and B. R. Holstein, *Phys. Lett. B* **119** (1982) 412.
- [82] J. Bijnens and J. Prades, *Nucl. Phys. B* **444** (1995) 523 and *Phys. Lett. B* **342** (1995) 331.
- [83] C. Bruno, *Phys. Lett. B* **320** (1994) 135.
- [84] W.A. Bardeen A.J. Buras and J.-M. Gérard, *Phys. Lett. B* **211** (1988) 343.
- [85] A. Pich and E. de Rafael, *Phys. Lett. B* **158** (1985) 477.
- [86] J. Prades, C. A. Domínguez, J. A. Peñarrocha, A. Pich and E. de Rafael, *Z. Physik C* **51** (1991) 287.
- [87] N. Bilić, C. A. Domínguez and B. Guberina, *Z. Physik C* **39** (1988) 351.
- [88] S. R. Sharpe, *Chiral Perturbation Theory and Weak Matrix Elements*, hep-lat/9609029.
- [89] J. F. Donoghue, E. Golowich and B. R. Holstein, *Phys. Lett. B* **135** (1984) 481.
- [90] I. I. Bigi and A. I. Sanda, *Phys. Lett. B* **148** (1984) 205.
- [91] P. Cea and G. Nardulli, *Phys. Lett. B* **152** (1985) 251.
- [92] M. R. Pennington, *Phys. Lett. B* **153** (1985) 439.
- [93] A. J. Buras and J. -M. Gérard, *Nucl. Phys. B* **264** (1986) 371.
- [94] K. Terasaki and S. Oneda, Preprint. RRK, 89-21 (1989).
- [95] T. Kurimoto, *Prog. Theor. Phys.* **84** (1990) 658.
- [96] J. Bijnens, J. -M. Gérard and G. Klein *Phys. Lett. B* **257** (1991) 191.
- [97] F. J. Gilman and M. B. Wise *Phys. Rev. D* **27** (1983) 1128.
- [98] J.M. Flynn *Mod. Phys. Lett. A* **5** (1990) 877;  
A. Datta, J. Froehlich and E. A. Paschos *Z. Physik C* **46** (1990) 63.
- [99] L. Wolfenstein, *Nucl. Phys. B* **160** (1979) 501.
- [100] J.J. de Swart, *Rev. Mod. Phys.* **35** (1963) 916.

[101] See the ref. [23] and see also:

A. Pich *Introduction to Chiral Perturbation Theory*, Lectures at V Mexican School of Particles and Fields 1992, hep-ph/9308351.

